PhD Thesis

Novel Electrocardiographic Biomarkers for Proarrhythmic Assessment of Drugs

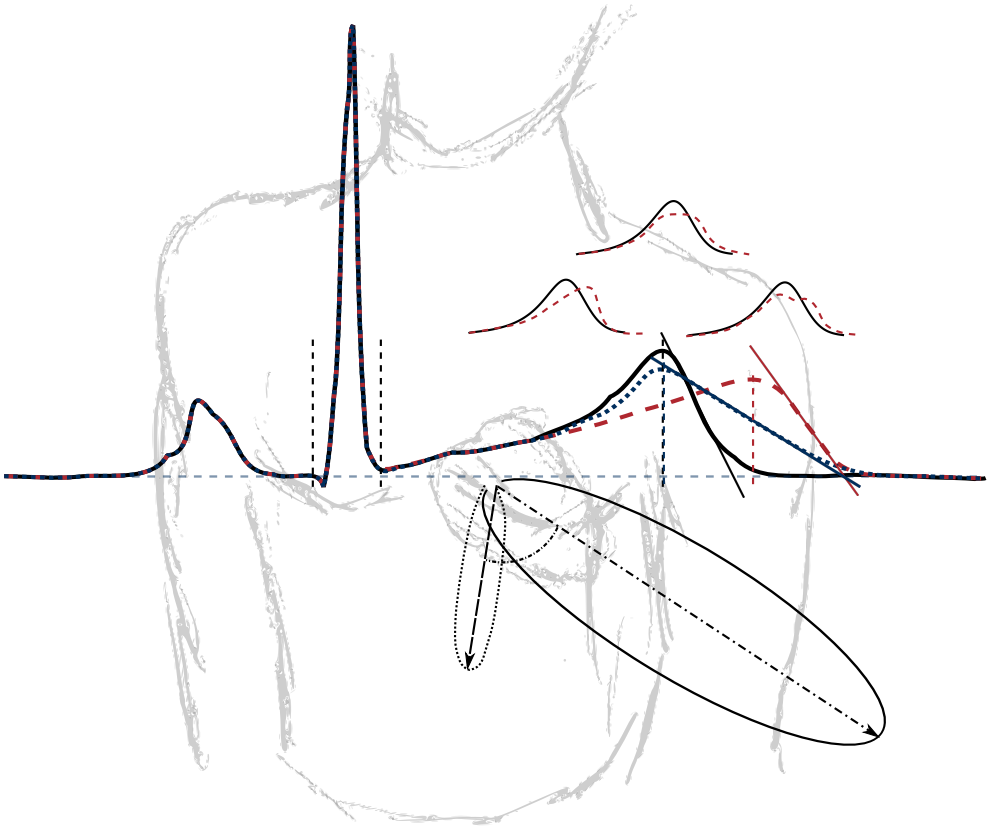

José Vicente Ruiz

Supervisors:
Esther Pueyo Paules, PhD
David G. Strauss, MD, PhD

Universidad Zaragoza
1542
December 2015

Instituto Universitario de Investigación
en Ingeniería de Aragón
Universidad Zaragoza

PhD Thesis

Novel Electrocardiographic Biomarkers for Proarrhythmic Assessment of Drugs

Nuevos Biomarcadores Electrocardiográficos para la Evaluación de Riesgo Proarrítmico de Fármacos

---

Doctoral Dissertation of:
José Vicente Ruiz

Supervisors:
Esther Pueyo Paules, PhD
David G Strauss, MD, PhD

University of Zaragoza
PhD in Biomedical Engineering

December 2015

This thesis was submitted to University of Zaragoza on December 11, 2015. The public defense of this thesis for the degree of Doctor of Philosophy in Biomedical Engineering will take place at Instituto de Investigación en Ingeniería de Aragón in Zaragoza, Spain, on March 14th, 2016.

Cover:
Illustration of drug-induced changes in the electrocardiogram (ECG). Drug effects on different ion channel currents cause changes in different ECG biomarkers, including the QT interval, its subintervals (QRS, J-T_{peak} and T_{peak}-T_{end}) and T-wave morphology. The main focus of this thesis is centered around these ECG biomarkers.

ISSN 2254-7606 Colección "*Tesis de la Universidad de Zaragoza*"
Instituto de Investigación en Ingeniería de Aragón
Universidad de Zaragoza
Zaragoza, España

Typeset using LaTeX and document layout based on Federico Maggi Memoir Thesis template.

pepoviru@gmail.com
http://www.pepovicente.com

This electronic version was compiled on July 2016 and includes author's versions of the manuscripts. See section "Tesis doctoral como compendio de publicaciones (List of publications included in this thesis)" for the corresponding publication references.

A Ofelia

Un día decidí
hacerle caso a la brisa
...
No me convenció nadie
me convenció tu sonrisa.
Y me fui tras de ti
persiguiendo mi instinto.
Si quieres cambio verdadero
pues, camina distinto.

Calle 13, La vuelta al mundo

Contents

Tesis doctoral como compendio de publicaciones

List of publications included in this thesis

Factores de impacto, áreas temáticas y contribuciones del doctorado en cada una de las publicaciones incluidas en esta tesis

For each study included in this thesis, the PhD student designed the study, analyzed the data and wrote the manuscript. A more detailed description of the PhD student contributions to each of the studies is outlined below:

1. Vicente J, Johannesen L, et al. Mechanisms of sex and age differences in ventricular repolarization in humans. *Am Heart J* 168(5):749–756, 2014

    - Factor the impacto: 4.463
    - Areas temáticas: Cardiac & cardiovascular systems.
    - Contribución del doctorando: The idea for this study came out of discussions between the student and Strauss and Johannesen. The design and planning of the study including software implementation and statistical analysis was carried out by the student. The manuscript was drafted by the student with help from Strauss and Johannesen and input from Galeotti. Journal correspondence was handled by the student and Strauss.

2. Vicente J, Simlund J, et al. Investigation of potential mechanisms of sex differences in quinidine-induced torsade de pointes risk. *J Electrocardiol* 48(4):533–538, 2015

    - Factor the impacto: 1.361
    - Areas temáticas: Cardiac & cardiovascular systems.
    - Contribución del doctorando: The idea for this study came out of discussions between the student and Strauss, Simlund, Johannesen and Wagner. The design and planning of the study including software implementation and statistical analysis was carried out by the student. Study data was curated by the student with help from Woosley and Johannesen. Semi-automatic adjudication of electrocardiograms (ECGs) was performed by the student with help from Johannesen and Simlund. ECGs were assessed with ECGlab, which was developed by the student. Compartmental model (hysteresis) analysis was performed by Johannesen with help from the student. The manuscript was drafted by the student and Simlund with help

from Strauss and Johannesen as well as input from all co-authors. Journal correspondence was handled by the student and Strauss.

3. Vicente J, Johannesen L, et al. Comprehensive T wave morphology assessment in a randomized clinical study of dofetilide, quinidine, ranolazine, and verapamil. *J Am Heart Assoc* 4(4):e001615, 2015

    - Factor the impacto: 4.306
    - Areas temáticas: Cardiac & cardiovascular systems.
    - Contribución del doctorando: The idea of assessing ECG biomarkers beyond QT and its subintervals was proposed by Strauss and further elaborated by the student together with Johannesen. The design and planning of the study including software implementation and statistical analysis was carried out by the student. The student and Johannesen performed analysis of all ECGs. ECG analysis software was developed with help from Johannesen. QTGuard+ (T-wave flatness, asymmetry and presence of notch) algorithms were provided by GE Healthcare and integrated in ECGlib by the student with help from Johannesen. The idea of plotting QT vs. other ECG biomarkers to visualize the ECG signatures of drugs was proposed by the student. Crumb conducted the voltage clamp experiments. The student analyzed the patch clamp data, fit Emax models and computed IC50 curves. Finally, the manuscript was drafted by the student with input from supervisors and all co-authors. Journal correspondence was handled by the student and Strauss.

4. Vicente J, Johannesen L, et al. Sex differences in drug-induced changes in ventricular repolarization. *J Electrocardiol* 48(6):1081–1087, 2015

    - Factor the impacto: 1.361
    - Areas temáticas: Cardiac & cardiovascular systems.
    - Contribución del doctorando: The idea of conducting sex-specific analysis came out of discussions between the student and Strauss and further elaborated by the student with input from Johannesen. Analysis of the ECGs was carried out by the student together with Johannesen. The statistical analysis plan was planned and carried out by the student with input from Johannesen. The student presented the results at the annual International Society for Computerized Electrocardiology

(ISCE), where he received the "Best poster award" and was invited to submit a full manuscript to Journal of Electrocardiology. The manuscript was drafted by the student with input from supervisors and all co-authors. Journal correspondence was handled by the student.

5. Vicente J, Johannesen L, et al. ECG biomarkers for detection of drug-induced late sodium current block. *Manuscript* , 2015

   - Factor de impacto: borrador.
   - Areas temáticas: Cardiac & cardiovascular systems.
   - Contribución del doctorando: The idea of assessing which biomarker would add value to assessing QTc alone was proposed by Stockbridge and further elaborated in discussions between the student, Strauss and Johannesen. The design and planning of the study including software implementation and statistical analysis was carried out by the student. The student and Johannesen performed analysis of all ECGs. ECG analysis software was developed with help from Johannesen. QTGuard+ (T-wave flatness, asymmetry and presence of notch) algorithms were provided by GE Healthcare and integrated in ECGlib by the student with help from Johannesen. The idea of using a receiver operating characteristic (ROC)-area under the curve (AUC) analysis was proposed by Johannesen and implemented and assessed by the student. The idea of using C4.5 decision tree was proposed by Hosseini and implemented and assessed by the student. The manuscript included in this thesis was drafted by the student with input from supervisors and all co-authors.

In addition and to support the research studies of this thesis, the PhD student played a lead role on the design and development of new ECG analysis tools (ECGlib and ECGlab). These tools are described in Section 9.2.1. Briefly, ECGlib is a C++ library for processing ECGs. It implements standard ECG signal processing methods that allow for automatic adjudication of ECGs. Its performance is comparable to state-of-the-art methods. ECGlib has a modular design and can be extended through plugins. ECGlab is a user friendly, graphical user interface for assessing results from automated analysis of ECGs in research environments. It is built on top of ECGlib library and plugins and allows for fast on-screen computer-assisted semi-automatic review and adjudication of large numbers of ECGs. ECGlib and ECGlab were developed using open source tools and libraries such us Armadillo, Boost, Qt and Qwt.

The PhD student is working together with other ECGlib and ECGlab developers to make the these tools publicly available under an open source license.

Lastly, the idea of the two FDA-sponsored prospective clinical trials was proposed by Stockbridge and led later by Strauss, Johannesen and the student with input from Stockbridge and Mason. The student played a lead role in both prospective clinical trials. The student contributed to the studies design, protocol, site initiation visits, data transfer and quality control, as well as follow-up with the clinic and making the data available through the Telemetric and Holter ECG Warehouse (`http://thew-project.org`, databases E-OTH-12-5232-020 and E-HOL-12-0109-021).

Acknowledgments / Agradecimientos

This thesis embraces all the efforts that I put during the last years as an ORISE cardiovascular research fellow at the U.S. Food and Drug Administration and as a PhD student at University of Zaragoza. I would like to thank my supervisors, colleagues, collaborators and co-authors for their contributions to this project.

I would like to thank my co-supervisor and mentor at FDA, **Dr. David Strauss**. Dave, you are the best mentor I have ever had. Thanks for everything you taught me. Not only about cardiovascular and regulatory science, but also about how to communicate better, keep focus and make the best of myself.

A mi co-directora de tesis **Dra. Esther Pueyo**. Esther, gracias por tu apoyo a lo largo de este viaje, en especial por todas esas reuniones fuera de horarios habituales. Gracias por enseñarme a ser mejor ingeniero y científico. Ha sido un viaje fantástico.

To my colleague and friend **Lars Johannesen**. Lars, thanks for being there in all those *sprints*. I still do not know how, but we always managed to get things done. Thanks for your help with writing, and for keeping alive the engineer I have in me. It has been a lot of fun.

Thanks to all my colleagues at FDA also, in particular to **Loriano Galeotti**, for all your help when I first arrive at White Oak and for all the scientific discussions we had. Some were more fruitful than others, but all were fun. To **Robbert Zusterzeel**, for your help with medical concepts, letting me to borrow your *super-computer* and of course for all those rides to FDA campus. Lastly I want to thank Dr. **Norman Stockbridge** for all his contributions and help with the resarch projects of this thesis.

I would like to thank also all people I met along the road that brought me here. To **David Moret**, for bringing me back to research and for awakening the scientist I have in me. To **Pablo Laguna** for trusting me since the first day we met, to **Raquel Bailón** for introducing me to cardiovasular physiology and for her mentoring and support during my last masters degree. To **Juan Bolea**. Juan, thanks for your help and teaching about ECG delination and methods. It is always great to talk to you and laugh out loud. To **Arantxa Trigo**, thank you so much for all your help with the paperwork. To all other members of *BSICoS* group at University of Zaragoza that taugh me how to be a better scientist.

Gracias también a todos aquellos que conocí en mi etapa en Alborán Informática. En especial a *mis chichos* **David**, **Coscu**, **Sergio**, **Luis** y **Juan Diego**, por enseñarme a ser mejor ingeniero y mentor. A **Angel** y **María** por animarme a acabar el proyecto final de carrera tantas veces, y por tantos otros momentos y cosas.

A mis padres, **Pepe** y **Encarna**, por su amor y por todo lo que me han enseñado. A mi hermana **María** y a **Agus**, y a mis "*in laws*" **Pedro**, **Ofelia**, **Teresa** y **Dani** por estar siempre ahí, para lo que haga falta.

Ofelia, mi compañera de viaje. Gracias por todo, por creer en mí, apoyarme y sacar lo mejor de mí. Te quiero infinito!

José Vicente Ruiz
Washington, DC
Fall 2015

Abstract and conclusions

In the 1990s there was an increasing recognition that non-cardiac drugs could cause torsade de pointes (torsade), a potentially fatal ventricular arrhythmia that disproportionately affects women. Most drugs that cause torsade block the human *ether-à-go-go* related gene (hERG) potassium channel and prolong the heart rate corrected QT interval (QTc) on the electrocardiogram (ECG). This resulted in fourteen drugs removed from the market worldwide due to potential for QTc prolongation and/or torsade. In addition, the extreme focus on drug-induced effects on the QTc interval and hERG potassium channel has likely led to drugs being inappropriately dropped from development. For example, QTc prolonging drugs with minimal torsade risk like ranolazine or verapamil may have not reached the market under the current regulatory paradigm. The minimal risk for torsade with these drugs is likely because they block inward currents (e.g. L-type calcium with verapamil or late sodium with ranolazine) in addition to hERG.

Through use of novel ECG morphology biomarkers and computer simulations, this thesis assesses whether there are sex differences in drug-induced changes in ventricular repolarization that can explain sex differences in drug-induced proarrhythmic risk. Moreover, the main goal of this thesis is to identify ECG biomarkers that can be used to differentiate drug-induced multi-ion channel current effects of relevance for torsade risk.

The thesis is composed of Studies I - V. Through an analysis of baseline ECGs from 30 thorough QT studies, Study I shows that age and sex differences in QTc are due to differences in the heart rate corrected J-T_{peak} interval (J-T_{peak}c). *In silico* simulations suggest that these differences are likely due to testosterone effects on the L-type calcium current.

Study II presents a sex-specific analysis of intravenous quinidine-induced changes on ventricular repolarization. Results show that women are not more sensitive to quinidine-induced effects on QTc and T_{peak}-T_{end} than men. Moreover, sex differences previously reported in the literature on data in Study II were due to a delay between plasma drug concentration and ECG changes (hysteresis), which was present in men but not in women.

The next two studies present a comprehensive assessment of ECG morphology biomarkers in a randomized clinical trial of dofetilide, quinidine, ranolazine and verapamil. Study III shows that there is a strong exposure-response relationship between selective hERG potassium channel blocking drugs and T-wave morphology changes. Multichannel blocking drugs still have a exposure-response relationship with T-wave morphology, in some cases having greater T-wave morphology changes at equivalent

amounts of QTc prolongation compared with selective hERG potassium channel block. Sex-specific analysis (Study IV) shows no sex differences in QTc prolongation induced by dofetilide, quinidine and ranolazine. Moreover, no systematic sex differences of other drug-induced ECG biomarker changes are present. Results of these studies suggest that J-T_{peak}c is the only biomarker that provides independent information from QTc to differentiate multichannel blocking drugs from selective hERG potassium channel blocking drugs.

Study V extends Study III with an analysis of data from a prospective clinical trial of moxifloxacin, dofetilide and dofetilide combined with either mexiletine or lidocaine. This study shows that drug-induced ECG signatures of selective hERG potassium channel block (moxifloxacin, dofetilide) and multichannel block (dofetilide + mexiletine, dofetilide + lidocaine, ranolazine) are reproducible and consistent. Analysis ranking ECG biomarkers by their ability to detect presence of inward current block shows that J-T_{peak}c is the best of all studied ECG biomarkers for detecting late sodium current block.

The studies in this thesis suggest that an integrated assessment of J-T_{peak}c and QTc can differentiate multichannel block from selective hERG potassium channel block on the ECG. This is important because this type of assessment could enhance the current clinical paradigm of proarrhythmic assessment of drugs. Specifically, such integrated assessment may be able to differentiate between selective hERG potassium channel blocking drugs that prolong QTc and have high torsade risk (e.g. dofetilide) from multichannel blocking drugs that also prolong QTc but have minimal risk for torsade (e.g. ranolazine). In addition, sex-specific analysis suggests that higher torsade risk in women is not because women are more sensitive to drug-induced QTc prolongation. Future strategies to use the ECG to detect multi-ion channel effects should use J-T_{peak}c to detect the presence of late sodium current block.

Resumen y conclusiones

Durante la decada de los 90 hubo un reconocimiento cada vez mayor de que fármacos no cardíacos podían causar torsade de pointes (torsade), una arritmia ventricular potencialmente mortal y que mayoritariamente afecta a las mujeres. La mayoría de los fármacos que causan torsade bloquean el canal de potasio codificado por el *human ether-à-go-go related gen* (hERG) y prolongan el intervalo QT corregido respecto al ritmo cardíaco (QTc) en el electrocardiograma (ECG). Como consecuencia, catorce fármacos fueron retirados del mercado en todo el mundo debido a su potencial para prologar QTc y/or causar torsade. Por otra parte, el excesivo foco en el potencial de fármacos para prolongar el intervalo QTc y bloquear el canal de potasio codificado por hERG ha llevado a abortar el desarrollo de algunos fármacos, en algunos casos de forma inapropiada. Por ejemplo, fármacos que prolongan el intervalo QTc pero tienen un riesgo de torsade mínimo como la ranolazina o el verapamilo probablemente no habrían llegado al mercado bajo el paradigma regulatorio actual. El bajo riesgo de torsade de estos fármacos es probablemente porque, además de hERG, estos fármacos también bloquean corrientes entrantes (p.ej. la corriente de calcio de tipo L en el caso del verapamilo o la corriente final de sodio en el caso de la ranolazina).

Mediante el uso de nuevos biomarcadores electrocardiográficos basados en la morfología del ECG y simulaciones computacionales de la electrofisiología cardiaca, esta tesis evalúa si existen diferencias entre hombres y mujeres en los cambios inducidos por fármacos en la repolarización ventricular que puedan explicar diferencias entre sexos en el riesgo proarrítmico asociado a la acción de determinados fármacos. Es más, el objetivo principal de esta tesis es identificar biomarcadores electrocardiográficos que puedan ayudar a distinguir fármacos que afectan a múltiples canales iónicos, frente a los que afectan únicamente a canales codificados por hERG, con importancia desde el punto de vista del riesgo proarrítmico.

Esta tesis está compuesta por cinco estudios (Estudios I - V). Mediante un análisis de ECGs basales procedentes de 30 "*thorough QT studies*", el Estudio I demuestra que las differencias entre sexos y grupos de edad en QTc son debidos a diferencias en el intervalo J-T_{peak} (del final del complejo QRS al pico de la onda T) corregido respecto al ritmo cardíaco (J-T_{peak}c). Simulaciones *in silico* sugieren que estas diferencias pueden ser debido a los efectos de la testosterona en la corriente de calcio L-type.

El Estuio II presenta un análisis específico por sexos de los efectos causados por dosis intravenosas de quinidina en la repolarización ventricular. Los resultados muestran que las mujeres no son más sensibles que los hombres a la prolongación de los intervalos QTc o T_{peak}-T_{end} (intervalo del pico al final de la onda T) inducidos por la quinidina. Es más, en esta

tesis se prueba que las differencias por sexos reportadas previamente en la literatura usando datos del Estudio II eran debidas al retardo existente entre los niveles de concentración de quinidina en plasma y los cambios en el ECG (histéresis), que estaba presente en los hombres pero no en las mujeres.

Los dos estudios siguientes presentan un analysis amplio de biomarcadores morfológicos del ECG en un ensayo clinico aleatorizado de dofetilida, quinidina, ranolazina y verapamilo. El Estudio III demuestra que hay una fuerte relación entre la exposición a fármacos que bloquean de forma selectiva el canal de potasio codificado por hERG y los cambios asociados en la morfología de la onda T. Fármacos que afectan a multiples canales iónicos también tienen esta relación entre exposición al fármaco y cambios morfológicos en la onda T, en algunos casos causando cambios mayores en la morfología de la onda T asociados a la misma cantidad de prolongación del QTc que los fármacos que bloquean el canal de potasio codificado por hERG de forma selectiva. En el análisis por sexos presentado en el Estudio IV no se encontraron differencias entre hombres y mujeres en la prolongación del QTc inducida por dofetilida, quinidina o verapamilo. Es más, no se hallaron diferencias sistemáticas entre sexos en ninguno de los biomarcadores electrocardiográficos evaluados en este estudio. Los resultados sugieren que J-T_{peak}c es el único biomarcardor que proporciona información independiente del QTc que permite diferenciar entre fármacos que bloquean múltiples canales iónicos de aquellos que bloquean el canal de potasio codificado por hERG de forma selectiva.

El Estudio V extiende el Estudio III con el análisis de datos de un estudio clinico prospectivo de moxifloxacino, dofetilida y dofetilida combinada con mexiletina o lidocaina. Este estudio demuestra que las "firmas" electrocardiográficas asociadas con el bloqueo selectivo del canal de potasio codificado por hERG (moxifloxacino, dofetilida) y bloqueo multicanal (dofetilida + mexiletina, dofetilida + lidocaina, ranolazina) son reproducibles y consistentes. El análisis ordenando los biomarcadores electrocardiográficos por su habilidad para detectar la presencia de bloqueo de corrientes entrantes demuestra que el intervalo J-T_{peak}c es el mejor de todos los biomarcadores electrocardiográficos evaluados para detectar el bloqueo de la corriente final de sodio.

En su conjunto, los estudios de esta tesis sugieren que una evaluación integrada de los intervalos J-T_{peak}c y QTc en el ECG puede diferenciar entre fármacos que bloquean multiples canales iónicos y aquellos que bloquean el canal de potasio codificado por hERG de forma selectiva. Este tipo de evaluación es importante porque puede mejorar el actual paradigma clínico de evaluación del riesgo proarrítmico de fármacos. Específicamente, una evaluación integrada como la presentada en esta tesis podría diferenciar entre bloqueo selectivo del canal de potasio codificado

por hERG asociado con alto riesgo de torsade (p.ej. dofetilida) y bloqueo multicanal con mínimo riesgo de torsade (p.ej. ranolazina). Además, los análisis por sexos sugieren que el mayor riesgo de torsade inducido por fármacos en las mujeres no es debido a que las mujeres sean más sensibles a la prolongación del intervalo QT inducida por fármacos. Adicionalmente, esta tesis sugiere que J-T_{peak}c debería ser utilizado como biomarcador de presencia de bloqueo de la corriente final de sodio en futuras estrategias que traten de detectar bloqueo multicanal inducido por fármacos en el ECG.

Funding

This work was supported by U.S. Food and Drug Administration's Critical Path Initiative, U.S. Food and Drug Administration's Office of Women's Health and appointments to the Research Participation Program at the Center for Devices and Radiological Health and the Center for Drug Evaluation and Research administered by the Oak Ridge Institute for Science and Education through an inter-agency agreement between the U.S. Department of Energy and the U.S. Food and Drug Administration.

Disclaimer

The mention of commercial products, their sources, or their use in connection with material reported herein is not to be construed as either an actual or implied endorsement of such products by the U.S. Department of Health and Human Services.

Y busqué en el fondo del mar, en las montañas y en el fuego
la manera de hacer realidad mis sueños.
Encontré en el corazón el mapa de los sentimientos.
Ya lo ves, no estaba tan lejos.

Platero y Tú, Al Cantar

CHAPTER 1

Introduction

This thesis focuses on assessing whether the *electrocardiogram* (ECG) can be used to differentiate ion channel current effects induced by drugs that prolong ventricular repolarization. This is important because drugs that prolong repolarization may have different degrees of proarrhythmic risk depending on whether they block a specific ion channel (high risk) or multiple ion channel currents (low risk). More specifically, the main focus of this thesis is to assess which ECG biomarkers could enhance the current clinical evaluation of proarrhythmic potential of drugs, the so-called thorough QT study [1].

This introduction starts with an overview of the global regulatory response to the increasing rate of fatal arrhythmias caused by non-cardiac drugs in the 1990s. Following this overview, the introduction describes the relationship between multiple ion channel currents, long QT syndrome, the occurrence of ventricular arrhythmias and different ECG morphologies. The introduction continues describing novel ECG biomarkers and their ability to detect multi-ion channel effects. Next, sex differences and other potential mechanisms that could explain the higher risk for drug-induced arrhythmias in women are introduced. Finally, the introduction describes the thematic unity and outline of this thesis.

1.1 Assessing proarrhythmic potential of drugs: current regulatory paradigm

Fourteen drugs have been removed from the market worldwide because of their potential for *heart rate corrected QT interval* (QTc) prolongation and/or *torsade de pointes* (torsade) (Table 1.1) [2], a potentially fatal

Table 1.1: Drugs withdrawn from the market due to potential for QTc prolongation and/or torsade [2].

Drug	Year of withdrawal
Prenylamine	1988
Lidoflazine	1989
Terodiline	1991
Terfenadine	1998
Sertindole	1998
Astemizole	1999
Grepafloxacin	1999
Cisapride	2000
Droperidol	2001
Levacetylmethadol	2001
Dofetilide	2004
Thioridazine	2005
Clobutinol	2007
Dextropropoxyphene	2009

ventricular arrhythmia (Figure 1.1) [3]. In the 1990s, there was an increasing recognition that non-cardiac drugs could cause torsade. In response to this drug-induced torsade epidemic two guidances for industry were established: the *International Conference on Harmonisation of Technical Requirements for Registration of Pharmaceuticals for Human Use* (ICH) S7B [4] and the ICH E14 [1]. The ICH S7B recommends an *in vitro* assay to assess whether a compound and its metabolites block the *human ether-à-go-go related gene* (hERG) potassium channel.The ICH E14 guidance describes a specific clinical study, the so-called thorough QT study. The thorough QT study assesses whether the drug prolongs QTc in healthy subjects. More specifically, the guidance states that "the threshold level of regulatory concern [...] is around 5 ms as evidenced by an upper bound of the 95% confidence interval around the mean effect on QTc of 10 ms" [1]. In summary, the current regulatory paradigm requires all new drugs to be screened for their ability to block the hERG potassium channel and prolong QTc.

Since the implementation of ICH S7B and ICH E14 guidances in 2005, no new marketed drugs have been associated with torsade. Thus, this has been a successful strategy from a torsade risk management standpoint. On the other hand, the extreme focus on hERG and QTc has resulted in drugs being dropped from development, sometimes inappropriately [2]. This is because not all drugs that block the hERG potassium channel

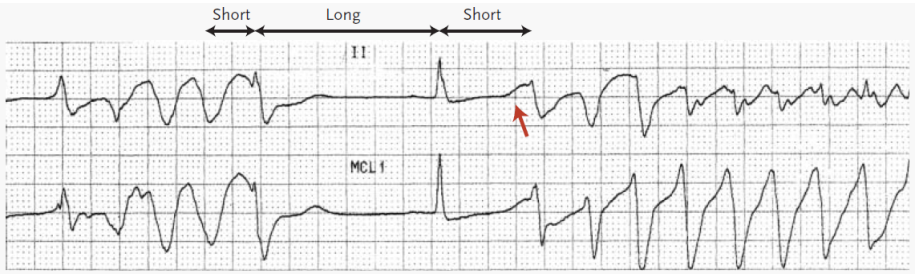

FIGURE 1.1: ECG showing torsade de pointes arrhythmia, which corresponds with the illusion of twisting of the QRS complexes around the isoelectric line following the short-long-short beats in this trace. Reproduced from Roden 2004 with permission [3].

or prolong QTc cause torsade. For example, there are marketed drugs like amiodarone [5], ranolazine [6] and verapamil [7] that block the hERG potassium channel and prolong QTc but have minimal risk for torsade because they block additional inward currents. Drugs like these may have not made it to the market under the current regulatory paradigm because pharmaceutical sponsors may have stopped the development of these drugs due to proarrhythmic potential concerns. Therefore, there is a need to improve the lack of specificity of the hERG assay and QTc prolongation for prediction of actual torsade risk.

1.2 Ion channel currents, long QT, torsade and T-wave morphology

There has been a regulatory focus on drug-induced QTc prolongation and hERG block because both are associated with an increased risk for torsade [3, 8]. The most common mechanism of drug-induced QTc prolongation is the block of the hERG potassium channel in the membrane of ventricular cells [9]. hERG potassium channel block reduces the *rapid delayed outward rectifier potassium current* (I_{Kr}). Reduction of I_{Kr} prolongs repolarization and may provide the necessary substrate for occurrence of *early afterdepolarizations* (EADs), which are the triggers for torsade (Figure 1.2) [10].

However, there are multiple ion channel currents in addition to I_{Kr} that regulate repolarization of ventricular cells in the heart (Figure 1.3) [11]. Non-clinical studies have demonstrated that block of inward current (*inward late sodium current* ($I_{Na,L}$) or *inward L-type calcium current* ($I_{Ca,L}$)) prevents the occurrence of EADs associated with drug-induced hERG potassium channel block [12, 13]. This explains why some QTc

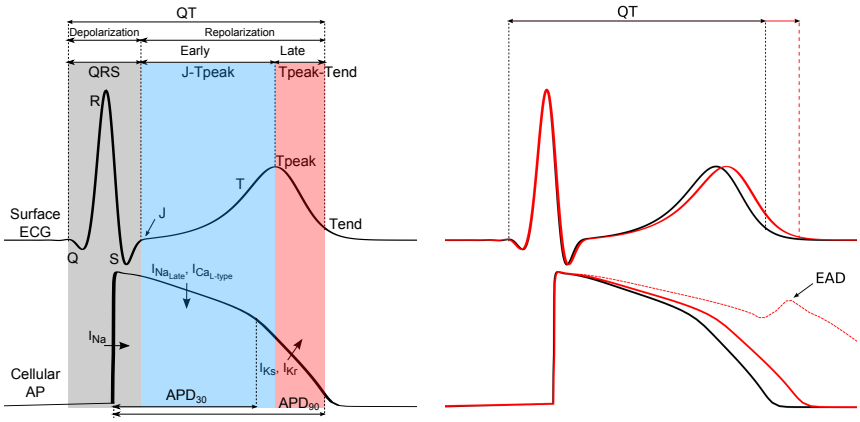

(a) The QT interval on the surface ECG reflects the entire ventricular electrical activity during depolarization (grey) and repolarization (blue and red). While early repolarization (blue) is mainly regulated by inward $I_{Ca,L}$ and $I_{Na,L}$ currents during the plateau phase of the ventricular action potential, late repolarization (red) is regulated by I_{Ks} and I_{Kr} currents.

(b) QT interval prolongation in the electrocardiogram resulting from ventricular action potential prolongation induced by reduced I_{Kr} (baseline black, prolongation red). Drug-induced hERG potassium channel block reduces the I_{Kr} current and provides the necessary substrate for occurrence of EADs (red dashed line in the action potential) which can trigger torsade (Figure 1.1).

Figure 1.2: Illustration of the relationship between the ECG (top traces) and a representative action potential of ventricular cells (bottom traces). AP, action potential; APD30, 30% of action potential duration; APD90, 90% of action potential duration; ECG, electrocardiogram; EAD, early after depolarization.

prolonging drugs that block inward currents in addition to the hERG potassium channel have minimal torsade risk (e.g. amiodarone[5], ranolazine[6] or verapamil[7]).

In addition, previous clinical studies have also demonstrated that $I_{Na,L}$ block (mexiletine) can mitigate QTc prolongation caused by strong hERG potassium channel block (quinidine) [14, 15, 16]. Moreover, recent clinical studies have shown that $I_{Na,L}$ block can reduce drug-induced QTc prolongation caused by hERG potassium channel block and mitigate recurrent torsade events caused by drug-induced long QT syndrome [17, 18]. Thus, detecting drug-induced inward current block on the ECG could help to better differentiate between low and high torsade risk drugs that prolong the QT interval.

There is more information beyond QT interval prolongation in the ECG that could inform about ion channel current disturbances of interest

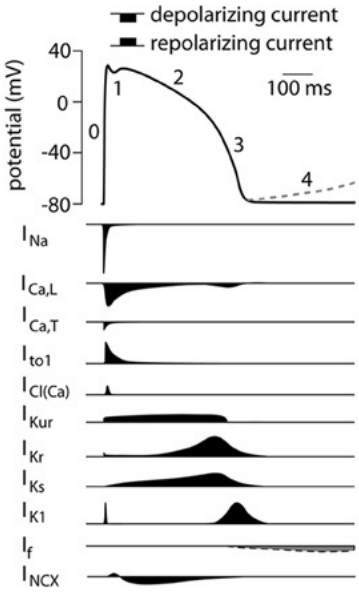

Figure 1.3: Ventricular cell action potential (top) as result of multiple ion channel currents (bottom traces) present in the membrane of cardiomyocytes. Reproduced from Hoekstkra et al 2012 with permission [11].

for proarrhythmic risk assessment. For example, genetic abnormalities in cardiac ion channels present in congenital long QT syndrome patients result in different ECG signatures depending on the individual ion channel currents affected [19]. More specifically, there are different T-wave patterns associated with the three major congenital long QT syndrome types (Figure 1.4) [20]. *Long QT syndrome type 1* (LQT1) patients have decreased *outward slow delayed rectifier potassium current* (I_{Ks}) and early onset broad-based T-waves. *Long QT syndrome type 2* (LQT2) patients have decreased I_{Kr} and low amplitude, bifid or notched T-waves. *Long QT syndrome type 3* (LQT3) patients have increased $I_{Na,L}$ and long isoelectric ST segment with late appearing, normal morphology T-waves.

1.3 Novel ECG biomarkers beyond QT

Recently, industry and academia have developed multiple ECG morphology algorithms in an attempt to go beyond QTc when identifying hERG potassium channel block on the surface ECG (Figure 1.5). For example, Andersen and colleagues developed an algorithm to quantify T-wave flatness, asymmetry and notching [21] associated with LQT2 [20]. T-wave morphology performed better than QTc assessment when separating LQT2 patients from normal healthy subjects [22]. Another example is the method developed by Couderc et al, which identifies repolarization changes associated with subtle hERG potassium channel block induced by moxifloxacin [23]. These ECG morphology biomarkers have been assessed and validated in a limited number of hERG potassium channel blocking

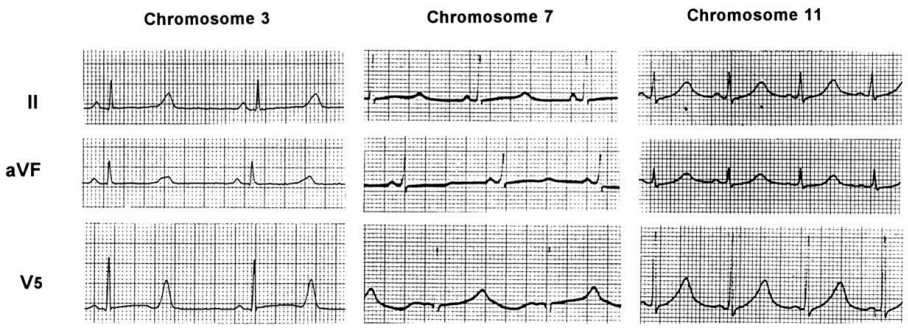

Figure 1.4: ECG traces from long QT syndrome patients. Chromosome 3 (LQT3, increased $I_{Na,L}$): long isoelectric ST segment with late appearing, normal morphology T-waves. Chromosome 7 (LQT2, reduced I_{Kr}): low amplitude, bifid or notched T-waves. Chromosome 11 (LQT1, decreased I_{Ks}): early onset broad-based T-waves. Reproduced from Moss et al 1995 with permission [20].

drugs [22, 23, 24]. Lastly, prior research has shown that vectorcardiographic measures of the relation between depolarization and repolarization vectors (QRS-T angle [25], ventricular gradient [26], and *total cosine R-to-T* (TCRT) [27]) can predict arrhythmic risk in some patient populations [27, 28, 29].

In addition to academia and industry, the *U.S. Food and Drug Administration* (FDA) has studied novel ECG biomarkers to identify drugs with multichannel block that have a balanced effect on outward (hERG potassium) and inward ($I_{Ca,L}$, $I_{Na,L}$) ion channel currents. In a retrospective study of 34 thorough QT studies together with computer simulations, it was demonstrated that the same amount of QT prolongation results in different "ECG signatures" depending on whether the drug is a selective hERG potassium channel or multichannel blocker (Figure 1.6) [31]. To confirm this observation, two prospective clinical trials were designed and conducted. The first clinical trial demonstrated that a separate analysis of the *heart rate corrected early repolarization interval* (J-T_{peak}c), measured from the end of the QRS to the peak of the T-wave, and the *late repolarization interval* (T_{peak}-T_{end}) can differentiate the effects of selective hERG potassium channel block (QTc prolongation by equal prolongation of J-T_{peak}c and T_{peak}-T_{end} intervals) from multichannel block (QTc prolongation preferentially caused by T_{peak}-T_{end} prolongation with minimal or no prolongation of J-T_{peak}c) (Figure 1.7) [32]. The second clinical trial demonstrated that $I_{Na,L}$ block with either mexiletine or lidocaine reduces drug-induced QTc prolongation caused by selective hERG potassium block (dofetilide). This QTc shortening occurs only in J-T_{peak}c, consistent with

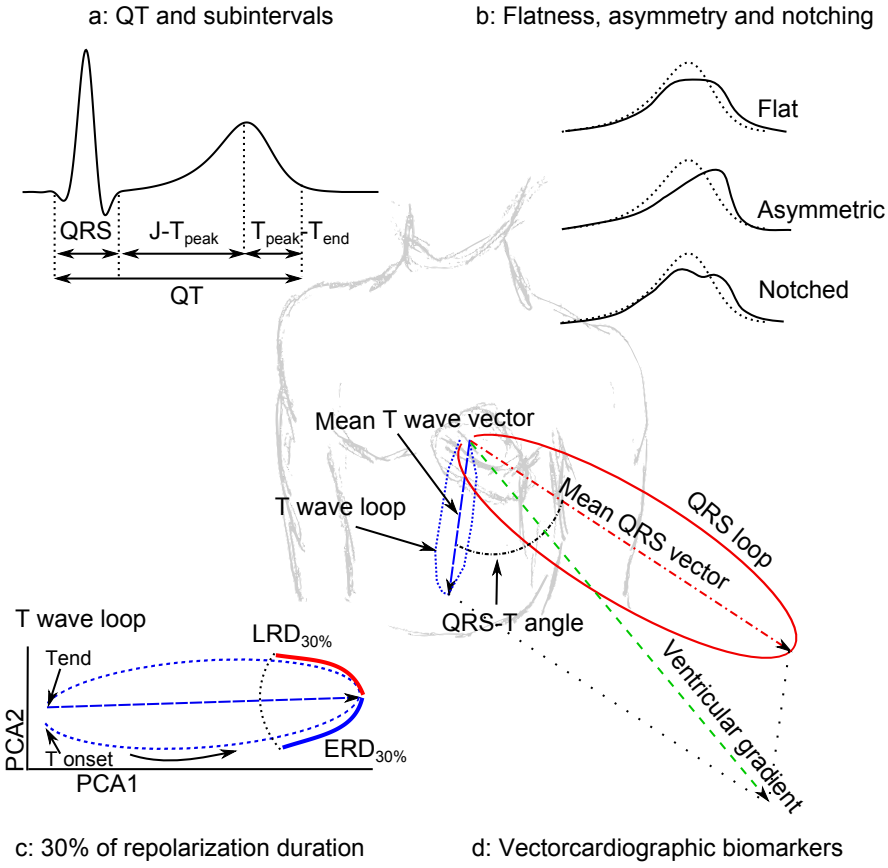

FIGURE 1.5: Illustration of novel ECG biomarkers assessed in this thesis: (a) QT and subintervals (QRS, J-T_{peak} and T_{peak}-T_{end}); (b) flat, asymmetric and notched T-waves (solid lines) vs. normal T-waves (dotted lines); (c) 30% of early ($ERD_{30\%}$) and late ($LRD_{30\%}$) repolarization duration in the preferential plane formed by the two-first Eigen leads from principal component analysis (PCA1 and PCA2); (d) other vectorcardiographic biomarkers (QRS-T angle, ventricular gradient and maximum magnitude of the T vector). Reproduced from Vicente et al 2015 with permission [30].

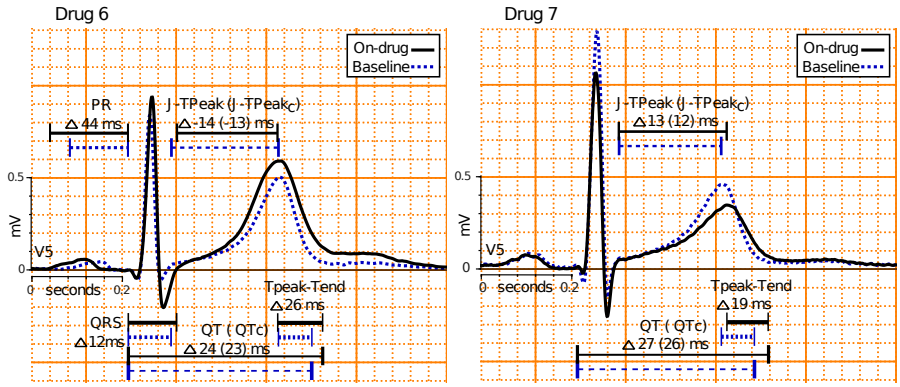

Figure 1.6: ECG signatures of multichannel blocker (Drug 6, left) and a selective hERG potassium channel blocker (Drug 7, right). ECGs on-drug (solid line) vs. baseline (dotted line). Reproduced from Johannesen et al 2014 with permission [31].

results from prior studies of individual drugs with multiple cardiac ion channel effects [17]. The studies presented in this thesis are an extension of this FDA research and include a comprehensive evaluation of the effect of selective hERG potassium channel block vs. multichannel block on multiple novel ECG morphology biomarkers described above (Figure 1.5).

1.4 Women at higher risk for drug-induced torsade de pointes

Women are at higher risk than men for drug-induced torsade [33, 34, 35]. The reason for this increased risk is not clear, and there are multiple factors that might make women more susceptible to drug-induced torsade. For example, women are often exposed to higher drug concentrations because they are on average smaller than men. Other contributing factors could be sex differences in the electrophysiology of the heart or differences in *absortion, distribution, metabolism and excretion* (ADME) of drugs that might make women more susceptible.

With regard to potential differences in cardiac electrophysiology, women have longer QTc than men [36] at baseline. This difference in QTc is not present in children and appears in puberty when men's QTc shortens by about 20 ms. Next, as men age their QTc values increase until the difference in QTc is no longer present in elderly populations [37]. These changes are inversely related to testosterone levels in men [38, 39].

Additional evidence suggests that testosterone levels play an impor-

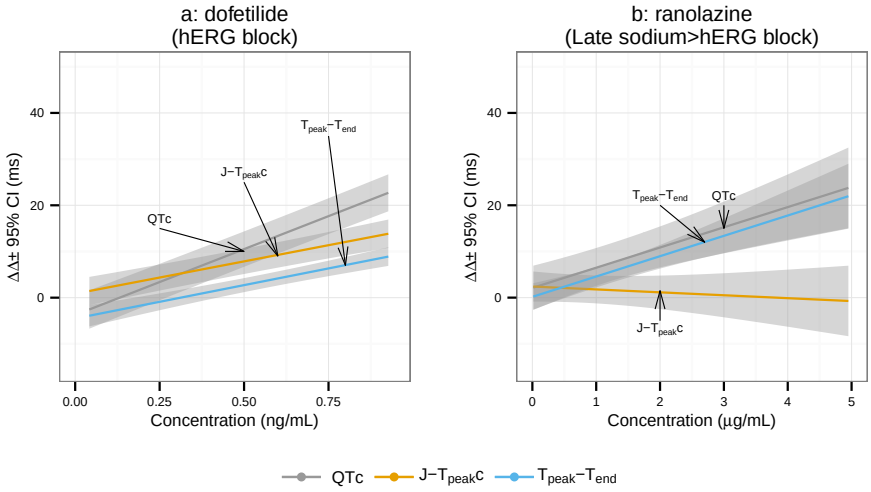

FIGURE 1.7: Drug-induced changes in J-T_{peak}c and T_{peak}-T_{end} for (a) a selective hERG potassium channel blocker (dofetilide) and (b) a hERG + late sodium current blocker (ranolazine). This zoomed plot of the concentrations of dofetilide that produce an amount of QTc prolongation comparable to that of ranolazine shows the ability of J-T_{peak}c and T_{peak}-T_{end} to detect multichannel block. Exposure response models showing predicted placebo corrected changes from baseline ($\Delta\Delta$, solid lines) together with 95% confidence intervals (gray). Reproduced from Johannesen et al 2014 with permission [32].

tant role in modulating cardiac repolarization in humans. Bidoggia et al [38] showed that subjects with high testosterone levels have shorter *early repolarization interval* (J-T_{peak}) (Figure 1.2a) than subjects with low testosterone levels. In addition, a non-clinical study in guinea pigs showed that testosterone shortens cardiac cell action potential duration by reducing $I_{Ca,L}$ and enhancing I_{Ks} [40]. In men, inhibition of $I_{Ca,L}$ by testosterone may prevent the occurrence of EADs [12, 13], which are the triggers for torsade. *In silico* studies also support that sex hormones are partly responsible for differences in cardiac repolarization [41, 42]. In addition, other age- and sex-specific factors (e.g. women having smaller ventricles than men [43]) and genomic-based differences [44] may contribute to sex differences in drug-induced torsade risk.

With regard to the sensitivity to drug-induced QTc prolongation, previous clinical studies in healthy subjects have shown that women are more sensitive to drug-induced QTc prolongation. In a study with *intravenous* (i.v.) quinidine, Benton and colleagues showed that quinidine caused greater QTc prolongation in women than in men at equivalent

serum concentrations [45]. Similar observations were made in subjects receiving i.v. ibutilide. In that study, women during the first half of the menstrual cycle had the greatest ibutilide-induced QTc prolongation compared to men and compared to the same group of women during the second half of the menstrual cycle, when progesterone levels peak [46]. A more recent study with oral rac-sotalol showed greater sensitivity in women compared to men for rac-sotalol-induced QTc prolongation [47]. These studies suggest that women are more susceptible to drug-induced QTc prolongation and that some sex hormones (e.g. testosterone and progesterone) may protect from drug-induced QTc prolongation and torsade risk.

In summary, women have generally smaller size and longer baseline QTc than men. This results in women being exposed to higher drug concentrations at a fixed dose, which may contribute to a higher risk for drug-induced torsade. However, there may be additional contributing factors (e.g. role of sex hormones) that might make women more susceptible to drug-induced QTc prolongation and torsade risk.

1.5 Thematic unity and outline of this thesis

The main theme of this thesis focuses on assessing whether novel ECG biomarkers can enhance the current paradigm of proarrhythmic assessment of drugs. More specifically, the main goals of this thesis are (i) to assess whether an integrated analysis of the ECG, including novel T-wave morphology biomarkers, can differentiate multichannel blocking drugs with minimal torsade risk from selective hERG potassium channel blocking drugs with high torsade risk; and (ii) to identify sex differences in ventricular repolarization that could provide additional insights about sex differences in drug-induced torsade risk. Together, this could lead to incorporation of automated analysis of T-wave morphology biomarkers into the current ECG analysis for proarrhythmic assessment of new drugs and a better understanding of sex-specific differences in drug-induced torsade risk.

To accomplish these goals, the research presented in this thesis was planned in five different studies. Study I (Chapter 2) investigates mechanisms of sex and age differences in ventricular repolarization. Study II (Chapter 3) assesses potential mechanisms of sex differences in ECG changes induced by quinidine, a potent hERG potassium channel blocking drug. Study III (Chapter 4) involves a comprehensive analysis of the effects of selective hERG potassium channel block vs. multichannel block on novel ECG morphology biomarkers. Study IV (Chapter 5) investigates sex differences in drug-induced changes in ECG biomarkers. Lastly, Study

V (Chapter 6) assesses the ability of multiple ECG morphology biomarkers to detect inward current block, which is important for assessing torsade risk.

The content of this thesis is organized as follows:

- **Introduction (Chapter 1):** The introduction gives a general overview of torsade risk, its relationship to drug-induced QTc prolongation and the current regulatory paradigm to assess drug-induced torsade risk. In addition, it describes different novel ECG biomarkers and outlines potential reasons why women are at higher risk for torsade than men. The introduction finishes with a description of the thematic unity and outline of this thesis.
- **Studies I-V (Chapters 2 - 6):** Manuscripts resulting from the research presented in this thesis.
- **Report - Memoria (Chapters 7 - 10):** This report summarizes:
  - the aims of the research presented in this thesis (Chapter 7),
  - the contributions of the PhD student to each study (Chapter 8),
  - the applied methodology (Chapter 9),
  - and the final conclusions (Chapter 10).

Studies I-V

CHAPTER 2

Study I

Mechanisms of sex and age differences in ventricular repolarization in humans

Vicente J, Johannesen L, et al. Mechanisms of sex and age differences in ventricular repolarization in humans. *Am Heart J* 168(5):749–756, 2014

Author's version. Published in Am Heart J, 2014 (http://dx.doi.org/10.1016/j.ahj.2014.07.010)

Mechanisms of Sex and Age Differences in Ventricular Repolarization in Humans

J Vicente[1,2], L Johannesen[1,3], L Galeotti[1], and DG Strauss[1,✉]

[1]*Office of Science and Engineering Laboratories, CDRH, US FDA, Silver Spring, MD, USA*
[2]*BSICoS Group, Aragón Institute for Engineering Research (I3A), IIS Aragón, University of Zaragoza, Spain*
[3]*Department of Clinical Physiology, Karolinska Institutet and Karolinska University Hospital, Stockholm, Sweden*

Abstract

Introduction: *QTc is shorter in postpubertal men than in women, however QTc lengthens as men age and testosterone levels decrease. Animal studies have demonstrated that testosterone decreases L-type calcium current and increases slow delayed rectifier potassium current (IKs); however it is not known how these contribute to QTc differences by sex and age in humans. We separately analyzed early versus late repolarization duration and performed simulations of the effect of testosterone on the ECG to examine the mechanism of sex and age differences in QTc in humans.* ***Methods:*** *12-lead ECGs from 2,235 healthy subjects (41% women) in Thorough QT studies were analyzed to characterize sex- and age-dependent differences in depolarization (QRS) early repolarization (J-Tpeak) and late repolarization (Tpeak-Tend). In addition, we simulated the effects of testosterone on calcium current, IKs and surface ECG intervals.* ***Results:*** *QTc was shorter in men than in women (394 ± 16 vs. 408 ± 15 ms, p<0.001), which was due to shorter early repolarization (213 ± 16 vs. 242 ± 16 ms, p<0.001), as men had longer depolarization (94 ± 7 vs. 89 ± 7 ms, p<0.001) and longer late repolarization (87 ± 10 vs. 78 ± 9 ms, p<0.001). Sex difference in QTc decreased with age and was due to changes in early repolarization. Simulations showed that the early repolarization changes were most influenced by testosterone's effect on calcium current.* ***Conclusions:*** *Shorter QTc in men compared to women is explained by shorter early repolarization, and this difference decreases with age. These sex and age differences in repolarization appear to be caused by testosterone effects on calcium current.*

Introduction

Women are at higher risk than men for the ventricular arrhythmia torsade de pointes [1, 2]. The reason for the increased risk is not clear, but sex differences in the electrophysiology of the heart might make women more susceptible to torsade. Women have a longer heart rate corrected QT interval (QTc) than men [3]. After puberty, QTc decreases in men resulting in a sex difference in QTc [4]. Subsequently, male QTc values increase as men age and elderly men and women have similar QTc values again. These changes are inversely related to testosterone levels in men [5, 6].

Testosterone has been shown to shorten cardiac cell action potential duration in guinea pigs by inhibiting L-type Calcium current (ICaL; an inward depolarizing current) and enhancing the slow delayed rectifier potassium current (IKs; an outward repolarizing current) [7]. However, significant differences in ion channel expression between species exist [8] and it is unclear what the primary mechanism is that contributes to sex and age differences in QTc in humans.

Through analysis of preclinical and clinical data from 34 Thorough QT studies [9] submitted to FDA, along with computer simulations, we demonstrated recently that drug-induced multi-ion channel block can be differentiated on the ECG [10]. One observation was that blocking ICaL primarily shortens early repolarization (J-Tpeak). In the present study, we use data from Thorough QT studies to characterize sex- and age-dependent differences in depolarization (QRS), early repolarization (J-Tpeak) and late repolarization (Tpeak-Tend) to elucidate the mechanisms for sex and age differences in QTc. In addition, we simulate the effect of decreasing testosterone levels on individual ion channel currents and early versus late repolarization on the ECG in order to understand the mechanism behind sex and age differences in ventricular repolarization in humans.

Methods

This study was approved by the Research Involving Human Subjects Committee of the U.S. Food and Drug Administration. For each of the individual clinical studies included in this analysis, the studies were approved by the local institutional review boards and all subjects gave informed consent. This project was supported in part by FDA's Critical Path Initiative, FDA's Office of Women's Health, and appointments to the Research Participation Program at the

✉David G. Strauss, MD, PhD. U.S. Food and Drug Administration. 10903 New Hampshire Avenue, WO62-1126. Silver Spring, MD, 20993, USA. E-mail: david.strauss@fda.hhs.gov. Telephone: 301-796-6323 - Fax: 301-796-9927

Author's version. Published in Am Heart J, 2014 (http://dx.doi.org/10.1016/j.ahj.2014.07.010)

Center for Devices and Radiological Health administered by the Oak Ridge Institute for Science and Education through an interagency agreement between the U.S. Department of Energy and the U.S. Food and Drug Administration. The authors are solely responsible for the design and conduct of this study, all study analyses, the drafting and editing of the paper and its final contents.

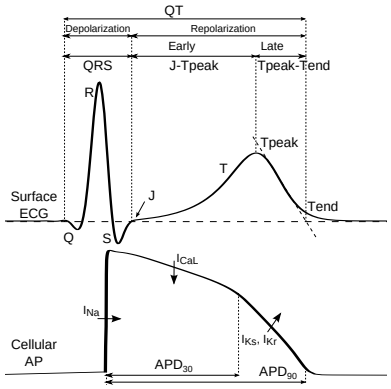

Figure 1: The QT interval of the surface ECG reflects the entire ventricular electrical activity during depolarization and repolarization. Figure illustrates the relationship between a representative ventricular action potential and the ECG. While early repolarization is mainly regulated by the inward L-type calcium current (ICaL) during the plateau phase of the ventricular action potential, late repolarization is regulated by outward potassium currents (IKs and hERG potassium current [IKr]). This is a simplified figure for illustration purposes only, and additional overlapping ion currents contribute to the different phases and morphology of the cellular action potential.

ECG Analysis

We analyzed resting 12-lead ECG recordings from 2,235 healthy subjects aged 18-78 years from 30 Thorough QT studies. Inclusion criteria for a typical Thorough QT study include healthy men or women without any clinically significant abnormalities, taking no medication (except oral contraceptives) and, for women, not to be pregnant or lactating before enrollment. Exclusion criteria include use of drugs, tobacco products or alcohol consumption, as well as ECG thresholds such as QTc >450ms for men and >470ms for women, PR >220ms, QRS >110ms and other cardiovascular abnormalities. Other inclusion and exclusion criteria limited weight, body mass index and vital signs measurements to ensure that all included subjects were considered healthy when enrolled in the study.

Every study protocol specified a set of time points at which multiple 10 second ECG recordings (ECG replicates) were extracted and individual cardiac beats were either manually or semi-automatically annotated by the sponsor ECG core laboratories. Information and details on the consistency of the quality of ECGs in Thorough QT studies has been described previously [11]. Subsequently, we used the same preprocessing and measurement methodology as described previously [10]. Briefly, ECGs with missing leads or excessive noise were excluded. The sponsors' provided ECG measurements were projected onto a median QRST waveform (or cardiac beat, Figure 1). Then, in the median cardiac beat, the peak of the T-wave was located automatically using the vector magnitude lead (from the vectorcardiogram constructed using Guldenring's transform [12]). Lastly, we computed early repolarization (sponsor provided QRSoffset [J point] to Tpeak) and late repolarization durations (Tpeak to sponsor provided T-wave offset [Tend]) in addition to sponsor provided QRS and QT. We computed the mean values of each ECG measurement for each time-point from the 24,345 analyzed ECG replicates. Finally, the average daily value for every single ECG biomarker was computed for each of the 2,235 subjects.

The primary analysis was performed with QTc calculated with Fridericia's [13] (QTcF) correction formula, however QTc with Bazett's [3] is also reported. The J-Tpeak interval was corrected for heart rate using a previously published correction (J-Tpeakc = J-Tpeak/RR0.58 with RR in seconds).10 Although Tpeak-Tend has been shown to be rate dependent [14], in this study we did not correct for heart rate because prior analysis demonstrated that Tpeak-Tend has minimal heart rate dependency within the limited range of heart rates included in this study where all ECGs were recorded with subjects in the resting supine state [10, 14].

Simulations of the Effect of Testosterone on the ECG

In order to study the relationship between the effects of testosterone on ICaL and IKs, along with early (J-Tpeak) and late repolarization (Tpeak-Tend) on the human surface ECG, we combined the O'Hara-Rudy ventricular cell model [15] with the van Oosteron and Oostendorp action potential-to-body surface ECG model (ECGSIM) [16], as described in a prior study [10]. To obtain approximate steady state behavior, the ventricular cell model was paced at 1 Hz for 1000 cycles [15]. The testosterone effects on ICaL and IKs were modelled by multiplying their conductance in the O'Hara-Rudy model by the corresponding scaling factors previously reported in isolated guinea pig ventricular myocytes [7]. Simulations were performed for testosterone's effects on ICaL block and IKs enhancement alone and in combination. Action potential duration was measured at 30% (APD30), 60% (APD60) and 90% (APD90) of repolarization in the simulated action potential for both endocardial

Author's version. Published in Am Heart J, 2014 (http://dx.doi.org/10.1016/j.ahj.2014.07.010)

and epicardial cells. To compute the effects of decreasing levels of testosterone as men age, we selected the highest testosterone concentration (20 years old male group) as the baseline, and then computed the relative action potential duration changes from this baseline as testosterone levels in men decrease as they age. In addition, we simulated the average value of testosterone in women. These testosterone values were taken from prior reports in the literature [17, 18].

ECGSIM is based on the equivalent double layer source model [16]. We used ECGSIM's 22 years old healthy male [19] example case as baseline and simulated ECGs for different testosterone levels by changing the repolarization time and slope in all endocardial and epicardial action potentials to match the corresponding relative changes in APD30, APD60 and APD90 measured in the O'Hara-Rudy model. Simulated ECGs were semi-automatically analyzed with a wavelet-based delineation algorithm [20, 21] in ECGlab [22].

Statistical analysis

Unpaired Student's t-tests were computed to assess differences in each ECG measurement by sex in the overall population and between age groups. We used a linear model for each sex to assess the effects of age on the ECG parameters separately in men and women. An additional linear model with sex and age as covariates and an interaction term between them was used to assess whether the age-ECG parameter relationship was different between men and women. P-values <0.05 were considered statistically significant. All statistical analysis was performed using R version 2.15.3 (Vienna, Austria) [23].

Results

Women represented 41% of the 2,235 subjects in the study population. Table I summarizes the population characteristics and the ECG measurements by sex for the whole population as well as for different age groups by decade.

In the overall population, QTc was shorter in men than in women (QTcF: [mean $\pm$ standard deviation] 394 $\pm$ 16 vs. 408 $\pm$ 15 ms, p<0.001). QTc increased more with age in men (QTcF: 2.7 ms per decade 95% confidence interval [CI]: 1.8 to 3.6 ms per decade, p<0.001) than in women (QTcF: 1.1 [0.2 to 1.9] ms per decade, p=0.015) (interaction QTcF: p=0.012), which resulted in a decreasing QTc difference between sexes as age increased (Table I and Figure 2a).

When dividing the QTc into its subintervals, depolarization (QRS duration) was 5 ms longer in men than in women (94 $\pm$ 8 vs. 89 $\pm$ 7 ms, p<0.001). A small decrease in QRS duration was observed with age in both men (-0.4 [-0.9 to 0.0] ms per decade, p=0.035) and women (-0.7 [-1.1 to -0.3] ms per decade, p=0.001). There was no significant difference in the age-QRS relationship between men and women (interaction p=0.48, Figure 2b). Early repolarization duration, measured as the heart rate corrected J-Tpeak interval (J- Tpeakc), was 29 ms shorter in men than in women (213 $\pm$ 16 vs. 242 $\pm$ 16 ms, p<0.001) and prolonged with age more in men (3.4 [2.5 to 4.3] ms per decade, p<0.001) than in women (1.4 [0.5 to 2.3] ms per decade, p=0.002) (interaction p=0.002). Consequently, the difference in early repolarization between men and women diminished with age (Table I and Figure 2c). Late repolarization duration, measured as Tpeak -Tend, was 9 ms longer in men than in women (87 $\pm$ 10 ms vs. 78 $\pm$ 9 ms, p<0.001). There was no significant relationship between age and late repolarization (Tpeak -Tend) in either men (p=0.30) or women (p=0.18) (Figure 2d).

Testosterone Induced-Effect Simulations

Decreasing levels of testosterone as men age resulted in action potential prolongation (endocardial cells: Figure 3A; epicardial cells: supplementary Figure S.1A) that was due to testosterone's effects on ICaL, but not on IKs (endocardial cells: Figure 3C; epicardial cells: supplementary Figure S.1B). This action potential duration prolongation was entirely due to prolongation of early repolarization (APD30), as there was no additional prolongation in APD90 compared to APD30 (Figure 3A, supplementary Figure S.1A). On the ECG, decreased testosterone levels prolonged early repolarization (J-Tpeak), with no additional effect on total QT (Figure 3B). These age-related changes in early repolarization were entirely due to testosterone effect's on ICaL (Figure 3D).

For women, the simulated level of testosterone was 1.1 nM, compared to a range of 14.2-22.5 nM in men. This lower level of testosterone caused an increased action potential duration (endocardial cells: Figure 3A; epicardial cells: supplementary Figure S.1A) due to testosterone's effects on both ICaL and IKs (endocardial cells: Figure 3C; epicardial cells: supplementary Figure S.1B), however ICaL had a larger effect than IKs. Similar to the clinical ECG data, the shorter QT in men compared to women was due to men having shorter early repolarization duration (J-Tpeak) (Figure 3B).

Discussion

This study demonstrated that in healthy adult subjects at rest, shorter QTc in men than in women is entirely explained by shorter early repolarization, and that this difference diminishes with increasing age. Simulations of testosterone's effects on ICaL and IKs confirmed this finding and revealed that testosterone's effects on ICaL play a larger role than its effects on IKs in shortening early repolarization. In the context of drug-induced arrhythmias, the decreased ICaL from testosterone may lower risk of torsade de pointes by

Author's version. Published in Am Heart J, 2014 (http://dx.doi.org/10.1016/j.ahj.2014.07.010)

Table I: Population summary and ECG measurements.

	Age group											
	All		20s		30s		40s		50s		60+	
	Men	Women	Men	Women	Men	Women	Men	Women	Men	Women	Men	Women
n	1322	913	610	402	385	231	254	203	62	58	11	19
Age (years)	32 ± 10	34 ± 11	24 ± 3	24 ± 3	34 ± 3	35 ± 3	44 ± 3	44 ± 3	53 ± 2	53 ± 2	65 ± 4	66 ± 6
QTcF (ms)	394 ± 16	408 ± 15*	392 ± 17	408 ± 15*	393 ± 15	407 ± 15*	397 ± 15	410 ± 14*	401 ± 14	411 ± 14*	409 ± 19	414 ± 16§
QTcB (ms)	395 ± 17	415 ± 16*	392 ± 17	408 ± 15*	395 ± 15	415 ± 16*	399 ± 17	415 ± 15*	402 ± 14	417 ± 16*	406 ± 23	416 ± 18‡
QRS (ms)	94 ± 8	89 ± 7*	95 ± 8	89 ± 7*	93 ± 7	88 ± 7*	93 ± 7	88 ± 8*	94 ± 8	88 ± 6*	96 ± 10	87 ± 7†
J-Tpeakc (ms)	213 ± 16	242 ± 16*	210 ± 17	241 ± 16*	213 ± 15	241 ± 16*	217 ± 15	243 ± 14*	219 ± 16	246 ± 16*	225 ± 19	244 ± 16†
Tpeak-Tend(ms)	87 ± 10	78 ± 9*	87 ± 10	78 ± 9*	87 ± 10	78 ± 8*	87 ± 10	79 ± 9*	87 ± 9	78 ± 10*	89 ± 5	84 ± 11‖

Results are presented as mean ± standard deviation. QTcB (QTc Bazett), QTcF (QTc Fridericia). Differences in ECG measurements between men and women within group. p<0.001 (*); p<0.05 (†); p=0.209 (‡); p= 0.419 (§); p= 0.105 (‖)

preventing early after depolarizations [24, 25], which are the trigger for initiating torsade de pointes. This deserves further study. While testosterone's effects on IKs do not seem to play a large role in regulating QTc at rest, IKs may have a greater effect in the presence of sympathetic stimulation [26, 27], which was not investigated in this study.

Prior Clinical Studies

Although there are other studies reporting different age- and sex-specific ECG measurements [4, 28], this is the first study reporting sex- and age-specific measurements for all the QT subintervals in healthy subjects [4, 14, 28, 29, 30, 31]. Our results regarding QTc measurements are in agreement with previous studies [4, 28, 29, 30, 31] and showed that men above the age of 18 have shorter QTc than women do and that this sex difference decreases with age. However, the age at which the QTc sex differences disappear is different in this study compared to that previously reported by Rautarhaju et al. [4]. While they reported that the sex differences in QTc were no longer present in subjects older than 50 years of age, sex differences in QTc were still present at such age in our study's population. When dividing by decade, the QTc difference trended to disappear in subjects above 60 years of age (supplementary Figure S.2). The difference in the age at which sex differences in QTc disappear can be due to multiple factors such as the different heart rate correction method (individual-subject correction vs. Fridericia), limited sample size of subjects aged above 60 or other differences in population characteristics.

When looking at the QTc subintervals, despite men having longer depolarization (QRS) and longer late repolarization (Tpeak-Tend) phases compared to women, our results showed that the shorter QTc in men was completely explained by men having shorter early repolarization (J-Tpeakc) than women do. Previous studies have also reported that men have longer QRS duration [4, 28, 29], which is likely due to men having larger hearts that take longer to depolarize [32]. Previous studies of sex differences in Tpeak-Tend are inconclusive [14, 30, 31], and our results are in concordance with those reporting that men have longer late repolarization than women at resting heart rates. Our results showed shorter J-Tpeakc in men than in women, and these findings are concordant with results from previous studies [30, 31]. This study demonstrated a weak relationship between age and QRS, no age related changes in Tpeak-Tend and that age related J- Tpeakc prolongation fully explains QTc prolongation with age in both men and women.

Mechanisms for Sex and Age Differences in QT

In animal studies, testosterone has been shown to decrease ICaL and enhance IKs [7]. Our simulations of testosterone-induced effects showed that testosterone's effects on both ICaL and IKs contributed to sex differences in early repolarization. In ventricular cells, our results were in concordance with previous simulations of sex-specific and testosterone-induced effects studies [27, 33]. Specifically, higher levels of testosterone in men compared to women resulted in men having shorter action potential duration, primarily caused by APD30 shortening. Simulations of body surface ECGs were in concordance with the clinical data and showed that men's shorter QT was fully explained by men having shorter early repolarization (J-Tpeakc) compared to women. When assessing age-related changes in men, simulations of age-group-matched levels of testosterone in men showed early repolarization prolongation as testosterone levels decreased with age. This prolongation was entirely due to the effect of testosterone on ICaL. These simulation results suggest that testosterone's effects on early repolarization play an important role in the sex difference in QTc observed in the clinical data.

While it is known that sympathetic activity affects how ICaL and IKs regulate the action potential duration, there is a lack of preclinical data on testosterone's effects on ICaL and IKs under sympathetic stimulation [26, 27]. All the ECGs in this study were acquired from healthy subjects in a controlled and quiet environment after a resting period in supine position, which minimizes the amount of

Author's version. Published in Am Heart J, 2014 (http://dx.doi.org/10.1016/j.ahj.2014.07.010)

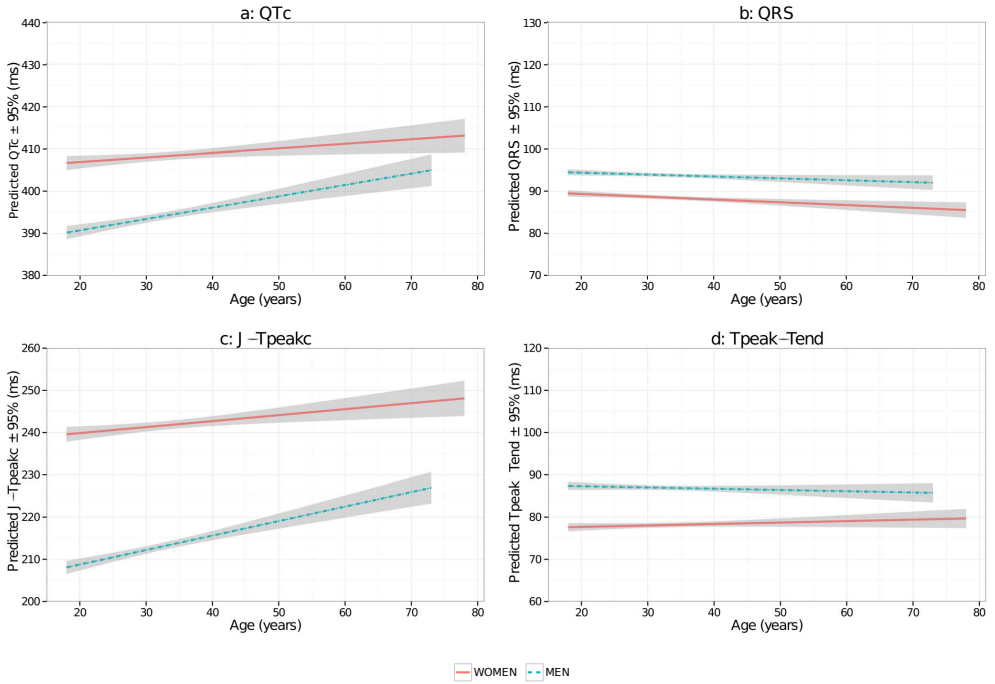

Figure 2: Linear model predictions for men (dashed lines) and women (solid lines) and 95% confidence intervals (gray area) of changes in QTcF (a), QRS (b), J-Tpeakc (c) and Tpeak-Tend (d) with age by sex. Vertical axes are scaled to the same range to facilitate visual comparison.

sympathetic activation. However, the lack of sympathetic activation in the computational models might result in an underestimated effect of ICaL and IKs in our simulations [27]. These potential underestimated effects may contribute to the differences in the magnitude of simulated changes when compared to the clinical data.

Testosterone-induced inhibition of ICaL may provide a protective effect in men by preventing the occurrence of early afterdepolarizations, which can initiate torsade de pointes [24, 25]. Furthermore, testosterone's effects on both ICaL and IKs might contribute to an increased "repolarization reserve" [6, 34, 35] in men. When introducing "repolarization reserve", Roden et al. [34] proposed that, in normal hearts, there are redundant mechanisms to accomplish normal repolarization. Thus, testosterone-induced IKs enhancement might provide the necessary redundancy to counteract the increasing torsade risk resulting from drug-induced hERG potassium current (IKr) block. This requires further investigation.

While this study focused on the potential relationship between testosterone and shortened early repolarization time (J-Tpeak), a separate recent study found a relationship between testosterone levels and ST-J elevation in leads other than V1-V3 ("early repolarization pattern") [36]. The relationship between testosterone, early repolarization duration and early repolarization pattern deserve further study.

Limitations

This was a cross-sectional study, which included same day baseline ECG recordings per subject, thus within-subject changes over time could not be assessed. However, it represents a clear snapshot of the sex and age normal limits of the studied ECG intervals. In addition, children were not included in this study and the number of subjects 60 years or older is limited. There is high variability (i.e. >10% within each age group) in the average testosterone levels in men reported in the literature [17, 37, 38]. Thus, although overall trends might be similar, quantitative results may vary depending on the average values selected for characterization of each age group of men. Finally, other age-specific, sex-

Author's version. Published in Am Heart J, 2014 (http://dx.doi.org/10.1016/j.ahj.2014.07.010)

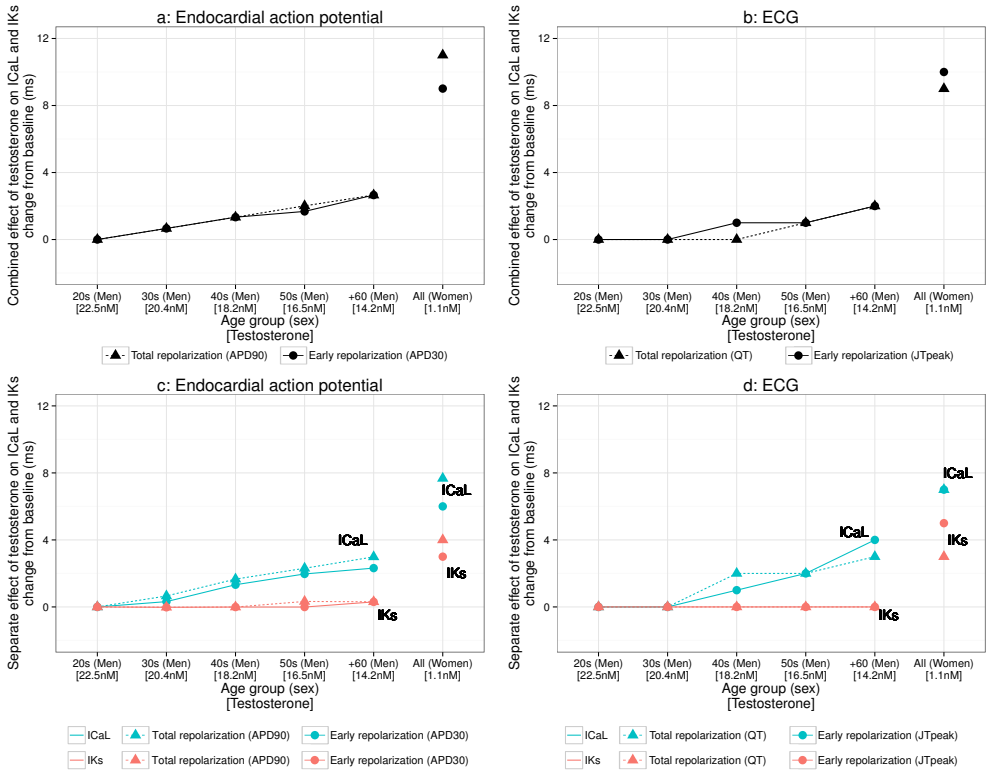

Figure 3: Combined effects of testosterone on total (triangles) and early (circles) repolarization on (a) endocardial action potential and (b) surface ECG in different age groups in men and in all women. Separate effects of testosterone on ICaL (blue) and IKs (red) and their contribution to total (triangles) and early (circles) repolarization on (c) endocardial action potential and (d) surface ECG. Changes in milliseconds from reference group (men in their 20s). Horizontal axis labels show each group's mean testosterone level from literature [17, 18].

specific (e.g. , women having smaller ventricles compared to men [32]) and genomic-based differences (e.g. differences in the expression of genes encoding key cardiac ion channels [27]) may also contribute to the observed differences in the clinical data.

Conclusions

In healthy adult subjects at rest, shorter QTc in men than women is due to shorter early repolarization (J-Tpeakc), and these differences diminish with increasing age because of a greater increase in early repolarization in men. Simulations suggested that the primary reason for lengthening QTc as men age (and testosterone levels decrease) is due to testosterone's effects on ICaL. With the larger difference in testosterone levels between women and men, testosterone's effects on IKs also contribute to differences in QTc, although the effect of ICaL is still larger. Further research should investigate how these findings translate to torsade de pointes risk, including under sympathetic stimulation which can increase the role of IKs.

Disclosures

The authors have no conflicts of interest to report.

References

[1] Makkar RR, Fromm BS, et al. Female gender as a risk factor for torsades de pointes associated with cardio-

Author's version. Published in Am Heart J, 2014 (http://dx.doi.org/10.1016/j.ahj.2014.07.010)

vascular drugs. *JAMA* 270(21):2590–7, 1993.

[2] Fung M, Hsiao-hui Wu H, et al. Evaluation of the profile of patients with qtc prolongation in spontaneous adverse event reporting over the past three decades—1969-1998. *Pharmacoepidemiol Drug Saf* 9(suppl 1):S24–5, 2000.

[3] Bazett HC. An analysis of the time-relations of electrocardiograms. *Heart* 7:353–370, 1920.

[4] Rautaharju Pm Fau Zhou SH, Zhou Sh Fau Wong S, et al. Sex differences in the evolution of the electrocardiographic qt interval with age. *Can J Cardiol* 8(7):690–5, 1992.

[5] Bidoggia H, Maciel JP, et al. Sex differences on the electrocardiographic pattern of cardiac repolarization: Possible role of testosterone. *Am Heart J* 140(4):678–683, 2000.

[6] Jonsson M, Vos M, et al. Gender disparity in cardiac electrophysiology: implications for cardiac safety pharmacology. *Pharmacol Ther* 127(1):9–18, 2010.

[7] Bai CX, Kurokawa J, et al. Nontranscriptional regulation of cardiac repolarization currents by testosterone. *Circulation* 112(12):1701–1710, 2005.

[8] Schram G, Pourrier M, et al. Differential distribution of cardiac ion channel expression as a basis for regional specialization in electrical function. *Circ Res* 90(9):939–950, 2002.

[9] ICH. Guidance for industry e14 clinical evaluation of qt/qtc interval prolongation and proarrhythmic potential for non-antiarrhythmic drugs, 2005. URL `http://www.fda.gov/downloads/RegulatoryInformation/Guidances/ucm129357.pdf`.

[10] Johannesen L, Vicente J, et al. Improving the assessment of heart toxicity for all new drugs through translational regulatory science. *Clin Pharmacol Ther* (95):501–508, 2014.

[11] Johannesen L, Garnett C, and Malik M. Electrocardiographic data quality in thorough qt/qtc studies. *Drug Saf* 37(3):191–197, 2014.

[12] Guldenring D, Finlay D, et al. Transformation of the mason-likar 12-lead electrocardiogram to the frank vectorcardiogram. In *Conf Proc IEEE Eng Med Biol Soc*, 677–680. IEEE.

[13] Fridericia LS. Die systolendauer im elektrokardiogramm bei normalen menschen und bei herzkranken. *Acta Med Scand* 53(1):469–486, 1920.

[14] Smetana P, Batchvarov V, et al. Sex differences in the rate dependence of the t wave descending limb. *Cardiovasc Res* 58(3):549–554, 2003.

[15] O'Hara T, Virag L, et al. Simulation of the undiseased human cardiac ventricular action potential: model formulation and experimental validation. *PLoS Comput Biol* 7(5):e1002061, 2011.

[16] Oosterom Av and Oostendorp TF. Ecgsim: an interactive tool for studying the genesis of qrst waveforms. *Heart* 90(2):165–168, 2004.

[17] Leifke E, Gorenoi V, et al. Age-related changes of serum sex hormones, insulin-like growth factor-1 and sex-hormone binding globulin levels in men: cross-sectional data from a healthy male cohort. *Clin Endocrinol (Oxf)* 53(6):689–695, 2000.

[18] Rodriguez I, Kilborn MJ, et al. Drug-induced qt prolongation in women during the menstrual cycle. *JAMA* 285(10):1322–6, 2001.

[19] van Dam PM, Oostendorp TF, and van Oosterom A. Ecgsim: Interactive simulation of the ecg for teaching and research purposes. In *Comput Cardiol*, 841–844. IEEE.

[20] Martínez J, Almeida R, et al. A wavelet-based ecg delineator: evaluation on standard databases. *IEEE Trans Biomed Eng* 51(4):570 –581, 2004.

[21] Johannesen L, Vicente J, et al. Ecglib: Library for processing electrocardiograms. In *Comput Cardiol*, 951–954. IEEE.

[22] Vicente J, Johannesen L, et al. Ecglab: User friendly ecg/vcg analysis tool for research environments. In *Comput Cardiol*, 775–778. IEEE.

[23] Team RC. R: A language and environment for statistical computing, 2013. URL `http://www.R-project.org`.

[24] January CT and Riddle JM. Early afterdepolarizations: mechanism of induction and block. a role for l-type ca2+ current. *Circ Res* 64(5):977–90, 1989.

[25] Guo D, Zhao X, et al. L-type calcium current reactivation contributes to arrhythmogenesis associated with action potential triangulation. *J Cardiovasc Electrophysiol* 18(2):196–203, 2007.

[26] Jost N, Virág L, et al. Restricting excessive cardiac action potential and qt prolongation a vital role for iks in human ventricular muscle. *Circulation* 112(10):1392–1399, 2005.

[27] Yang PC and Clancy CE. In silico prediction of sex-based differences in human susceptibility to cardiac ventricular tachyarrhythmias. *Front Physiol* 3:360, 2012.

Author's version. Published in Am Heart J, 2014 (http://dx.doi.org/10.1016/j.ahj.2014.07.010)

[28] Mason JW, Ramseth DJ, et al. Electrocardiographic reference ranges derived from 79,743 ambulatory subjects. *J Electrocardiol* 40(3):228–234.e8, 2007.

[29] Macfarlane P, Oosterom Av, et al. *Adult normal limits*, chapter Appendix 1, 2057–2125, 2011.

[30] Merri M, Benhorin J, et al. Electrocardiographic quantitation of ventricular repolarization. *Circulation* 80(5):1301–8, 1989.

[31] Nakagawa M, Takahashi N, et al. Gender differences in ventricular repolarization. *Pacing Clin Electrophysiol* 26(1p1):59–64, 2003.

[32] Dhingra R, Nam BH, et al. Cross-sectional relations of electrocardiographic qrs duration to left ventricular dimensionsthe framingham heart study. *J Am Coll Cardiol* 45(5):685–689, 2005.

[33] Yang PC, Kurokawa J, et al. Acute effects of sex steroid hormones on susceptibility to cardiac arrhythmias: a simulation study. *PLoS computational biology* 6(1):e1000658, 2010.

[34] Roden D. Long qt syndrome: reduced repolarization reserve and the genetic link. *J Intern Med* 259(1):59–69, 2006.

[35] Silva J and Rudy Y. Subunit interaction determines iks participation in cardiac repolarization and repolarization reserve. *Circulation* 112(10):1384–1391, 2005.

[36] Junttila MJ, Tikkanen JT, et al. Relationship between testosterone level and early repolarization on 12-lead electrocardiograms in men. *J Am Coll Cardiol* 62(17):1633–4, 2013.

[37] Simon D, Preziosi P, et al. The influence of aging on plasma sex hormones in men: the telecom study. *Am J Epidemiol* 135(7):783–791, 1992.

[38] Rohrmann S, Platz EA, et al. The prevalence of low sex steroid hormone concentrations in men in the third national health and nutrition examination survey (nhanes iii). *Clin Endocrinol (Oxf)* 75(2):232–239, 2011.

Author's version. Published in Am Heart J, 2014 (http://dx.doi.org/10.1016/j.ahj.2014.07.010)

Supplementary materials

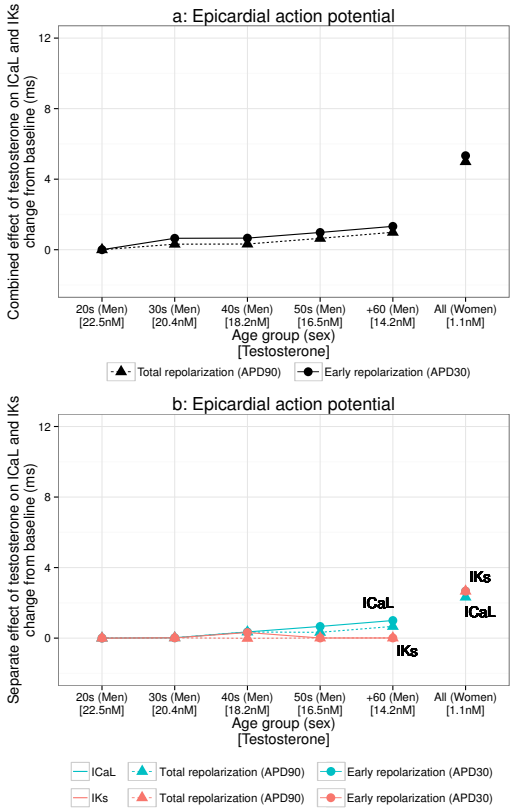

Figure S.1: a) Combined effects of testosterone on total (triangles) and early repolarization (circles) on epicardial action potential in different age groups in men and in all women. (b) Separate effects of testosterone on ICaL (blue) and IKs (red) and their contribution to total (triangles) and early (circles) repolarization on epicardial action potential. Changes in milliseconds from reference group (men in their 20s). Horizontal axis labels show each group's mean testosterone level from literature [17, 18].

Author's version. Published in Am Heart J, 2014 (http://dx.doi.org/10.1016/j.ahj.2014.07.010)

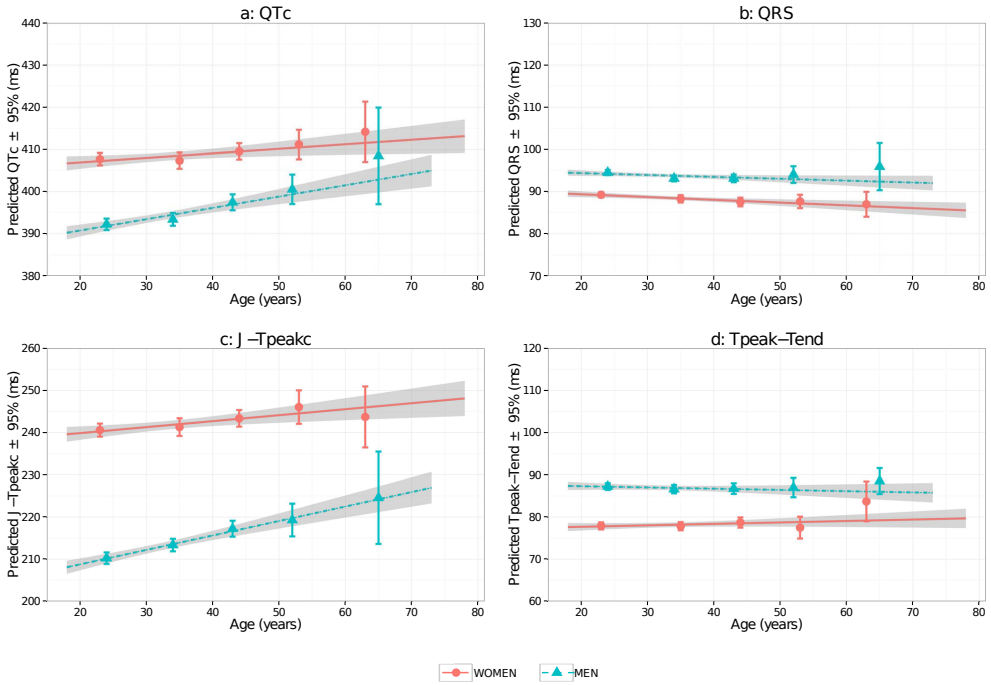

Figure S.2: Linear model predictions for men (blue dashed lines) and women (red solid lines) and 95% confidence intervals (gray area) of changes in QTc (a), QRS (b), J-Tpeakc (c) and Tpeak-Tend (d) with age by sex vs. observed measurements by age group. Men (triangles) and women (circles) were grouped by decade except for the oldest group, which contains subjects aged 60 or over, and plotted with the x-axis location of the median age per group and mean ± 95% confidence intervals on the y-axis. Vertical axes are scaled to the same range to facilitate visual comparisons of differences between sexes, age groups and intervals. Sample size and mean values of each age group are reported in Table I.

CHAPTER 3

Study II

Investigation of potential mechanisms of sex differences in quinidine-induced torsade de pointes risk

Vicente J, Simlund J, et al. Investigation of potential mechanisms of sex differences in quinidine-induced torsade de pointes risk. *J Electrocardiol* 48(4):533–538, 2015

Author's version. Published in J Electrocardiol, 2015 (http://dx.doi.org/10.1016/j.jelectrocard.2015.03.011)

Investigation of potential mechanisms of sex differences in quinidine-induced Torsade de Pointes risk

J Vicente[1,2,3], J Simlund[4,5], L Johannesen[1,5,6], F Sundh[4,5], J Florian[6], M Ugander[5], GS Wagner[4], RL Woosley[7], and DG Strauss[1,5,✉]

[1]*Division of Biomedical Physics, Office of Science and Engineering Laboratories, CDRH, US FDA, Silver Spring, MD, USA*
[2]*Division of Cardiovascular and Renal Products, Office of New Drugs, CDER, US FDA , Silver Spring, MD, USA*
[3]*BSICoS Group, Aragón Institute for Engineering Research (I3A), IIS Aragón, University of Zaragoza, Spain*
[4]*Duke Clinical Research Institute, Durhan, North Carolina, USA*
[5]*Department of Clinical Physiology, Karolinska Institutet and Karolinska University Hospital, Stockholm, Sweden*
[6]*Division of Pharmacometrics, Office of Clinical Pharmacology, Office of Translational Sciences, CDER, US FDA, Silver Spring, Maryland, USA*
[7]*AZCERT, Inc., Oro Valley, AZ, USA*

Abstract

Introduction: *The electrocardiographic index Tpeak-Tend has been proposed as a marker of dispersion of repolarization and may be a stronger predictor of torsade de pointes risk than QTc prolongation.* ***Methods and Results:*** *We assessed whether quinidine-induced Tpeak-Tend prolongation is greater in women than men. The relationship between QTc prolongation and quinidine concentration was greater in women than men (38±10 vs. 28±9 ms/μg/ml, p=0.02), but there was no difference for Tpeak-Tend prolongation (39±13 vs. 32±13 ms/μg/ml, p=0.21). There was a delay (hysteresis) between peak concentration and both maximum QTc and Tpeak-Tend prolongation and a trend toward higher serum quinidine concentration in men than women. Analysis controlling for hysteresis showed no sex difference for QTc (55±18 vs. 43±19 ms/μg/ml, p=0.14), without changing the lack of sex difference with Tpeak-Tend (61±22 vs. 55±21 ms/μg/ml, p=0.49).* ***Conclusions:*** *Women do not have a greater quinidine-induced Tpeak-Tend prolongation than men. Sex differences in hysteresis and serum quinidine concentration in this study may have contributed to sex differences in quinidine-induced QTc prolongation.*

Conflicts of interest*: none.*
Keywords*: QTc prolongation; Quinidine; Torsade de pointes; Sex differences; T wave notching*

Introduction

Torsade de pointes (torsade) is a potentially fatal polymorphic ventricular tachycardia characterized by a cyclic shifting of the QRS axis [1]. It is known that both cardiac and non-cardiac drugs, including antiarrhythmics, antibiotics, antidepressants, antipsychotics and antiemetics can cause torsade [2] and that women have a higher risk of developing drug-induced torsade [3]. All drugs that have been removed from the market due to high risk of developing torsade also had a blocking effect on the human ether a gogo related (hERG) potassium channel [4].

The incidence of torsade is difficult to estimate because it is often a transient, rare event that requires an ECG recording for diagnosis. However, many patients who experience syncope or sudden cardiac death do not have an ECG recording at the time of the event making diagnosis of torsade difficult if not impossible. In the U.S. >400,000 people die every year from sudden cardiac death and 10 – 20% have no evidence of structural heart disease [5]. As women 35 – 44 years old are a subgroup with an increased incidence of sudden cardiac death [5], it is a priority to further understand the underlying mechanisms of sudden cardiac death due to torsade in women.

Prior studies have suggested that the time from the peak to the end of the T wave (Tpeak-Tend) is a marker of dispersion of repolarization [6, 7, 8] and may be a stronger predictor of arrhythmic risk than prolongation of the heart-rate corrected QT interval (QTc) alone [9]. In addition, we previously showed that Tpeak-Tend is a specific marker of hERG potassium channel block [10]. Quinidine was the first drug recognized to prolong QTc and cause torsade [11]. It has previously been demonstrated that quinidine-induced QTc prolongation is greater in women than men [12]; however that study did not examine possible sex differences in Tpeak-Tend. Determination of sex differences in the individual components of the T wave could provide insight into the mechanism of sex differences in torsade risk. The aim of this study was to test the hypothesis that quinidine-induced Tpeak-Tend prolongation is greater in women than men.

✉David G. Strauss, MD, PhD. U.S. Food and Drug Administration. 10903 New Hampshire Avenue, WO62-1126. Silver Spring, MD, 20993, USA. E-mail: david.strauss@fda.hhs.gov. Telephone: 301-796-6323 - Fax: 301-796-9927

Author's version. Published in J Electrocardiol, 2015 (http://dx.doi.org/10.1016/j.jelectrocard.2015.03.011)

Methods

This study population has been previously described [12]. Briefly, 24 healthy nonsmoking volunteers (12 women, 12 men) between 18-35 years old participated in the study. The protocol was a randomized, single-blinded comparison of single doses of intravenous quinidine gluconate (4 mg/kg of base, Eli Lilly, Indianapolis, Indiana, USA) and matching intravenous placebo (saline). Quinidine gluconate (80 mg/ml) was diluted to a total volume of 20 ml with saline solution and infused over 20 minutes. Blood was collected through an intravenous catheter into plain vacutainer tubes from the opposite arm of the infusion at 28 nominal time points postdose. The samples were prepared for quantification of quinidine and 3-hydroxyquinidine and non-protein bound (free) concentrations were determined by ultrafiltration and high performance liquid chromatography, as previously described [12].

ECG acquisition and analysis

Digital 12-lead ECGs were recorded with a MacVu ECG machine (Marquette Electronics, Marquette, WI) immediately before the collection of each blood sample. There were 2 visits per subject, intravenous placebo and intravenous quinidine. Each visit had 28 nominal time points, with the last time point being 12 hours postdose, where ECGs were acquired for 10 seconds [12].

ECGs were analyzed independently from the prior analysis reported by Benton et al. [12]. Two independent ECG readers blinded to treatment and sex assessed each 10 second ECG using semi-automated ECG analysis software [13]. Briefly, ECGs with missing leads or with excessive low- and high-frequency noise were discarded. QRS complexes were detected, baseline wander was corrected and a representative median beat was computed. Measurements were made in lead V5, as Tpeak-Tend in V5 has been described previously as a good predictor of torsade [9]. Of the 24 enrolled subjects, one subject was excluded from analysis due to a short PR interval of approximately 100 ms.

The majority of subjects developed T wave notching, also known as bifid waves or humps, after administration of quinidine. T wave notching includes both biphasic T waves and two positive peaks with a nadir in between. If there were two T peaks, Tpeak was selected as the first peak maximum [6, 14]. If any maximum or minimum was in the form of a plateau, annotations were placed at the earliest point of the plateau. In order to minimize intra-observer variability, ECGs for each patient (56 ECGs each) were evaluated in one sitting and the ECGs were viewed in chronological order to better differentiate T wave notches versus T-U waves. Disagreements on a T wave being measureable, presence of a notch, or a difference of more than 5 ms in either Tpeak or Tend were re-reviewed and adjudicated by an expert ECG reader.

QT intervals were heart rate corrected by the method of Frederica (QTC = QT/((RR/1000 ms)1/3), where RR is in ms). Smetana et al. showed that Tpeak-Tend is rate dependent and differs between gender at shorter RR-intervals (faster heart rate) [15]. In our calculations for Tpeak-Tend, we did not correct for heart rate, as the heart rate in this study was between 62-78 bpm and this range of heart rates is not associated with a significant change in the Tpeak-Tend interval [15].

Statistical analysis

The relationships between the serum quinidine concentration and change in QTc and Tpeak-Tend were evaluated using two approaches: analysis of the direct relationship between serum quinidine concentrations and ECG effect and using an effect-compartment model, using Nonmem 7.3 (ICON plc, Dublin, Ireland) [12, 16]. Prior work by Holford et al. [16], has shown that the delayed effect of quinidine can be modeled by using a sequential approach. In the first step of the sequential approach, a two-compartment model is fitted to the pharmacokinetic data alone, and afterwards the pharmacokinetic model is reapplied to the data with an added effect compartment. The effect compartment is then characterized by a parameter keo, which quantifies the clearance of drug from the effect compartment, and the equilibrium half life is log(2)/keo. Unpaired Student's t-test was used to compare values between women and men and all values are reported using mean values $\pm$ SD. Statistical testing was performed using R 3.0.2 (R Foundation for Statistical Computing, Vienna, Austria). Results were considered significant if two-sided p-values were <0.05.

Results

While women had a longer QTc than men at baseline, there was no difference in Tpeak-Tend (Table 1). Quinidine infusion resulted in substantial QTc prolongation and T wave morphology changes in both women and men (Table 1). Twenty of 23 (87%) subjects showed T wave notching after quinidine infusion (9 of 11 women vs. 11 of 12 men, p=0.99). Example ECGs in Figure 1 show QTc and Tpeak-Tend prolongation as well as notched T waves in two subjects.

Quinidine induced similar maximum placebo- and baseline-corrected QTc prolongation in women and men ([mean$\pm$SD] 143$\pm$44 ms; p<0.001 vs. 130$\pm$36 ms, p<0.001; women vs. men p=0.47). The placebo- and baseline-corrected quinidine-induced prolongation in Tpeak-Tend was also similar in women when compared to men (140$\pm$57 ms; p<0.001 vs. 147$\pm$34 ms; p<0.001; women vs. men p=0.73). There were no significant differences between women and men in quinidine-induced maximum QTc (541$\pm$40 vs. 510$\pm$38 ms; p=0.07) or maximum Tpeak-Tend

Author's version. Published in J Electrocardiol, 2015 (http://dx.doi.org/10.1016/j.jelectrocard.2015.03.011)

Table I: Comparison between baseline characteristics and drug induced changes in men and women

	Women n=11	Men n=12	p Value
Baseline			
Age (years)	26 ± 8	30 ± 7	0.28
Height (m)	1.69 ± 0.06	1.79 ± 0.08	<0.01
Weight (Kg)	65 ± 11	75 ± 13	0.047
Body mass index (Kg/m^2)	23 ± 4	22 ± 3	0.57
Heart Rate (bpm)	64 ± 7	63 ± 10	0.58
QTc (ms)	405 ± 10	389 ± 17	<0.01
Tpeak-Tend (ms)	77 ± 11	73 ± 4	0.10
After quinidine infusion			
Max Quinidine concentration (μg/ml)	2.9 ± 0.7	3.7 ± 1.2	0.07
Max Delta QTc (ms)	143 ± 44	130 ± 36	0.47
Max QTc (ms)	541 ± 40	510 ± 38	0.07
QTc slope (not hysteresis corrected) (ms/μg/ml)	38 ± 10	28 ± 9	0.02
QTc slope (hysteresis corrected) (ms/μg/ml)	55 ± 18	43 ± 19	0.14
Max Delta Tpeak-Tend (ms)	140 ± 57	147 ± 34	0.73
Max Tpeak-Tend (ms)	216 ± 60	222 ± 37	0.76
Tpeak-Tend slope (not hysteresis corrected) (ms/μg/ml)	39 ± 13	32 ± 13	0.21
Tpeak-Tend slope (hysteresis corrected) (ms/μg/ml)	61 ± 22	55 ± 21	0.49

(216±60 vs. 222±37 ms; p=0.76). However there was a trend toward a lower maximum serum quinidine concentration in women compared to men (2.9±0.7 vs. 3.7±1.2 μg/ml; p=0.07).

Figure 2 shows scatterplots and regression lines comparing serum quinidine concentration to change in QTc and Tpeak-Tend for women (red) and men (blue). The slope describing the relationship between serum quinidine concentration and QTc prolongation was greater in women than in men (38±10 ms/μg/ml vs. 28±9 ms/μg/ml; p=0.02) (Figure 2a). However, the slope for Tpeak-Tend was not different between women and men (39±13 ms/μg/ml vs. 32±13 ms/μg/ml, p=0.21) (Figure 2b).

Further analysis revealed that when grouping the concentration-dependent effects by time point (Figure 3), differences between women and men occurred primarily in the first 20 minutes after quinidine infusion, when serum quinidine concentrations were higher in men than women. In men (blue), but not in women (red), there is an apparent delay (concentration-effect hysteresis) between reaching the maximum serum concentration and observing the maximum QTc and Tpeak-Tend effects, which is reflected by a wider loop in men (Figure fig:Fig3). A prior intravenous quinidine study only in men demonstrated that an effect-compartment model is appropriate to model the delayed effect of intravenous quinidine [16]. Using this effect-compartment analysis controlling for hysteresis resulted in no sex difference for QTc (55±18 ms/μg/ml vs. 43±19 ms/μg/ml, p=0.14), without changing the lack of sex difference for Tpeak-Tend (61±22 ms/μg/ml vs. 55±21 ms/μg/ml, p=0.49). In the QTc model, the time to steady state in the effect compartment was 15.1±10.4 min (p<0.01) in women and 18.8±9.8 min (p<0.001) in men (women vs. men p=0.39), which was similar with Tpeak-Tend (15.4±9.2 min; p<0.001 vs. 19.4±8.6 min; p<0.001; women vs. men p=0.30).

Discussion

Quinidine caused a prolongation of Tpeak-Tend, which has been proposed as a marker of dispersion of repolarization in the heart [6, 7, 8, 9]. However, there was no difference in Tpeak-Tend prolongation between women and men (Figure 2b). The majority of the subjects (20 of 23) developed T wave notching, and there was no difference between women and men in the occurrence of T wave notching. This suggests that quinidine-induced increase of Tpeak-Tend and T wave notching do not explain differences in torsade risk between women and men. However, we did observe a delay (concentration-effect hysteresis) between maximum serum quinidine concentration and maximum ECG effect. This trended toward greater delays and higher serum quinidine concentrations in men than women. One explanation for the observed concentration-effect hysteresis may be because quinidine blocks the hERG potassium channel in the intracellular space [17], whereby the delay could be due to the time required for quinidine to accumulate inside ventricular cells [16]. Sex differences in cardiac ion channel composition and distribution and protein binding in drug metabolism and membrane transport have been reported previously [18]. Whether sex differences in quinidine membrane trans-

Author's version. Published in J Electrocardiol, 2015 (http://dx.doi.org/10.1016/j.jelectrocard.2015.03.011)

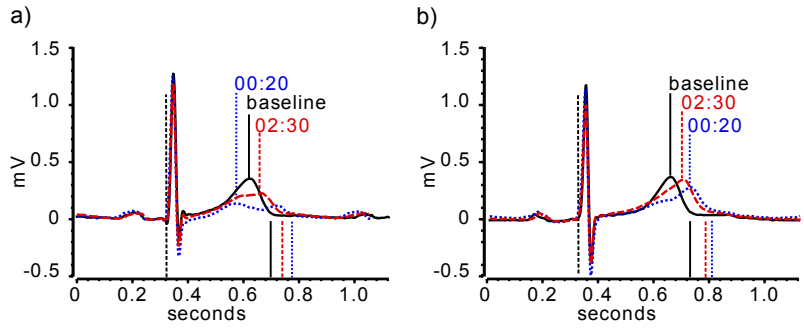

Figure 1: The figure illustrates lead V5 from ECGs at 3 time points (baseline [black solid line], 20 minutes post quinidine [00:20, blue dotted line], and 2 hours and 30 minutes post quinidine [02:30, red dashed line]) for 2 female subjects (A and B). The time points for QRS onset, Tpeak and Tend, respectively, are denoted with vertical lines. At baseline the subjects have similar QTc and Tpeak-Tend durations. At 00:20 subject A developed T wave notching and showed a greater QTc and Tpeak-Tend prolongation due to T wave notching than subject B who did not develop T wave notching. At 02:30 the notching had disappeared and both subjects had similar QTc and Tpeak-Tend durations.

port contribute to the observed greater sensitivity of QTc prolongation to serum quinidine concentration in women deserves further study. Alternatively, the apparent sex difference may have been due to the higher serum quinidine concentrations observed in men in this study.

Effect of sex-hormones on cardiac electrophysiology

The QTc does not differ between women and men in childhood [19]. At the onset of puberty, the QTc interval shortens in males and then slowly increases in later years until women and men have equivalent QTc again sometime after 50 years of age [19]. This QTc shortening in men is likely due to the effects of testosterone [20, 21]. Preclinical studies in guinea pig ventricular myocytes have demonstrated that testosterone shortens action potential duration (and thus QTc) by decreasing L-type calcium current and increasing the slow potassium current (IKs) [22]. The decreased calcium current from testosterone may prevent early after depolarizations (the trigger for torsade) [23], while increased IKs current from testosterone increases repolarization reserve [24]. Both of these may contribute to the lower drug-induced torsade risk in men compared to women.

Testosterone is not the only sex hormone that affects the QTc interval. Preclinical studies have demonstrated that progesterone, like testosterone, shortens action potential duration by decreasing L-type calcium current and increasing the IKs current [25]. A previous study demonstrated that the ibutilide-induced QTc interval prolongation showed an inverse relationship with progesterone levels and the magnitude of the prolongation depended on the menstrual phase [26]. Therefore, the potential protective effects of progesterone against torsade in women might be masked by, and dependent on, the menstrual phase.

ECG Markers of Dispersion of Repolarization

Previous studies have suggested that Tpeak-Tend is a marker of dispersion of repolarization, and that it may be a better predictor of torsade than QTc [6, 7, 8, 9]. Since women have a higher incidence of torsade than men [3], and quinidine is known to cause torsade, we hypothesized that women would exhibit greater quinidine-induced Tpeak-Tend prolongation than men at similar drug concentrations. However, no difference between women and men was identified between either maximum Tpeak-Tend prolongation or the slope describing the relationship between serum quinidine concentration and Tpeak-Tend. While it is possible that women have a higher drug-induced dispersion of repolarization, results of this study suggest that measuring drug-induced changes in the Tpeak-Tend interval alone might not suffice to assess drug-induced changes in dispersion of repolarization. This study did demonstrate that quinidine substantially prolongs Tpeak-Tend in both women and men.

Previous studies have suggested that Q-Tpeak reflects the repolarization time in the region with shorter repolarization time [7, 8]. While we did not assess Q-Tpeak, results suggest that the sex difference in Q-Tpeak (=QTc-(Tpeak-Tend)) increased by 15 ms after quinidine infusion (Table 1). On the other hand, hysteresis analysis (Figure 3) suggests that this increase may be explained by concentration-effect delay. This approximation of Q-Tpeak must be interpreted with caution because maximum effects on each interval

Author's version. Published in J Electrocardiol, 2015 (http://dx.doi.org/10.1016/j.jelectrocard.2015.03.011)

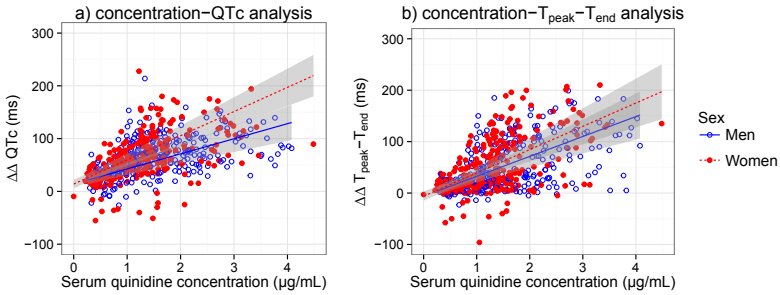

Figure 2: Women (red solid circles) and men (blue open circles) mean baseline- and placebo-corrected serum quinidine concentration dependent changes (red dashed lines [women] and blue solid lines [men]) and 95% confidence intervals (shaded areas) from the model predictions for (a) QTc and (b) Tpeak-Tend. Circles correspond with the observed data. For QTc, a difference in slope between women and men was observed (p = 0.02). No sex difference in slope was observed for Tpeak-Tend (p = 0.21).

happened at different time points in women than in men (Figure 3). Sex-differences in drug-induced prolongation of Q-Tpeak or other markers of early repolarization (e.g. J-Tpeak) deserve further investigation.

A majority of the subjects (87%) developed notched T waves with quinidine and the occurrence was similar in women and men. Previous studies in canine left ventricular wedge models have demonstrated that the ventricular myocardium is not homogenous, but likely comprised of three cell types, epicardial, endocardial and midmyocardial (M-cells), which display electrical and functional differences [27]. Due to these differences, the response to drugs differs between cell types. The T wave notching may be a representation of heterogeneity in the myocardium that is accentuated by hERG potassium channel blocking drugs like quinidine.

Potential Mechanisms for Hysteresis

We observed that there was a delay between reaching maximum serum concentration and obtaining the maximum QTc and Tpeak-Tend prolongation, and the wider counterclockwise loops in men compared to women (Figure 3) suggested that a sex difference might be present. Sex-related differences in the activity of cell membrane transport of drugs have been reported for some drugs, though no such studies have been identified for quinidine [28]. Because quinidine acts as a blocker on the internal mouth of the hERG potassium channel [17], differences in cell membrane transport could cause sex differences in concentration-effect hysteresis. In a previous paper by Benton et al, they used the same dataset as in this study and showed that women had a significantly longer QTc prolongation than men after quinidine infusion [12]. The results of our analyses without using the effect compartment analysis were similar, but the magnitude of delay differed slightly between women and men and correction for concentration-effect hysteresis accounted for the differences in concentration-dependent QTc prolongation between sexes.

As shown in the analyses by Benton et al [12], women in this study had a trend toward a greater weight-adjusted clearance of quinidine (5.2 $\pm$ 1.1 versus 4.3 $\pm$ 1.6 ml/min/kg) and a slightly higher free fraction of the metabolite 3-hydroxyquinidine than men (0.53 $\pm$ 0.05 versus 0.47 $\pm$ 0.05; $p < 0.01$). Faster metabolism of quinidine by women may contribute to the lower serum concentrations of quinidine and higher quinidine metabolites in women than in men. However, it is unlikely that sex differences in drug metabolism fully explain the difference in hysteresis loops (Figure 3) early after drug administration. In this study, subjects received weight-based dosing of quinidine with men (on average 10 kg heavier than women) being administered a total higher quinidine dose than women over the same 20 minute infusion period. Thus, men were likely subjected to a more rapid change in drug concentration and a greater disequilibrium between quinidine serum and intracellular concentration, where quinidine binds to the hERG potassium channel. This larger hysteresis effect with rapid changes in drug concentration was also observed in the prior study by Holford et al [16].

Limitations

The T wave morphology changes produced by quinidine make detection of the end of the T wave difficult. To address this difficulty, software was used to make automatic annotations, which were controlled, and if needed corrected, manually. As opposed to preclinical studies that invasively measure Tpeak-Tend directly on the myocardium, we measured Tpeak-Tend from lead V5. Thus, Tpeak-Tend is a

Author's version. Published in J Electrocardiol, 2015 (http://dx.doi.org/10.1016/j.jelectrocard.2015.03.011)

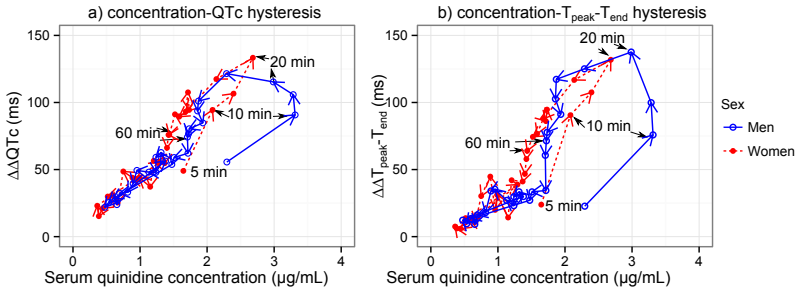

Figure 3: Relationship between mean serum quinidine concentration and mean prolongation in (a) QTc and (b) Tpeak-Tend for women (red solid circles) and men (blue open circles) over time. The connected dots show the concentration for time points from 0–12 hours post dose for women (red dashed lines) and men (blue solid lines). Time points at 5, 10, 20, and 60 minutes post dose are labeled. Men trended to reach higher maximum serum quinidine concentrations (p = 0.07) with a trend toward a delay between maximum serum concentration and maximum ECG effect (p = 0.26), which caused the appearance of a wide loop in men, but not in women. The maximum ECG effects were reached by 20–25 minutes (the fourth or fifth measurement points).

more indirect measure of dispersion of repolarization, however this method has been used in prior clinical studies [9]. Women received their first infusion (quinidine or placebo) within 5 days after the first day of menstruation and received the second infusion 7-17 days later. Consequently, the variability in the phase of the menstrual cycle may have influenced ECG measurements [26]. The small sample size and retrospective nature of the findings related to concentration-effect hysteresis means that these observations should be further evaluated in prospective studies.

Conclusions

We found that both women and men had substantial QTc and Tpeak-Tend prolongation after quinidine infusion and almost all subjects developed T wave notching. Women had a greater slope than men in the relationship between serum quinidine concentration and QTc, but not Tpeak-Tend. However, there was a delay between peak serum concentration and ECG effect, and analysis controlling for the concentration-effect hysteresis found no statistically significant difference in QTc or Tpeak-Tend prolongation between women and men. The observed concentration-effect hysteresis may be because quinidine blocks the hERG potassium channel in the intracellular space and the delay is due to the time required for quinidine to accumulate inside ventricular cells. Potential sex differences in concentration-effect hysteresis should be considered in future research on drug-induced torsade risk.

Acknowledgements

This study was supported by FDA's Critical Path Initiative, FDA's Office of Women's Health and appointments to the Research Participation Program at the Center for Devices and Radiological Health administered by the Oak Ridge Institute for Science and Education through an interagency agreement between the U.S. Department of Energy and the U.S. Food and Drug Administration. The mention of commercial products, their sources, or their use in connection with material reported herein is not to be construed as either an actual or implied endorsement of such products by the U.S. Department of Health and Human Services.

References

[1] Dessertenne F. Ventricular tachycardia with 2 variable opposing foci. *Arch Mal Coeur Vaiss* 59(2):263–72, 1966.

[2] CredibleMedsorg. Qt drugs list. URL `https://www.crediblemeds.org/new-drug-list/`.

[3] Makkar RR, Fromm BS, et al. Female gender as a risk factor for torsades de pointes associated with cardiovascular drugs. *JAMA* 270(21):2590–7, 1993.

[4] Stockbridge N, Morganroth J, et al. Dealing with global safety issues : was the response to qt-liability of noncardiac drugs well coordinated? *Drug Saf* 36(3):167–82, 2013.

[5] Zheng ZJ, Croft JB, et al. Sudden cardiac death in the united states, 1989 to 1998. *Circulation* 104(18):2158–63, 2001.

[6] Emori T and Antzelevitch C. Cellular basis for complex t waves and arrhythmic activity following combined i(kr) and i(ks) block. *J Cardiovasc Electrophysiol* 12(12):1369–78, 2001.

Author's version. Published in J Electrocardiol, 2015 (http://dx.doi.org/10.1016/j.jelectrocard.2015.03.011)

[7] Rautaharju PM, Zhang ZM, et al. Electrocardiographic predictors of coronary heart disease and sudden cardiac deaths in men and women free from cardiovascular disease in the atherosclerosis risk in communities study. *J Am Heart Assoc* 2(3):e000061, 2013.

[8] Rautaharju PM, Zhang ZM, et al. Electrocardiographic repolarization-related predictors of coronary heart disease and sudden cardiac deaths in men and women with cardiovascular disease in the atherosclerosis risk in communities (aric) study. *J Electrocardiol* 48(1):101–11, 2015.

[9] Yamaguchi M, Shimizu M, et al. T wave peak-to-end interval and qt dispersion in acquired long qt syndrome: a new index for arrhythmogenicity. *Clin Sci (Lond)* 105(6):671–6, 2003.

[10] Johannesen L, Vicente J, et al. Differentiating drug-induced multichannel block on the electrocardiogram: randomized study of dofetilide, quinidine, ranolazine, and verapamil. *Clin Pharmacol Ther* 96(5):549–58, 2014.

[11] Selzer A and Wray HW. Quinidine syncope. paroxysmal ventricular fibrillation occurring during treatment of chronic atrial arrhythmias. *Circulation* 30:17–26, 1964.

[12] Benton RE, Sale M, et al. Greater quinidine-induced qtc interval prolongation in women. *Clin Pharmacol Ther* 67(4):413–8, 2000.

[13] Vicente J, Johannesen L, et al. Ecglab: User friendly ecg/vcg analysis tool for research environments. *Comput Cardiol* 775–778, 2013.

[14] Goldenberg I, Moss AJ, and Zareba W. Qt interval: how to measure it and what is "normal". *J Cardiovasc Electrophysiol* 17(3):333–6, 2006.

[15] Smetana P, Batchvarov V, et al. Sex differences in the rate dependence of the t wave descending limb. *Cardiovasc Res* 58(3):549–54, 2003.

[16] Holford NH, Coates PE, et al. The effect of quinidine and its metabolites on the electrocardiogram and systolic time intervals: concentration–effect relationships. *Br J Clin Pharmacol* 11(2):187–95, 1981.

[17] Yeola SW, Rich TC, et al. Molecular analysis of a binding site for quinidine in a human cardiac delayed rectifier k+ channel. role of s6 in antiarrhythmic drug binding. *Circ Res* 78(6):1105–14, 1996.

[18] Gaborit N, Varro A, et al. Gender-related differences in ion-channel and transporter subunit expression in non-diseased human hearts. *J Mol Cell Cardiol* 49(4):639–46, 2010.

[19] Rautaharju PM, Zhou SH, et al. Sex differences in the evolution of the electrocardiographic qt interval with age. *Can J Cardiol* 8(7):690–5, 1992.

[20] Bidoggia H, Maciel JP, et al. Sex differences on the electrocardiographic pattern of cardiac repolarization: Possible role of testosterone. *Am Heart J* 140(4):678–683, 2000.

[21] Vicente J, Johannesen L, et al. Mechanisms of sex and age differences in ventricular repolarization in humans. *American heart journal* 168(5):749–756, 2014.

[22] Bai CX, Kurokawa J, et al. Nontranscriptional regulation of cardiac repolarization currents by testosterone. *Circulation* 112(12):1701–1710, 2005.

[23] January CT and Riddle JM. Early afterdepolarizations: mechanism of induction and block. a role for l-type ca2+ current. *Circ Res* 64(5):977–90, 1989.

[24] Jonsson M, Vos M, et al. Gender disparity in cardiac electrophysiology: implications for cardiac safety pharmacology. *Pharmacol Ther* 127(1):9–18, 2010.

[25] Nakamura H, Kurokawa J, et al. Progesterone regulates cardiac repolarization through a nongenomic pathway: An in vitro patch-clamp and computational modeling study. *Circulation* 116(25):2913–2922, 2007.

[26] Rodriguez I, Kilborn MJ, et al. Drug-induced qt prolongation in women during the menstrual cycle. *JAMA* 285(10):1322–6, 2001.

[27] Antzelevitch C. Cellular basis for the repolarization waves of the ecg. *Ann N Y Acad Sci* 1080:268–81, 2006.

[28] Meissner K, Jedlitschky G, et al. Modulation of multidrug resistance p-glycoprotein 1 (abcb1) expression in human heart by hereditary polymorphisms. *Pharmacogenetics* 14(6):381–5, 2004.

CHAPTER 4

Study III

Comprehensive T-wave morphology assessment in a randomized clinical study of dofetilide, quinidine, ranolazine, and verapamil

Vicente J, Johannesen L, et al. Comprehensive T wave morphology assessment in a randomized clinical study of dofetilide, quinidine, ranolazine, and verapamil. *J Am Heart Assoc* 4(4):e001615, 2015

Author's version. Published in J Am Heart Assoc, 2015 (http://dx.doi.org/10.1161/JAHA.114.001615)

Comprehensive T wave Morphology Assessment in a Randomized Clinical Study of Dofetilide, Quinidine, Ranolazine and Verapamil

J Vicente[1,2,3], L Johannesen[1,4], JW Mason [5], WJ Crumb[6], E Pueyo[7,3], N Stockbridge[2], and DG Strauss[1,4,✉]

[1]*Office of Science and Engineering Laboratories, CDRH, US FDA, Silver Spring, MD, USA*
[2]*Division of Cardiovascular and Renal Products, Office of New Drugs, CDER, US FDA , Silver Spring, MD, USA*
[3]*BSICoS Group, Aragón Institute for Engineering Research (I3A), IIS Aragón, University of Zaragoza, Spain*
[4]*Department of Clinical Physiology, Karolinska Institutet and Karolinska University Hospital, Stockholm, Sweden*
[5]*Spaulding Clinical Research, West Bend, WI, USA*
[6]*Zenas Technologies, Metairie, Louisiana, USA*
[7]*Biomedical Research Networking Center in Bioengineering, Biomaterials and Nanomedicine (CIBER-BBN), Spain*

Abstract

Background: *Congenital long QT syndrome type 2 (abnormal hERG potassium channel) patients can develop flat, asymmetric and notched T waves. Similar observations have been made with a limited number of hERG blocking drugs. However, it is not known how additional calcium or late sodium block, that can decrease torsade risk, affects T wave morphology.* ***Methods and Results:*** *Twenty-two healthy subjects received a single dose of a pure hERG blocker (dofetilide) and three drugs that also block calcium or sodium (quinidine, ranolazine and verapamil) as part of a five period, placebo controlled cross-over trial. At predose and 15 time points post-dose, ECGs and plasma drug concentration were assessed. Patch clamp experiments were performed to assess block of hERG, calcium (L-type) and late sodium currents for each drug. Pure hERG block (dofetilide) and strong hERG block with lesser calcium and late sodium block (quinidine) caused substantial T wave morphology changes ($p<0.001$). Strong late sodium current and hERG block (ranolazine) still caused T wave morphology changes ($p<0.01$). Strong calcium and hERG block (verapamil) did not cause T wave morphology changes. At equivalent QTc prolongation, multichannel blockers (quinidine and ranolazine) caused equal or greater T wave morphology changes compared to pure hERG block (dofetilide).* ***Conclusion:*** *T wave morphology changes are directly related to amount of hERG block; however, with quinidine and ranolazine, multichannel block did not prevent T wave morphology changes. A combined approach of assessing multiple ion channels, along with ECG intervals and T wave morphology may provide the greatest insight into drug-ion channel interactions and torsade de pointes risk.*

Clinical Trial Registration Information*: http://clinicaltrials.gov/ct2/show/NCT01873950 (NCT01873950)*
Keywords*: electrocardiography, ion channels, pharmacology, torsade de pointes, long-QT syndrome*

Long QT syndrome can be caused by congenital or acquired (e.g., drug-induced or electrolyte) abnormalities in cardiac ion channel currents regulating ventricular repolarization [1]. Long QT syndrome patients are at increased risk for torsade de pointes, a potentially fatal ventricular arrhythmia [2]. Conventionally, physicians and drug regulators have focused solely on the QT interval in assessing risk for torsade; however, more information may be present in the ECG. Moss and colleagues [3] identified different T wave patterns associated with the three major congenital long QT syndrome types. LQT1 patients (decreased IKs current) have early onset broad-based T waves, LQT2 patients (decreased hERG potassium current, IKr) have low amplitude, bifid or notched T waves, and LQT3 patients (increased late sodium current, INa_{late}) have long isoelectric ST segments with late-appearing, normal morphology T waves.

In the 1990s, there was recognition of an epidemic of drug-induced QT prolongation and torsade de pointes resulting in many drugs being withdrawn from the market [4]. It was also recognized that nearly all drugs that increased torsade risk blocked the hERG potassium channel [5]. This resulted in all new drugs being required to be screened for their ability to block the hERG potassium channel and prolong QT in Thorough QT studies [6, 7]. However, the extreme focus on hERG and QT has resulted in drugs being dropped from development, sometimes inappropriately, as not all drugs with hERG block or QT prolongation cause torsade [4].

Multiple examples exist of drugs on the market which

✉David G. Strauss, MD, PhD. U.S. Food and Drug Administration. 10903 New Hampshire Avenue, WO62-1126. Silver Spring, MD, 20993, USA. E-mail: david.strauss@fda.hhs.gov. Telephone: 301-796-6323 - Fax: 301-796-9927

Author's version. Published in J Am Heart Assoc, 2015 (http://dx.doi.org/10.1161/JAHA.114.001615)

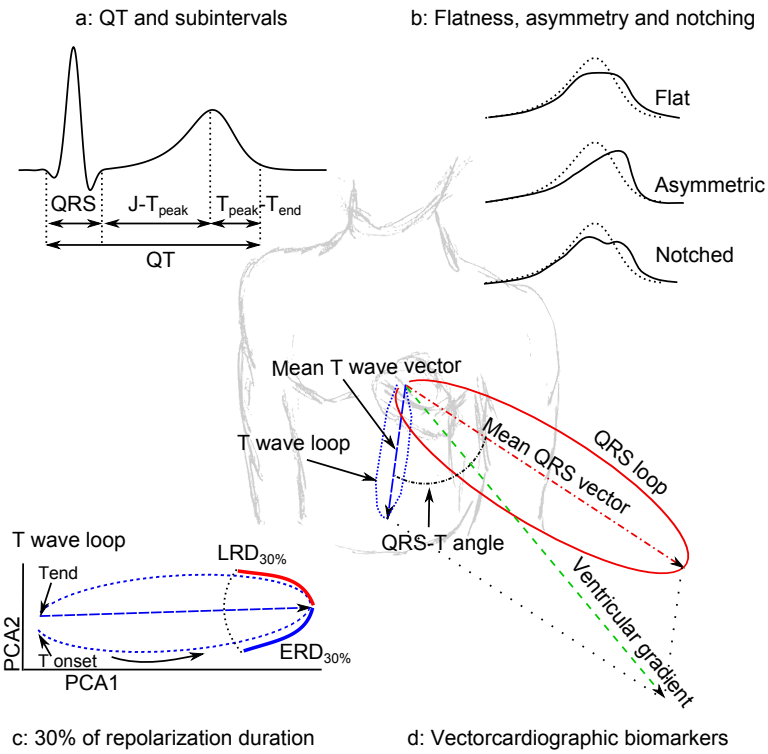

Figure 1: Illusration showing the ECG biomarkers assessed in this study: (a) QT and subintervlas (J-Tpeak and Tpeak-Tend); (b) flat, asymmetric and notched T waves (solid lines) vs. normal T waves (dotted lines); (c) 30% of early ($ERD_{30\%}$) and late ($LRD_{30\%}$)repolarization duration in the preferential plane formed by the two-first Eigen leads from principal component analysis (PCA1 and PCA2); (d) other vectorcardiographic biomarkers (QRS-T angle, ventricular gradient, total cosine R-to-T [TCRT] and maximum magnitude of the T vector). See methods.

block hERG channel (an outward potassium current), but have minimal-to-no risk for torsade due to their concurrent block of either L-type calcium or late sodium (inward currents) [8, 9]. Nonclinical studies have suggested that inward current block can lessen torsade risk from hERG block by decreasing dispersion of repolarization (e.g., shortening action potential duration) and preventing early after depolarizations, which are the trigger for torsade [10, 11]. In order to understand whether drug-induced multi-ion channel block can be detected and differentiated on the electrocardiogram as in congenital long QT syndrome, we conducted a prospective, placebo-controlled clinical study of dofetilide, quinidine, ranolazine and verapamil. Dofetilide is a pure strong hERG potassium channel blocker [12] with a high risk of torsade [5]. Quinidine is a strong hERG potassium channel blocker that has additional weaker block of calcium and late sodium [12]. Torsade has been observed to occur more frequently at lower quinidine concentrations [13, 14] where hERG block is present, but there is lesser calcium and sodium block. Ranolazine blocks the late sodium current and hERG approximately equally and has not been associated with torsade, and may be anti-arrhythmic [15]. Verapamil blocks calcium stronger than hERG and has low torsade risk [5, 12].

A separate study [16] analyzed the J-Tpeak and Tpeak-Tend intervals and demonstrated that pure hERG block prolonged both J-Tpeak and Tpeak-Tend while additional inward current block preferentially shortened J-Tpeak. The

Author's version. Published in J Am Heart Assoc, 2015 (http://dx.doi.org/10.1161/JAHA.114.001615)

objective of the current study was to evaluate the effect of pure hERG block versus multichannel block on multiple previously developed T wave morphology metrics (Figure 1). This included quantitative measures of T wave flatness, asymmetry and notching, which were developed to detect the ECG signature of LQT2 (abnormal hERG current) [17]. In addition, we studied the 30% early and late repolarization duration ($ERD_{30\%}$ and $LRD_{30\%}$) of the T wave loop [18, 19], previously shown to detect hERG block, and other vectorcardiographic measures of the relation between depolarization and repolarization vectors (QRS-T angle, ventricular gradient and total cosine R-to-T [TCRT]), which have been shown to predict arrhythmic risk in some patient populations [20, 21, 22].

Methods

Clinical study design

The design of this clinical study has been previously described [16]. The study's inclusion and exclusion criteria were similar to those used in dedicated QT studies [6]. Briefly, healthy subjects between 18 and 35 years old, weighting between 50 and 85 Kg and without a family history of cardiovascular disease or unexplained sudden cardiac death were eligible for participation in the study. In addition, the subjects had to have less than 12 ventricular ectopic beats during a 3 hour continuous recording at screening, as well as a baseline QTc of less than 450 ms for men (470ms for women), using Fridericia's correction [23]. The study was designed as a randomized double-blind 5-period crossover clinical trial at a phase 1 clinical research unit (Spaulding Clinical, West Bend, Wisconsin, USA). William's Latin square design balanced for first-order carryover effects [24] was used for randomization.

In the morning of each period, subjects received a single dose of 500 μg dofetilide (Tikosyn, Pfizer, New York, NY), 400 mg quinidine sulfate (Watson Pharma, Corona, CA), 1,500 mg ranolazine (Ranexa, Gilead, Foster City, CA), 120 mg verapamil hydrochloride (Heritage Pharmaceuticals, Edison, NJ) or placebo under fasting conditions. For dofetilide and quinidine, the selected dose was the maximum single dose allowed in the label [25, 26] to ensure substantial ECG changes after a single dose. The ranolazine dose was selected to achieve plasma levels close to the chronic/steady state levels, but with a single dose. This resulted in a dose higher than the clinical dose but lower than the maximum daily dose in the label [27]. For verapamil, the highest initial single dose in the label was selected, and not pushed further due to concern for extreme PR prolongation and heart block in healthy subjects [28].

There was a 7-day washout period between each 24-hour treatment period. During each period, continuous ECGs were recorded at 500 Hz and with an amplitude resolution of 2.5 μV. From the continuous recording, triplicate 10-second ECGs were extracted at predose and 15 predefined time-points postdose (0.5, 1, 1.5, 2, 2.5, 3, 3.5, 4, 5, 6, 7, 8, 12, 14, 24 h) during which the subjects were resting in a supine position for 10 minutes. A blood sample was drawn for pharmacokinetic analysis after each ECG extraction time-point period and plasma drug concentration was measured using a validated liquid chromatography with tandem mass spectroscopy method by Frontage Laboratories (Exton, Philadelphia, PA). The study was approved by the U.S. Food and Drug Administration Research Involving Human Subjects Committee and the local institutional review board. All subjects gave written informed consent.

ECG analysis

At each of the 16 time-points, three optimal 10-second 12-lead ECGs were extracted with stable heart rates and maximum signal quality using Antares software (AMPS-LLC, New York City, NY, USA) [29]. The resulting 5,232 ECGs were up-sampled from 500 Hz to 1,000 Hz. The semi-automatic evaluation, which included computerized interval annotations (i.e. Fridericia's QTc [23]) by ECG readers blinded to treatment and time, has been described elsewhere [16]. T wave flatness, asymmetry and the presence of notch were automatically assessed with QTGuard+ (GE Healthcare, Milwaukee, Wisconsin, USA). All the other T wave morphology and vectorcardiographic biomarkers described below were automatically assessed with ECGlib [30].

T wave flatness, asymmetry and notching

The computation of T wave flatness, asymmetry and the presence of notch has been described elsewhere (Figure 1.b) [17]. Briefly, a median beat was derived from the independent leads (I-II, V1-V6) of the 10-second 12-lead ECG, and morphology measures were assessed in the first Eigen lead (PCA1) after applying principal component analysis (PCA). T wave flatness is based on the inverse kurtosis (1 - kurtosis) of the unit area of the T wave, thus increasing values reflect increasing flatness of the T wave (dimensionless units [d.u.]). Asymmetry score (d.u.) evaluates differences in the slope profile and duration of the ascending and descending parts of the T wave, where low values correspond with symmetric T waves and higher values with more asymmetric T waves. The presence of notch was obtained from the inverse, signed radius of curvature of the T wave, where values different from 0 correspond with the presence of notch. Notch was labeled as present if at least 1 out of the 3 ECGs of the triplicate in the corresponding time-point had a notch score greater than 0.

Author's version. Published in J Am Heart Assoc, 2015 (http://dx.doi.org/10.1161/JAHA.114.001615)

Percentage of early and late repolarization duration

Vectorcardiographic measurements 30% of early ($ERD_{30\%}$) and late ($LRD_{30\%}$) repolarization duration were based on the PCA transform from the ST-T segment of the independent leads (I-II, V1-V6) of the 12-lead ECG median beat. The maximum amplitude of the T vector in the preferential plane formed by the two first Eigen leads (PCA1 and PCA2) was selected as reference, and $ERD_{30\%}$ and $LRD_{30\%}$ were then measured at the time at which the amplitude decreased by 30% (Figure 1.c) [18].

Other vectorcardiographic biomarkers

For each 12-lead ECG median beat, we derived the Frank vectorcardiogram using Guldenring's transformation matrix [31]. The QRS-T angle was defined as the angle between the QRS and T vectors, which were defined as the summation in the X, Y and Z leads from the QRS onset to QRS offset and QRS offset to T offset respectively. The ventricular gradient was defined as the magnitude of the sum of the QRS and T vectors [32]. The vector with the maximum magnitude between QRS offset and T offset (maximum T vector) was also computed (Figure 1.d).

In addition to the QRS-T angle described above, we also assessed the concordance between ventricular depolarization and repolarization sequences computing the total cosine R-to-T (TCRT, Figure 1.d) [22]. This descriptor is defined as the average of the cosines of the angles between a subset of QRS and T vectors in the 3 first Eigen leads (PCA1-PCA3) derived from the PCA transform of the independent leads (I-II, V1-V6) of the 12-lead ECG median beat.

Analysis and removal of heart rate dependency

We determined if the T wave morphology biomarkers were dependent on heart rate, by considering if there was a statistically significant heart rate relationship as well as a meaningful change [33]. For biomarkers with dependency on heart rate, we developed a study-specific correction factor using an exponential model and allowed the relationship to be sex dependent. The heart rate correction was performed using PROC MIXED in SAS 9.3 (SAS Institute, Cary, North Carolina, USA), wherein a significance level of 0.05 was used to determine if there was a difference by sex.

Patch clamp experiments

Patch clamp experiments were conducted to assess the relative block of hERG, late sodium (Nav1.5) and calcium (Cav1.2) currents caused by each drug. Stably transfected hERG,r Nav1.5 cells (HEK-293), or Cav1.2 cells (CHO) were obtained from Cytocentrics Biosciences (Rostock, Germany). Cells were maintained in minimum essential medium with Earle's salts supplemented with nonessential amino acids, sodium pyruvate, penicillin, streptomycin, and fetal bovine serum.

Drugs were dissolved in either dimethyl sulfoxide (DMSO) or deionized H2O to make stock solutions. Dilutions of stock solutions were made immediately before the experiment to create the desired concentrations. The external solution (solution bathing the cell) had an ionic composition of (in mM): 137 NaCl, 4 KCl, 1.8 CaCl2, 1.2 MgCl2, 11 dextrose, 10 HEPES, adjusted to a pH of 7.4 with NaOH. The internal (pipette) solution had an ionic composition of (in mM): 130 KCl; 1 MgCl2, 5 NaATP, 7 NaCl, 5 EGTA, 5 HEPES, pH=7.2 using KOH. Experiments were performed at 36 $\pm$ 1°C. Drugs were obtained from Tocris Bioscience (Minneapolis, MN, USA).

Currents were measured using the whole-cell variant of the patch clamp method as previously described [34]. After rupture of the cell membrane (entering whole-cell mode), current amplitude and kinetics were allowed to stabilize (3-5 min) before experiments were begun. All three currents (hERG, Nav1.5, Cav1.2) were elicited using a ventricular action potential waveform paced at 0.1Hz.

Statistical analysis

The placebo-corrected change from baseline was computed using PROC MIXED in SAS 9.3 (SAS institute, Cary, North Carolina, USA), where the change from baseline for each T wave morphology biomarker by time-point was the dependent variable. Sequence, period, time, drug, and an interaction between treatment and time were included as fixed effects, and subject was included as a random effect. Afterwards, a linear-mixed effects model was used to evaluate the relationship between each of the T wave morphology biomarkers (except notch) and plasma concentrations. This was done using PROC MIXED in SAS 9.3, and having a random effect on both intercept and slope (i.e., allowing each subject to have their own drug concentration-biomarker relationship). A logistic regression model was used to evaluate the relationship between presence of notch and drug concentration including a random effect on intercept in SAS (PROC GLIMMIX). P-values <0.05 were considered statistically significant.

Patch clamp results are given as percent reduction of current amplitude, which was measured as current reduction after a steady-state effect had been reached in the presence of drug relative to current amplitude before drug was introduced (control). Each cell served as its own control. Log-linear plots were created from the mean percent block $\pm$ S.E.M. at the concentrations that were tested. A nonlinear least square fitting routine was used to fit a three-parameter Hill equation to the results in R 3.0.2 (R Foundation for Statistical Computing, Vienna, Austria). The equation is of

Author's version. Published in J Am Heart Assoc, 2015 (http://dx.doi.org/10.1161/JAHA.114.001615)

the following form

$$B(\%) = 100\frac{D^n}{IC_{50}^n + D^n}$$

where B(%) is the percentage of current blockage at drug concentration D, IC_{50} is the concentration of drug that causes 50% block, and n is the Hill coefficient.

Results

Twenty-two healthy subjects (11 females) participated in this randomized controlled clinical trial; see Table 1 for baseline characteristics. All subjects completed the study except for one subject who withdrew prior to the last treatment period (quinidine period for that subject). There were no unexpected treatment related adverse events (supplementary Figure S.1). Placebo changes from baseline are shown in supplementary Figure S.2.

Table 1: Baseline characteristics

	All subjects (N=22)
Demographic	
Age (years)	26.9 ± 5.5
Female	11 (50%)
Body mass index (kg/m2)	23.1 ± 2.7
ECG	
Heart rate (beats per minute)	56.8 ± 6.4
QTc (ms)	395.9 ± 17.1
JTpeakc (ms)	225.6 ± 19.8
Tpeak-Tend (ms)	73.1 ± 6.4
T wave morphology	
Flatness (d.u.)	0.41 ± 0.04
Asymmetry (d.u.)	0.16 ± 0.05
Presence of Notch (%)	0
Repolarization duration	
$ERD_{30\%}$ (ms)	44.5 ± 5.1
$LRD_{30\%}$ (ms)	27.5 ± 4.1
Vectorcardiographic	
QRS-T angle (°)	34.5 ± 9.9
TCRT (radians)	0.67 ± 0.24
Tmagmax (μV)	578.5 ± 173.0
Ventricular gradient (mV·ms)	112.3 ± 30.2

Continuous variables are represented as mean ± SD of each subject's 5-day baseline average

Analysis and removal of heart rate dependency

Substantial heart rate dependent change was observed for T wave flatness, maximum magnitude of the T vector and ventricular gradient. No sex-specific differences in the heart rate dependency were found. The heart rate dependent biomarkers were corrected for heart rate in all subsequent analysis using an exponential model (biomarkerc= biomarker/RR^{α}), where the values of α coefficient were 0.58 for T wave flatness, 0.96 for maximum magnitude of the T vector and 0.85 for ventricular gradient.

Dofetilide: Pure hERG potassium channel block

From our ion channel patch clamp experiments, dofetilide was associated with ∼55% hERG potassium channel block at the population's mean maximum concentration (Cmax); see Table 2. Dofetilide did not block calcium or late sodium currents (Figure 2).

Figure 3 shows the relationships between plasma drug concentration and each T wave morphology biomarker, where the plasma concentration for each drug is normalized to the population Cmax. The actual drug concentration ranges are shown in Table 3. In addition to causing significant concentration-dependent QTc prolongation, pure hERG potassium channel block (dofetilide) caused concentration-dependent T wave flatness, asymmetry and notching (see Figure 4 for ECG examples), consistent with ECG findings from LQT2 patients (abnormal hERG potassium channel) [35]. T wave flatness had a more consistent response than asymmetry, illustrated by the smaller confidence intervals (Figure 3), and 14 of 22 subjects developed notched T waves (Table 2). There was also strong decrease in the maximum magnitude of the T vector (Figure 3), which is consistent with the observed T wave flatness (Figure 3).

As with prior pure hERG blockers [18, 19], dofetilide caused an increase in both $ERD_{30\%}$ and $LRD_{30\%}$ (Figure 3). While prior literature has suggested that a wider QRS-T angle is associated with increased arrhythmic risk, pure hERG block caused a small decrease in the QRS-T angle (Figure 3). A similar finding was observed for TCRT, while there was no concentration-dependent change in the ventricular gradient (Figure 3).

Quinidine: Strong hERG block with additional calcium and sodium block

Our patch clamp experiments (Figure 2) showed that at Cmax quinidine was associated with ∼71% hERG potassium channel block, ∼8% calcium current block and ∼3% of late sodium current block (Table 2). Thus, quinidine had stronger hERG potassium channel block than dofetilide, however quinidine had additional calcium and sodium channel block, but resulted in a similar amount of concentration-dependent QTc prolongation for the two drugs (Figure 3). Quinidine was associated with similar to greater amounts of T wave flatness, asymmetry, notching (see Figure4 for ECG examples) and a decrease in the maximum magnitude of the T vector ($p<0.001$ for all) compared to dofetilide (Figure 3). Notched T waves developed in 18 of 21 subjects (Table 2).

Similar to dofetilide, quinidine increased $ERD_{30\%}$ and $LRD_{30\%}$ (Figure 3). In contrast to the small decrease in QRS-

Author's version. Published in J Am Heart Assoc, 2015 (http://dx.doi.org/10.1161/JAHA.114.001615)

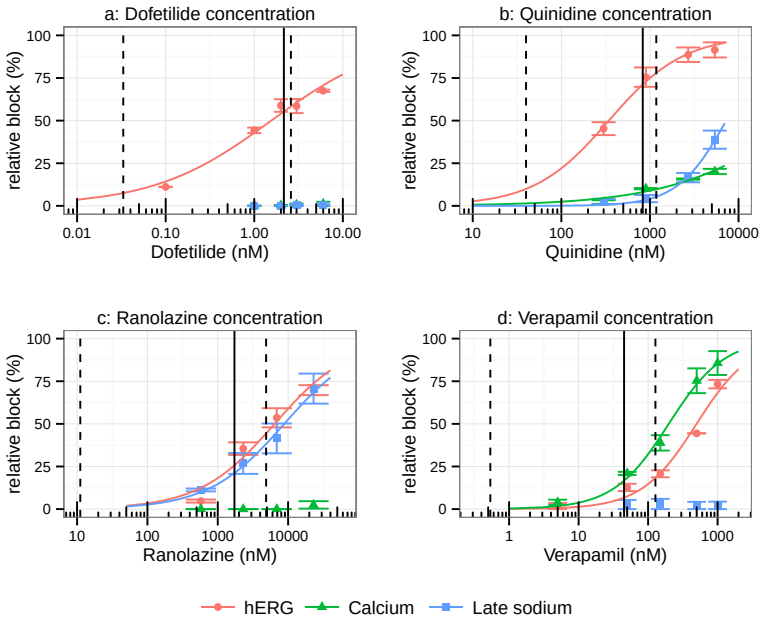

Figure 2: Patch clamp experiments results for (a) dofetilide, (b) quinidine, (c) ranolazine and (d) verapamil for hERG (red), calcium (green) and late sodium (blue). The lines in each plot correspond to a fit between the observed means per concentration and data (see text). The error bars denote ± SEM. The dashed lines in each panel correspond to the range of observed clinical concentrations and the solid line is the population average maximum concentration (Cmax).

T angle with dofetilide, quinidine caused a small increase in the QRS-T angle, while it had no change in TCRT or the ventricular gradient (Figure 3).

Ranolazine: Similar hERG and late sodium block

From our ion channel patch clamp experiments (Figure 2), at Cmax ranolazine was associated with ∼26% hERG potassium channel block and ∼21% late sodium current block (Table 2). Ranolazine produced modest concentration-dependent QTc prolongation of ∼13 ms at Cmax (Table 2); however it still produced significant amounts of T wave flatness and asymmetry (p<0.001) (Figure 3), along with a decrease in the maximum magnitude of the T vector (p<0.01). Furthermore, while ranolazine produced statistically significant notching for the population overall (Figure 3, supplementary S.1), only 2 of 22 subjects developed notching (Table 2). Figure 4(b) shows the ECG traces of one of the subjects who developed notching with ranolazine. Of note, this woman had the second highest plasma concentration of ranolazine (6.14 μg/ml) of all subjects in this study, and notches in the T wave were observed at concentrations exceeding 2.45 μg/ml. This subject had even more severe T wave morphology changes with dofetilide and quinidine (Figure 4(b)). Like dofetilide and quinidine, ranolazine caused an increase in both $ERD_{30\%}$ and $LRD_{30\%}$ (Figure 3). Ranolazine did not cause a change in the QRS-T angle, TCRT or ventricular gradient (Figure 3).

Verapamil: Calcium block stronger than hERG block

From our ion channel patch clamp experiments (Figure 2), at Cmax verapamil was associated with ∼17% of calcium current block and ∼7% hERG potassium channel block (Table 2).Verapamil did not cause a meaningful change in QTc (Figure 3) or any of the T wave morphology markers (Figure 3) at the plasma concentrations observed in this study. Of note, as described previously [16], verapamil did cause a substantial 32.1 [26.7 to 37.4] ms (p<0.001) increase in the PR interval, demonstrating that the plasma concentrations

Author's version. Published in J Am Heart Assoc, 2015 (http://dx.doi.org/10.1161/JAHA.114.001615)

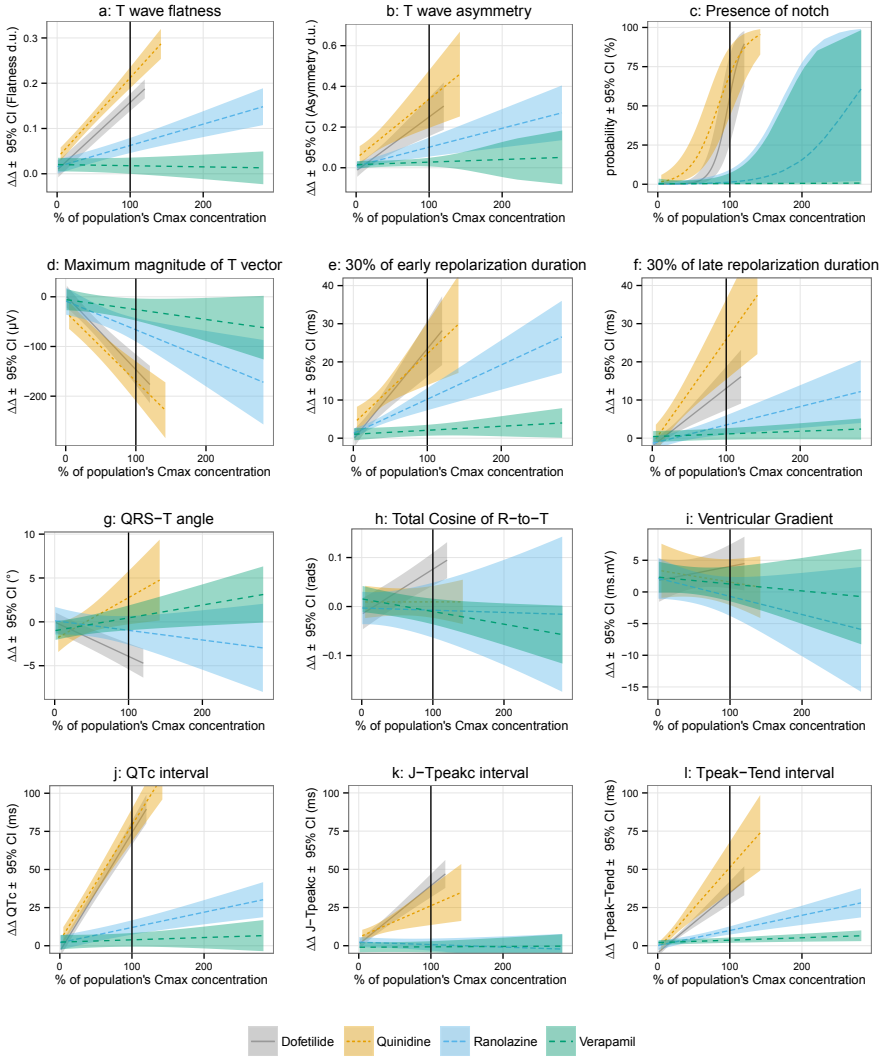

Figure 3: Mean baseline- and placebo-corrected plasma drug concentration-dependent changes (lines) and 95% confidence intervals (shaded areas) for T wave (a) flatness, (b) asymmetry, (c) probability of presence of notch, (d) maximum magnitude of T vector, (e) 30% of early, (f) late repolarization duration, (g) QRS-T angle, (h) total cosine of R to T, (i) spatial ventricular gradient, (j) QTc interval, (k) early repolarization interval (J-Tpeakc) and (l) late repolarization interval (Tpeak-Tend). X axis shows % of population Cmax for each drug (mean ±SD): dofetilide (2.7 ±0.3 ng/mL, solid gray), quinidine (1.8 ±0.4 μg/mL, dotted orange line), ranolazine (2.3 ±1.4 μg/mL, blue dashed line) and verapamil (130.4 ±75.8 ng/mL, dashed green line). See Table 3 for detailed drug concentration ranges. Mean slopes together with 95% confidence interval values are reported in supplementary Table S.1. Supplementary figures S.3, S.4 and S.5 show similar information in a drug by drug basis together with relative block of hERG, calcium and late sodium currents from the patch clamp experiments. Corresponding time profile plots of drug plasma concentration and drug-induced changes are shown in supplementary figures S.6, S.7 and S.8.

Author's version. Published in J Am Heart Assoc, 2015 (http://dx.doi.org/10.1161/JAHA.114.001615)

in this study were sufficient to elicit an electrophysiological effect. The lack of T wave morphology changes observed in this study suggests that competing effects of inward current block from calcium and outward current block from hERG potassium during ventricular repolarization are very well balanced with verapamil.

Relation between QTc and T wave morphology metrics

We used the concentration-response models to predict the individual drug-induced changes for QTc and each T wave morphology biomarker at 25% increments of the population's Cmax of each drug. Figure 5 shows the relationship between changes in QTc and changes in T wave morphology biomarkers for dofetilide, quinidine and ranolazine. At equivalent drug-induced QTc prolongation, quinidine and ranolazine (multichannel blockers) induced similar to or slightly greater T wave morphology changes than did dofetilide (pure hERG potassium channel blocker).

Discussion

This study observed that pure hERG potassium channel block with dofetilide causes substantial concentration-dependent T wave flatness, asymmetry and notching, along with a decrease in the maximum magnitude of the T vector. These quantitative T wave biomarkers were originally developed to detect the ECG signature of congenital LQT2 (decreased hERG potassium channel current), and this study strongly supports that these biomarkers capture that ECG phenotype. This study was novel and unique in that the same subjects received three additional hERG potassium channel blockers (quinidine, ranolazine and verapamil) that also block inward currents (calcium or late sodium) during repolarization. hERG blocking drugs that also block inward currents have been observed to have a lower torsade risk, either because they decrease dispersion of repolarization (the substrate for re-entry) [10] or they prevent early afterdepolarizations (the trigger for torsade) [11]. We observed that quinidine and ranolazine both still caused T wave morphology changes, despite inward current block.

This raises the question of how T wave morphology changes relate to risk for drug-induced torsade de pointes. While quinidine, ranolazine and verapamil are multichannel blockers, only quinidine is associated with a significant torsade risk. This is likely due to quinidine's substantially greater hERG block (∼71%) than calcium and late sodium block (∼8% and ∼3%, respectively) at Cmax. Furthermore, at lower concentrations (see Figure 2) quinidine is a relatively pure hERG blocker, and torsade de pointes events with quinidine have been observed to occur more frequently at lower concentrations [13]. Compared to quinidine, ranolazine was associated with less hERG block (∼26%) and more late sodium current block (∼21%), while verapamil was associated with only ∼7% hERG block and ∼17% calcium block. Moreover, there was no increase in QTc or change in T wave morphology associated with verapamil in this study, suggesting that verapamil has almost perfectly balanced inward (calcium) and outward (hERG) current block. Thus, it is likely not just the presence of calcium or late sodium current block that can prevent torsade, but rather the balance between inward and outward current block that is most important.

Taken together with our prior observations that calcium and late sodium block primarily affect early repolarization by shortening the J-Tpeakc interval [16, 33], this suggests that the strongest effect of calcium and late sodium block may be to shift the T wave to the left (shorter ST segment duration), with a lesser effect on T wave morphology. The opposite effect is seen with LQT3, where the abnormally increased late sodium current results in a long ST segment duration, with a late appearing T wave of unchanged morphology [3]. Overall, while flat, asymmetric and notched T waves appear to be biomarkers of hERG block, these T wave morphology markers likely do not always correlate with torsade de pointes risk, as has also been observed for QTc. The relationship between events of torsade de pointes and the relative amount of hERG block compared to additional calcium or late sodium block deserves further investigation with a large number of drugs, as has been proposed under the Comprehensive *in vitro* Proarrhythmia Assay (CiPA) initiative [36].

T wave loop biomarkers

In addition to assessing T wave flatness, asymmetry and notching, we assessed a series of T wave loop biomarkers. $ERD_{30\%}$ and $LRD_{30\%}$ measure the time from the peak of the T wave loop to 30% of the baseline toward the beginning of the T wave ($ERD_{30\%}$) and end of the T wave ($LRD_{30\%}$), respectively. These markers were developed to be sensitive detectors of hERG potassium channel block and were previously assessed with moxifloxacin [18] and d,l-sotalol [37]. The results of the present study confirm that $ERD_{30\%}$ and $LRD_{30\%}$ are indeed sensitive markers of hERG block from dofetilide, quinidine and ranolazine. When assessing the relative changes of these biomarkers compared to the amount of QTc change (Figure 5), there was a similar amount of change in $LRD_{30\%}$ for dofetilide, quinidine and ranolazine. For $ERD_{30\%}$, dofetilide and quinidine were similar, while ranolazine induced a greater relative change in $ERD_{30\%}$; how this relates to cardiac safety is unknown.

Prior research has suggested that patients with a wide QRS-T angle are at increased risk for ventricular arrhythmias and sudden death [20, 21]. Similar observations have been reported with the TCRT in other patient populations (hypertrophic cardiomyopathy [22] and post–myocardial

Author's version. Published in J Am Heart Assoc, 2015 (http://dx.doi.org/10.1161/JAHA.114.001615)

Table 2: Predicted relative channel block and changes in ECG biomarkers at Cmax.

	Dofetilide	Quinidine	Ranolazine	Verapamil
Population's Cmax	2.7 ±0.3 ng/mL	1.8 ±0.4 μg/mL	2.3 ±1.4 μg/mL	130.4 ±75.8 ng/mL
Relative block				
hERG (%)	55	71	26	7
Calcium (%)	No block	8	No block	17
Late sodium (%)	No block	3	21	No block
ECG intervals				
QTc (ms)	74.7 ***	80.3 ***	12.7 **	-
	(66.7 to 82.6)	(69.3 to 91.2)	(8.1 to 17.3)	-
JTpeakc (ms)	39.2 ***	26.2 **	-	-
	(31.7 to 46.8)	(13.5 to 38.9)	-	-
Tpeak-Tend (ms)	36.3 ***	52.9 ***	11.6 ***	-
	(29.0 to 43.6)	(37.7 to 68.2)	(7.6 to 15.5)	-
T wave morphology				
Flatness (d.u.)	0.16 ***	0.21 ***	0.06 ***	-
	(0.14 to 0.18)	(0.19 to 0.34)	(0.05 to 0.08)	-
Asymmetry (d.u.)	0.25 ***	0.34 **	0.10 **	-
	(0.16 to 0.34)	(0.20 to 0.48)	(0.05 to 0.15)	-
Notch (%)	57.6 ***	70.4 ***	1.4 **	-
	(26.9 to 83.3)	(43.9 to 87.8)	(0.2 to 9.4)	-
Repolarization duration				
$ERD_{30\%}$ (ms)	23.4 ***	22.2 **	10.2 ***	-
	(16.1 to 30.8)	(13.9 to 30.5)	(7.3 to 13.2)	-
$LRD_{30\%}$ (ms)	13.1 ***	26.0 ***	3.5 **	-
	(7.4 to 18.7)	(15.5 to 36.5)	(0.9 to 6.0)	-
Vectorcardiographic				
QRST (°)	-3.9 ***	2.8 *	-	0.5 *
	(-5.4 to -2.4)	(-0.3 to 5.8)	-	(-1.0 to 1.9)
TCRT(rads)	0.08 ***	-	-	-0.01 *
	(0.04 to 0.11)	-	-	(-0.04 to 0.02)
Tmagmax (μV)	-146.6 ***	-170.3 ***	-66.6 **	-
	(-177.5 to -115.8)	(-210.3 to -130.2)	(-90.3 to -42.9)	-
Ventricular gradient (mV·ms)	-	-	-	-

Drug concentrations mean± SD. Relative ion channel block is from the Hill equation curve shown in Figure 2 at Cmax. ECG biomarker changes reported as mean values and 95% confident intervals. * p<0.5; ** p<0.01; *** p<0.001; (-) means there was no relationship between drug concentration and the ECG biomarker.

infarction [38]), where a decrease in TCRT is equivalent to a wider QRS-T angle. However, in this study pure hERG potassium channel block (dofetilide) did not cause an increase in the QRS-T angle, but rather caused a small decrease. In contrast, quinidine caused a small increase in the QRS-T angle. The small magnitude of the changes (∼5 degrees at Cmax) suggests that these changes are likely not clinically meaningful and these indices do not appear to have value for detecting hERG potassium channel block. There was also no change in the ventricular gradient with any drug, which has been proposed as a global marker of action potential morphology heterogeneity [32].

Our results show heart rate dependency for the maximum magnitude of the T vector, which is in concordance with previous studies [39, 40]. Andersen et al. [40] reported T wave flatness as heart rate independent, but our results show T wave flatness being heart rate dependent. The present study had a larger range of heart rates, and thus T wave flatness likely is heart rate dependent.

Limitations

This study involved only a single dose of each drug and it is possible that different doses or chronic dosing would have different effects on T wave morphology. We partially addressed this limitation by administering large doses

Author's version. Published in J Am Heart Assoc, 2015 (http://dx.doi.org/10.1161/JAHA.114.001615)

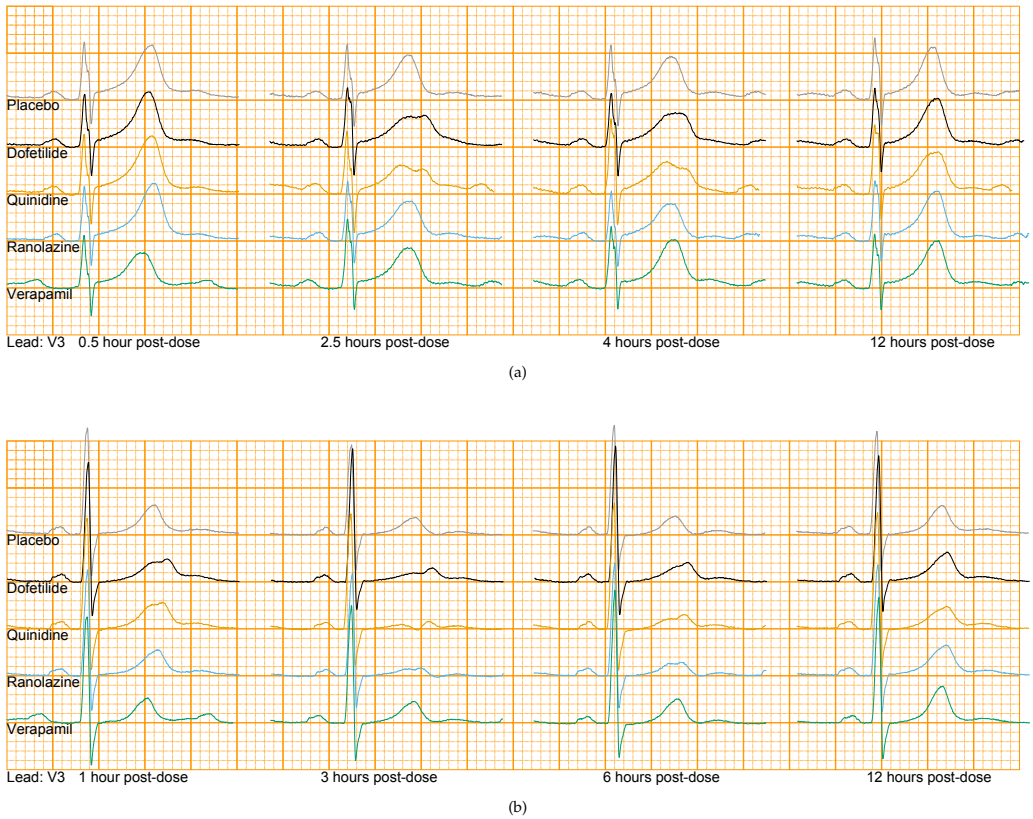

Figure 4: Lead V3 of median beats of time-matched placebo (gray), dofetilide (black), quinidine (orange), ranolazine (blue) and verapamil (green). Top panel (a): ECGs at 0.5, 2.5, 4 and 12 hours post dose from a woman with notches present in dofetilide and quinidine but not in ranolazine. Bottom panel (b): ECGs at 1, 3, 6 and 12 hours post dose from a woman with notches induced by ranolazine. See supplementary S.2 for heart rate and QT/QTc measurements.

of dofetilide, quinidine and ranolazine and performing concentration-dependent analysis with fifteen matched ECG and plasma samples for each subject with each drug. This resulted in a large range of plasma concentrations representative of chronic/steady state dosing levels for all drugs, although the population Cmax values for quinidine and verapamil were at the low end of the clinical range. All 4 drugs included in this study block hERG potassium channel, thus late sodium or calcium effects on T wave morphology could not be assessed independently. To address this limitation, we assessed each of the drugs in a standardized patch clamp protocol on hERG, calcium and late sodium currents.

All T wave morphology biomarkers were computed automatically, so incorrect determination of the peak of the T wave could affect the results. However, the large number of pharmacokinetic samples (15) after each drug administration coupled with triplicate ECG measurements minimizes this limitation. Although ECGs were extracted during periods of 10 minutes of supine resting, quinidine and verapamil induced heart rate changes. This effect was minimized by assessing the heart rate dependency for each biomarker and developing correction formulas when indicated.

Author's version. Published in J Am Heart Assoc, 2015 (http://dx.doi.org/10.1161/JAHA.114.001615)

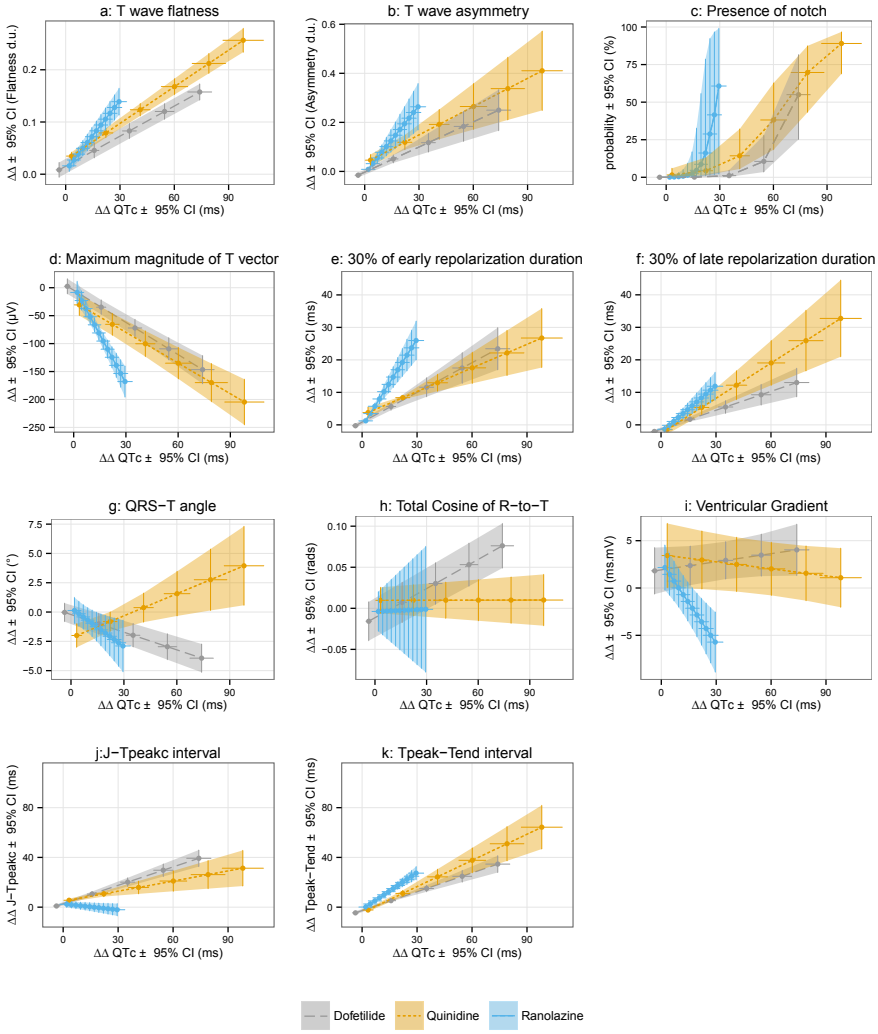

Figure 5: Relationship between predicted drug-induced baseline- and placebo-corrected changes in QTc (x axis) and T wave (a) flatness, (b) asymmetry, (c) probability of presence of notch, (d) maximum magnitude of T vector, (e) 30% of early and (f) late repolarization duration, (g) QRS-T angle, (h) total cosine of R to T, (i) spatial ventricular gradient, (j) early repolarization interval (J-Tpeakc) and (j) late repolarization interval (Tpeak-Tend) (y axis). Average predictions (dots) and 95% confidence intervals (horizontal and vertical lines) from concentration dependent models for QTc (x axis) and the different T wave morphology biomarkers (y axis) at baseline and 25% increments of population's Cmax for dofetilide (solid gray line) quinidine (dotted orange line) and ranolazine (dashed blue line).

Author's version. Published in J Am Heart Assoc, 2015 (http://dx.doi.org/10.1161/JAHA.114.001615)

Table 3: Drug concentration ranges

	Minimum (Individual)	**Mean** (Population's Cmax)	**Maximum** (Individual)
Dofetilide			
Plasma (ng/mL)	0	2.7	3.3
Estimated unbound free fraction (nM)	0	2.2	2.6
Relative to population Cmax (%)	0	100	120
Quinidine			
Plasma (μg/mL)	0.1	1.8	2.6
Estimated unbound free fraction (nM)	40.0	829.4	1179.1
Relative to population Cmax (%)	5	100	142
Ranolazine			
Plasma (μg/mL)	0	2.3	6.5
Estimated unbound free fraction (nM)	11.1	1726.7	4867.5
Relative to population Cmax (%)	0	100	282
Verapamil			
Plasma (ng/mL)	1.6	130.3	368
Estimated unbound free fraction (nM)	0.5	45.1	127.4
Relative to population Cmax (%)	0	100	282

Conclusion

This study demonstrated that there is a strong dose-response relationship between hERG potassium channel block and T wave morphology changes. While nonclinical studies have suggested that late sodium current block can reduce dispersion of repolarization from hERG block, we observed that ranolazine still had a dose-dose dependent relationship with T wave morphology, in some cases having greater T wave morphology changes at equivalent amounts of QTc prolongation compared to the pure hERG blocker dofetilide. Thus, the presence of T wave morphology changes is not a perfect predictor of torsade de pointes risk. However, this study supports that T wave morphology biomarkers (e.g. flatness, asymmetry and notching) likely have value in determining if QT prolongation is due to hERG block. Subsequently, analysis of J-Tpeak and Tpeak-Tend intervals may be able to inform whether a hERG blocking drug has additional late sodium or calcium current block that can mitigate torsade risk, as with ranolazine. Overall, the ECG signatures of drug-induced ion channel block closely parallel the ECG signatures seen with congenital long QT syndromes and a combined approach of assessing multiple ion channels, subintervals of the QT (e.g., J-Tpeak and Tpeak-Tend) and T wave morphology can provide the greatest insight into drug-ion channel interactions and torsade de pointes risk.

Acknowledgements

QTGuard+ was provided by GE Healthcare through a material transfer agreement. The mention of commercial products, their sources, or their use in connection with material reported herein is not to be construed as either an actual or implied endorsement of such products by the U.S. Department of Health and Human Services.

Funding sources

This study was supported by FDA's Critical Path Initiative, FDA's Office of Women's Health, appointments to the Research Participation Program at the Center for Devices and Radiological Health administered by the Oak Ridge Institute for Science and Education through an interagency agreement between the U.S. Department of Energy and the U.S. Food and Drug Administration. E.P. is funded by Ministerio de Economía y Competitividad (MINECO), Spain, under project TIN2013-41998-R and by Grupo Consolidado BSICoS from DGA (Aragón) and European Social Fund (EU).

Conflict of Interest Disclosures

None.

References

[1] Antzelevitch C and Shimizu W. Cellular mechanisms underlying the long qt syndrome. *Curr Opin Cardiol* 17(1):43–51, 2002.

[2] Sauer AJ and Newton-Cheh C. Clinical and genetic determinants of torsade de pointes risk. *Circulation* 125(13):1684–94, 2012.

Author's version. Published in J Am Heart Assoc, 2015 (http://dx.doi.org/10.1161/JAHA.114.001615)

[3] Moss AJ, Zareba W, et al. Ecg t-wave patterns in genetically distinct forms of the hereditary long qt syndrome. *Circulation* 92(10):2929–2934, 1995.

[4] Stockbridge N, Morganroth J, et al. Dealing with global safety issues: Was the response to qt-liability of non-cardiac drugs well coordinated? *Drug Saf* 36:167–82, 2013.

[5] Redfern WS, Carlsson L, et al. Relationships between preclinical cardiac electrophysiology, clinical qt interval prolongation and torsade de pointes for a broad range of drugs: evidence for a provisional safety margin in drug development. *Cardiovasc Res* 58(1):32–45, 2003.

[6] Food U and Administration D. Guidance for industry e14 clinical evaluation of qt/qtc interval prolongation and proarrhythmic potential for non-antiarrhythmic drugs, 2005. URL `http://www.fda.gov/downloads/drugs/guidancecomplianceregulatoryinformation/guidances/ucm073153.pdf`.

[7] on Harmonisation IC. Ich topic s7b the nonclinical evaluation of the potential for delayed ventricular repolarization (qt interval prolongation) by human pharmaceuticals., 2005. URL `http://www.ich.org/fileadmin/Public_Web_Site/ICH_Products/Guidelines/Safety/S7B/Step4/S7B_Guideline.pdf`.

[8] Hohnloser SH, Klingenheben T, and Singh BN. Amiodarone-associated proarrhythmic effects. a review with special reference to torsade de pointes tachycardia. *Ann Intern Med* 121(7):529–535, 1994.

[9] Aiba T, Shimizu W, et al. Cellular and ionic mechanism for drug-induced long qt syndrome and effectiveness of verapamil. *J Am Coll Cardiol* 45(2):300–7, 2005.

[10] Antzelevitch C. Role of transmural dispersion of repolarization in the genesis of drug-induced torsades de pointes. *Heart Rhythm* 2(11, Supplement 2):S9–S15, 2005.

[11] January CT and Riddle JM. Early afterdepolarizations: mechanism of induction and block. a role for l-type ca2+ current. *Circ Res* 64(5):977–90, 1989.

[12] Kramer J, Obejero-Paz CA, et al. Mice models: superior to the herg model in predicting torsade de pointes. *Sci Rep* 3:2100, 2013.

[13] Roden D, Woosley R, and Primm R. Incidence and clinical features of the quinidine-associated long qt syndrome: implications for patient care. *Am Heart J* 111:1088–93, 1986.

[14] Wu L, Guo D, et al. Role of late sodium current in modulating the proarrhythmic and antiarrhythmic effects of quinidine. *Heart Rhythm* 5(12):1726–34, 2008.

[15] Antzelevitch C, Belardinelli L, et al. Electrophysiological effects of ranolazine, a novel antianginal agent with antiarrhythmic properties. *Circulation* 110(8):904–10, 2004.

[16] Johannesen L, Vicente J, et al. Differentiating drug-induced multichannel block on the electrocardiogram: randomized study of dofetilide, quinidine, ranolazine, and verapamil. *Clin Pharmacol Ther* 96(5):549–58, 2014.

[17] Andersen MP, Xue J, et al. A robust method for quantification of ikr-related t-wave morphology abnormalities. In *Comput Cardiol*, 341–344. Comput Cardiol.

[18] Couderc JP, Vaglio M, et al. Electrocardiographic method for identifying drug-induced repolarization abnormalities associated with a reduction of the rapidly activating delayed rectifier potassium current. In *Conf Proc IEEE Eng Med Biol Soc*, 4010–15. IEEE.

[19] Couderc JP, McNitt S, et al. Improving the detection of subtle i(kr)-inhibition: assessing electrocardiographic abnormalities of repolarization induced by moxifloxacin. *Drug Saf* 31(3):249–60, 2008.

[20] Kardys I, Kors JA, et al. Spatial qrs-t angle predicts cardiac death in a general population. *Eur Heart J* 24(14):1357–1364, 2003.

[21] Whang W, Shimbo D, et al. Relations between qrs | t angle, cardiac risk factors, and mortality in the third national health and nutrition examination survey (nhanes iii). *Am J Cardiol* 109(7):981–987, 2012.

[22] Acar B, Yi G, et al. Spatial, temporal and wavefront direction characteristics of 12-lead t-wave morphology. *Med Biol Eng Comput* 37(5):574–84, 1999.

[23] Fridericia LS. Die systolendauer im elektrokardiogramm bei normalen menschen und bei herzkranken. *Acta Med Scand* 53(1):469–486, 1920.

[24] Williams E. Experimental designs balanced for the estimation of residual effects of treatments. *Aust J Chem* 2(2):149–168, 1949.

[25] Drugs@FDA. Dofetilide label, 2013. URL `http://www.accessdata.fda.gov/drugsatfda_docs/label/2013/020931s007lbl.pdf`.

[26] DailyMed. Quinidine sulfate label, 2013. URL `http://dailymed.nlm.nih.gov/dailymed/drugInfo.cfm?setid=a90a03b0-ffbe-4cf6-90b5-bfb0412a1cb2`.

[27] Drugs@FDA. Ranolazine label, 2013. URL `http://www.accessdata.fda.gov/drugsatfda_docs/label/2013/021526s026lbl.pdf`.

Author's version. Published in J Am Heart Assoc, 2015 (http://dx.doi.org/10.1161/JAHA.114.001615)

[28] DailyMed. Verapamil label, 2014. URL `http://dailymed.nlm.nih.gov/dailymed/drugInfo.cfm?setid=10881745-3a16-44c3-9b94-60433218f1d6`.

[29] Badilini F, Vaglio M, and Sarapa N. Automatic extraction of ecg strips from continuous 12-lead holter recordings for qt analysis at prescheduled versus optimized time points. *Ann Noninvasive Electrocardiol* 14(Suppl 1):S22–9, 2009.

[30] Johannesen L, Vicente J, et al. Egclib: Library for processing electrocardiograms. In *Comput Cardiol*, 951–954. IEEE.

[31] Guldenring D, Finaly D, et al. Transformation of the mason-likar 12-lead electrocardiogram to the frank vectorcardiogram. In *Conf Proc IEEE Eng Med Biol Soc*, 677–680. IEEE.

[32] Draisma HH, Schalij MJ, et al. Elucidation of the spatial ventricular gradient and its link with dispersion of repolarization. *Heart rhythm : the official journal of the Heart Rhythm Society* 3:1092–1099, 2006.

[33] Johannesen L, Vicente J, et al. Improving the assessment of heart toxicity for all new drugs through translational regulatory science. *Clin Pharmacol Ther* 95(5):501–508, 2014.

[34] Crumb WJ, Pigott JD, and Clarkson CW. Description of a nonselective cation current in human atrium. *Circ Res* 77(5):950–956, 1995.

[35] Lupoglazoff JM, Denjoy I, et al. Notched t waves on holter recordings enhance detection of patients with lqt2 (herg) mutations. *Circulation* 103(8):1095–101, 2001.

[36] Sager PT, Gintant G, et al. Rechanneling the cardiac proarrhythmia safety paradigm: a meeting report from the cardiac safety research consortium. *Am Heart J* 167(3):292–300, 2014.

[37] Couderc JP, Zhou M, et al. Investigating the effect of sotalol on the repolarization intervals in healthy young individuals. *J Electrocardiol* 41(6):595–602, 2008.

[38] Zabel M, Acar B, et al. Analysis of 12-lead t-wave morphology for risk stratification after myocardial infarction. *Circulation* 102(11):1252–1257, 2000.

[39] Couderc J, Vaglio M, et al. Impaired T-amplitude adaptation to heart rate characterizes IKr inhibition in the congenital and acquired forms of the long QT syndrome. *J Cardiovasc Electrophysiol* 18(12):1299–1305, 2007.

[40] Andersen M, Xue J, et al. New descriptors of t-wave morphology are independent of heart rate. *Journal of electrocardiology* 41(6):557–561, 2008.

Supplementary materials

Supplementary tables

Table S.1: Relationship between plasma drug concentrations and ECG measurements that correlate with graphs in Figure 3.

	Dofetilide ng/mL	**Quinidine** μg/mL	**Ranolazine** μg/mL	**Verapamil** ng/mL
ECG intervals				
QTc (ms)	28.5 ***	42.3 ***	4.3 ***	0.01
	(25.4 to 31.6)	(35.9 to 46.6)	(2.3 to 6.4)	(-0.02 to 0.04, p=0.39)
JTpeakc (ms)	14.1 ***	11.6 **	-0.7	0.0
	(11.0 to 17.3)	(3.3 to 19.8)	(-2.4 to 1.0, p=0.39)	(-0.02 to 0.02, p=0.85)
Tpeak-Tend (ms)	14.5 ***	29.9 ***	4.4 ***	0.01 *
	(11.0 to 17.9)	(19.2 to 40.7)	(2.6 to 6.2)	(0.0 to 0.02)
T wave morphology				
Flatness (d.u.)	0.05 ***	0.10 ***	0.02 ***	0.0
	(0.05 to 0.06)	(0.08 to 0.11)	(0.01 to 0.03)	(0.0 to 0.0, p=0.68)
Asymmetry (d.u.)	0.10 ***	0.16 **	0.04 **	0.0
	(0.06 to 0.14)	(0.07 to 0.25)	(0.02 to 0.06)	(0.0 to 0.0, p=0.24)
Notch probability	3.48***	2.93 ***	1.13 **	2.23
(logit units†)	(2.38 to 4.58)	(2.09 to 3.77)	(0.28 to 1.97)	(-25.77 to 30.24, p=0.88)
Repolarization duration				
$ERD_{30\%}$ (ms)	8.7 ***	10.0 **	3.9 ***	0.01
	(5.5 to 11.9)	(4.1 to 16.4)	(2.3 to 5.5)	(0.0 to 0.02, p=0.11)
$LRD_{30\%}$ (ms)	5.6 ***	15.3 ***	2.1 **	0.01
	(3.0 to 8.1)	(8.5 to 22.0)	(0.7 to 3.5)	(0.0 to 0.01, p=0.16)
Vectorcardiographic				
QRST (°)	-1.4 ***	2.6 *	-0.5	0.01*
	(-1.9 to -1.0)	(0.4 to 4.9)	(-1.4 to 0.4, p=0.28)	(0.0 to 0.02)
TCRT(rads)	0.03 ***	0.0	0.0	0.0*
	(0.02 to 0.05)	(-0.02 to 0.02, p=0.99)	(-0.04 to 0.04, p=0.86)	(0.0 to 0.0)
Tmagmax (μV)	-54.8 ***	-77.5 ***	-25.2 **	-0.1
	(-69.1 to -40.4)	(-102.5 to -52.5)	(-41.1 to 0.1)	(-0.4 to 0.0, p=0.12)
Ventricular gradient	0.8	-1.0	-1.2	-0.01
(m·Vms)	(-1.0 to 2.7, p=0.37)	(-3.7 to 1.6, p=0.41)	(-3.0 to 0.5, p=0.15)	(-0.03 to 0.01, p=0.44)

Mean slopes± 95% confident intervals. * p<0.5; ** p<0.01; *** p<0.001. † from logistic regression model.

Table S.2: Global measurements of ECGs shown in Figure 4

Subject		**Measuements per time point**											
			0.5			2.5			4			12	
A	Treatment	HR	QT	QTc	HR	QT	QTc	HR	QT	QTc	HR	QT	QTc
	Placebo	64	398	409	72	379	403	74	378	407	83	355	397
	Dofetilide	65	387	397	71	462	489	76	419	453	82	374	415
	Quinidine	65	403	416	82	454	506	82	441	489	87	390	443
	Ranolazine	62	410	415	71	392	415	80	373	411	78	373	407
	Verapamil	79	373	411	73	389	415	76	406	439	75	376	407
		Measuements per time point											
			0.5			2.5			4			12	
B	Treatment	HR	QT	QTc	HR	QT	QTc	HR	QT	QTc	HR	QT	QTc
	Placebo	65	405	418	67	402	419	75	381	412	67	397	412
	Dofetilide	66	460	477	66	478	496	72	442	472	66	418	431
	Quinidine	68	457	479	72	470	502	75	448	485	69	441	462
	Ranolazine	65	424	435	73	399	426	74	399	430	65	414	427
	Verapamil	81	379	421	70	397	420	73	386	412	68	389	406

Time point (hours post-dose); heart rate ([HR] beats per minute); QT (ms); QTc (ms).

Supplementary figures

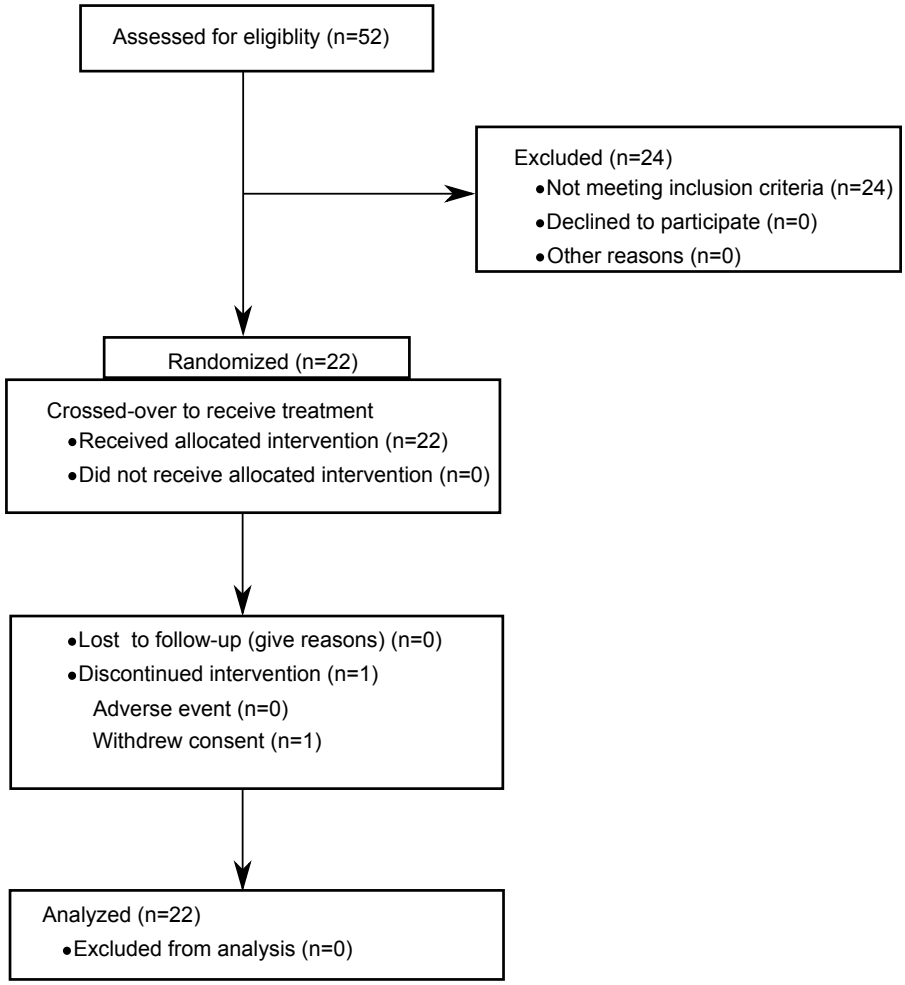

Figure S.1: CONSORT diagram for the study. Twenty four of the 52 screened subjects did not meet the inclusion criteria. Twenty two of the 28 subjects who met the inclusion criteria were randomized. All subjects completed the study, except one who withdrew prior to the last treatment period.

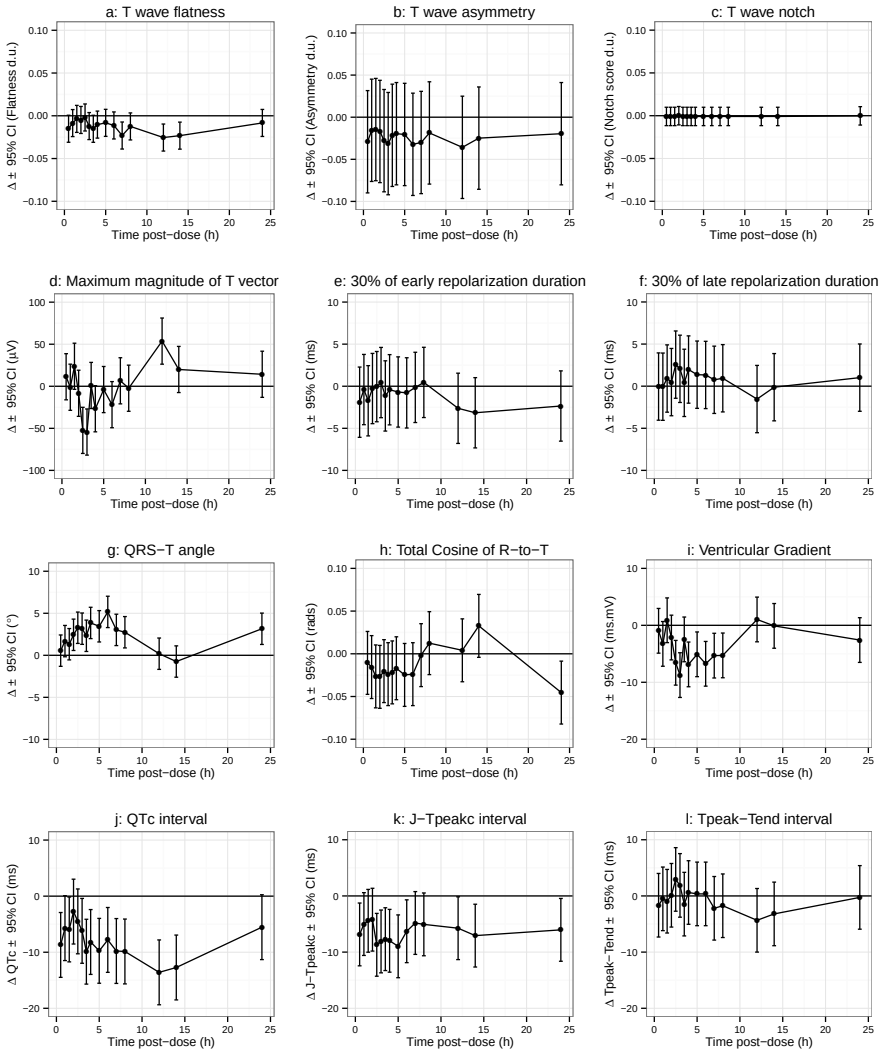

Figure S.2: Placebo changes from baseline for (a) T wave flatness, (b) asymmetry, (c) probability of notch, (d) maximum magnitude of the T vector, (e) 30% of early repolarization duration, (f) 30% of late repolarization duration, (g) QRS-T angle, (h) total cosine R-to-T, (i) ventricular gradient, (j) QTc, (k) J-Tpeakc and (l) Tpeak-Tend.

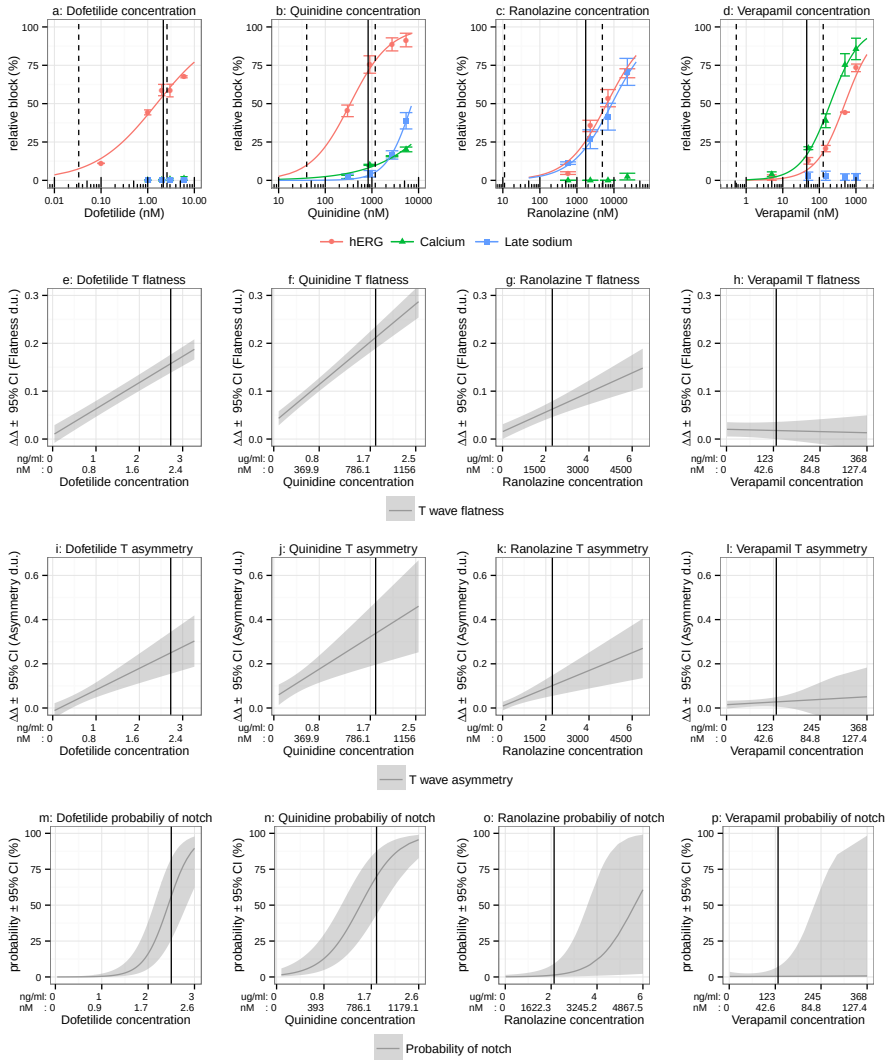

Figure S.3: Patch clamp experiments results for (a) dofetilide, (b) quinidine, (c) ranolazine and (d) verapamil for hERG (red), calcium (green) and late sodium (blue). The lines in each plot correspond to a fit between the observed means per concentration and data (see text). The error bars denote ± SEM. The dashed lines in each panel correspond to the range of observed clinical concentrations and the solid line is the population average maximum concentration (Cmax). Corresponding mean baseline- and placebo-corrected plasma drug concentration-dependent changes (lines) and 95% confidence intervals (shaded areas) for drug-induced effects on: T wave flatness for (e) dofetilide, (f) quinidine, (g) ranolazine and (h) verapamil; T wave asymmetry for (i) dofetilide, (j) quinidine, (k) ranolazine and (l) verapamil; and probability of notch for (m) dofetilide, (n) quinidine, (o) ranolazine and (p) verapamil. X axis shows plasma drug concentrations and the corresponding estimated unbound free fraction in nM (see Table 3).

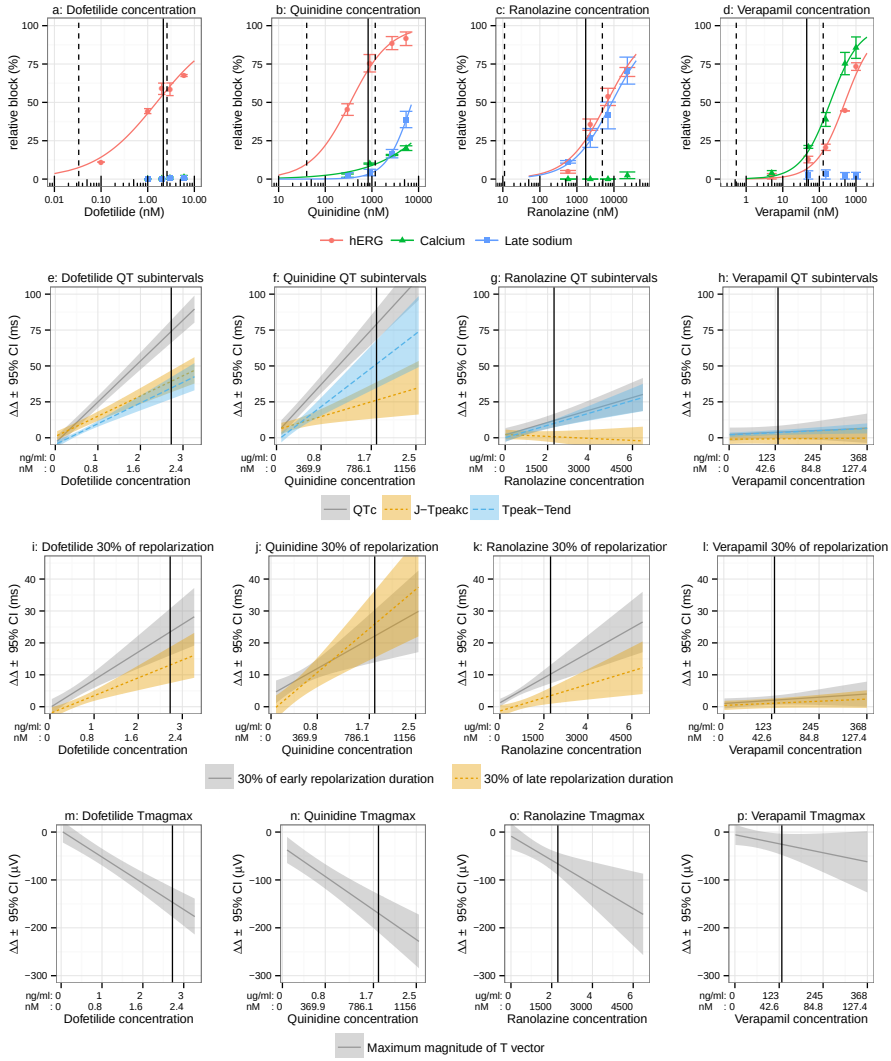

Figure S.4: Patch clamp experiments results for (a) dofetilide, (b) quinidine, (c) ranolazine and (d) verapamil for hERG (red), calcium (green) and late sodium (blue). The lines in each plot correspond to a fit between the observed means per concentration and data (see text). The error bars denote ± SEM. The dashed lines in each panel correspond to the range of observed clinical concentrations and the solid line is the population average maximum concentration (Cmax). Corresponding mean baseline- and placebo-corrected plasma drug concentration-dependent changes (lines) and 95% confidence intervals (shaded areas) for drug-induced effects: on QT subintervals for (e) dofetilide, (f) quinidine, (g) ranolazine and (h) verapamil (QTc [solid gray], early repolarization interval [J-Tpeakc, dotted orange] and late repolarization [Tpeak-Tend, blue dashed]); on 30% of early (solid gray) and late (dotted orange) repolarization duration for (i) dofetilide, (j) quinidine, (k) ranolazine and (l) verapamil; and maximum magnitude of the T vector for (m) dofetilide, (n) quinidine, (o) ranolazine and (p) verapamil. X axis shows plasma drug concentrations and the corresponding estimated unbound free fraction in nM (see Table 3). QT subintervals as previously reported [16].

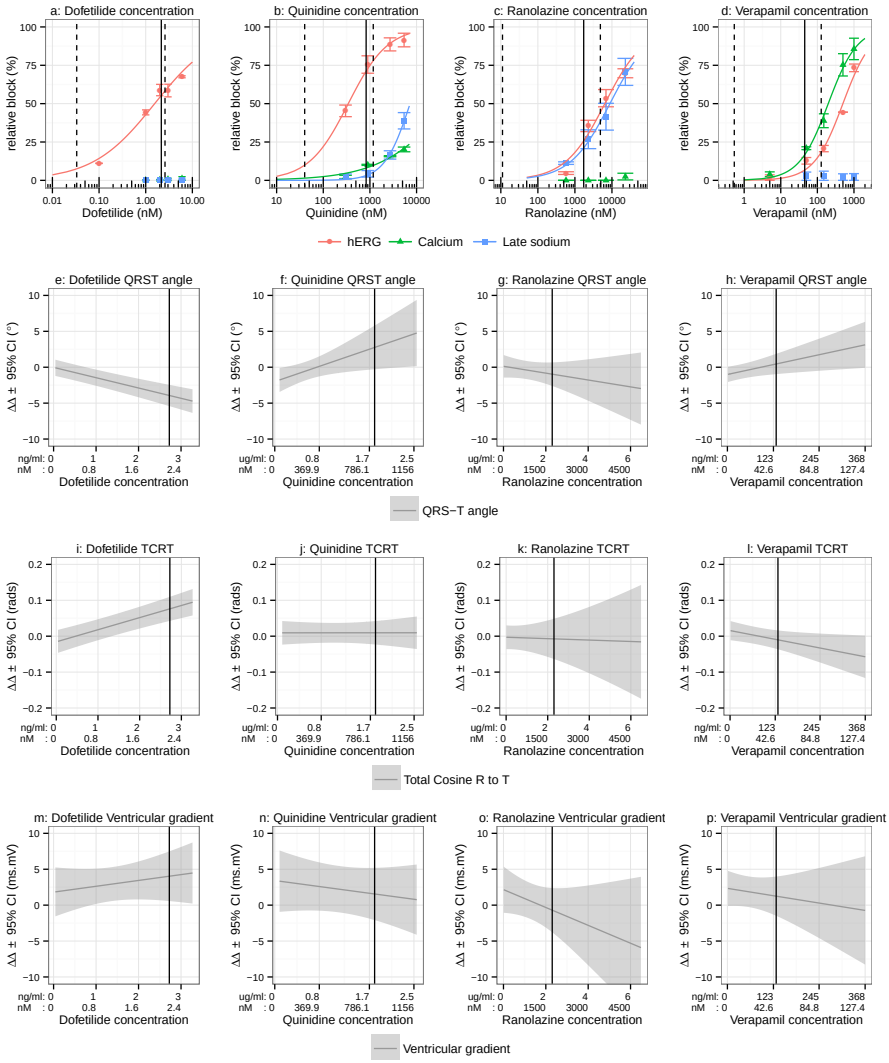

Figure S.5: Patch clamp experiments results for (a) dofetilide, (b) quinidine, (c) ranolazine and (d) verapamil for hERG (red), calcium (green) and late sodium (blue). The lines in each plot correspond to a fit between the observed means per concentration and data (see text). The error bars denote ± SEM. The dashed lines in each panel correspond to the range of observed clinical concentrations and the solid line is the population average maximum concentration (Cmax). Corresponding mean baseline- and placebo-corrected plasma drug concentration-dependent changes (lines) and 95% confidence intervals (shaded areas) for drug-induced effects on: QRS-T angle for (e) dofetilide, (f) quinidine, (g) ranolazine and (h) verapamil; total cosine R to T for (i) dofetilide, (j) quinidine, (k) ranolazine and (l) verapamil; and spatial ventricular gradient for (m) dofetilide, (n) quinidine, (o) ranolazine and (p) verapamil. X axis shows plasma drug concentrations and the corresponding estimated unbound free fraction in nM (see Table 3).

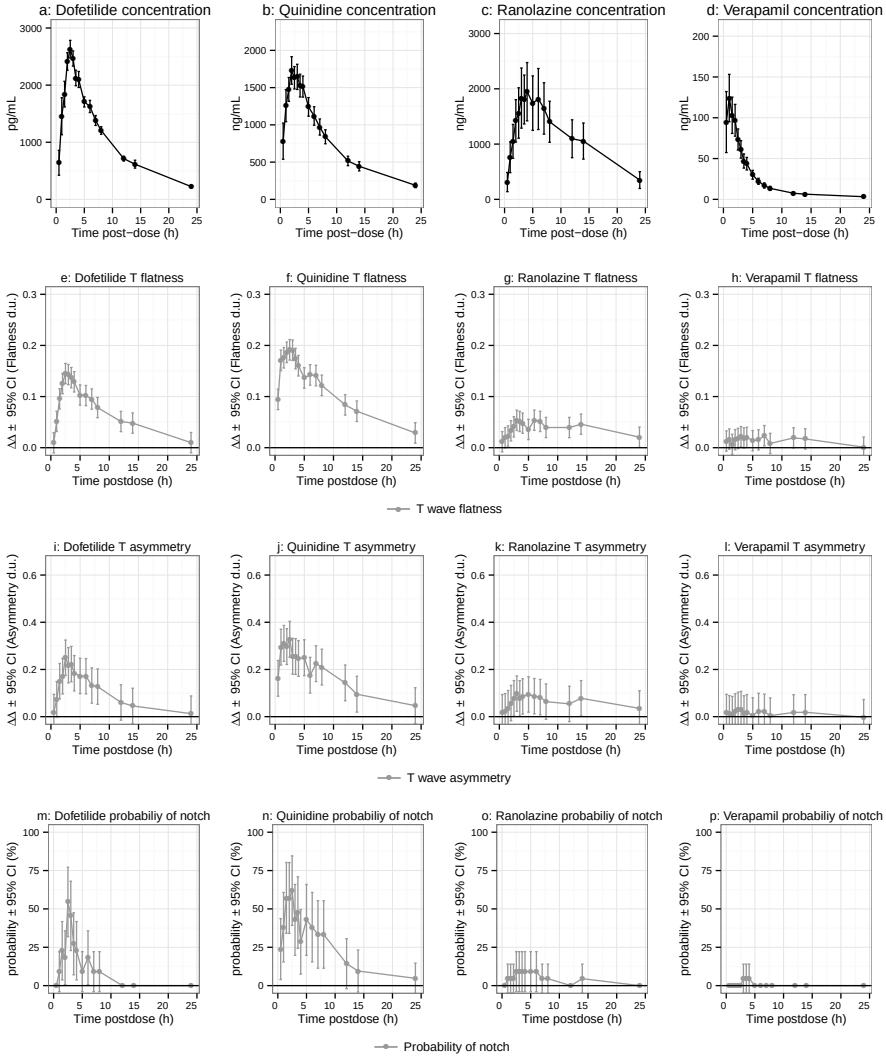

Figure S.6: Time profiles of average plasma drug concentration for (a) dofetilide, (b) quinidine, (c) ranolazine and (d) verapamil for hERG (red), calcium (green) and late sodium (blue). The error bars denote ± 95% confidence intervals. Time-matched mean baseline- and placebo-corrected drug-induced changes (lines) and 95% confidence intervals (error bars) on T wave flatness for (e) dofetilide, (f) quinidine, (g) ranolazine and (h) verapamil; T wave asymmetry for (i) dofetilide, (j) quinidine, (k) ranolazine and (l) verapamil; and probability of notch for (m) dofetilide, (n) quinidine, (o) ranolazine and (p) verapamil. X axis shows time post dose in hours. Plasma drug concentrations as previously reported [16].

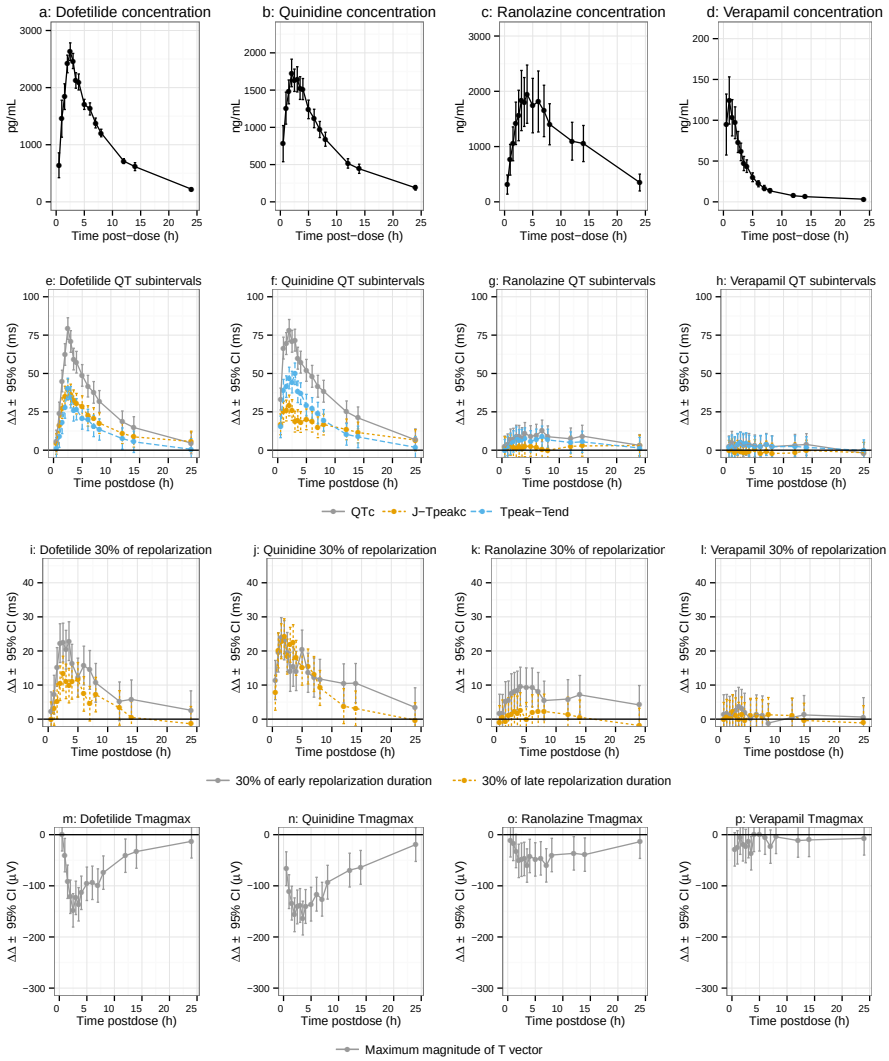

Figure S.7: Time profiles of average plasma drug concentration for (a) dofetilide, (b) quinidine, (c) ranolazine and (d) verapamil for hERG (red), calcium (green) and late sodium (blue). The error bars denote ± 95% confidence intervals. Time-matched mean baseline- and placebo-corrected drug-induced changes (lines) and 95% confidence intervals (error bars) on QT subintervals for (e) dofetilide, (f) quinidine, (g) ranolazine and (h) verapamil (QTc [solid gray], early repolarization interval [J-Tpeakc, dotted orange] and late repolarization [Tpeak-Tend, blue dashed]); on 30% of early (solid gray) and late (dotted orange) repolarization duration for (i) dofetilide, (j) quinidine, (k) ranolazine and (l) verapamil; and maximum magnitude of the T vector for (m) dofetilide, (n) quinidine, (o) ranolazine and (p) verapamil. X axis shows time post dose in hours. Panels of plasma drug concentrations and QT subintervals as previously reported [16].

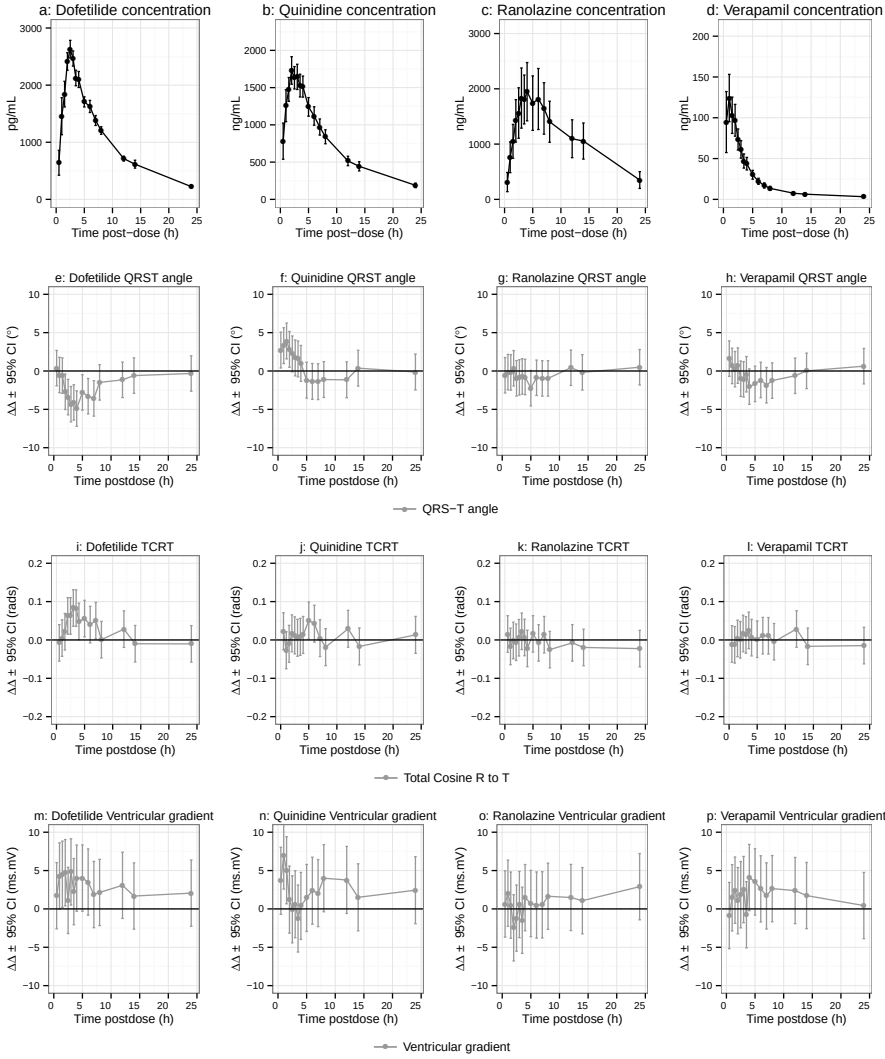

Figure S.8: Time profiles of average plasma drug concentration for (a) dofetilide, (b) quinidine, (c) ranolazine and (d) verapamil for hERG (red), calcium (green) and late sodium (blue). The error bars denote ± 95% confidence intervals. Time-matched mean baseline- and placebo-corrected drug-induced changes (lines) and 95% confidence intervals (error bars) on QRS-T angle for (e) dofetilide, (f) quinidine, (g) ranolazine and (h) verapamil; total cosine R to T for (i) dofetilide, (j) quinidine, (k) ranolazine and (l) verapamil; and spatial ventricular gradient for (m) dofetilide, (n) quinidine, (o) ranolazine and (p) verapamil.. X axis shows time post dose in hours. Plasma drug concentrationss as previously reported [16].

CHAPTER 5

Study IV

Sex differences in drug-induced changes in ventricular repolarization

Vicente J, Johannesen L, et al. Sex differences in drug-induced changes in ventricular repolarization. *J Electrocardiol* 48(6):1081–1087, 2015

Author's version. Published in J Electrocardiol, 2015 (http://dx.doi.org/10.1016/j.jelectrocard.2015.08.004)

Sex Differences in Drug-Induced Changes in Ventricular Repolarization

J Vicente[1,2,6,✉], L Johannesen[1,3], JW Mason [4], E Pueyo[5,6], N Stockbridge[2], and DG Strauss[1]

[1]*Office of Science and Engineering Laboratories, CDRH, US FDA, Silver Spring, MD, USA*
[2]*Division of Cardiovascular and Renal Products, Office of New Drugs, CDER, US FDA , Silver Spring, MD, USA*
[3]*Department of Clinical Physiology, Karolinska Institutet and Karolinska University Hospital, Stockholm, Sweden*
[4]*Spaulding Clinical Research, West Bend, WI, USA*
[5]*Biomedical Research Networking Center in Bioengineering, Biomaterials and Nanomedicine (CIBER-BBN), Spain*
[6]*BSICoS Group, Aragón Institute for Engineering Research (I3A), IIS Aragón, University of Zaragoza, Spain*

Abstract

Introduction: *Heart rate corrected QT (QTc) interval prolongation is a predictor of drug-induced torsade de pointes, a potentially fatal ventricular arrhythmia that disproportionately affects women. This study assesses whether there are sex differences in the ECG changes induced by four different hERG potassium channel blocking drugs.* ***Methods and Results:*** *Twenty-two healthy subjects (11 women) received a single oral dose of dofetilide, quinidine, ranolazine, verapamil and placebo in a double-blind 5-period crossover study. ECGs and plasma drug concentrations were obtained at pre-dose and at 15 time-points post-dose. Dofetilide, quinidine and ranolazine prolonged QTc. There were no sex differences in QTc prolongation for any drug, after accounting for differences in exposure. Sex differences in any ECG biomarker were observed only with dofetilide, which caused greater J-Tpeakc prolongation (p=0.045) but lesser Tpeak-Tend prolongation (p=0.006) and lesser decrease of T wave amplitude (p=0.003) in women compared to men.* ***Conclusions:*** *There were no sex differences in QTc prolongation for any of the studied drugs. Moreover, no systematic sex differences in other drug-induced ECG biomarker changes were observed in this study. This study suggests that the higher torsade risk in women compared to men is not due to a larger concentration-dependent QTc prolongation.*

Clinical Trial Registration Information*: http://clinicaltrials.gov/ct2/show/NCT01873950 (NCT01873950)*
Keywords*: sex differences; QTc prolongation; T wave morphology; torsade de pointes; drugs; hERG block*

Women are at higher risk for drug-induced torsade de pointes, a potentially fatal ventricular arrhythmia [1]. The reason for the higher drug-induced torsade risk in women is not entirely clear. It might be because women are smaller than men and thus are exposed to higher drug concentrations, there may be sex differences in the electrophysiology of the heart that make women more susceptible or there may be sex differences in drug metabolism and transport that make women more susceptible.

Almost all drugs that cause torsade block the human ether-a-go-go related gene (hERG) potassium channel [2] and prolong the heart rate corrected QT interval (QTc) on the electrocardiogram (ECG) [3]. Previous clinical studies with different drugs (e.g. quinidine [4], ibutilide [5], rac-sotalol [6]) have shown greater drug-induced QTc prolongation relative to serum drug concentration in women compared to men. However, it has been shown recently that sex differences in the delay between serum quinidine concentration and ECG changes (hysteresis [7]) in a study of intravenous quinidine may have contributed to observed sex differences in quinidine-induced QTc prolongation [8].

Sex- and age-differences in ventricular repolarization at baseline have been reported since the 1920s [9, 10, 11]. Specifically, longer QTc in women compared to men is explained by longer early repolarization (J-Tpeak), despite women having shorter depolarization (QRS) and shorter late repolarization (Tpeak-Tend) than men do [11]. The shorter J-Tpeak interval in men is likely due to reduced calcium current by testosterone [11]. Testosterone-induced calcium block may prevent occurrence of early after depolarizations [12, 13], which are the triggers for torsade, and therefore may lower the risk for torsade in men. However, it is still not clear how other physiological mechanisms contribute to these baseline differences and how they might be related to drug-induced torsade risk.

Sex differences in drug-induced ECG changes may provide insights for the higher risk for drug-induced torsade in women. In this study we assess whether there are sex differences in the ECG changes (QTc, but also QT subintervals and T wave morphology) induced by a selective hERG potassium channel drug (dofetilide) and three drugs that

✉Jose Vicente, MSc. U.S. Food and Drug Administration. 10903 New Hampshire Avenue, WO62-1125B. Silver Spring, MD, 20993, USA. E-mail: jose.vicente@fda.hhs.gov. Telephone: 301-796-8442 - Fax: 301-796-9927

Author's version. Published in J Electrocardiol, 2015 (http://dx.doi.org/10.1016/j.jelectrocard.2015.08.004)

block the hERG potassium channel but also block calcium or late sodium inward currents (quinidine, ranolazine and verapamil).

Methods

Clinical study design

The design of this clinical study has been described previously [14]. Briefly, 22 healthy subjects (11 women) received a single oral dose of dofetilide, quinidine, ranolazine, verapamil and placebo in a double-blind 5-period crossover study at a clinical research unit (Spaulding Clinical, West Bend, Wisconsin, USA). ECGs and plasma drug concentrations were obtained pre-dose and at 15 time-points post-dose (0.5, 1, 1.5, 2, 2.5, 3, 3.5, 4, 5, 6, 7, 8, 12, 14, 24 h), during which the subjects were resting in a supine position for 10 min. Continuous 12-lead ECGs were recorded at 500 Hz and with an amplitude resolution of 2.5 μV using the Mason-Likar electrode configuration [15]. Plasma drug concentration was measured using a validated liquid chromatography with tandem mass spectroscopy method by Frontage Laboratories (Exton, Philadelphia, PA). The study was approved by the U.S. Food and Drug Administration Research Involving Human Subjects Committee and the local institutional review board. All subjects gave written informed consent.

ECG analysis

From the continuous recording and within the 10 min resting supine period at each of the 16 predefined time-points, triplicate non-overlapping 10-second ECGs with more stable heart rates and maximum signal quality were extracted using Antares software (AMPS-LLC, New York City, NY, USA)[16]. The extracted ECGs were up-sampled from 500 Hz to 1000 Hz and semi-automatically evaluated by ECG readers blinded to treatment and time as described elsewhere [14, 17]. Briefly, global measures of PR, QT, QRS, J-Tpeak and Tpeak-Tend intervals were semi-automatically measured in the vectormagnitude lead. In addition to these ECG intervals, different T wave morphology (e.g., T wave amplitude, flatness, asymmetry and notching) and vectorcardiographic biomarkers were automatically measured [18]. T wave flatness, asymmetry and presence of notch [19] were assessed with QTGuard+ (GE Healthcare, Milwaukee, Wisconsin, USA). All the other T wave morphology (30% of repolarization duration [20]) and vectorcardiographic biomarkers (QRS-T angle, ventricular gradient, maximum magnitude of the T vector [T wave amplitude] and total cosine R-to-T [TCRT][21]) were automatically assessed with ECGlib [22].

Heart rate corrected QT (QTc) was computed using Fridericia's correction formula [23]. All heart rate dependent ECG biomarkers were corrected using an exponential model ($\text{biomarker}_c = \frac{\text{biomarker}}{(\text{RR}/1000)^{\alpha}}$), allowing the relationship to be sex dependent as previously described [18]. No sex-specific differences in the heart rate dependency were found [18] and the values of α coefficient were 0.58 for J-Tpeak, 0.96 for T wave amplitude (measured as the maximum magnitude of the T vector), 0.85 for ventricular gradient and 0.58 for T wave flatness.

Statistical analysis

Unpaired Student's t-tests were computed to assess baseline differences between women and men in each ECG biomarker using R version 3.1.2 (R Foundation for Statistical Computing, Vienna, Austria). The placebo-corrected change from baseline was computed using PROC MIXED in SAS 9.3 (SAS institute, Cary, North Carolina, USA), where the change from baseline for each ECG biomarker by time-point was the dependent variable. Sequence, period, time, drug, and an interaction between treatment and time were included as fixed effects, and subject was included as a random effect. Afterwards, we performed an exposure-response analysis similar to the one proposed for early QT assessment [24] but for a single-dose placebo-controlled randomized crossover study design. Briefly, a linear-mixed effects model was used to evaluate the relationship between each ECG biomarker (except notch) and plasma drug concentrations. This was done using PROC MIXED in SAS 9.3, and having a random effect on both intercept and slope (i.e., allowing each subject to have his own drug concentration-biomarker change relationship). A logistic regression model was used to evaluate the relationship between presence of notch and drug concentration including a random effect on intercept in SAS (PROC GLIMMIX). Sex differences were evaluated by the interaction between slope and intercept of effect by drug level (to adjust for differences in exposure) and sex in a linear mixed effects model with PROX MIXED in SAS. p-values <0.05 were considered statistically significant without adjustment for multiplicity.

Results

Twenty-two healthy subjects (11 females) with a mean age of 26.9 $\pm$ 5.5 years participated in this randomized controlled clinical trial. All subjects completed the study except for one subject who withdrew prior to the last treatment period (quinidine period for that subject). This resulted in 5232 of the 5280 planned ECGs. There were no unexpected treatment related adverse events.

At baseline (supplementary table S1), women had higher heart rates, but shorter QRS duration (p=0.010), late repolarization interval (Tpeak-Tend , p=0.044), 30% of early (ERD30%, p=0.002) and late (LRD30%, p=0.011) repolarization duration and smaller ventricular gradient (p =0.009)

Author's version. Published in J Electrocardiol, 2015 (http://dx.doi.org/10.1016/j.jelectrocard.2015.08.004)

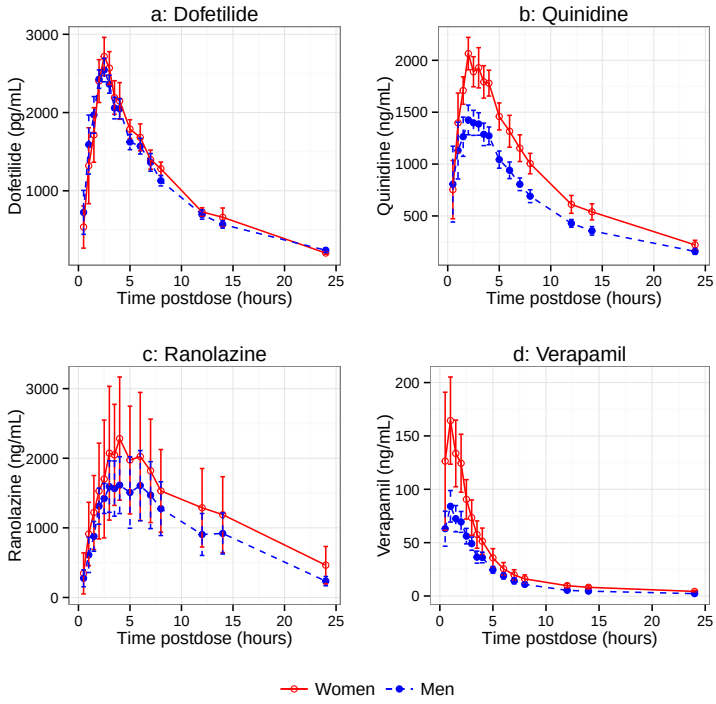

Figure 1: Measured plasma drug concentration (mean ± 95% confidence intervals) in women (red open circles) and men (closed blue circles) for (a) dofetilide, (b) quinidine, (c) ranolazine and (d) verapamil.

than men did. Early repolarization interval (J-Tpeakc) was longer (p = 0.001) in women compared with men. There were trends toward women having longer QTc (p = 0.065), greater TCRT (p = 0.064) and smaller T wave amplitude (p = 0.064) than men at baseline. No additional sex differences were observed at baseline.

Time-dependent Analysis

Results of the pharmacokinetic analysis are shown in Figure 1 for each drug: (a) dofetilide, (b) quinidine, (c) ranolazine and (d) verapamil. There were no differences between women and men in the pharmacokinetic profiles of dofetilide and ranolazine. However, the maximum plasma drug concentration of quinidine and verapamil were higher in women than in men (2074 [95% confidence interval 1897 to 2268] vs. 1506 [1340 to 1693] ng/mL, p < 0.001 and 156.9 [11.5 to 220.9] vs. 82.21 [66.4 to 101.9] ng/mL, p = 0.002 respectively, Figure 1).

Figure 2 shows the time-matched placebo- and baseline-corrected drug-induced QTc changes (ΔQTc) for each drug: (a) dofetilide, (b) quinidine, (c) ranolazine and (d) verapamil. There were no differences between women and men in the ΔQTc prolongation induced by dofetilide, quinidine or ranolazine (Figure 2). Verapamil increased the heart rate and PR interval, but did not cause ΔQTc prolongation or any other changes in the additional ECG biomarkers assessed in this study.

Concentration-dependent Analysis

There were no sex differences in the relationship between plasma drug concentration and ΔQTc prolongation induced by dofetilide (Figure 3), quinidine (supplementary Figure 1) or ranolazine (supplementary Figure 2). Sex differences were observed only with dofetilide, which caused greater concentration dependent ΔJ-Tpeakc prolongation (17 [95% confidence interval: 13 - 21.1] vs. 11.1 [7 - 15.2] ms per ng/mL, p = 0.045), but a lesser increase in ΔTpeak-Tend (10.1 [6 - 14.2] vs. 18.8 [14.7 - 23] ms per ng/mL, p = 0.006)

Author's version. Published in J Electrocardiol, 2015 (http://dx.doi.org/10.1016/j.jelectrocard.2015.08.004)

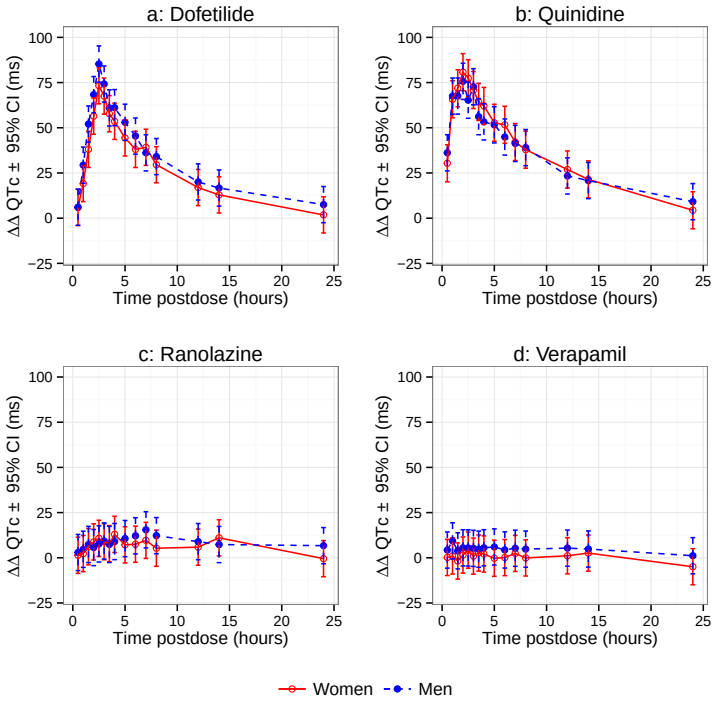

Figure 2: Pharmacodynamic time profiles of mean baseline- and placebo-corrected drug-induced QTc changes in women (red open circles) and men (closed blue circles) for (a) dofetilide, (b) quinidine, (c) ranolazine and (d) verapamil. The errors bars denote the ±95% confidence intervals.

and lesser decrease of ΔT wave amplitude (-35.9 [-52.3 to -19.6] vs. -73.9 [-90.6 to -57.2] μV per ng/mL, p = 0.003) in women compared with men (Figure 3). There were no other sex-specific differences in the exposure-response relationships between any of the drugs and ECG biomarkers (supplementary tables S2-S5 and supplementary Figure S1-S8).

Discussion

This study showed no sex differences in the QTc prolongation caused by dofetilide, quinidine and ranolazine. Additional assessment of other ECG subintervals and morphology biomarkers showed sex-specific differences only with dofetilide (selective hERG potassium channel block). Specifically, women had greater dofetilide-induced increase in J-Tpeakc (early repolarization), but a lesser increase in Tpeak-Tend (late repolarization) and lesser decrease of T wave amplitude. No other sex differences in the exposure-response relationship were observed for any of the other drugs and ECG biomarkers. While sex differences with dofetilide were consistent with differences between women and men in the absence of drug, these few sex differences were not present with other drugs. Therefore, few-to-no sex differences in drug-induced changes in ventricular repolarization were observed consistently across the study drugs.

Sex differences in ECG changes induced by dofetilide

There was no difference in dofetilide-induced prolongation of repolarization (QTc) between women and men in this study. However, dofetilide caused greater increase of early repolarization (J-Tpeakc) but lesser prolongation of late repolarization (Tpeak-Tend) and lesser T wave amplitude decrease in women than in men. Adult women have longer QTc than men at baseline, but this difference diminishes

Author's version. Published in J Electrocardiol, 2015 (http://dx.doi.org/10.1016/j.jelectrocard.2015.08.004)

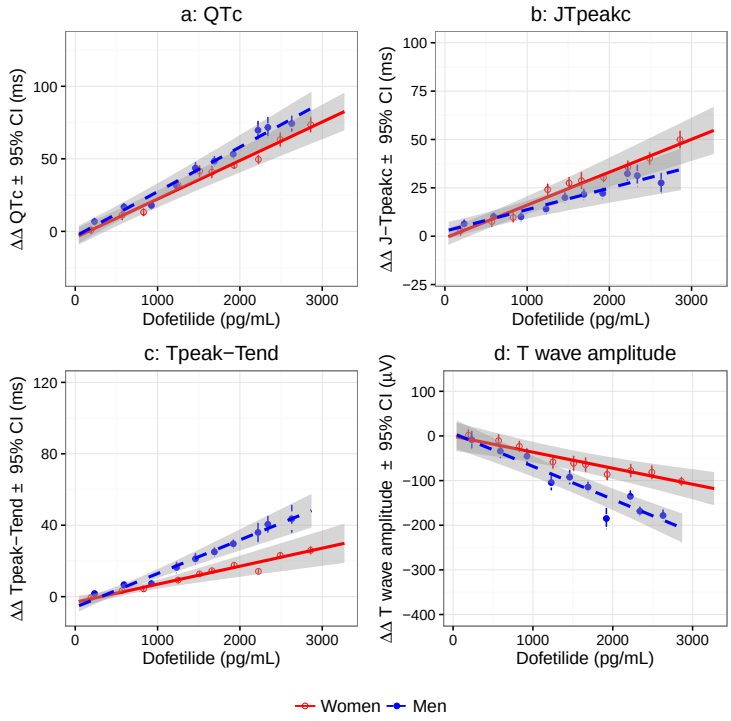

Figure 3: Mean baseline- and placebo-corrected plasma dofetilide concentration-dependent changes (PK/PD response) in women (red solid line) and men (blue dashed line) in (a) QTc, (b) J-Tpeakc, (c) Tpeak-Tend, and (d) T wave amplitude measured as the maximum magnitude to the T vector. Shaded areas show the 95% confidence intervals from the model predictions. For clarity, the observed data is grouped in 10 bins (deciles) represented by the circles (median concentration and mean ΔΔECG change) and error bars (95% confidence intervals) for women (red open circles) and men (blue closed circles). See supplementary table S2 for the population and sex-specific slopes values, and supplementary figure S5 for the observed data. Sex-specific PK/PD relationships for quinidine, ranolazine and verapamil are shown in supplementary figures S1-S3.

with age [10]. These sex- and age-differences in the QTc interval are fully explained by women having longer J-Tpeakc. The shorter J-Tpeakc in men is likely due to the block of L-type calcium current by testosterone, which may shorten the plateau phase of the ventricular action potential [11] but also may prevent the occurrence of early after depolarizations [12, 13], which are the triggers for torsade de pointes. Therefore, in this study selective hERG potassium channel block (dofetilide) increased the sex differences in early and late repolarization intervals without increasing the sex differences in QTc.

Previous studies reporting sex differences in drug-induced QTc prolongation

Previous clinical studies have shown greater drug-induced QTc prolongation relative to serum drug concentration in women compared to men with different drugs. Benton and colleagues found greater intravenous quinidine-induced QTc prolongation in women [4]. However, a recent retrospective analysis [8] of that study showed no sex differences in quinidine-induced QTc or Tpeak-Tend prolongation when accounting for sex differences in the delay between serum quinidine concentration and ECG changes (hysteresis [7]). This is consistent with the lack of sex differences in quinidine-induced ECG changes observed in this study.

Sex differences in ibutilide-induced QTc prolongation

Author's version. Published in J Electrocardiol, 2015 (http://dx.doi.org/10.1016/j.jelectrocard.2015.08.004)

have been previously reported [5]. Ibutilide prolongs the QTc interval by blocking the hERG potassium channel and increasing the late sodium inward current. Enhancement of late sodium current may result in early repolarization interval (J-Tpeakc) prolongation, which is seen in long QT syndrome type 3 patients [25]. Whether hysteresis effects and additional late sodium current enhancement contributed to the sex differences in QTc prolongation observed with intravenous ibutilide deserves further investigation.

Darpo and colleagues reported women having higher rac-sotalol plasma levels as well as a steeper concentration dependent QTc prolongation [6]. While we did not study rac-sotalol, which blocks the hERG potassium channel, we observed women having higher plasma concentration of quinidine, which also blocks the hERG potassium channel. However, there were no sex differences in the quinidine concentration dependent response in this study. While there were few-to-no sex differences in the four drugs of this study, sex differences in drug-induced changes might be present with other drugs.

Sex differences in dofetilide-induced torsade de pointes risk

Recent studies have shown that female sex, longer baseline QTc and greater drug-induced QTc prolongation are significant risk factors for torsade in patients taking dofetilide [26, 27]. The few sex differences in drug-induced ECG changes in this study suggest that, in patient populations, women may have longer ΔΔQTc prolongation because women are exposed to higher plasma drug concentrations than men. This, together with women having longer baseline QTc [9, 10, 11], may partially explain the higher risk for drug-induced torsade in women. However, this should be interpreted with caution because the reduced sample size of this study and the differences between populations (e.g. age or healthy vs. not healthy subjects) participating in this vs. other studies.

Limitations

The difference between women and men in dofetilide-induced J-Tpeakc prolongation was statistically significant (p=0.045), however this result should be interpreted with caution because p-values were not adjusted for multiple comparisons and the reduced sample size of this study (11 women vs. 11 men). Lower p-values would be required to consider a finding statistically significant when adjusting for multiple comparisons. Therefore, adjusting for multiplicity could minimize or even result in no sex differences in the drug-induced changes in the present study. The study sample size was similar to cohorts used in a previous quinidine study (12 women vs. 12 men) [4]. In addition, retrospective assessment showed that the study was powered to detect sex differences in the drug concentration vs. QTc slope similar to those reported previously with rac-sotalol [6]. The use of other heart rate correction formulas for QT might produce different results [28]. However, sensitivity analysis using either a study based heart rate correction and the so-called model-based QT correction (QTcMod= QT(120 + HR)/180)[29] did not change the observed sex differences in drug-induced ECG effects (results not shown).

Conclusions

There were no sex differences in the relationship between plasma drug concentration and ΔΔQTc prolongation induced by dofetilide, quinidine and ranolazine. In addition, no systematic sex differences of other drug-induced ECG biomarker changes were observed in this study. This study suggests that the higher torsade risk in women compared to men is not due to a larger concentration-dependent QTc prolongation. However, women have a longer QTc at baseline and are often exposed to higher drug concentrations than men, which likely contribute to their higher torsade risk.

Acknowledgements

This study was supported by U.S. Food and Drug Administration's Critical Path Initiative, U.S. Food and Drug Administration's Office of Women's Health and appointments to the Research Participation Program at the Center for Devices and Radiological Health and the Center for Drug Evaluation and Research administered by the Oak Ridge Institute for Science and Education through an interagency agreement between the U.S. Department of Energy and the U.S. Food and Drug Administration. E.P. is funded by Ministerio de Economía y Competitividad (MINECO), Spain, under project TIN2013-41998-R and by Grupo Consolidado BSICoS from DGA (Aragón) and European Social Fund (EU). QTGuard+ was provided by GE Healthcare through a material transfer agreement. The mention of commercial products, their sources, or their use in connection with material reported herein is not to be construed as either an actual or implied endorsement of such products by the U.S. Department of Health and Human Services.

Conflict of Interest Disclosures

None.

References

[1] Makkar RR, Fromm BS, et al. Female gender as a risk factor for torsades de pointes associated with cardiovascular drugs. *JAMA* 270(21):2590–7, 1993.

Author's version. Published in J Electrocardiol, 2015 (http://dx.doi.org/10.1016/j.jelectrocard.2015.08.004)

[2] Trudeau M, Warmke J, et al. Herg, a human inward rectifier in the voltage-gated potassium channel family. *Science* 269(5220):92–5, 1995.

[3] Fung M, Hsiao-hui Wu H, et al. Evaluation of the profile of patients with qtc prolongation in spontaneous adverse event reporting over the past three decades—1969-1998. *Pharmacoepidemiol Drug Saf* 9(suppl 1):S24, 2000.

[4] Benton RE, Sale M, et al. Greater quinidine-induced qtc interval prolongation in women. *Clin Pharmacol Ther* 67(4):413–8, 2000.

[5] Rodriguez I, Kilborn MJ, et al. Drug-induced qt prolongation in women during the menstrual cycle. *JAMA* 285(10):1322–6, 2001.

[6] Darpo B, Karnad DR, et al. Are women more susceptible than men to drug-induced qt prolongation? concentration-qtc modeling in a phase 1 study with oral rac-sotalol. *Br J Clin Pharmacol* , 2013.

[7] Holford NH, Coates PE, et al. The effect of quinidine and its metabolites on the electrocardiogram and systolic time intervals: concentration–effect relationships. *Br J Clin Pharmacol* 11(2):187–95, 1981.

[8] Vicente J, Simlund J, et al. Investigation of potential mechanisms of sex differences in quinidine-induced torsade de pointes risk. *Journal of electrocardiology* , 2015.

[9] Bazett HC. An analysis of the time-relations of electrocardiograms. *Heart* 7:353–370, 1920.

[10] Rautaharju PM, Zhou SH, et al. Sex differences in the evolution of the electrocardiographic qt interval with age. *Can J Cardiol* 8(7):690–5, 1992.

[11] Vicente J, Johannesen L, et al. Mechanisms of sex and age differences in ventricular repolarization in humans. *American heart journal* 168(5):749–756, 2014.

[12] January CT and Riddle JM. Early afterdepolarizations: mechanism of induction and block. a role for l-type ca2+ current. *Circ Res* 64(5):977–90, 1989.

[13] Guo D, Zhao X, et al. L-type calcium current reactivation contributes to arrhythmogenesis associated with action potential triangulation. *J Cardiovasc Electrophysiol* 18(2):196–203, 2007.

[14] Johannesen L, Vicente J, et al. Differentiating drug-induced multichannel block on the electrocardiogram: Randomized study of dofetilide, quinidine, ranolazine, and verapamil. *Clin Pharmacol Ther* 96(5):549–558, 2014.

[15] Mason RE and Likar I. A new system of multiple-lead exercise electrocardiography. *Am Heart J* 71(2):196–205, 1966.

[16] Badilini F, Vaglio M, and Sarapa N. Automatic extraction of ecg strips from continuous 12-lead holter recordings for qt analysis at prescheduled versus optimized time points. *AnnNoninvasive Electrocardiol* 14 Suppl 1:S22–S29, 2009.

[17] Vicente J, Johannesen L, et al. Ecglab: User friendly ecg/vcg analysis tool for research environments. *Comput Cardiol* 40(775-778), 2013.

[18] Vicente J, Johannesen L, et al. Comprehensive t wave morphology assessment in a randomized clinical study of dofetilide, quinidine, ranolazine, and verapamil. *J Am Heart Assoc* 4(4), 2015.

[19] Andersen MP, Xue J, et al. A robust method for quantification of ikr-related t-wave morphology abnormalities. In *Computers in Cardiology, 2007*, 341–344. IEEE.

[20] Couderc J, Vaglio M, et al. Electrocardiographic method for identifying drug-induced repolarization abnormalities associated with a reduction of the rapidly activating delayed rectifier potassium current. In *Engineering in Medicine and Biology Society, 2006. EMBS'06. 28th Annual International Conference of the IEEE*, 4010–4015. IEEE.

[21] Acar B, Yi G, et al. Spatial, temporal and wavefront direction characteristics of 12-lead t-wave morphology. *Medical & biological engineering & computing* 37(5):574–584, 1999.

[22] Johannesen L, Vicente J, et al. Ecglib: Library for processing electrocardiograms. In *Computing in Cardiology*, In–Press.

[23] Fridericia LS. Die systolendauer im elektrokardiogramm bei normalen menschen und bei herzkranken. *Acta Med Scand* 53(1):469–486, 1920.

[24] Darpo B, Sarapa N, et al. The iq-csrc prospective clinical phase 1 study: "can early qt assessment using exposure response analysis replace the thorough qt study?". *Ann Noninvasive Electrocardiol* 19(1):70–81, 2014.

[25] Moss AJ, Zareba W, et al. Ecg t-wave patterns in genetically distinct forms of the hereditary long qt syndrome. *Circulation* 92(10):2929–2934, 1995.

[26] Pedersen HS, Elming H, et al. Risk factors and predictors of torsade de pointes ventricular tachycardia in patients with left ventricular systolic dysfunction receiving dofetilide. *Am J Cardiol* 100(5):876–80, 2007.

Author's version. Published in J Electrocardiol, 2015 (http://dx.doi.org/10.1016/j.jelectrocard.2015.08.004)

[27] Abraham JM, Saliba WI, et al. Safety of oral dofetilide for rhythm control of atrial fibrillation and atrial flutter. *Circ Arrhythm Electrophysiol* , 2015.

[28] Garnett CE, Zhu H, et al. Methodologies to characterize the qt/corrected qt interval in the presence of drug-induced heart rate changes or other autonomic effects. *American heart journal* 163(6):912–30, 2012.

[29] Rautaharju PM, Mason JW, and Akiyama T. New age- and sex-specific criteria for qt prolongation based on rate correction formulas that minimize bias at the upper normal limits. *Int J Cardiol* 174(3):535–540, 2014.

Supplementary materials

Supplementary tables

Supplementary Table S.1: Baseline characteristics.

	Women (n=11)	Men (n=11)	
Demographics			
Age (years)	26.6±4.7	27.2±6.5	p=0.82
Height (cm)	167.7±7.8	176.7±5.4	**p=0.006**
Weight (kg)	66.2±9.3	70.4±6.7	p=0.24
BMI (kg/m^2)	23.5±2.5	22.7±2.8	p=0.48
Heart rate (bpm)	60.9±6.1	52.7±3.5	**p=0.001**
ECG intervals			
PR (ms)	156.7±19.4	167.4±23.3	p=0.26
QTc (ms)	402.6±15.6	389.2±16.6	p=0.065
QRS (ms)	93.8±4.1	101.0±7.0	**p=0.010**
J-Tpeakc (ms)	238.2±12.9	212.9±17.4	**p=0.001**
Tpeak-Tend (ms)	70.4±3.8	75.9±7.4	**p=0.044**
T-wave morphology			
T wave flatness (d.u.)	0.40±0.04	0.42±0.05	p=0.42
T wave asymmetry (d.u.)	0.15±0.05	0.16±0.05	p=0.66
T wave notching (% of subjects)	0.00±0.00	0.00±0.00	p=0.21
ERD 30% (ms)	41.2±2.8	47.7±5.0	**p=0.002**
LRD 30% (ms)	25.3±1.4	29.7±4.7	**p=0.011**
QRS-T angle (°)	31.8±7.5	37.3±11.4	p=0.20
TCRT (radians)	0.76±0.15	0.57±0.28	p=0.064
T wave amplitude (μV)	510.6±154.1	646.4±170.1	p=0.064
Ventricular gradient (mV·ms)	95.8±26.0	127.0±24.9	**p=0.009**

Continuous variables reported as mean ± SD of each subjects 5-day baseline average. T-wave amplitude measured as the heart rate corrected maximum amplitude of the T vector. ERD30%:30% of early repolarization duration, LRD30%: 30% of late repolarization duration; TCRT: Total Cosine R-to-T; d.u., dimensionless units.

Supplementary Table S.2: Sex-specific plasma dofetilide concentration dependent ECG changes

ΔΔ per ng/mL	Population	Women (n=11)	Men (n=11)	Women vs. Men
Heart rate (bpm)	-1.2 (-2.1 to -0.4)**	-1.1 (-2.2 to 0.1)	-1.4 (-2.6 to -0.2)*	p=0.69
PR (ms)	-0.1 (-1.0 to 0.9)	-0.3 (-1.6 to 1.1)	0.2 (-1.2 to 1.6)	p=0.65
QTc (ms)	28.7 (25.5 to 31.8)**	26.6 (22.2 to 30.9)**	30.8 (26.3 to 35.2)**	p=0.17
QRS (ms)	0.2 (-0.5 to 0.9)	-0.3 (-1.2 to 0.6)	0.7 (-0.3 to 1.6)	p=0.14
J-Tpeakc (ms)	14.1 (11.2 to 16.9)**	17.0 (13.0 to 21.1)**	11.1 (7.0 to 15.2)**	**p=0.045**
Tpeak-Tend (ms)	14.5 (11.5 to 17.4)**	10.1 (6.0 to 14.2)**	18.8 (14.7 to 23.0)**	**p=0.006**
T wave flatness (d.u.)	0.05 (0.05 to 0.06)**	0.06 (0.05 to 0.07)**	0.05 (0.04 to 0.06)**	p=0.37
T wave asymmetry (d.u.)	0.09 (0.05 to 0.13)**	0.12 (0.07 to 0.18)**	0.06 (0.01 to 0.12)*	p=0.13
ERD 30% (ms)	8.7 (5.5 to 11.9)**	8.9 (4.3 to 13.4)**	8.5 (3.9 to 13.1)**	p=0.91
LRD 30% (ms)	5.6 (3.2 to 7.9)**	3.4 (0.1 to 6.8)*	7.7 (4.3 to 11.0)**	p=0.078
QRS-T angle (°)	-1.4 (-1.8 to -1.0)**	-1.9 (-2.4 to -1.2)**	-1.0 (-1.7 to -0.4)**	p=0.081
TCRT (radians)	0.03 (0.02 to 0.05)**	0.03 (0.02 to 0.05)**	0.03 (0.02 to 0.05)**	p=0.82
T wave amplitude (uV)	-54.9 (-66.6 to -43.2)**	-35.9 (-52.3 to -19.6)**	-73.9 (-90.6 to -57.2)**	**p=0.003**
Ventricular gradient (mV.ms)	0.8 (-1.0 to 2.6)	2.2 (-0.2 to 4.7)	-0.7 (-3.2 to 1.9)	p=0.10

Values reported as mean ECG changes induced drug concentration unit. ±95% confidence intervals reported in parenthesis. * p< 0.05; ** p < 0.01; T-wave amplitude measured as the heart rate corrected maximum amplitude of the T vector. ERD30%:30% of early repolarization duration, LRD30%: 30% of late repolarization duration; TCRT: Total Cosine R-to-T;
d.u., dimensionless units.

Supplementary Table S.3: Sex-specific plasma quinidine concentration dependent ECG changes

ΔΔ per μgmL	Population	Women (n=10)	Men (n=11)	Women vs. Men
Heart rate (bpm)	4.7 (3.3 to 6.1)**	4.9 (3.1 to 6.8)**	4.5 (2.3 to 6.6)**	p=0.73
PR (ms)	-0.1 (-2.7 to 2.4)	-0.3 (-3.8 to 3.2)	0.0 (-3.6 to 3.6)	p=0.90
QTc (ms)	42.4 (36.0 to 48.8)**	39.4 (30.3 to 48.5)**	45.5 (36.4 to 54.5)**	p=0.33
QRS (ms)	0.1 (-1.2 to 1.3)	0.0 (-1.7 to 1.8)	0.1 (-1.8 to 1.9)	p=0.99
J-Tpeakc (ms)	11.5 (3.3 to 19.7)**	15.7 (4.0 to 27.4)*	7.4 (-4.1 to 18.9)	p=0.30
Tpeak-Tend (ms)	29.6 (19.5 to 39.7)**	22.3 (7.9 to 36.8)**	36.9 (22.7 to 51.1)**	p=0.15
T wave flatness (d.u.)	0.10 (0.08 to 0.11)**	0.10 (0.08 to 0.12)**	0.10 (0.08 to 0.12)**	p=0.99
T wave asymmetry (d.u.)	0.16 (0.06 to 0.25)**	0.15 (0.01 to 0.28)*	0.17 (0.04 to 0.3)*	p=0.81
ERD 30% (ms)	10.3 (4.0 to 16.6)**	8.7 (-0.1 to 17.6)	11.8 (3.0 to 20.7)*	p=0.61
LRD 30% (ms)	15.2 (8.3 to 22.1)**	14.4 (4.5 to 24.3)**	16.0 (6.2 to 25.7)**	p=0.82
QRS-T angle (°)	2.7 (0.4 to 4.9)*	2.1 (-1.1 to 5.3)	3.2 (0.0 to 6.4)*	p=0.60
TCRT (radians)	-	-	-	-
T wave amplitude (uV)	-77.98 (-102.57 to -53.38)**	-60.83 (-95.44 to -26.21)**	-95.12 (-130.11 to -60.14)**	p=0.16
Ventricular gradient (mV.ms)	-0.97 (-3.65 to 1.7)	-1.52 (-5.25 to 2.21)	-0.43 (-4.28 to 3.43)	p=0.67

Values reported as mean ECG changes induced drug concentration unit. ±95% confidence intervals reported in parenthesis. * p< 0.05; ** p < 0.01; T-wave amplitude measured as the heart rate corrected maximum amplitude of the T vector. ERD30%:30% of early repolarization duration, LRD30%: 30% of late repolarization duration; TCRT: Total Cosine R-to-T; d.u., dimensionless units.
Dashes (-) indicate the model did not converged (i.e. there was not relationship between the ECG changes and plasma drug concentration).

Supplementary Table S.4: Sex-specific plasma ranolazine concentration dependent ECG changes

ΔΔ per μg/mL	Population	Women (n=11)	Men (n=11)	Women vs. Men
Heart rate (bpm)	0.4 (-0.6 to 1.5)	0.6 (-1.1 to 2.4)	0.2 (-1.2 to 1.7)	p=0.67
PR (ms)	1.1 (0.2 to 2.1)*	0.9 (-0.3 to 2.0)	1.4 (-0.1 to 3)	p=0.55
QTc (ms)	4.2 (2.3 to 6.1)**	5.5 (2.7 to 8.2)**	2.9 (0.1 to 5.7)*	p=0.18
QRS (ms)	0.5 (-0.1 to 1.1)	0.4 (-0.4 to 1.2)	0.6 (-0.3 to 1.6)	p=0.66
J-Tpeakc (ms)	-	-	-	-
Tpeak-Tend (ms)	4.4 (2.6 to 6.3)**	4.1 (1.6 to 6.7)**	4.8 (2.1 to 7.4)**	p=0.72
T wave flatness (d.u.)	-	-	-	-
T wave asymmetry (d.u.)	0.03 (0.01 to 0.06)**	0.04 (0 to 0.07)*	0.03 (0 to 0.07)	p=0.89
ERD 30% (ms)	3.9 (2.3 to 5.5)**	4.4 (2.2 to 6.6)**	3.4 (1.0 to 5.7)**	p=0.53
LRD 30% (ms)	2.1 (0.7 to 3.6)**	2.0 (0.0 to 4.1)*	2.2 (0.1 to 4.3)*	p=0.91
QRS-T angle (°)	-0.5 (-1.4 to 0.5)	-0.6 (-1.9 to 0.6)	-0.3 (-1.6 to 1.1)	p=0.68
TCRT (radianss)	0.00 (-0.03 to 0.02)	0.00 (-0.09 to 0.09)	0.00 (-0.03 to 0.02)	p=0.91
T wave amplitude (μV)	-25.3 (-41.6 to -9.0)**	-25.6 (-48.3 to -3.0)*	-25.0 (-48.5 to -1.5)*	p=0.97
Ventricular gradient (mV.ms)	-1.2 (-3.1 to 0.6)	-1.4 (-3.9 to 1.2)	-1.1 (-3.8 to 1.5)	p=0.89

Values reported as mean ECG changes induced drug concentration unit. ±95% confidence intervals reported in parenthesis. * $p < 0.05$; ** $p < 0.01$; T-wave amplitude measured as the heart rate corrected maximum amplitude of the T vector. ERD30%:30% of early repolarization duration, LRD30%: 30% of late repolarization duration; TCRT: Total Cosine R-to-T; d.u., dimensionless units.
Dashes (-) indicate the model did not converged (i.e. there was not relationship between the ECG changes and plasma drug concentration).

Supplementary Table S.5: Sex-specific plasma verapamil concentration dependent ECG changes

ΔΔ per μg/mL	Population	Women (n=11)	Men (n=11)	Women vs. Men
Heart rate (bpm)	0.1 (0.0 to 0.1)**	0.1 (0.0 to 0.1)**	0.1 (0.0 to 0.1)**	p=0.56
PR (ms)	0.2 (0.2 to 0.3)**	0.3 (0.2 to 0.3)**	0.2 (0.1 to 0.3)**	p=0.38
QTc (ms)	0.0 (0.0 to 0.0)	0.0 (0.0 to 0.0)	0.0 (0.0 to 0.1)	p=0.45
QRS (ms)	0.0 (0.0 to 0)*	0.0 (0.0 to 0.0)	0.0 (0.0 to 0)*	p=0.15
J-Tpeakc (ms)	0.0 (0.0 to 0.0)	0.0 (0.0 to 0.0)	0.0 (0.0 to 0.1)	p=0.32
Tpeak-Tend (ms)	-	-	-	-
T wave flatness (d.u.)	0.0 (0.0 to 0.0)	0.0 (0.0 to 0.0)	0.0 (0.0 to 0.0)	p=0.023
T wave asymmetry (d.u.)	0.0 (0.0 to 0.0)	0.0 (0.0 to 0.0)	0.0 (0.0 to 0.0)	p=0.91
ERD 30% (ms)	0.0 (0 to 0.0)*	0.0 (0.0 to 0.0)	0.0 (0 to 0.0)*	p=0.23
LRD 30% (ms)	-	-	-	-
QRS-T angle (°)	0.0 (0 to 0.0)*	0.0 (0 to 0.0)*	0.0 (0 to 0.0)	p=0.84
TCRT (radians)	0 (0 to 0)	0 (0 to 0)	0 (0 to 0)	p=0.14
T wave amplitude (μV)	-0.1 (-0.3 to 0.1)	-0.2 (-0.5 to 0.1)	0.0 (-0.4 to 0.3)	p=0.43
Ventricular gradient (mV·ms)	0 (0.0 to 0.0)	0.0 (0.0 to 0.0)	0.0 (0.0 to 0.0)	p=0.27

Values reported as mean ECG changes induced drug concentration unit. ±95% confidence intervals reported in parenthesis. * $p < 0.05$; ** $p < 0.01$; T-wave amplitude measured as the heart rate corrected maximum amplitude of the T vector. ERD30%:30% of early repolarization duration, LRD30%: 30% of late repolarization duration; TCRT: Total Cosine R-to-T; d.u., dimensionless units.
Dashes (-) indicate the model did not converged (i.e. there was not relationship between the ECG changes and plasma drug concentration).

Supplementary figures

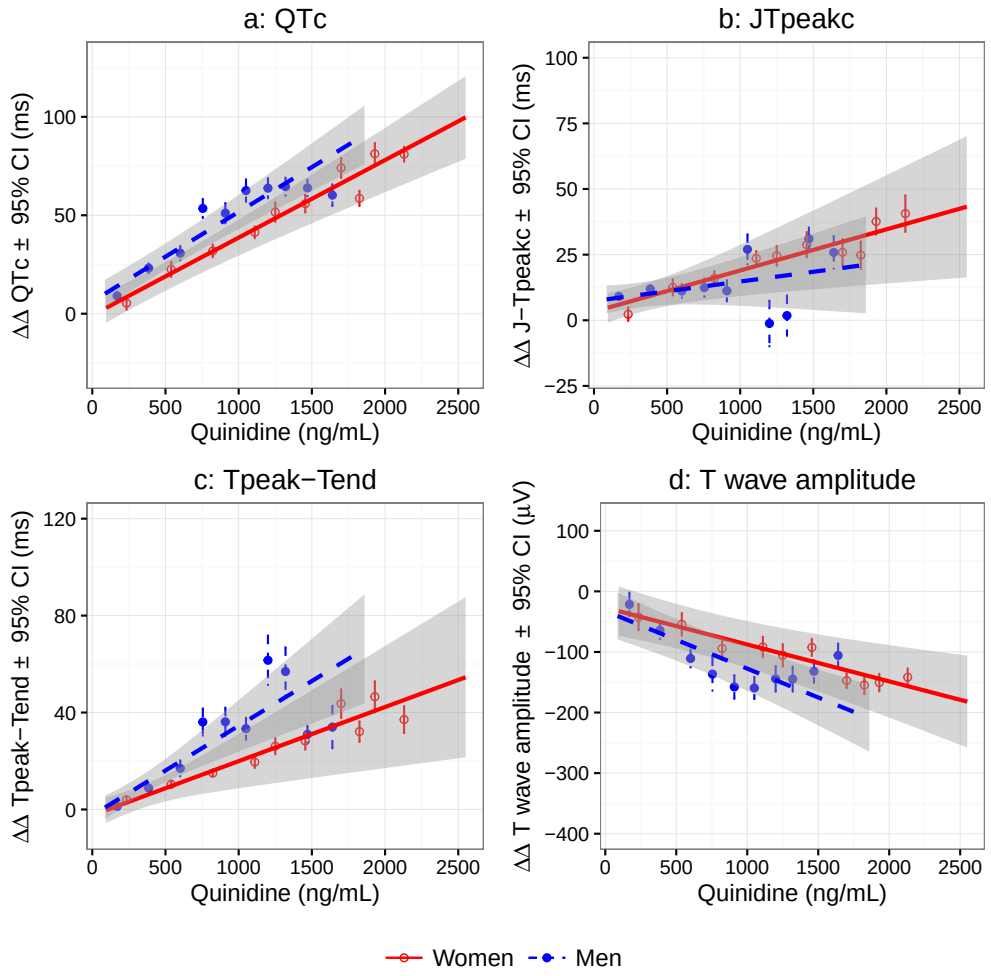

Supplementary Figure S.1: Mean baseline- and placebo-corrected plasma quinidine concentration-dependent changes (PK/PD response) in women (red solid line) and men (blue dashed line) in (a) QTc, (b) J-Tpeakc, (c) Tpeak-Tend, and (d) T wave amplitude measured as the maximum magnitude to the T vector. Shaded areas show the 95% confidence intervals from the model predictions. For clarity, the observed data is grouped in 10 bins (deciles) represented by the circles (median concentration and mean ΔΔECG change) and error bars (95% confidence intervals) for women (red open circles) and men (blue closed circles). See supplementary table S3 for the population and sex-specific slopes values, and supplementary figure S6 for the observed data.

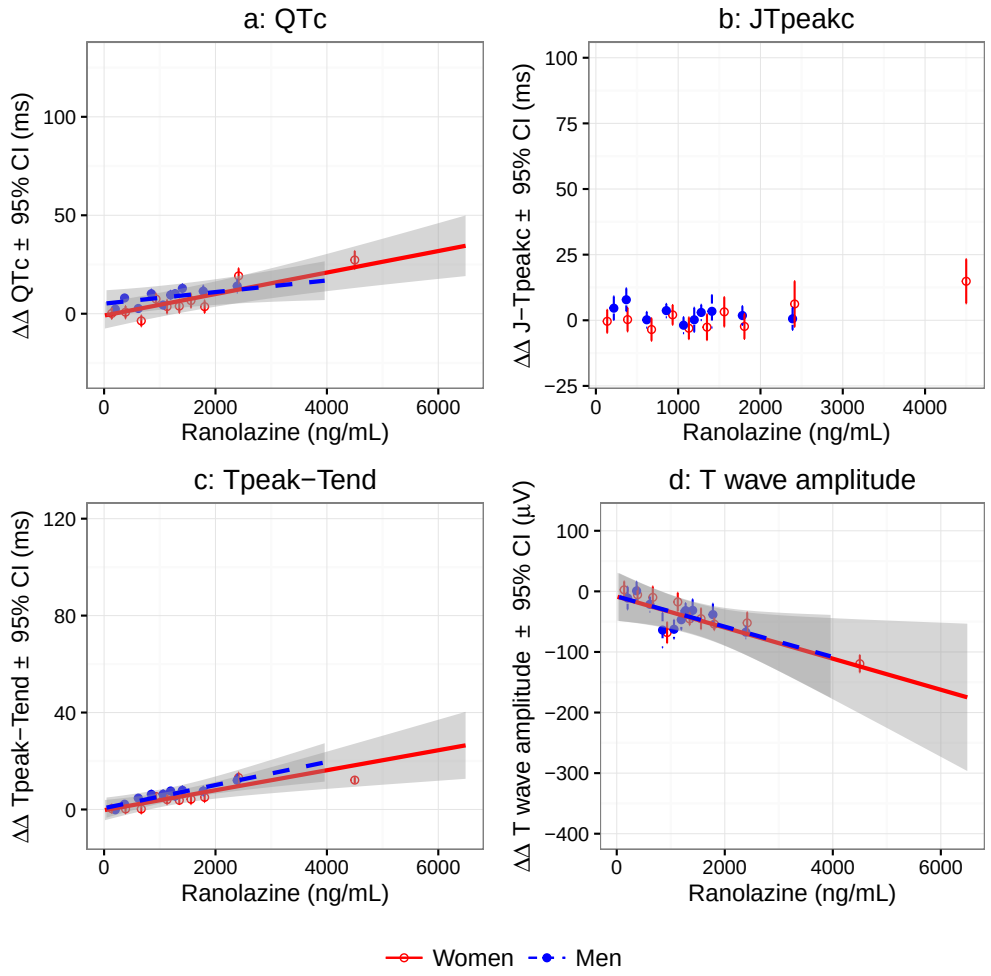

Supplementary Figure S.2: Mean baseline- and placebo-corrected plasma ranolazine concentration-dependent changes (PK/PD response) in women (red solid line) and men (blue dashed line) in (a) QTc, (b) J-Tpeakc, (c) Tpeak-Tend, and (d) T wave amplitude measured as the maximum magnitude to the T vector. Shaded areas show the 95% confidence intervals from the model predictions. For clarity, the observed data is grouped in 10 bins (deciles) represented by the circles (median concentration and mean ΔΔECG change) and error bars (95% confidence intervals) for women (red open circles) and men (blue closed circles). See supplementary table S4 for the population and sex-specific slopes values, and supplementary figure S7 for the observed data.

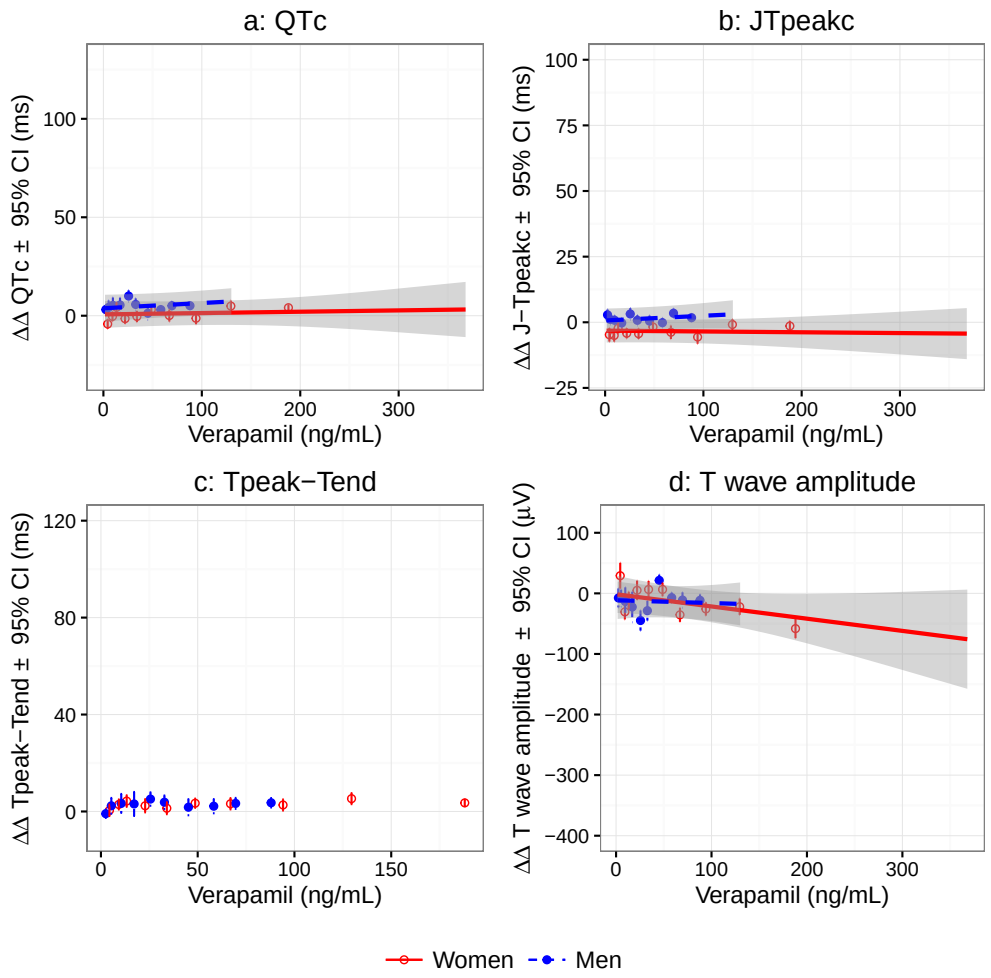

Supplementary Figure S.3: Mean baseline- and placebo-corrected plasma verapamil concentration-dependent changes (PK/PD response) in women (red solid line) and men (blue dashed line) in (a) QTc, (b) J-Tpeakc, (c) Tpeak-Tend, and (d) T wave amplitude measured as the maximum magnitude to the T vector. Shaded areas show the 95% confidence intervals from the model predictions. For clarity, the observed data is grouped in 10 bins (deciles) represented by the circles (median concentration and mean ΔΔECG change) and error bars (95% confidence intervals) for women (red open circles) and men (blue closed circles). See supplementary table S5 for the population and sex-specific slopes values, and supplementary figure S8 for the observed data.

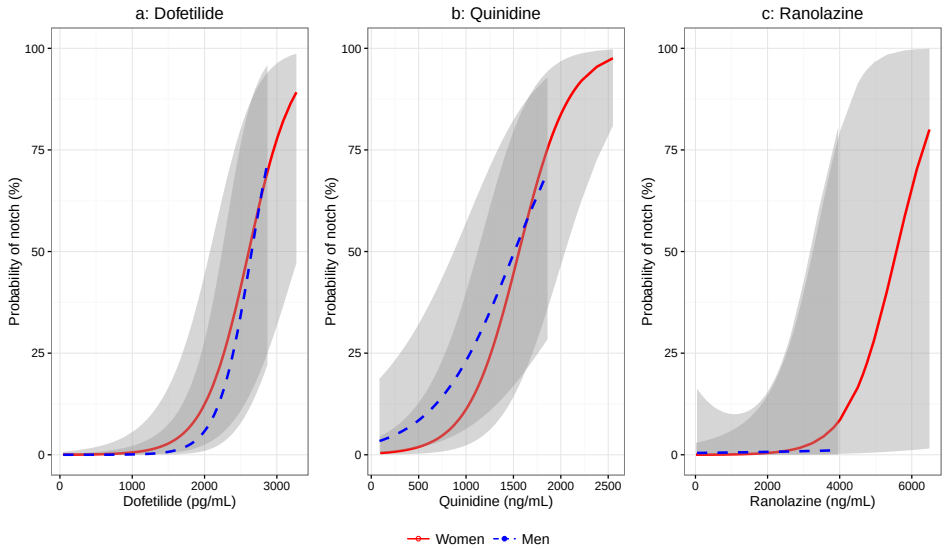

Supplementary Figure S.4: Average probability of developing notches vs. drug concentration in women (red solid line) and men (blue dashed line). Shaded areas show the 95% confidence intervals from the model predictions. Only two subjects (1 woman) developed notches with ranolazine. No subjects developed notches with verapamil (not shown).

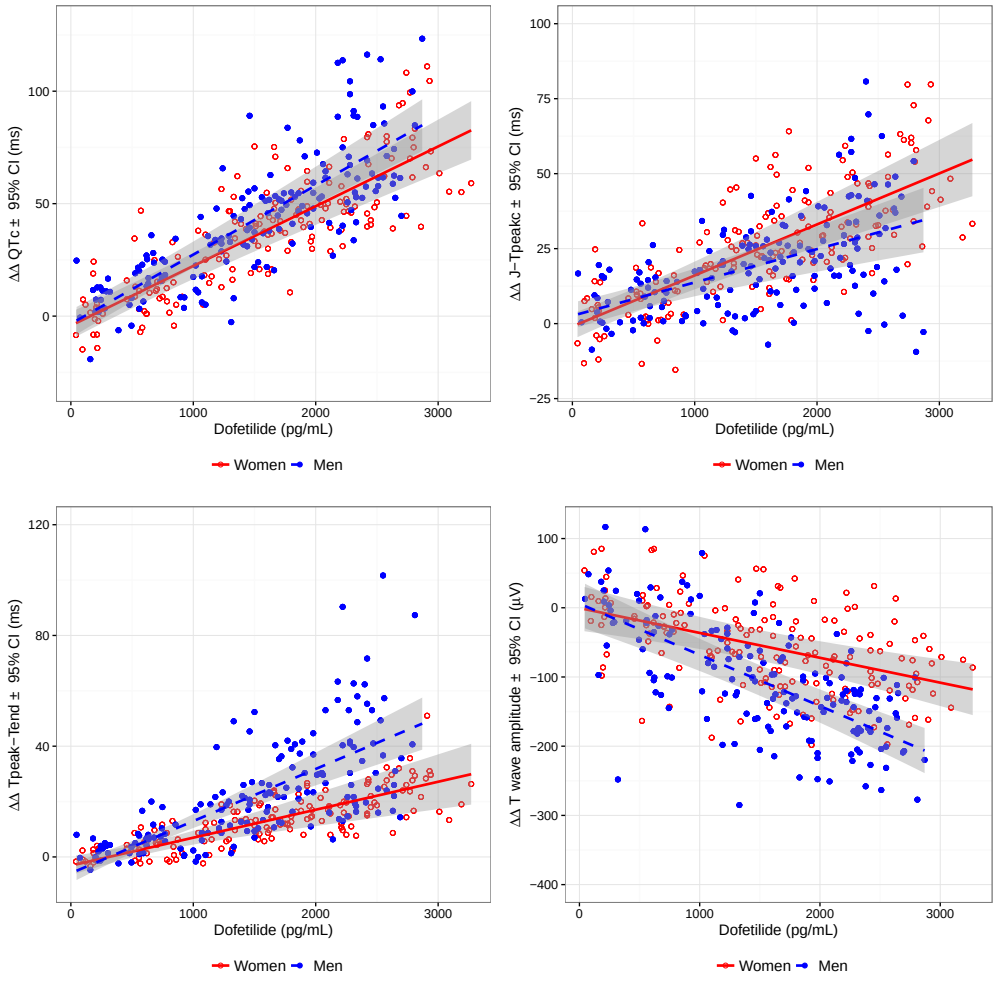

Supplementary Figure S.5: Dofetilide slopes with all observations.

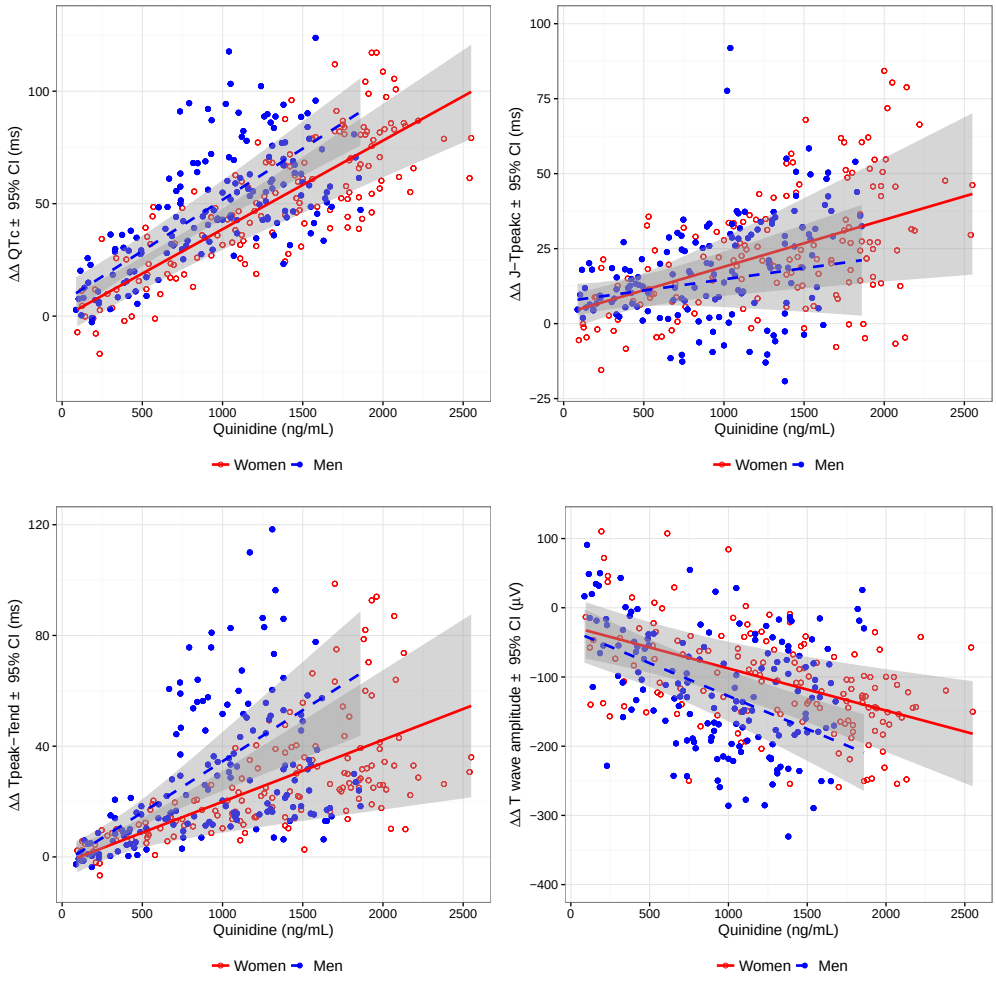

Supplementary Figure S.6: Quinidine slopes with all observations.

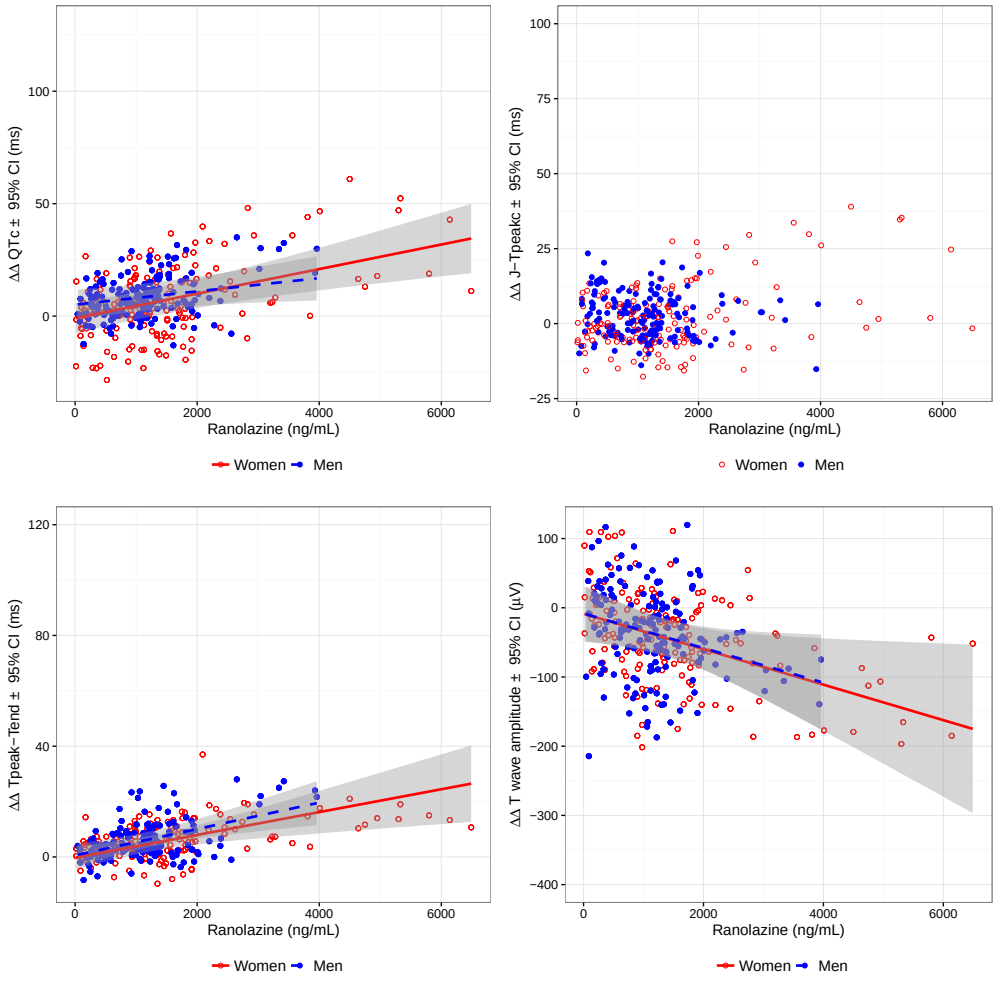

Supplementary Figure S.7: Ranolazine slopes with all observations.

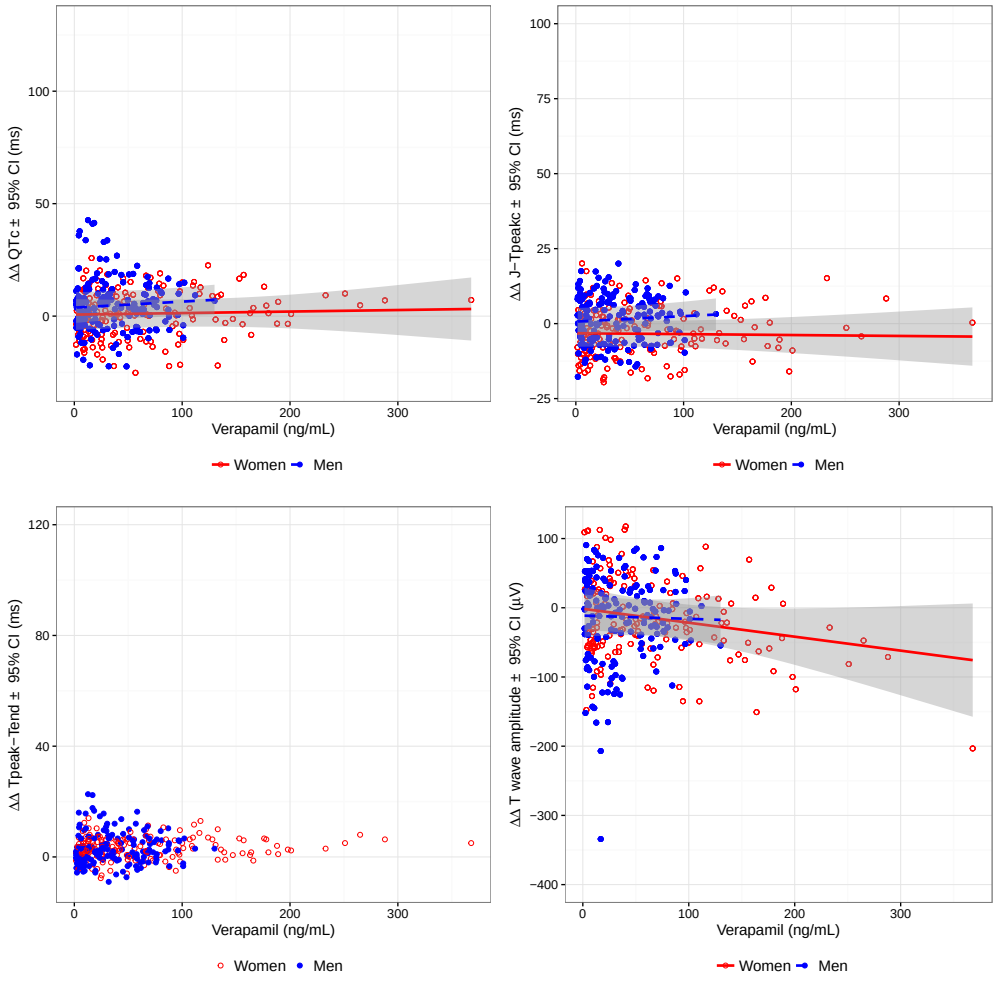

Supplementary Figure S.8: Verapamil slopes with all observations.

CHAPTER 6

Study V

ECG biomarkers for detection of drug-induced late sodium current block

Vicente J, Johannesen L, et al. ECG biomarkers for detection of drug-induced late sodium current block. *Manuscript* , 2015

Manuscript

ECG biomarkers for detection of drug-induced late sodium current block

J Vicente[1,2,5], L Johannesen[1,3], M Hosseini[2], E Pueyo[4,5], N Stockbridge[6], and DG Strauss[2,✉]

[1]*Office of Science and Engineering Laboratories, CDRH, US FDA, Silver Spring, MD, USA*
[3]*Office of Clinical Pharmacology, Office of Translational Sciences, CDER, US FDA, Silver Spring, MD, USA*
[3]*Department of Clinical Physiology, Karolinska Institutet and Karolinska University Hospital, Stockholm, Sweden*
[4]*Biomedical Research Networking Center in Bioengineering, Biomaterials and Nanomedicine (CIBER-BBN), Spain*
[5]*BSICoS Group, Aragón Institute for Engineering Research (I3A), IIS Aragón, University of Zaragoza, Spain*
[6]*Division of Cardiovascular and Renal Products, Office of New Drugs, CDER, US FDA , Silver Spring, MD, USA*

Abstract

Recent clinical studies have shown that late sodium current block can reduce prolongation of the heart rate corrected QT interval (QTc) induced by hERG potassium channel blocking drugs. Detection of late sodium current block on the ECG can add value beyond assessing QTc alone. In this study we assess the ability of multiple ECG morphology biomarkers to detect inward current block. We demonstrate that, in addition to shortening QTc by shortening heart-rate corrected J-Tpeak interval (J-Tpeakc), late sodium current block mitigates T-wave flatness changes induced by selective hERG potassium channel block. However, area under the curve of receiver operating characteristic analysis shows that T-wave flatness does not add value to QTc assessment alone. Moreover, of all studied ECG biomarkers, J-Tpeakc was the best biomarker for detecting late sodium current block. Future methodologies assessing drug effects on cardiac ion channel currents on the ECG should use J-Tpeakc to detect the presence of late sodium current block.

***Clinical Trial Registration Information**: http://clinicaltrials.gov/ct2/show/NCT02308748 (NCT02308748)*
***Keywords**: long QT, ion channel, torsade de pointes, ECG*

Previous clinical studies have demonstrated that mexiletine can mitigate heart rate corrected QT interval (QTc) prolongation caused by quinidine [1, 2, 3], a strong hERG potassium channel blocker. Moreover, recent clinical studies have demonstrated that late sodium current block can reduce drug-induced QTc prolongation caused by hERG potassium channel block [4], but also mitigate recurrent torsade de pointes caused by acquired long QT syndrome [5]. Thus, detecting drug-induced inward current block on the electrocardiogram (ECG) could help to better differentiate between minimal and high torsade risk drugs that prolong QTc.

The current regulatory paradigm for assessing torsade risk of new drugs focuses on whether the new drug or its metabolites block the hERG potassium channel [6] and prolong QTc on the ECG in the so-called thorough QT study [7]. This paradigm can be considered successful because no new marketed drugs have been associated with unexpected torsade risk since its implementation in 2005. On the other hand, this approach may have prevented potentially effective medicines from reaching the market, sometimes inappropriately [8]. This is because there are QTc prolonging drugs that block the hERG potassium channel, but have low torsade risk (e.g. ranolazine [9], amiodarone [10], verapamil [11]). In addition to hERG potassium channel block, these drugs block other inward currents (e.g. late sodium, L-type calcium), which can prevent the occurrence of early afterdepolarizations, the triggers for torsade [12, 13].

The U.S. Food and Drug Administration (FDA) is studying novel ECG biomarkers beyond the QTc interval to differentiate selective hERG potassium channel blocking drugs (high torsade risk) from drugs that block additional inward currents (minimal torsade risk). These studies have shown that drug-induced shortening of the heart rate corrected J-Tpeak interval (J-Tpeakc) is a sign of late sodium current block [4, 14]; and that drug-induced changes in T-wave morphology are directly related to the amount of hERG potassium channel block [15].

In this study we assess the effects of late sodium current block (mexiletine or lidocaine) on T-wave morphology changes caused by selective hERG potassium channel block (dofetilide). In addition, we rank 12 ECG biomarkers by their ability to detect late sodium current block.

Methods

This study was approved by the US Food and Drug Administration Research Involving Human Subjects Committee

✉David G Strauss, MD, PhD U.S. Food and Drug Administration. 10903 New Hampshire Avenue, WO64-2062. Silver Spring, MD, 20993, USA. E-mail: David.Strauss@fda.hhs.gov. Telephone: 301-796-6323 - Fax: 301-796-9927

and the local institutional review board. All subjects gave written informed consent and the study was performed at a phase 1 clinic (Spaulding Clinical, West Bend, WI, USA).

Clinical trial design

The study design of this phase 1 clinical trial has been described previously [4]. Briefly, this was a five-period, randomized, cross-over trial designed to study the ability of late sodium or calcium current block to balance the ECG effects of selective hERG potassium channel block. There was one week between treatment periods. In each treatment period subjects were dosed three times during the day with placebo, selective hERG potassium channel block (dofetilide [Tikosyn, Pfizer, USA] or moxifloxacin) or late sodium current block (mexiletine [Teva Pharmaceuticals USA Inc.,USA] or lidocaine [B. Braun Medical, Inc., USA]) alone or in combination (mexiletine combined with dofetilide, lidocaine combined with dofetilide), or selective hERG potassium channel block (moxifloxacin) alone or in combination with calcium channel block (diltiazem). Plasma drug concentration was measured using a validated liquid chromatography with tandem mass spectroscopy method by Frontage Laboratories (Exton, Philadelphia, PA). The present study focuses on the effects of late sodium current block when combined with selective hERG potassium channel block on multiple ECG biomarkers. Therefore, time-points from the combination of diltiazem with moxifloxacin were not included in this study. One female was excluded from this analysis because in the evening time-point of dofetilide alone arm, plasma dofetilide concentration was lower despite the evening oral dose, but she still had larger placebo- and baseline-corrected changes in all ECG biomarkers.

ECG measurement methodology

Continuous ECG recordings were performed using the Mortara Surveyor system (Mortara, Milwaukee, WI, USA) sampled at 500 Hz with an amplitude resolution of 2.5 μV. Three 10 seconds non overlapping 12 lead ECGs were extracted prior to the draw of each pharmacokinetic sample, based on heart rate stability and signal quality using Antares software (AMPS LLC, New York, NY, USA). All extracted 10s ECGs were up-sampled to 1000 Hz. T-wave morphology biomarkers were automatically assessed in the 10s ECGs as previously described [15]. Briefly, T-wave flatness and asymmetry were automatically assessed with QTGuard+ (GE Healthcare, Milwaukee, WI, USA). T-wave amplitude as well as 30% of early and late repolarization duration (ERD30% and LRD30% [16]) were automatically assessed with ECGlib [17]. The semi-automatic evaluation of QT, J-Tpeak and Tpeak-Tend subintervals included in this analysis has been described elsewhere [4].

Analysis and correction of heart rate dependency

T-wave morphology biomarkers dependent on heart rate were corrected for heart rate as previously described [15]. Briefly, population based heart rate correction factor was developed using baseline data from the present study. In all subsequent analysis, the heart rate dependent biomarkers (T-wave flatness and T-wave amplitude) were corrected for heart rate using an exponential model. The heart rate correction was performed using PROC MIXED in SAS 9.3 (SAS Institute, Cary, NC), wherein a significance level of 0.05 was used to determine if there was a difference by sex.

Statistical methods

We assessed whether there was a mitigation of dofetilide-induced ECG changes by either mexiletine of lidocaine at the maximum plasma drug concentration (Cmax) time-point during the evening dose. This was done using a paired t-test between the individual placebo-corrected changes from baseline with the combination vs. the individual predicted placebo-corrected changes from baseline at the individual measured dofetilide concentrations at Cmax time-point in R version 3.2.2 (R Foundation for Statistical Computing, Vienna, Austria). The placebo-corrected change from baseline was computed using PROC MIXED in SAS 9.3 (SAS institute, Cary, NC), where the change from baseline for each ECG biomarker by time-point was the dependent variable. Sequence, period, time, drug, and an interaction between treatment and time were included as fixed effects, and subject was included as a random effect. Afterwards, a linear-mixed effects model was used to evaluate the relationship between each of the ECG biomarkers and plasma concentrations for dofetilide and moxifloxacin alone. This was done using PROC MIXED in SAS 9.3 using a random effect on both intercept and slope (i.e., allowing each subject to have his or her own drug concentration-biomarker relationship).

ECG signature of selective hERG potassium channel block

We used a previously described method [15] to assess the ECG signatures of selective hERG potassium channel block associated with dofetilide and moxifloxacin. Briefly, we used the concentration-response models to predict the individual drug-induced changes for QTc and each ECG biomarker at 25% increments of the population's Cmax of each drug. Then, predicted changes together with 95% confidence intervals were plotted for each ECG biomarker vs. QTc.

Receiver operating characteristic (ROC) analysis

Using the ECG biomarkers with statistically significant changes at Cmax, we developed logistic regression models to classify selective hERG potassium channel block (dofetilide and moxifloxacin alone arms) vs. multichannel block (mexiletine with dofetilide and lidocaine with dofetilide arms) using placebo-corrected changes from baseline in QTc, J-Tpeakc and T-wave flatnessc pooled from all time-points (afternoon and evening time-points for dofetilide alone, mexiletine with dofetilide, and lidocaine with dofetilide; morning and afternoon time-points for moxifloxacin alone) . We computed the receiver operating characteristic (ROC) area under the curve (AUC) to assess the performance of each model. 95% confidence intervals (CI) of AUC were computed with 2000 stratified bootstrap replicates. We compared the performances of the models using Delong's test [18]. This analysis was done in R 3.2.2.

Decision tree

Lastly, we developed a C4.5 decision tree [19] to assess the relationship between the identified ECG biomarkers and selective hERG potassium channel block vs. multichannel block. The decision tree was developed using 10 fold cross-validation on all data from selective hERG potassium channel block (dofetilide [afternoon and evening time-points] and moxifloxacin [morning and afternoon] alone) vs. multichannel block (afternoon and evening time-points of mexiletine with dofetilide and lidocaine with dofetilide) (training set). We assessed the performance of the decision tree in the training set, but also using all data from our previous clinical study [14], where dofetilide and quinidine were labeled as strong hERG potassium channel blockers and ranolazine and verapamil as multichannel blockers (validation set). Decision tree was computed using the J48 algorithm in WEKA data mining software [20] version 3.6.

The "positive" class for all classification methods (ROC-AUC and decision tree) was "multichannel block". P values <0.05 were considered statistically significant without adjustment for multiplicity, and should be interpreted with an appropriate level of caution.

Results

The study included 21 healthy subjects (8 female). No serious adverse events were observed [4]. Table 1 reports the baseline characteristics of the subjects included in this analysis.

Selective hERG potassium channel block: dofetilide and moxifloxacin

At equivalent drug-induced QTc prolongation, T-wave morphology changes induced by moxifloxacin were similar to those caused by dofetilide. Moreover, the ECG "signature" of dofetilide was consistent with the ECG "signature" observed in our previous clinical study [15] (Figure 1).

Table 1: Baseline characteristics

	All subjects (N=21)
Demographic	
Age (years)	26.9 ± 5.5
Female	8 (38%)
Body mass index (kg/m2)	23.7 ± 2.3
Heart rate (beats per minute)	68.6 ± 8.2
QT and subintervals	
QTc (ms)	397.2 ± 15.0
JTpeakc (ms)	227.6 ± 18.9
Tpeak-Tend (ms)	82.2 ± 6.2
T wave morphology	
Flatness (d.u.)	0.43 ± 0.05
Asymmetry (d.u.)	0.17 ± 0.06
$ERD_{30\%}$ (ms)	50.1 ± 8.6
$LRD_{30\%}$ (ms)	31.5 ± 5.4
T-wave amplityde (μV)	574.3 ± 162.6

Continuous variables are represented as mean ± SD. QTc, Fridericia's heart rate corrected QT interval; J-Tpeakc, heart rate corrected J-Tpeak interval; T-wave flatnessc, heart rate corrected T-wave flatness; EDR30%, 30% of early repolarization duration; LRD30%, 30% of late repolarization duration; T-wave amplitudec, heart rate corrected T-wave amplitude; d.u., dimensionless units.

Mitigation of ECG changes by mexiletine and lidocaine

When administered in combination with dofetilide, Cmax of mexiletine and lidocaine were achieved after the third dose of the corresponding treatment period (Table 2). Figure 2 shows the ECG signatures of dofetilide alone, mexiletine+dofetilide and lidocaine+dofetilide together with the ECG "signature" of ranolazine from previous clinical study [15]. Late sodium current block by both mexiletine and lidocaine caused a numerical reduction of the ECG changes induced by dofetilide alone for all assessed ECG biomarkers except for 30% of late repolarization duration (Table 3). However, the changes were statistically significant only for QTc (p<0.001), J-Tpeakc (p<0.001) and T-wave flatnessc (p<0.001 and p=0.015 for mexiletine+dofetilide and lidocaine+dofetilide, respectively).

Ability of ECG biomarkers to detect late sodium current block

In the ROC-AUC analysis, J-Tpeakc had the largest AUC (0.83 [95% CI 0.8 to 0.83]) of all assessed ECG biomarkers (Figure 3). QTc had smaller AUC than J-Tpeakc (p<0.001)

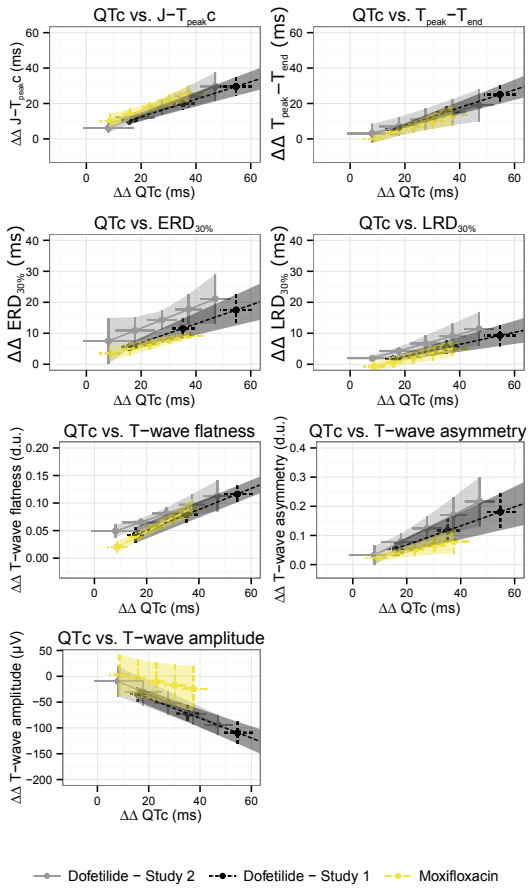

Figure 1: ECG "signature" of selective hERG potassium channel block shown as the relationship between predicted drug-induced placebo-corrected changes from baseline in QTc and (a) J-Tpeakc, (b) Tpeak-Tend, (c) 30% of early repolarization duration, (d) 30% of late repolarization duration, (e) T-wave flatnessc, (f)T-wave asymmetry and (g) T-wave amplitudec. Average predictions (dots) and 95% confidence intervals (horizontal and vertical lines) from concentration dependent models for QTc (x axis) and the different T-wave morphology biomarkers (y axis) at baseline and 25% increments of population's Cmax for dofetilide alone (light gray) and moxifloxacin (yellow) arms in this study together with dofetilide arm from previous clinical study [14, 15]. QTc, Fridericia's heart rate corrected QT; J-Tpeakc, heart rate corrected J-Tpeakc interval; T-wave flatnessc, heart rate corrected T-wave flatness; EDR30%, 30% of early repolarization duration; LRD30%, 30% of late repolarization duration;T-wave amplitudec, heart rate corrected T-wave amplitude.

but greater than T-wave flatnessc (p<0.001). AUC of the model including both J-Tpeakc and QTc was similar to AUC of J-Tpeakc alone (p=0.63). Lastly, AUC of the model including both T-wave flatnessc and QTc was not different from QTc alone (p=0.47). Table 4 summarizes AUC and the highest combined sensitivity + specificity from the ROC curve for all assessed models.

Decision tree analysis selected the ECG biomarkers in the same order as the ROC-AUC analysis (J-Tpeakc, QTc and T-wave flatnessc). Figure 4 shows the decision tree developed using the best features in the ROC-AUC analysis (QTc and J-Tpeakc). The accuracy of the decision tree differ-

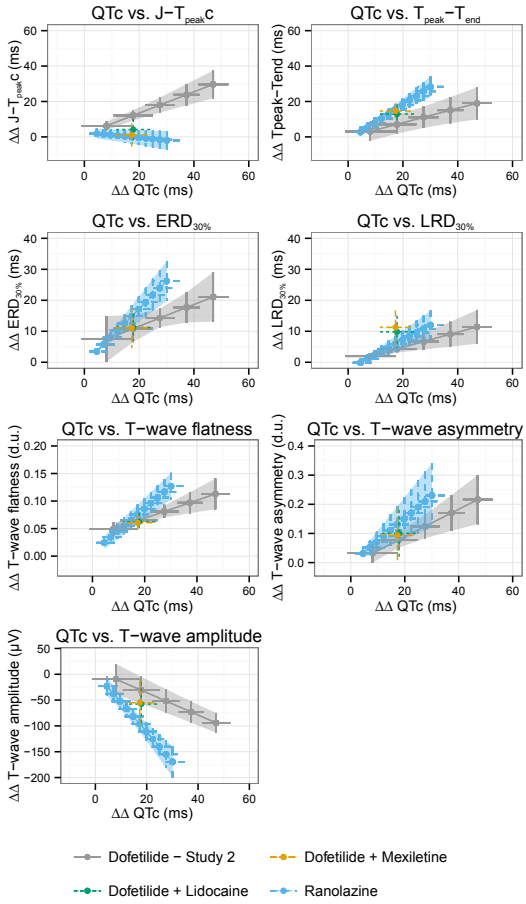

Figure 2: ECG "signature" of dofetilide (light gray), ranolazine (blue), mexiletine+dofetilide (orange) and lidocaine+dofetilide (green) shown as the relationship between predicted drug-induced placebo-corrected changes from baseline in QTc and (a) J-Tpeakc, (b) Tpeak-Tend, (c) 30% of early repolarization duration, (d) 30% of late repolarization duration, (e) T-wave flatnessc, (f)T-wave asymmetry and (g) T-wave amplitudec. Average predictions (dots) and 95% confidence intervals (horizontal and vertical lines) from concentration dependent models for QTc (x axis) and the different T-wave morphology biomarkers (y axis) at baseline and 25% increments of population's Cmax for dofetilide alone (light gray) and ranolazine (blue) arms in this study together with dofetilide arm from previous clinical study [14, 15]. Average (dots) and 95% confidence intervals (vertical and horizontal bars) of placebo-corrected changes from baseline for mexiletine+dofetilide (orange) and lidoacaine+dofetilide (green). QTc, Fridericia's heart rate corrected QT; J-Tpeakc, heart rate corrected J-Tpeakc interval; T-wave flatnessc, heart rate corrected T-wave flatness; EDR30%, 30% of early repolarization duration; LRD30%, 30% of late repolarization duration;T-wave amplitudec, heart rate corrected T-wave amplitude.

entiating multichannel block from hERG potassium channel block was 0.80 [0.76 to 0.83] (sensitivity 0.85, specificity 0.77) in the training set and 0.83 [0.81 to 0.85] in the validation set (sensitivity 0.83, specificity 0.82).

Discussion

In this study we assessed the effects of drug-induced late sodium current block on ECG changes caused by drug-

Table 2: Cmax time-points and plasma drug concentrations of mexiletine and lidocaine when given in combination with dofetilide.

Arm	Time	Drug	Concentration (ng/mL)
Mexiletine + Dofetilide	13	Dofetilide	1.83 [1.71 to 1.95]
	13	Mexiletine	1426 [1312 to 1540]
Lidocaine + Dofetilide	12.5	Dofetilide	1.83 [1.71 to 1.95]
	12.5	Lidocaine	2261 [2072 to 2450]

Time: hours after first dose of day; Concentration: mean and 95% confidence intervals.

Table 3: Placebo- and baseline-corrected drug-induced ECG changes at time-points reported in Table 2.

Biomarker	Dofetilide	Combination	P
Mexiletine + Dofetilide			
QT and subintervals			
QTc (ms)	45.2 [37.8 to 52.6]	17.3 [11.6 to 23]	**<0.001**
JTpeakc (ms)	29.1 [20.2 to 38]	1.1 [-5.5 to 7.7]	**<0.001**
Tpeak-Tend (ms)	17.9 [9.0 to 26.7]	14.6 [10.0 to 19.2]	0.36
T wave morphology			
Flatness (d.u.)	0.11 [0.08 to 0.14]	0.06 [0.04 to 0.08]	**<0.001**
Asymmetry (d.u.)	0.20 [0.11 to 0.29]	0.09 [0.00 to 0.19]	0.056
$ERD_{30\%}$ (ms)	19.8 [11.5 to 28.1]	11.1 [4.5 to 17.7]	0.12
$LRD_{30\%}$ (ms)	9.8 [5.0 to 14.6]	11.3 [5.8 to 16.7]	0.57
T-wave amplityde (μV)	-87.9 [-106.3 to -69.5]	-55.1 [-98.3 to -11.9]	0.16
Lidocaine + Dofetilide			
QT and subintervals			
QTc (ms)	45 [35.5 to 54.6]	17.9 [11.7 to 24.1]	**<0.001**
JTpeakc (ms)	28.3 [18.2 to 38.3]	4.1 [-1.9 to 10.2]	**<0.001**
Tpeak-Tend (ms)	18.4 [8.2 to 28.7]	12.9 [7.6 to 18.2]	0.23
T wave morphology			
Flatness (d.u.)	0.11 [0.07 to 0.14]	0.06 [0.05 to 0.08]	**0.015**
Asymmetry (d.u.)	0.19 [0.09 to 0.29]	0.1 [0.02 to 0.18]	0.14
$ERD_{30\%}$ (ms)	18.4 [8.8 to 27.9]	11.2 [6.8 to 15.6]	0.19
$LRD_{30\%}$ (ms)	10.0 [4.5 to 15.4]	9.8 [4.6 to 15.0]	0.90
T-wave amplityde (μV)	-82.5 [-107.6 to -57.5]	-57.6 [-99.8 to -15.4]	0.27

Values reported as mean and 95% confidence intervals.QTc, Fridericia's heart rate corrected QT interval; J-Tpeakc, heart rate corrected J-Tpeak interval; T-wave flatnessc, heart rate corrected T-wave flatness; EDR30%, 30% of early repolarization duration; LRD30%, 30% of late repolarization duration; T-wave amplitudec, heart rate corrected T-wave amplitude; d.u., dimensionless units.

induced selective hERG potassium channel block. The ECG signature of selective hERG potassium channel block was consistent between dofetilide and moxifloxacin, but also reproducible across studies for dofetilide. QTc, J-Tpeakc and T-wave flatnessc were the only three ECG biomarkers for which late sodium current block (mexiletine, lidocaine) caused statistically significant mitigation of changes induced by selective hERG potassium channel block (dofetilide). ROC-AUC analysis showed that J-Tpeakc was the best ECG biomarker for detecting late sodium current block, followed by QTc and then T-wave flatnessc. Decision tree analysis showed that J-Tpeakc and QTc can be used to detect late sodium current block in the presence of QTc prolongation caused by selective hERG potassium channel block. Future methodologies assessing drug effects on the ECG should use J-Tpeakc to detect drug-induced late sodium current block.

The ECG signatures of selective hERG block were consistent between drugs (dofetilide and moxifloxacin) and reproducible for dofetilide across studies (Figure 1). Moxifloxacin is commonly used as a positive control in thorough QT studies[7] because it is a weak hERG potassium channel blocker at clinical concentrations that prolongs the QTc by 10 to 14 ms (between 2 and 4 hours after 400mg oral dose), but has minimal torsade risk [21, 22, 23]. The similarity between moxifloxacin and dofetilide ECG "signatures" (Figure 1) suggests that the low torsade risk of moxifloxacin may be because moxifloxacin therapeutic doses cause limited hERG potassium channel block.[4] However, rare cases of moxifloxacin-induced torsade have been reported in pa-

Manuscript

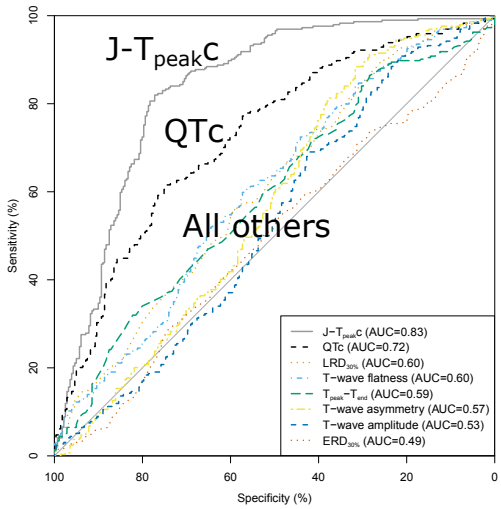

Figure 3: ROC curves for multiple logistic regression models. QTc, Fridericia's heart rate corrected QT interval; J-Tpeakc, heart rate corrected J-Tpeakc interval; T-wave flatnessc, heart rate corrected T-wave flatness. Area under the curve of each model reported in parenthesis.

Table 4: Logistic regression by performance.

model	AUC	Se	Sp
J-Tpeakc	0.83 [0.80 to 0.87]	0.82	0.77
QTc + J-Tpeakc	0.83 [0.80 to 0.87]	0.84	0.74
QTc + T-wave flatnessc	0.73 [0.69 to 0.77]	0.58	0.77
QTc	0.72 [0.68 to 0.77]	0.62	0.74
T-wave flatnessc	0.60 [0.56 to 0.65]	0.60	0.57
LRD30%	0.60 [0.56 to 0.65]	0.89	0.26
Tpeak-Tend	0.59 [0.55 to 0.64]	0.86	0.28
T-wave asymmetry	0.57 [0.52 to 0.62]	0.88	0.32
T-wave amplitudec	0.53 [0.48 to 0.58]	0.89	0.23
ERD30%	0.49 [0.45 to 0.54]	0.54	0.49

Performance reported as area under the curve [AUC] to predict when additional inward current block is present. AUC brackets show 95% confidence intervals. Sensitivity and specificity are the highest combination of sensitivity + specificity on the ROC curve. QTc, Fridericia's heart rate corrected QT interval; J-Tpeakc, heart rate corrected J-Tpeak interval; T-wave flatnessc, heart rate corrected T-wave flatness; EDR30%, 30% of early repolarization duration; LRD30%, 30% of late repolarization duration;T-wave amplitudec, heart rate corrected T-wave amplitude; Se, sensitivity; Sp, specificity.

tients at higher risk for torsade [24, 25, 26, 27]. Therefore, in patients exposed to higher moxifloxacin concentrations or with reduced "repolarization reserve" [28], moxifloxacin may exhibit an ECG profile more similar to dofetilide with larger QTc prolongation and higher risk for torsade.

There are multiple drugs that prolong QTc with minimal torsade risk [9, 10, 11], likely because they block inward currents [12, 29] in addition to the hERG potassium channel.

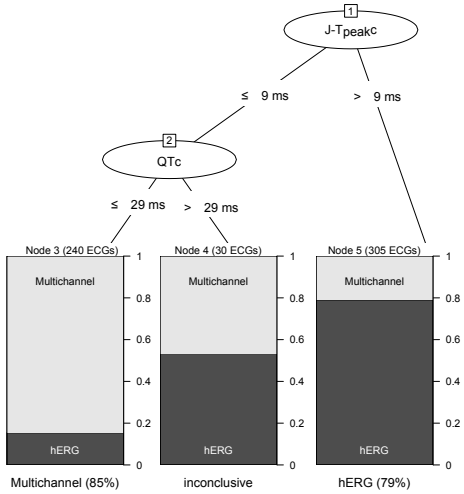

Figure 4: Decision tree classifies the drug effects on any ECG from any time point based on the time-matched placebo-corrected changes from baseline (ΔΔ) as selective of strong hERG potassium channel block (right bucket class), multichannel block (left bucket class) or inconclusive (middle bucket class). More specifically, if ΔΔJ-Tpeakc is greater than 9ms the ECG is classified as strong or selective hERG potassium channel block. If ΔΔJ-Tpeakc is less than or equal to 9ms and ΔΔQTc less than or equal to 29ms, then the ECG is classified as multichannel block. Otherwise the classification is inconclusive. The number of ECGs from each class in the training set reported in parenthesis on top of each class bucket. The percentage of ECGs correctly classified within each class is reported below each class bucket. See text for more details on classification performance in both training (hERG [dofetilide and moxifloxacin] vs. multichannel [dofetilide + mexiletine and dofetilide + lidocaine]) and validation (hERG [dofetilide and quinidine] vs. multichannel [ranolazine and verapamil]) sets. QTc, Fridericia's heart rate corrected QT interval; J-Tpeakc, heart rate corrected J-Tpeak interval; hERG, selective or strong hERG potassium channel block; Multichannel, inward (late sodium or calcium) current and hERG potassium channel block.

We have previously shown that shortening of J-Tpeakc is a sign of inward (late sodium or calcium) current block [4, 14, 30]. We have also shown that drug-induced changes in T-wave morphology biomarkers are directly related to the amount of hERG potassium channel block, and that multichannel blockers caused greater T-wave morphology changes than selective hERG potassium channel blockers at equivalent amount of QTc prolongation [15]. In this study we assessed which of all these ECG biomarkers can differentiate multichannel block (late sodium current block + hERG potassium channel block) from selective hERG potassium channel block on the ECG and therefore add value to QTc assessment. While there was a numerical reduction of hERG potassium channel induced changes for almost all ECG biomarkers after addition of late sodium current block, the effect was statistically significant only for QTc, J-Tpeakc and T-wave flatnessc (Table 3). This may have been due to larger inter-subject variability in the drug-induced changes in the T-wave morphology biomarkers compared to the more consistent response in QTc, J-Tpeakc and T-wave flatnessc (assessed as Cohen's d effect size [31], results not shown).

When comparing the ability of ECG biomarkers to detect the presence of late sodium current block, J-Tpeakc had the largest AUC in the ROC-AUC analysis. T-wave flatnessc did not add value to QTc assessment alone. Moreover, J-Tpeakc model performed better than QTc alone or in combination with either J-Tpeakc or T-wave flatnessc (Figure 3). The performance of the C4.5 decision tree developed with J-Tpeakc and QTc identifying inward current block using ECG data from this study was similar to the performance achieved with ECG data of drugs from our previous clinical study[14] (accuracy of 0.80 [0.76 to 0.83] vs. 0.83[0.81 to 0.84]). This suggests that, while appropriate thresholds still have to be established, a methodology using J-Tpeakc and QTc can identify multichannel block vs. selective hERG potassium channel block, in particular in the presence of QTc prolongation.

There are two main initiatives that may affect the future of the current regulatory paradigm of proarrhythmic assessment of drugs. The Consortium for Innovation and Quality in Pharmaceutical Development and the Cardiac

Safety Research Consortium (IQ-CSRC) have recently shown that exposure-response analysis of ECG and pharmacokinetic data from first-in-human studies can be used to assess drug-induced QTc prolongation with high confidence. This 'Early QT assessment' could be used in lieu of thorough QT studies in some cases [32], which could potentially reduce drug development costs. However, this approach does not address the distinction between high and low torsade risk QTc prolonging drugs [33]. Thus, the ability of J-Tpeakc to detect inward current block in small sample sizes should be assessed and considered as a potential enhancement of the IQ-CSRC proposed paradigm.

The second initiative is the Comprehensive in Vitro Proarrhythmia Assay (CiPA) initiative [33], which proposes an assessment of torsade risk beyond hERG potassium channel block and QTc prolongation. In particular, a mechanistically driven assessment of in vitro drug effects on multiple ion channels coupled with an in silico model of human cardiomyocytes with verification of predicted responses in human induced pluripotent stem cell derived cardiomyocytes. The current proposal is that the preclinical CiPA paradigm would include clinical confirmation. This clinical confirmation would include an ECG assessment in a Phase 1 clinical study to confirm that no unanticipated clinical ECG changes are found. Results of this study suggest that J-Tpeakc should be considered as a biomarker to detect late sodium current block in Phase 1 clinical studies under CiPA.

Limitations

Classes in the training set were defined as "selective hERG potassium channel block" vs. "late sodium current + hERG potassium channel block", while in the validation set, the corresponding classes are "strong hERG block" (dofetilide, quinidine) and "multichannel block" (ranolazine [late sodium current + hERG potassium channel block] and verapamil [strong calcium current block with some hERG potassium channel block]). However, this divides the drugs in the test set into those with high torsade risk and predominant hERG block (dofetilide and quinidine) vs. low torsade risk and balanced inward and outward current block (ranolazine and verapamil). Thresholds of the decision tree should be interpreted with caution because differences in statistical methods may result in different values.

Conclusion

J-Tpeakc was the best of all studied ECG biomarkers for detecting late sodium current block. ROC-AUC and decision tree analysis showed that an integrated assessment of J-Tpeakc and QTc can differentiate drug-induced multichannel block from selective hERG potassium channel block. Future methodologies assessing drug effects on cardiac ion channel currents on the ECG should consider J-Tpeakc to detect the presence of late sodium current block.

Study highlights

What is the current knowledge on the topic?

Drugs that block the hERG potassium channel and the late sodium current (e.g. ranolazine) have a low risk of torsade de pointes. A previous clinical study demonstrated that shortening of the J-Tpeakc interval is an ECG sign of late sodium current block.

What question did this study address?

Which ECG biomarkers would add value to current QT/QTc assessment? In other words, which ECG biomarkers are useful to detect inward current block on the ECG, in particular in presence of QTc prolongation.

What this study adds to our knowledge?

Late sodium current block mitigates T-wave flatness induced by selective hERG potassium channel block. However, T-wave flatness does not add value to QTc assessment for detecting late sodium current block. Moreover, of all assessed ECG biomarkers, J-Tpeakc performed best to detect late sodium current block.

How this might change clinical pharmacology and therapeutics?

Future strategies for assessing drug effects on cardiac ion channel currents on the ECG should consider J-Tpeakc to detect the presence of late sodium current block.

Acknowledgements

QTGuard+ was provided by GE Healthcare through a material transfer agreement. The mention of commercial products, their sources, or their use in connection with material reported herein is not to be construed as either an actual or implied endorsement of such products by the U.S. Department of Health and Human Services. This project was supported by FDA's Critical Path Initiative, Office of Women's Health and appointments to the Research Participation Programs at the Oak Ridge Institute for Science and Education through an interagency agreement between the Department of Energy and FDA. Pueyo is funded by Ministerio de Economía y Competitividad (MINECO), Spain, under project TIN2013-41998-R and by Grupo Consolidado BSICoS from DGA (Aragón) and European Social Fund (EU).

Disclosures

None.

Author contributions

J.V., D.G.S., L.J., M.H., E.P. and N.S. wrote the manuscript. J.V., D.G.S., L.J. and N.S. designed the research. J.V., L.J. and M.H. analyzed the data.

References

[1] Duff HJ, Roden D, et al. Mexiletine in the treatment of resistant ventricular arrhythmias: enhancement of efficacy and reduction of dose-related side effects by combination with quinidine. *Circulation* 67(5):1124–1128, 1983.

[2] Duff HJ, Mitchell LB, et al. Mexiletine-quinidine combination: electrophysiologic correlates of a favorable antiarrhythmic interaction in humans. *Journal of the American College of Cardiology* 10(5):1149–1156, 1987.

[3] Giardina EGV and Wechsler ME. Low dose quinidine-mexiletine combination therapy versus quinidine monotherapy for treatment of ventricular arrhythmias. *Journal of the American College of Cardiology* 15(5):1138–1145, 1990.

[4] Johannesen L, Vicente J, et al. Late sodium current block for drug-induced long qt syndrome: Results from a prospective clinical trial. *Clin Pharmacol Ther* , 2015.

[5] Badri M, Patel A, et al. Mexiletine prevents recurrent torsades de pointes in acquired long qt syndrome refractory to conventional measures. *JACC Clin Electrophysiol* 1(4):315–322, 2015.

[6] ICH. Ich topic s7b the nonclinical evaluation of the potential for delayed ventricular repolarization (qt interval prolongation) by human pharmaceuticals, 2005.

[7] ICH. Guidance for industry e14 clinical evaluation of qt/qtc interval prolongation and proarrhythmic potential for non-antiarrhythmic drugs, 2005. URL `http://www.fda.gov/downloads/drugs/guidancecomplianceregulatoryinformation/guidances/ucm073153.pdf`.

[8] Stockbridge N, Morganroth J, et al. Dealing with global safety issues - was the response to qt-liability of non-cardiac drugs well coordinated? *Drug Saf* 36(3):167–82, 2013.

[9] Antzelevitch C, Belardinelli L, et al. Electrophysiological effects of ranolazine, a novel antianginal agent with antiarrhythmic properties. *Circulation* 110(8):904–10, 2004.

[10] Wu L, Rajamani S, et al. Augmentation of late sodium current unmasks the proarrhythmic effects of amiodarone. *Cardiovasc Res* 77(3):481–8, 2008.

[11] Redfern WS, Carlsson L, et al. Relationships between preclinical cardiac electrophysiology, clinical qt interval prolongation and torsade de pointes for a broad range of drugs: evidence for a provisional safety margin in drug development. *Cardiovasc Res* 58(1):32–45, 2003.

[12] January CT and Riddle JM. Early afterdepolarizations: mechanism of induction and block. a role for l-type ca2+ current. *Circ Res* 64(5):977–90, 1989.

[13] Guo D, Zhao X, et al. L-type calcium current reactivation contributes to arrhythmogenesis associated with action potential triangulation. *J Cardiovasc Electrophysiol* 18(2):196–203, 2007.

[14] Johannesen L, Vicente J, et al. Differentiating drug-induced multichannel block on the electrocardiogram: randomized study of dofetilide, quinidine, ranolazine, and verapamil. *Clin Pharmacol Ther* 96(5):549–58, 2014.

[15] Vicente J, Johannesen L, et al. Comprehensive t wave morphology assessment in a randomized clinical study of dofetilide, quinidine, ranolazine, and verapamil. *J Am Heart Assoc* 4(4), 2015.

[16] Couderc J, Vaglio M, et al. Electrocardiographic method for identifying drug-induced repolarization abnormalities associated with a reduction of the rapidly activating delayed rectifier potassium current. In *Engineering in Medicine and Biology Society, 2006. EMBS'06. 28th Annual International Conference of the IEEE*, 4010–4015. IEEE, 2006.

[17] Johannesen L, Vicente J, et al. Ecglib: Library for processing electrocardiograms. In *Comput Cardiol*, 951–954. IEEE, 2013.

[18] DeLong ER, DeLong DM, and Clarke-Pearson DL. Comparing the areas under two or more correlated receiver operating characteristic curves: a nonparametric approach. *Biometrics* 837–845, 1988.

[19] Quinlan JR. *C4.5: programs for machine learning*. Morgan Kaufmann Publishers Inc., 1993.

[20] Hall M, Frank E, et al. The weka data mining software: an update. *ACM SIGKDD explorations newsletter* 11(1):10–18, 2009.

[21] Drugs@FDA. Moxifloxacin label, 2015. URL `http://www.accessdata.fda.gov/drugsatfda_docs/label/2015/205572s000lbl.pdf`.

[22] Demolis JL, Kubitza D, et al. Effect of a single oral dose of moxifloxacin (400 mg and 800 mg) on ventricular repolarization in healthy subjects. *Clin Pharmacol Ther* 68(6):658–66, 2000.

[23] Florian JA, Tornøe CW, et al. Population pharmacokinetic and concentration—qtc models for moxifloxacin: Pooled analysis of 20 thorough qt studies. *J Clin Pharmacol* 51(8):1152–1162, 2011.

[24] Altin T, Ozcan O, et al. Torsade de pointes associated with moxifloxacin: A rare but potentially fatal adverse event. *Can J Cardiol* 23(11):907–908, 2007.

[25] Dale KM, Lertsburapa K, et al. Moxifloxacin and torsade de pointes. *Ann Pharmacother* 41(2):336–40, 2007.

[26] Sherazi S, DiSalle M, et al. Moxifloxacin-induced torsades de pointes. *Cardiol J* 15(1):71–3, 2008.

[27] Badshah A, Janjua M, et al. Moxifloxacin-induced qt prolongation and torsades: an uncommon effect of a common drug. *Am J Med Sci* 338(2):164–6, 2009.

[28] Roden D. Long qt syndrome: reduced repolarization reserve and the genetic link. *J Intern Med* 259(1):59–69, 2006.

[29] Guo D, Zhao X, et al. L-type calcium current reactivation contributes to arrhythmogenesis associated with action potential triangulation. *J Cardiovasc Electrophysiol* 18(2):196–203, 2007.

[30] Johannesen L, Vicente J, et al. Improving the assessment of heart toxicity for all new drugs through translational regulatory science. *Clin Pharmacol Ther* (95):501–508, 2014.

[31] Cohen J. *Statistical power analysis for the behavioral sciences*. Lawrence Erlbaum, 1988.

[32] Darpo B, Garnett C, et al. Implications of the iq-csrc prospective study: Time to revise ich e14. *Drug Saf* 38(9):773–80, 2015.

[33] Sager PT, Gintant G, et al. Rechanneling the cardiac proarrhythmia safety paradigm: a meeting report from the cardiac safety research consortium. *Am Heart J* 167(3):292–300, 2014.

Report - Memoria

The following chapters summarize:

- Aims of this research.
- Contributions of the PhD student.
- Methods applied in the studies presented in the previous chapters.
- Final conclusions

CHAPTER 7

Aims

The main goal of this thesis is to assess whether an integrated analysis of the ECG, including novel T-wave morphology biomarkers, can differentiate multichannel blocking drugs with minimal torsade risk from selective hERG potassium channel blocking drugs with high torsade risk. More specifically, studies in this thesis identify which ECG biomarkers can enhance the current clinical evaluation of proarrhythmic potential of drugs. A secondary goal is to identify sex differences in drug-induced changes in the ECG that provide insights into why women are at higher risk for torsade than men.

The specific aims for each study included in this thesis are described below:

- **Study I**: To characterize sex- and age-dependent differences in depolarization (QRS), early repolarization interval (J-T_{peak}c), and late repolarization interval (T_{peak}-T_{end}) to elucidate the mechanisms for sex and age differences in QTc. In addition, we simulated the effect of decreasing testosterone levels on individual ion channel currents and early versus late repolarization on the ECG to understand the mechanism behind sex and age differences in ventricular repolarization in humans.

- **Study II**: To test the hypothesis that quinidine-induced T_{peak}-T_{end} prolongation is greater in women than men.

- **Study III**: To evaluate the effect of selective hERG block versus multichannel block on multiple T-wave morphology biomarkers. This included quantitative measures of T-wave flatness, asymmetry,

and notching, which were developed to detect the ECG signature of LQT2 (abnormal hERG current). In addition, we studied the 30% early and late repolarization duration ($ERD_{30\%}$ and $LRD_{30\%}$) of the T-wave loop, previously shown to detect hERG potassium channel block, and other vectorcardiographic measures of the relation between depolarization and repolarization vectors (QRS-T angle, ventricular gradient, and total cosine R-to-T [TCRT]), which have been shown to predict arrhythmic risk in some patient populations.

- **Study IV**: To assess whether there are sex differences in the ECG changes (QTc, but also QT subintervals and T-wave morphology) induced by a selective hERG potassium channel drug (dofetilide) and three drugs that block the hERG potassium channel but also block calcium or late sodium inward currents (quinidine, ranolazine and verapamil).

- **Study V**: To assess which ECG biomarkers are useful to detect inward current block on the ECG, in particular in presence of QTc prolongation. More specifically, we assess the effects of late sodium current block (mexiletine or lidocaine) on T-wave morphology changes caused by selective hERG potassium channel block (dofetilide). In addition, we rank multiple ECG biomarkers (QTc, its subintervals and T-wave morphology) by their ability to detect late sodium current block, which is important for torsade risk assessment.

CHAPTER 8

Contributions

To support the research studies of this thesis, the PhD student played a lead role on the design and development of new ECG analysis tools (ECGlib [52] and ECGlab [53]). These tools are described in Section 9.2.1. Briefly, ECGlib is a C++ library for processing ECGs. It implements standard ECG signal processing methods that allow for automatic adjudication of ECGs. Its performance is comparable to state-of-the-art methods. ECGlib has a modular design and can be extended through plugins. ECGlab is a user friendly, graphical user interface for assessing results from automated analysis of ECGs in research environments. It is built on top of ECGlib library and plugins and allows for fast on-screen computer-assisted semi-automatic review and adjudication of large numbers of ECGs. ECGlib and ECGlab were developed using open source tools and libraries such us Armadillo [54], Boost [55], Qt [56] and Qwt [57]. The PhD student is working together with other ECGlib and ECGlab developers to make these tools publicly available under an open source license.

For each study included in this thesis, the PhD student designed the study, analyzed the data and wrote the manuscript. A more detailed description of the PhD student contributions to each of the studies is outlined below:

- **Study I**: The idea for this study came out of discussions between the student and Strauss and Johannesen. The design and planning of the study including software implementation and statistical analysis was carried out by the student. The manuscript was drafted by the student with help from Strauss and Johannesen and input from Galeotti. Journal correspondence was handled by the student and Strauss.

- **Study II**: The idea for this study came out of discussions between the student and Strauss, Simlund, Johannesen and Wagner. The design and planning of the study including software implementation and statistical analysis was carried out by the student. Study data was curated by the student with help from Woosley and Johannesen. Semi-automatic adjudication of ECGs was performed by the student with help from Johannesen and Simlund. ECGs were assessed with ECGlab, which was developed by the student. Compartmental model (hysteresis) analysis was performed by Johannesen with help from the student. The manuscript was drafted by the student and Simlund with help from Strauss and Johannesen as well as input from all co-authors. Journal correspondence was handled by the student and Strauss.

- **Study III**: The idea of assessing ECG biomarkers beyond QT and its subintervals was proposed by Strauss and further elaborated by the student together with Johannesen. The design and planning of the study including software implementation and statistical analysis was carried out by the student. The student and Johannesen performed analysis of all ECGs. ECG analysis software was developed with help from Johannesen. QTGuard+ (T-wave flatness, asymmetry and presence of notch) algorithms were provided by GE Healthcare and integrated in ECGlib by the student with help from Johannesen. The idea of plotting QT vs. other ECG biomarkers to visualize the ECG signatures of drugs was proposed by the student. Crumb conducted the voltage clamp experiments. The student analyzed the patch clamp data, fit Emax models and computed IC50 curves. Finally, the manuscript was drafted by the student with input from supervisors and all co-authors. Journal correspondence was handled by the student and Strauss. The manuscript was "*featured article*" of April 2015 issue of the *Journal of the American Heart Association*.

- **Study IV**: The idea of conducting sex-specific analysis came out of discussions between the student and Strauss and further elaborated by the student with input from Johannesen. Analysis of the ECGs was carried out by the student together with Johannesen. The statistical analysis plan was planned and carried out by the student with input from Johannesen. The student presented the results at the annual International Society for Computerized Electrocardiology (ISCE), where he received the "*Best poster award*" and was invited to submit a full manuscript to *Journal of Electrocardiology*. The manuscript was drafted by the student with input from supervisors

and all co-authors. Journal correspondence was handled by the student.

- **Study V**: The idea of assessing which biomarker would add value to assessing QTc alone was proposed by Stockbridge and further elaborated in discussions between the student, Strauss and Johannesen. The design and planning of the study including software implementation and statistical analysis was carried out by the student. The student and Johannesen performed analysis of all ECGs. ECG analysis software was developed with help from Johannesen. QTGuard+ (T-wave flatness, asymmetry and presence of notch) algorithms were provided by GE Healthcare and integrated in ECGlib by the student with help from Johannesen. The idea of using a *receiver operating characteristic* (ROC)-*area under the curve* (AUC) analysis was proposed by Johannesen and implemented and assessed by the student. The idea of using C4.5 decision tree was proposed by Hosseini and implemented and assessed by the student. The manuscript included in this thesis was drafted by the student with input from supervisors and all co-authors.

Lastly, the idea of the two FDA-sponsored prospective clinical trials was proposed by Stockbridge and led later by Strauss, Johannesen and the student with input from Stockbridge and Mason. The student played a lead role in both prospective clinical trials. The student contributed to the studies design, protocol, site initiation visits, data transfer and quality control, as well as follow-up with the clinic and making the data available through the Telemetric and Holter ECG Warehouse (`http://thew-project.org`, databases E-OTH-12-5232-020 and E-HOL-12-0109-021).

CHAPTER 9

Materials and Methods

9.1 Study populations and study designs

All the studies presented in this thesis were approved by the Research Involving Human Subjects Committee of the U.S. Food and Drug Administration. For each of the individual clinical studies included in this thesis, the studies were approved by the local institutional review boards and all subjects gave written informed consent.

9.1.1 Baseline data from 30 Thorough QT studies (Study I)

The population in this study consisted of 2,235 healthy subjects aged 18-78 years from 30 Thorough QT studies. Inclusion criteria for a typical thorough QT study include healthy men or women without any clinically significant abnormalities, taking no medication (except for hormonal contraceptives) and, for women, not to be pregnant or lactating before enrollment. Exclusion criteria include use of drugs, tobacco products or alcohol consumption, as well as ECG thresholds such as QTc $>$ 450 ms for men and $>$ 470 ms for women, PR $>$ 220 ms, QRS $>$ 110 ms and other cardiovascular abnormalities. Other inclusion and exclusion criteria included assessment of limited weight, body mass index and vital signs measurements to ensure that all included subjects were considered healthy when enrolled in the study. Sex and age differences were assessed by analyzing resting 12-lead ECG recordings acquired at baseline.

Table 9.1: Study II baseline characteristics by sex

	Women	Men	*P*
N	11	12	
Age (years)	26 ± 8	30 ± 7	0.28
Height (m)	1.69 ± 0.06	1.79 ± 0.08	<0.01
Weight (kg)	65 ± 11	75 ± 13	0.047
Body mass index (kg/m^2)	23 ± 4	22 ± 3	0.57
Heart Rate (bpm)	64 ± 7	63 ± 10	0.58
QTc (ms)	405 ± 10	389 ± 17	<0.01
T_{peak}-T_{end} (ms)	77 ± 11	73 ± 4	0.10

9.1.2 Intravenous quinidine clinical study (Study II)

This study population included 24 healthy nonsmoking volunteers (12 women, 12 men) between 18-35 years old. One woman was excluded from this analysis because she had a short PR interval of approximately 100 ms. Table 9.1 reports baseline characteristics by sex. The protocol was a randomized, single-blinded comparison of single doses of intravenous quinidine gluconate (4 mg/kg of base, Eli Lilly, Indianapolis, Indiana, USA) and matching intravenous placebo (saline). Quinidine gluconate (80 mg/ml) was diluted to a total volume of 20 ml with saline solution and infused over 20 minutes. Blood was collected through an intravenous catheter into plain vacutainer tubes from the opposite arm of the infusion at 28 nominal time points postdose. The samples were prepared for quantification of quinidine and 3-hydroxyquinidine and non-protein bound (free) concentrations were determined by ultrafiltration and high performance liquid chromatography, as previously described [45].

9.1.3 First FDA-sponsored clinical trial (Studies III - IV)

The inclusion and exclusion criteria in this study were similar to those used in thorough QT studies [1]. Briefly, healthy subjects between 18 and 35 years old, weighing between 50 and 85 kg and without a family history of cardiovascular disease or unexplained sudden cardiac death were eligible for participation in the study. In addition, the subjects had to have less than 12 ventricular ectopic beats during a 3 hour continuous ECG recording at screening, as well as a baseline QTc of less than 450 ms for men (470 ms for women), using Fridericia's correction [58]. Baseline characteristics are summarized in Table 9.2.

The study was designed as a randomized double-blind 5-period crossover clinical trial. Briefly, subjects received a single dose of 500 μg dofetilide

Table 9.2: Study III baseline characteristics

	All subjects (N=22)
Demographic	
Age (years)	26.9 ± 5.5
Female	11 (50%)
Body mass index (kg/m2)	23.1 ± 2.7
ECG	
Heart rate (beats per minute)	56.8 ± 6.4
QTc (ms)	395.9 ± 17.1
J-T_{peak}c (ms)	225.6 ± 19.8
T_{peak}-T_{end} (ms)	73.1 ± 6.4
T wave morphology	
Flatness (d.u.)	0.41 ± 0.04
Asymmetry (d.u.)	0.16 ± 0.05
Presence of Notch (%)	0
Repolarization duration	
$ERD_{30\%}$ (ms)	44.5 ± 5.1
$LRD_{30\%}$ (ms)	27.5 ± 4.1
Vectorcardiographic	
QRS-T angle (°)	34.5 ± 9.9
TCRT (radians)	0.67 ± 0.24
Tmagmax (μV)	578.5 ± 173.0
Ventricular gradient (mV·ms)	112.3 ± 30.2

Continuous variables are represented as mean ± SD of each subject's 5-day baseline average

(Tikosyn, Pfizer, New York, NY), 400 mg quinidine sulfate (Watson Pharma, Corona, CA), 1,500 mg ranolazine (Ranexa, Gilead, Foster City, CA), 120 mg verapamil hydrochloride (Heritage Pharmaceuticals, Edison, NJ) or placebo under fasting conditions in the morning of each period. To ensure substantial ECG changes after a single dose, the selected dose was the maximum single dose allowed in the label for dofetilide and quinidine [59, 60]. The ranolazine dose was selected to achieve plasma levels close to the chronic/steady state levels, but with a single dose. This resulted in a dose higher than the clinical dose but lower than the maximum daily dose in the label [61]. The highest initial single dose in the label was selected for verapamil. However, verapamil was not pushed further due to concern for extreme PR prolongation and heart block in healthy subjects [62]. There was a 7-day washout period between each 24-hour treatment period. The study was conducted at a phase 1 clinical research unit (Spaulding

Clinical, West Bend, Wisconsin, USA). William's Latin square design balanced for first-order carryover effects [63] was used for randomization.

Continuous ECGs were recorded at 500 Hz and with an amplitude resolution of 2.5 μV during each period. From the continuous recording, triplicate 10-second 12-lead ECGs were extracted at predose and 15 predefined time-points postdose (0.5, 1, 1.5, 2, 2.5, 3, 3.5, 4, 5, 6, 7, 8, 12, 14, 24 h) during which the subjects were resting in a supine position for 10 minutes. At each time-point period and after each ECG extraction, a blood sample was drawn for pharmacokinetic analysis. Plasma drug concentration was measured using a validated liquid chromatography with tandem mass spectroscopy method by Frontage Laboratories (Exton, Philadelphia, PA).

9.1.4 Second FDA-sponsored clinical trial (Study V)

This clinical trial involved a five-period, randomized, cross-over trial designed to study the ability of $I_{Na,L}$ or $I_{Ca,L}$ current block to balance the ECG effects of selective hERG potassium channel block. There was one week between treatment periods. Figure 9.1 shows the study design. Briefly, in each treatment period subjects were dosed three times during the day to evaluate the effects of $I_{Na,L}$ current block by itself in the morning (mexiletine or lidocaine), and increasing levels of late sodium combined with selective hERG potassium channel block in the afternoon and evening (mexiletine combined with dofetilide or lidocaine combined with dofetilide). It was not possible to combine diltiazem ($I_{Ca,L}$ current blocker) with dofetilide because of pharmacokinetic interactions. Therefore, high-dose of moxifloxacin (selective hERG potassium channel blocker) was given in the morning and afternoon doses and a combination of moxifloxacin with diltiazem in the evening dose.

The study inclusion and exclusion criteria were similar to those used in thorough QT studies [1] and the first FDA-sponsored clinical trial described above (Section 9.1.3), but with a stricter baseline QTc criteria ($<$430 ms using Fridericia's correction [58]). Twenty-two healthy subjects (9 female) participated in the study. Twenty subjects started the placebo treatment day, 20 the dofetilide alone day, 21 the mexiletine and dofetilide day, 19 the lidocaine and dofetilide day, and 20 the moxifloxacin and diltiazem day. No serious adverse events were observed. One female was excluded from this analysis because in the evening time-point of dofetilide alone arm, plasma dofetilide concentration was lower despite the evening oral dose, but she still had larger placebo- and baseline-corrected changes in all ECG biomarkers. Table 9.3 reports the baseline characteristics of the 21 subjects included in this analysis.

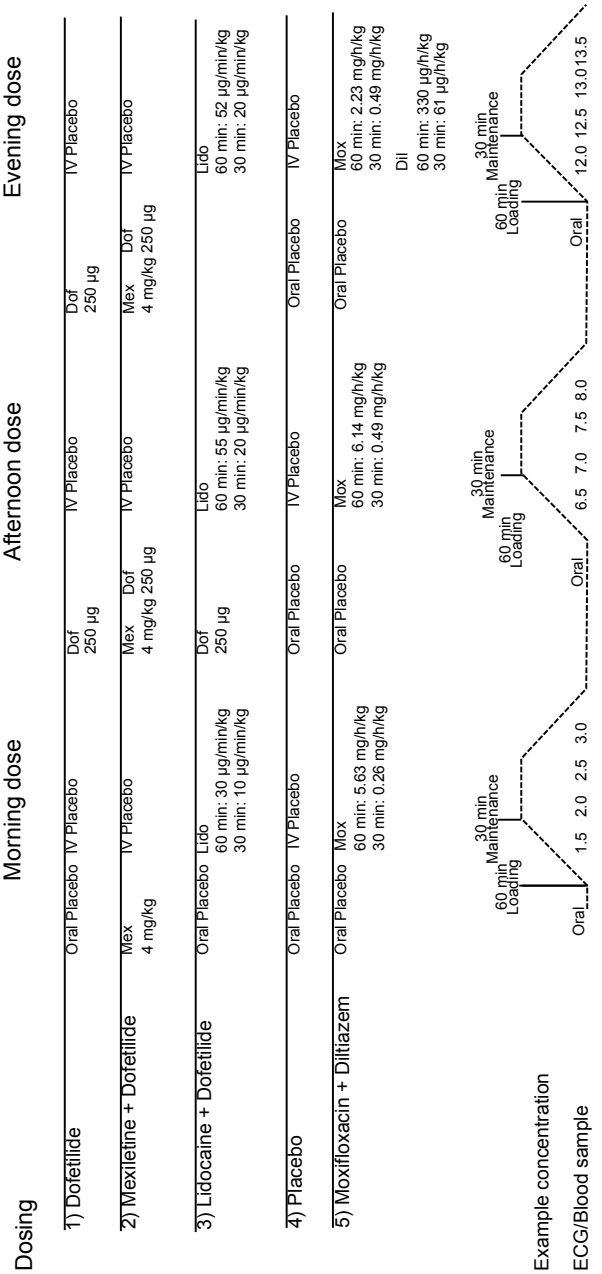

FIGURE 9.1: Study design of the second FDA-sponsored clinical trial (Study V). The table shows the morning, afternoon and evening doses for each of the five treatment periods. Below the table, an illustration of the plasma drug level is shown to indicate when oral and intravenous dosing took place as well as when ECGs and plasma samples were taken (in hours after first oral dose). Dof, dofetilide; mex, mexiletine; lido, lidocaine; mox, moxifloxacin; dil, diltiazem. Reprinted from Johannesen et al 2016 with permission [17].

Table 9.3: Study V baseline characteristics

	All subjects (N=21)
Demographic	
Age (years)	26 ± 5
Female	8 (38%)
Body mass index (kg/m^2)	23.7 ± 2.3
ECG	
Heart rate (beats per minute)	68.6 ± 8.2
QTc (ms)	397.2 ± 15.0
J-T_{peak}c (ms)	227.6 ± 18.9
T_{peak}-T_{end} (ms)	82.2 ± 6.2
T-wave morphology	
Flatness (d.u.)	0.43 ± 0.05
Asymmetry (d.u.)	0.17 ± 0.06
Tmagmax (μV)	574.3 ± 162.6

Continuous variables are represented as mean ± SD of each subject's 5-day baseline average

9.2 ECG analysis

All the ECGs analyzed in the multiple studies of this thesis were 10-second 12-lead ECGs obtained while subjects were resting in a supine position. According to each study design, three or more non-overlapping 10-second ECGs were obtained at pre-specified time-points. In particular, triplicate non-overlapping 10-second ECGs were extracted from continuous recordings (Holters) at the pre-specified time-point windows with stable heart rates and maximum signal quality [64] using Antares software (AMPS-LLC, New York City, NY) in the two FDA-sponsored clinical trials (Studies III - V) .

9.2.1 ECG analysis tools (Studies I - V)

All 10-second 12-lead ECGs were automatically assessed with ECGlib or semi-automatically assessed with ECGlib and ECGlab [52, 53]. ECGlib and ECGlab are ECG analysis tools developed and maintained by the PhD student. These ECG analysis tools were developed to support the research studies of this thesis and are described in subsection 9.2.1. Subsections 9.2.2 and 9.2.3 provide an overview of the methods implemented in these tools and that allow to assess the QT interval, QT subintervals and multiple T-wave morphology biomarkers.

In addition to the research studies in this thesis, ECGlib and ECGlab

have been used in other research projects [17, 31, 32, 65]. The PhD student is working together with other ECGlib and ECGlab developers on making the these tools publicly available under an open source license.

9.2.1.1 ECGlib: library for processing ECGs

ECGlib [52] is a library developed in C++ to facilitate evaluation of ECGs in the FDA ECG warehouse (Study I) as well as public databases (e.g. Physionet [66]) and clinical trials (Studies II-V). ECGlib supports multiple ECG file formats (e.g. ISHNE [67], Physionet and FDA HL7) and implements standard ECG signal processing methods. The performance of the different components of ECGlib has been reported before and is comparable to state-of-the-art methods [52].

The design of ECGlib is modular. It provides an *Application Programming Interface* (API) that allows developers to write ECGlib compatible plugins to extend its functionality. For example, a developer can write a plugin to add support for a new ECG file format or a plugin that implements a new ECG analysis method. To allow rapid algorithm development, ECGlib provides a MATLAB^{TM}/Octave interface also. ECGlib is multi-platform and can be compiled and executed in both Linux and Microsoft Windows© operating systems.

To enable researches to quickly process large number of ECGs, ECGlib includes a set of command line tools that process ECG files from indexed databases automatically and in parallel. These tools use ECGlib and ECGlib compatible plugins to access ECG files, analyze them and store the analysis results.

Figure 9.2 shows the default ECG analysis workflow implemented by ECGlib library and command line tools. The default workflow was used in the automatic analysis of the ECGs of this thesis. After loading an ECG, QRS complexes were detected and delineated using the so-called U3 method [68, 69] (Figure 9.2.a). Next, high frequency noise was removed applying a 4^{th} order butterworth 40 Hz lowpass filter (Figure 9.2.b). Then, baseline wander was removed fitting a cubic spline through a point in the PQ segment (Figure 9.2.c). ECGs with excessive baseline wander (average of the residual of the baseline wander filter $\geq$ 200 μV), high-frequency noise (average residual of butterflow highpass filter $\geq$ 40 μV), not enough number of noise-free beats to construct the median beat (number of noisy beats $\geq$ 4), unstable heart rate (standard deviation of beat to beat heart rate $\geq$ 10 beats per minute), or intermittent lead problems (e.g. large spread of QRS onset across leads assessed as mean of the standard deviation across leads $\geq$ 20 ms) were excluded from subsequent analysis [70].

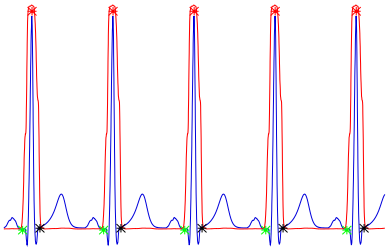

(a) QRS detection

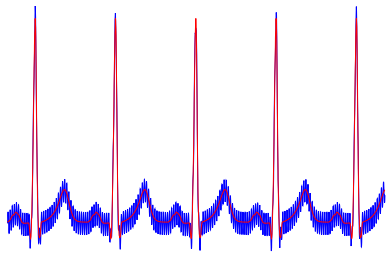

(b) Powerline noise filtering

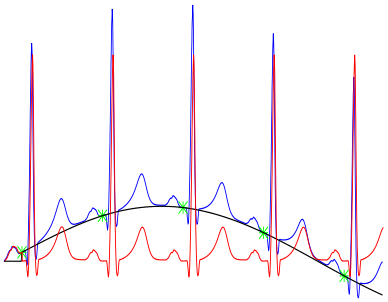

(c) Baseline wander removal

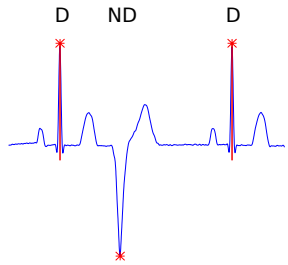

(d) Beat classification

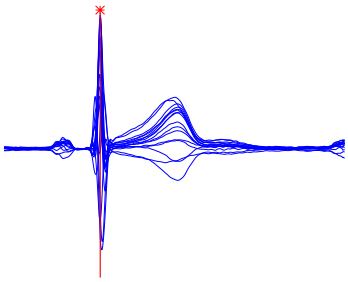

(e) Median beat construction

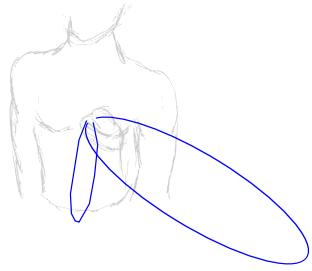

(f) Derived vectorcardiogram

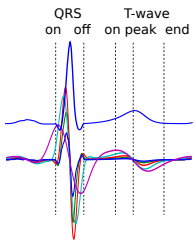

(g) Wavelet-based delination

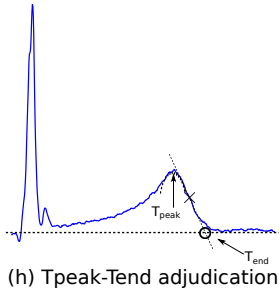

(h) Tpeak-Tend adjudication

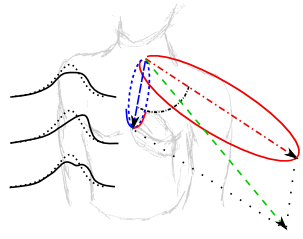

(i) T-wave morphology

Figure 9.2: ECGlib automatic ECG analysis steps. See text.

Next, median beats were created to increase the *signal-to-noise ratio* (SNR) under the assumption that noise is random and uncorrelated with the signal. To avoid reduction of SNR caused by inclusion ectopic beats, false QRS detections or other noise artifacts, detected beats were classified into dominant (D) and non-dominant (ND) beats. ECGlib implements a template-based beat classifier, which is based on waveform similarity and the regularity of the RR interval for each beat (Figure 9.2.d). Under the assumption that sinus beats are the most frequent, only dominant beats were included in when constructing the median beats. When two semi-equal classess were identified, the class with narrowest QRS complex was selected as dominant. (Figure 9.2.e).

Then, the vectorcardiogram was derived from the 12-lead median beat using Guldenring transform [71] and the vectormagnitude lead was computed (Figure 9.2.f). Lastly, multiple ECG biomarkers were assessed in the median beat. Automatic delineation of the QRST complex (Figure 9.2.g and Figure 9.2.h) and computation of T-wave morphology biomarkers (Figure 9.2.i) are described in section 9.2.2 ans section 9.2.3 below.

9.2.1.2 ECGlab: user friendly ECG analysis tool

ECGlab is a C++, cross-platform, user friendly, graphical user interface for assessing results from automated analysis of ECGs in research environments [53]. It allows visual inspection and semi-automatic adjudication of ECGs. ECGlab uses ECGlib library and plugins to load and save ECG files and annotations. It provides visual helpers as well as assisted annotation capabilities that are built using ECGlib methods and plugins. This increases both intra- and inter-reader consistency and reproducibility of semi-automatic ECG adjudications. Annotations can be introduced in a manual fashion also.

To facilitate the review of large amount of ECGs, ECGlab provides a database navigation assistant. The navigation assistant is built on top of ECGlib indexing methods and facilitates searching, filtering and sorting ECGs. The assistant includes a tree and a table views. The tree view allows to display hierarchical indexes (e.g. ECGs organized by subject, visit and time-point in unblinded clinical databases). Other metadata associated with the index can be loaded from a *comma separated values* (CSV) file into the table view. Metadata files can contain any arbitrary variables such us demographics, individual or global lead interval durations, noise metrics or any other statistical values. These files can be generated during automatic ECG analysis by ECGlib command line tools and plugins, but also using external tools for data analysis (such as R, Mathworks MATLAB^{TM}or Microsoft EXCEL^{TM}). The table can be filtered and sorted by any variable. ECGs can be opened with a mouse

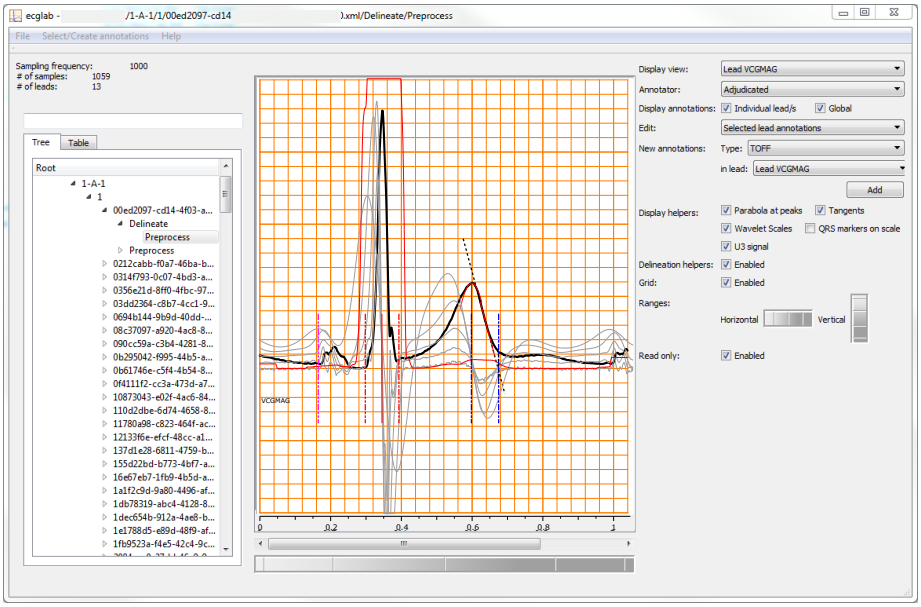

Figure 9.3: ECGlab screenshot: Database navigation assistant (search box, tree and table views in the left panel). ECG display in the central panel, which in the figure displays a vectormagnitude lead of a median beat on top of standard ECG grid, together with annotated fiducial points (vertical lines), line fitted to the descending part of T-wave (dashed black line), parabola fitted to T-wave peak and U3 transform in red and scales of wavelet transform in gray. Right panel shows controls to customize ECG display, including display view (e.g. single lead, 4x3 matrix), zoom level or delineation helpers check box, which allows for semi-automatic point-and-click adjudication using the same ECGlib methods used by the automatic command line tools and the ECG display visual helpers.

double-click on the corresponding table row. This facilitates the evaluation of outliers but also identifying ECGs that match other criteria of interest for the user.

Lastly, ECGlab provides some other features such as exporting the display as *scalable vector graphics* (SVG) files or adding notes to the ECG. Note that notes will be saved to the ECG format only if the file format supports notes. Figure 9.3 shows a screen shot of ECGlab's user interface.

9.2.2 QT and subintervals (Studies I - V)

While there are some study specific differences, delineation of the QRST complex was usually performed in four steps. First, the vectorcardiogram was derived from the 12 leads using Guldenring transform [71] and the

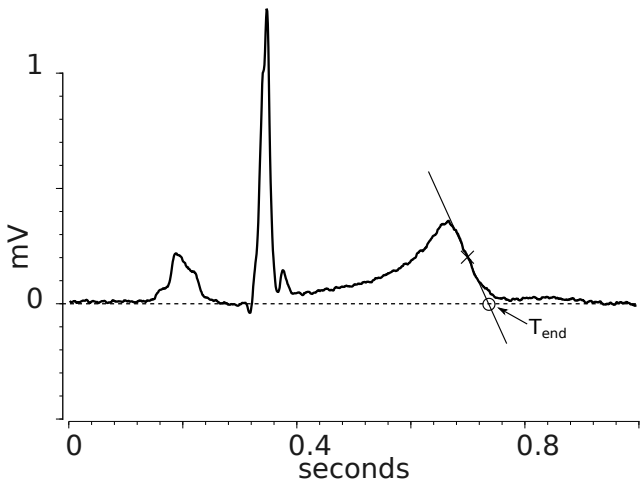

FIGURE 9.4: The end of the T-wave was determined using the least-squares approach method, which involves locating the intersection between the line through the terminal descending part of the T-wave and the isoelectric line [72, 73].

vectormagnitude lead was computed (Figure 9.2.f). Next, the wave peaks and boundaries (QRS_{onset}, R_{peak}, QRS_{offset}, T_{peak} and T_{end}) were determined using a wavelet-based delineator (Figure 9.2.g) [74]. Then, the least-squares approach, which involves locating the intersection between the tangent line fitted to the terminal descending part of the T-wave and the isoelectric line, was used to locate the offset of the T-wave [72, 73] using T_{peak} and T_{end} fiducial points obtained in the previous steps to establish the search boundaries (Figure 9.4). Lastly, the peak of the T-wave was assessed as the maximum of the parabola fitted around the peak of the T-wave [75] using T_{peak} from the wavelet-based delineation as seeding point (Figure 9.2.h). The tangent-based approach was used instead of other methods such as wavelet-based delineation [74] because it has been traditionally used by cardiologists when assesing ECGs at contract research organizations. In addition to the fiducial point annotations, ECGlib analysis tools also reported QT (QRS_{onset} to T_{end}), QRS (QRS_{onset} to QRS_{offset}), J-T_{peak} (QRS_{offset} [J point] to T_{peak}) and T_{peak}-T_{end} (T_{peak} to T_{end}) as ECG biomarkers for use in subsequent analysis.

In Study I, sponsors' provided ECG measurements (QRS_{onset}, QRS_{offset} and T_{end}) were projected onto the median QRST waveform. Briefly, if sponsor provided annotations on a median beat, then the median beat provided by the sponsor was aligned with the median beat computed by ECGlib and sponsor annotations were projected onto ECGlib's median beat using the location of the peak of the R wave as reference. If fidu-

cial points were measured in consecutive beats in one lead (e.g. three consecutive beats in lead II), individual beats were aligned with the corresponding lead of ECGlib's median beat, annotations were projected using the location of the peak of the R wave as reference and the median value of the projected fiducial points was used as the location of the annotation in the median beat. Lastly, sponsor's QRS_{onset}, QRS_{offset} and T_{end} were then used together with ECGlib's automatically assessed T_{peak} on the vectormagnitude lead to compute the QT subintervals (QRS, J-T_{peak} and T_{peak}-T_{end}).

QT and T_{peak}-T_{end} were assessed in lead V5 in Study II. V5 was selected because prolonged T_{peak}-T_{end} interval in V5 has been described previously as a good predictor of torsade [76]. ECGlib automatic annotations were reviewed and manually adjusted as determined by visual inspection in ECGlab by two independent ECG readers blinded to treatment and sex. Most subjects developed notched T-wave after administration of quinidine. Notched T-waves included both biphasic T-waves and two positive peaks with a nadir in between. If there were two T-wave peaks, T_{peak} was selected as the first peak maximum [77, 78]. If any maximum or minimum was in the form of a plateau, annotations were placed at the earliest point of the plateau. In order to minimize intra-observer variability in this study, ECGs for each patient were evaluated in one sitting and the ECGs were viewed in chronological order to better differentiate T-wave notches versus T-U waves. An expert ECG reader re-reivewed and adjudicated ECGs with disagreements on a T-wave being measurable, presence of a notch, or a difference of more than 5 ms in either T_{peak} or T_{end}.

ECGs from the first FDA-sponsored clinical trial (Studies III - IV) were all evaluated with computerized interval annotations on high-resolution images by an ECG reader, who was blinded to treatment and time. The same ECG reader evaluated all ECGs from the same subject and determined QRS_{onset} and QRS_{offset} using lead II. T_{peak} and T_{end} were determined by two ECG readers blinded to treatment and time on the vectormagnitude lead of the vectorcardiogram in ECGlab. T_{peak} was defined as the first discernible peak in the T-wave. T_{end} was determined using the tangent method [72, 73]. If the maximum was in the form of a plateau, T_{peak} was placed in the middle point of the plateau. T_{peak} determination criterion was different from Study II because Studies III and IV assessed global changes in repolarization. Disagreements on a T-wave being measurable, presence of a notch, or a difference of more than 5 ms in either T_{peak} or T_{end} were re-reviewed and adjudicated by an expert ECG reader. The global measurement of T_{peak}-T_{end} is different than T_{peak}-T_{end} measured in a precordial lead, which has been proposed as a measure of transmural dispersion [79]. However, the relationship between T_{peak}-T_{end} and transmural dispersion is subject to discussion [80, 81].

T_{peak}-T_{end} was measured globally because it is likely more consistent in the presence of complex T-wave patterns [82].

In the second FDA-sponsored clinical trial (Study V), ECGs were semi-automatically assessed by two ECG readers blinded to treatment and time. ECGlib automatic annotations (QRS_{onset}, QRS_{offset}, T_{peak} and T_{end}) on the vectormagnitude lead were reviewed and manually adjusted as determined by visual inspection in ECGlab. T_{peak} and T_{end} were determined following the same criteria used in Studies III - IV. Disagreements on a T-wave being measurable, presence of a notch, or a difference of more than 5 ms in any annotation were re-reviewed and adjudicated by an expert ECG reader.

9.2.3 T-wave morphology (Studies III - V)

T-wave flatness, asymmetry and the presence of notch were automatically assessed with QTGuard+ (GE Healthcare, Milwaukee, Wisconsin, USA). All the other T-wave morphology and vectorcardiographic biomarkers described below were implemented as ECGlib plugins by the PhD student and were automatically assessed with ECGlib [52].

T-wave flatness, asymmetry and notching

The computation of T-wave flatness, asymmetry and the presence of notch has been described elsewhere (Figure 1.5.b) [21]. Briefly, a median beat was derived from the independent leads (I-II, V1-V6) of the 10-second 12-lead ECG, and morphology measures were assessed in the first Eigen lead (PCA1) after applying principal component analysis (PCA). T-wave flatness is based on the inverse kurtosis (1 - kurtosis) of the unit area of the T-wave, thus increasing values reflect increasing flatness of the T-wave. Asymmetry score evaluates differences in the slope profile and duration of the ascending and descending parts of the T-wave, where low values correspond with symmetric T-waves and higher values with more asymmetric T-waves. The presence of notch was obtained from the inverse, signed radius of curvature of the T-wave, where values different from 0 correspond with the presence of notch. Notch was labeled as present if at least 1 out of the 3 ECGs of the triplicate in the corresponding time-point had a notch score greater than 0.

Percentage of early and late repolarization duration

Vectorcardiographic measurements 30% of early ($ERD_{30\%}$) and late ($LRD_{30\%}$) repolarization duration were based on the PCA transform from the ST-T segment of the independent leads (I-II, V1-V6) of the 12-lead ECG median beat. The maximum amplitude of the T vector in the preferential plane

formed by the two first Eigen leads (PCA1 and PCA2) was selected as reference, and $ERD_{30\%}$ and $LRD_{30\%}$ were then measured at the time at which the amplitude decreased by 30% (Figure 1.5.c) [83].

Other vectorcardiographic biomarkers

For each 12-lead ECG median beat, the Frank vectorcardiogram was derived using Guldenring's transformation matrix [71]. The QRS-T angle was defined as the angle between the QRS and T vectors, which were defined as the summation in the X, Y and Z leads from the QRS onset to QRS offset and QRS offset to T offset respectively. The ventricular gradient was defined as the magnitude of the sum of the QRS and T vectors [84]. The vector with the maximum magnitude between QRS offset and T offset (maximum T vector) was also computed (Figure 1.5.d).

In addition to the QRS-T angle described above, we also assessed the concordance between ventricular depolarization and repolarization by computing the total cosine R-to-T (TCRT, Figure 1.5.d) [27]. This descriptor is defined as the average of the cosines of the angles between a subset of QRS and T vectors in the 3 first Eigen leads (PCA1- PCA3) derived from the PCA transform of the independent leads (I-II, V1-V6) of the 12-lead ECG median beat.

9.3 Mathematical models and data analysis

Statistical analysis was performed using SAS 9.3 (SAS institute, Cary, North Carolina, USA) and R version 3.1.2 (R Foundation for Statistical Computing, Vienna, Austria) unless otherwise specified. A C++ implementation of the O'Hara-Rudy ventricular cell model [85] was used to simulate drug-induced changes in the ventricular action potential. The van Oosteron and Oostendorp action potential-to-body surface ECG model (ECGSIM) [86] was used to simulate ECG changes associated with drug-induced changes in ventricular action potential. Effect-compartment models were computed using Nonmem 7.3 (ICON plc, Dublin, Ireland). Decision tree analysis was computed in WEKA data mining software [87] version 3.6. P-values <0.05 were considered statistically significant without adjustment for multiplicity, and should be interpreted with an appropriate level of caution.

9.3.1 *In silico* models (Study I)

Two *in silico* models were used to study the relationship between the effects of testosterone on $I_{Ca,L}$ and I_{Ks} currents, along with early ($J\text{-}T_{peak}$) and late repolarization ($T_{peak}\text{-}T_{end}$) on the human surface ECG. The

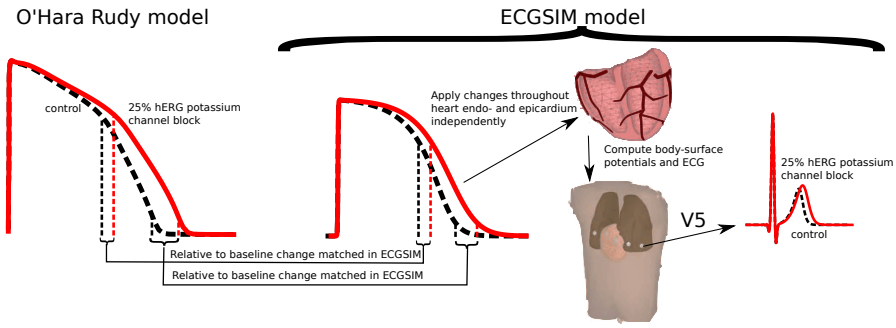

FIGURE 9.5: Example of simulated hERG potassium channel block. The left panel shows a simulated action potential (control: black dashed, hERG potassium channel block: red) and the measurement of the relative (to control) changes in action potential from the O'Hara-Rudy model [85]. The relative changes from the O'Hara-Rudy action potential are then applied to the action potential in ECGsim [86] and a 12-lead electrocardiogram is simulated. Reprinted from Johannesen et al with permission [31].

O'Hara-Rudy ventricular cell model [85] was combined with the van Oosteron and Oostendorp action potential-to-body surface ECG model (ECGSIM) [86] (Figure 9.5).

The ventricular cell model was paced at 1 Hz for 1000 cycles to obtain approximate steady state behavior [85]. The testosterone effects on $I_{Ca,L}$ and I_{Ks} were modeled by multiplying their conductance in the O'Hara-Rudy model by the corresponding scaling factors previously reported in isolated guinea pig ventricular myocytes [40]. Testosterone's effects on $I_{Ca,L}$ block and I_{Ks} enhancement were simulated alone and in combination. Action potential duration was measured at 30% (APD30), 60% (APD60) and 90% (APD90) of repolarization in the simulated action potential for both endocardial and epicardial cells. The highest testosterone concentration (20 years old male group) was selected as the baseline, and the relative action potential duration changes from this baseline was computed as testosterone levels in men decrease as they age. The average value of testosterone in women was simulated also. Testosterone values were taken from prior reports in the literature [46, 88].

ECGSIM is based on the equivalent double layer source model [86]. ECGSIM's 22 years old healthy male example case [89] was used as baseline. ECGs for different testosterone levels were simulated by changing the repolarization time and slope in all endocardial and epicardial action potentials to match the corresponding relative changes in APD30, APD60 and APD90 measured in the O'Hara-Rudy model. Simulated ECGs were semi-automatically analyzed with a wavelet-based delineation algorithm

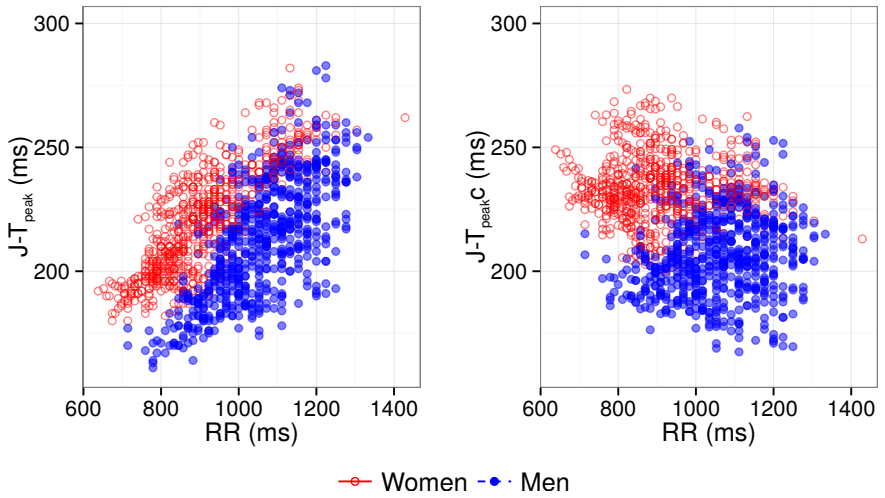

Figure 9.6: Example of heart rate dependent ECG biomarker. Panels show J-T_{peak} (Y axis) vs. RR interval (X axis) before (left) and after (right) heart rate correction for women (red, open circles) and men (blue, solid circles). Each dot correspond with an ECG.

[52, 74] in ECGlab [53].

9.3.2 Heart rate dependency of T-wave morphology biomarkers (Studies III - V)

T-wave morphology biomarkers were assessed for their dependency on heart rate, by considering if there was a statistically significant heart rate relationship as well as a meaningful change [31]. For biomarkers with dependency on heart rate, a correction factor was developed using an exponential model (Equation 9.1) that allowed the relationship to be sex

$$\text{biomarker}_c = \frac{\text{biomarker}}{(\text{RR}/1000)^{\alpha}} \tag{9.1}$$

dependent. Figure 9.6 shows an example of one heart rate dependent ECG biomarker before (left panel) and after (right panel) applying heart rate correction. The heart rate correction was performed by first log transforming the QT and RR intervals and modeling the relationship using PROC MIXED in SAS 9.3 (SAS Institute, Cary, North Carolina, USA) with a random effect on both intercept and slope (i.e. allowing each subject to have its own relationship) as well as an interaction between slope and sex, wherein a significance level of 0.05 was used to determine if there was a difference by sex.

9.3.3 Drug-induced changes in the electrocardiogram (Studies II - V)

The placebo-corrected change from baseline was computed using PROC MIXED in SAS, where the change from baseline for each ECG biomarker by time-point (e.g. Equation 9.2 for QTc) was the dependent variable. Sequence, period, time, drug, and an interaction between treatment and time were included as fixed effects, and subject was included as a random effect. More specifically, to compute the drug-induced changes from baseline in each ECG biomarker, an analysis of covariance (ANCOVA) was performed for the change from baseline in the ECG biomarker as the dependent variable and drug, time, sex, period and treatment-sequence as fixed-effects and with a random intercept by subject. Using QTc as example:

$$\Delta\mathrm{QTc}_{s,j,t} = \mathrm{QTc}_{s,j,t} - \mathrm{QTc}_{s,j,t_0} \tag{9.2}$$

where $\Delta\mathrm{QTc}_{s,j,t}$ is the difference between QTc for subject s on treatment j at time t minus the subject's QTc at baseline (t=t_0) . Lastly, the placebo-corrected change from baseline was computed as the difference in the least-squares mean for drug and placebo per time-point and sex.

Afterwards, a linear-mixed effects model was used to evaluate the relationship between each of the ECG biomarkers (except notch) and plasma concentrations. This was done using PROC MIXED in SAS. A random effect on both intercept and slope was included (i.e., allowing each subject to have their own drug concentration-biomarker relationship). Using QTc as example:

$$\begin{aligned} \Delta\Delta\mathrm{QTc}_{s,j,t} &= \Delta\mathrm{QTc}_{i,j,t} - \Delta\mathrm{QTc}_{i,PBO,t} \\ \Delta\Delta\mathrm{QTc}_{s} &= (\alpha + \alpha_s) + (\beta + \beta_s) \cdot \mathrm{drug} + \mathrm{sex} \cdot \mathrm{drug} + \varepsilon \end{aligned} \tag{9.3}$$

where $\Delta\Delta\mathrm{QTc}_s$ are the time-matched placebo-corrected changes from baseline from subject s for each treatment, α is the intercept and β is the slope, and drug is the measured concentrations. Sex is a categorical variable (e.g. 0 for males and 1 for females) and subscripts s for α and β indicate that subject's random effect.

Sex and age differences in the drug-induced response were assessed as follows. In Studies I and II (chapters 2 and 3), unpaired Student's t-test was used to compare values between age and sex groups in R. In Study IV (chapter 5), sex differences were evaluated by the interaction between slope and intercept of effect by drug concentration (to account for differences in exposure) and sex in a linear mixed effects model with PROX MIXED in SAS.

If a linear model was not appropriate a non linear model was used. This was the case for the presence of notch, which is a binary variable

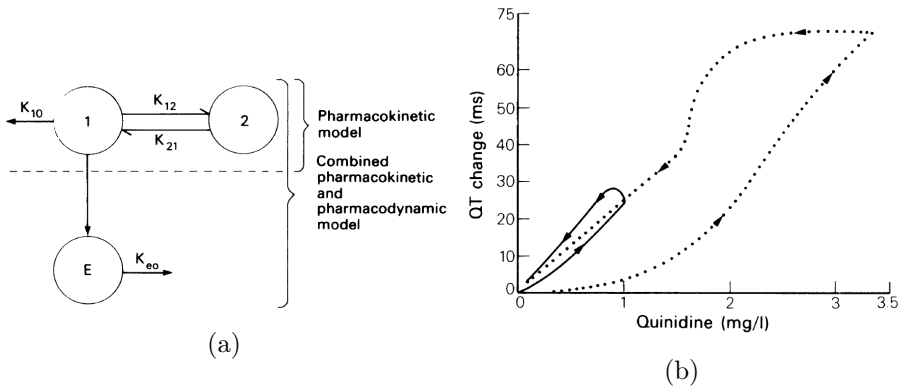

Figure 9.7: (a) Diagram of the combined pharmacokinetic and pharmacodynamic model. (b) Change in QT interval predicted by the combined pharmacokinetic and pharmacodynamic model after i.v. (dotted line) and oral (solid line) administration of quinidine. Relationship to plasma concentration predicted from pharmacokinetic model. Reprinted from Holford et al with premission [90].

that takes the value 'Yes' when the T-wave notch score is greater than 0 and 'No' otherwise. Therefore in Studies III and IV, a logistic regression model was used to evaluate the relationship between presence of notch and drug concentration including a random effect on intercept in SAS (PROC GLIMMIX). If there was a significant delay (hysteresis) between maximum drug concentration and maximum response (e.g. QTc prolongation as determined by visual inspection) an effect compartmental model was used to account for hysteresis.

9.3.4 Compartmental models for hysteresis (Study II)

Prior work by Holford et al. [90] has shown that the delayed effect of quinidine in the ECG (hysteresis) can be modeled by using a sequential approach (Figure 9.7). In the first step of the sequential approach, a two-compartment model was fitted to the *pharmacokinetic* (PK) data alone, and afterwards the PK model was reapplied to the data with an added effect compartment to compute the *pharmacodynamic* (PD) response. The effect compartment was then characterized by a parameter K_{eo}, which quantifies the clearance of drug from the effect compartment, and the equilibrium half life is $log(2)/K_{eo}$. The two compartment model was described by the following set of equations:

$$
\left.\begin{array}{l}
\left.\begin{array}{l}
\mathrm{K_{12}} = \frac{\mathrm{Q}}{\mathrm{V_1}} \\
\mathrm{K_{21}} = \frac{\mathrm{Q}}{\mathrm{V_2}} \\
\mathrm{K_{10}} = \frac{\mathrm{CL}}{\mathrm{V_1}} \\
\frac{d\mathrm{A_1}}{dt} = \mathrm{A_2K_{21}} - \mathrm{A_1(K_{10} + K_{12})} \\
\frac{d\mathrm{A_2}}{dt} = \mathrm{A_1K_{12}} - \mathrm{A_2K_{21}}
\end{array}\right\} \text{PK model} \\
\\
\mathrm{K_{1E}} = \frac{\mathrm{V_E}}{\mathrm{V_1}}\mathrm{K_{eo}} \\
\frac{d\mathrm{A_E}}{dt} = \mathrm{A_1K_{1E}} - \mathrm{A_EK_{eo}} \\
\mathrm{Y_{ecg}} = \alpha + \beta \cdot \mathrm{CE} + \varepsilon
\end{array}\right\} \text{PK and PD model} \quad (9.4)
$$

where the drug is administered as a bolus into the central compartment (compartment 1 in Figure 9.7a), V_1 is the volume of the central compartment, CL is the clearance rate of the central compartment, V_2 is the volume of the peripheral compartment, Q is the clearance rate of the peripheral compartment (compartment 2 in Figure 9.7a), K_{12} is the rate of drug flow from the central compartment to the peripheral compartment, K_{21} is the rate of drug flow from the peripheral compartment to the central compartment and K_{10} is the drug elimination rate from the central compartment, $\frac{dA_1}{dt}$ is the change in amount of drug in the central compartment over time as the flow from the peripheral compartment minus the amount of drug that leaves the main compartment (elimination flow plus flow to peripheral compartment), $\frac{dA_2}{dt}$ is the change in amount of drug in the peripheral compartment over time, K_{eo} is the elimination rate from the effect compartment, V_E is the volume of the effect compartment (modeled as a negligibly small volume), K_{12} and K_{21} are the flow rates between the main and peripheral compartments computed when fitting the pharmacokinetic model in the first step, K_{1E} is the rate of drug flow from the central compartment to the effect compartment, and $\frac{dA_E}{dt}$ is the change in amount of drug in the effect compartment over time as the flow from the central compartment minus the amount of drug that leaves the effect compartment. Lastly, drug-induced changes in the ECG are predicted with the linear model Y_{ecg}, where CE is the concentration of drug present in the effect compartment ($CE = \frac{A_E}{V_E}$), α and β are the intercept and slope of the concentration-response relationship, and ε the error of the predicted response.

9.3.5 Patch clamp experiments (Study III)

Patch clamp experiments were conducted to assess the relative block of hERG, late sodium (Nav1.5) and calcium (Cav1.2) currents caused by each

drug. Stably transfected hERG, Nav1.5 cells (HEK-293), or Cav1.2 cells (CHO) were obtained from Cytocentrics Biosciences (Rostock, Germany). Cells were maintained in minimum essential medium with Earle's salts supplemented with nonessential amino acids, sodium pyruvate, penicillin, streptomycin, and fetal bovine serum.

Drugs were dissolved in either dimethyl sulfoxide (DMSO) or deionized H_2O to make stock solutions. Dilutions of stock solutions were made immediately before the experiment to create the desired concentrations. The external solution (solution bathing the cell) had an ionic composition of (in mM): 137 NaCl, 4 KCl, 1.8 CaCl2, 1.2 MgCl2, 11 dextrose, 10 HEPES, adjusted to a pH of 7.4 with NaOH. The internal (pipette) solution had an ionic composition of (in mM): 130 KCl; 1 MgCl2, 5 NaATP, 7 NaCl, 5 EGTA, 5 HEPES, pH=7.2 using KOH. Experiments were performed at 36 ± 1°C. Drugs were obtained from Tocris Bioscience (Minneapolis, MN, USA).

Currents were measured using the whole-cell variant of the patch clamp method as previously described [91]. After rupture of the cell membrane (entering whole-cell mode), current amplitude and kinetics were allowed to stabilize (3-5 min) before experiments were begun. All three currents (hERG, Nav1.5, Cav1.2) were elicited using a ventricular action potential waveform paced at 0.1Hz.

Patch clamp results were given as percent reduction of current amplitude, which was measured as current reduction after a steady-state effect had been reached in the presence of drug relative to current amplitude before drug was introduced (control). Each cell served as its own control. Log-linear plots were created from the mean percent block ± *standard error of the mean* (SEM) at the concentrations that were tested. A non-linear least square fitting routine was used to fit a three-parameter Hill equation to the results in R 3.0.2 (R Foundation for Statistical Computing, Vienna, Austria). The equation was of the following form

$$B(\%) = 100\frac{C^h}{{IC_{50}}^h + C^h} \tag{9.5}$$

where B(%) is the percentage of current blockage at drug concentration C, IC_{50} is the concentration of drug that causes 50% block, and h is the Hill coefficient.

9.3.6 Ability of ECG biomarkers to detect late sodium current block (Study V)

Logistic regression models were used to classify selective hERG potassium channel block (dofetilide and moxifloxacin alone) vs. multichannel block

(mexiletine with dofetilide and lidocaine with dofetilide) using placebo-corrected changes from baseline. Only ECG biomarkers that had a statistically significant effect were selected. A ROC-AUC analysis was performed to assess the performances of the models, which were compared using Delong's test [92] in R 3.2.2 (R Foundation for Statistical Computing, Vienna, Austria). Individual ECG biomarkers were then ranked by the AUC of each corresponding model.

In addition to the ROC-AUC analysis, a C4.5 decision tree [93] was developed to assess the relationship between the identified ECG biomarkers and selective hERG potassium channel block vs. multichannel block. The decision tree was developed using 10-fold cross-validation on a training set that included all data from selective hERG potassium channel block (dofetilide and moxifloxacin alone) vs. multichannel block (mexiletine with dofetilide and lidocaine with dofetilide) in the second FDA-sponsored clinical trial. Next the decision tree was validated using all data from the first FDA-sponsored clinical study (Studies III - IV), where dofetilide and quinidine were labeled as strong hERG potassium channel blockers and ranolazine and verapamil as multichannel blockers (validation set). The performance of the decision tree was assessed for the training and validation sets separately. The decision tree was computed using the J48 algorithm in WEKA data mining software [87] version 3.6.

The "positive" class for all classification methods (ROC-AUC and decision tree) was "multichannel block". Performance was reported as accuracy, sensitivity and specificity.

CHAPTER 10

Conclusions and summary

The studies in this thesis suggest that the J-T_{peak}cand QTc intervals are the best ECG biomarkers to differentiate selective hERG potassium channel block (high torsade risk) from multichannel block (low risk). This is important because this type of assessment could enhance the current clinical paradigm of proarrhythmic assessment of drugs in thorough QT studies. Specifically, such integrated assessment may be able to differentiate between selective hERG potassium channel blocking drugs that prolong QTc and have high torsade risk (e.g. dofetilide) from multichannel blocking drugs that also prolong QTc but have minimal risk for torsade (e.g. ranolazine). In addition, sex-specific analysis results suggest that higher torsade risk in women is not because women are more sensitive to drug-induced QTc prolongation.

The main outcomes for each study were:

- **Study I**: In the overall population QTc was shorter in men than in women. Men had shorter J-T_{peak}c but longer QRS and T_{peak}-T_{end} intervals than women. Difference in QTc was due to men having shorter J-T_{peak}c than women. QTc increased more with age in men than in women, which resulted in a decreasing QTc differences between sexes as age increased. QRS and T_{peak}-T_{end} did not change with age in either men or women. Similarly to QTc, J-T_{peak}c increased more with age in men than in women. Therefore, age- and sex-differences in the QTc interval are fully explained by J-T_{peak}c interval. Lastly, simulations suggested that lengthening of QTc as men age (and testosterone levels decrease) is due to testosterone's effects on $I_{Ca,L}$.

- **Study II**: Both women and men had substantial QTc and T_{peak}-T_{end} prolongation after quinidine infusion and almost all subjects developed T-wave notching. Women had a greater slope than men in the relationship between serum quinidine concentration and QTc, but not T_{peak}-T_{end}. However, there was a delay between maximum concentration of quinidine and maximum quinidine-induced ECG changes in men (hysteresis). When taking this hysteresis into account, there were no sex-differences in quinidine-induced QTc or T_{peak}-T_{end} prolongation. Thus, in this study women did not have a greater quinidine-induced T_{peak}-T_{end} prolongation than men. Sex differences in hysteresis and serum quinidine concentration in this study may have contributed to sex differences in quinidine-induced QTc prolongation.

- **Study III**: There was a strong dose-response relationship between hERG potassium channel block (dofetilide, quinidine) and T-wave morphology changes. Multichannel block (ranolazine) still had a dose dependent relationship with T-wave morphology, in some cases having greater T-wave morphology changes at equivalent amounts of QTc prolongation compared with selective hERG potassium channel block (dofetilide). ECG signatures of drug-induced ion channel block closely parallel the ECG signatures seen with congenital long QT syndromes. This study supports that T-wave morphology biomarkers (e.g. flatness, asymmetry, and notching, along with a decrease in the maximum magnitude of the T vector) likely have value in determining if QTc prolongation is due to hERG potassium channel block. A combined approach of assessing multiple ion channels, QTc, J-T_{peak}c, T_{peak}-T_{end} and T-wave morphology can provide the greatest insight into drug-ion channel interactions of relevance for torsade risk.

- **Study IV**: There were no sex differences in the relationship between plasma drug concentration and the placebo-corrected changes from baseline QTc prolongation induced by dofetilide, quinidine and ranolazine. In addition and consistently with Study II, no systematic sex differences of other drug-induced ECG biomarker changes were observed in this study. This study suggests that the higher torsade risk in women compared to men is not due to a larger concentration-dependent QTc prolongation. However, women have longer QTc at baseline and are often exposed to higher drug concentrations than men, which may contribute to their higher torsade risk.

- **Study V**: In this study J-T_{peak}c was the best of all studied ECG biomarkers for detecting $I_{Na,L}$ current block. ROC-AUC and deci-

sion tree analysis showed that an integrated assessment of J-T_{peak}c and QTc can differentiate drug-induced multichannel block from selective hERG potassium channel block. More specifically, selective hERG potassium channel blockers prolong both J-T_{peak}c and QTc, while multichannel blocking drugs prolong QTc with minimal effect in J-T_{peak}c. Future methodologies assessing drug effects on cardiac ion channel currents on the ECG should use J-T_{peak}c to detect the presence of late sodium current block.

Clinical relevance

There are two global initiatives that will likely affect future thorough QT studies. One focuses on using exposure-response data from early phase 1 clinical studies *in lieu* of dedicated thorough QT studies. The other focuses on a better understanding of multichannel effects to improve the lack of specificity of hERG potassium channel block and QTc prolongation for prediction of actual proarrhythmic risk.

For the first effort, a collaboration between the *Consortium for Innovation and Quality in Pharmaceutical Development and the Cardiac Safety Research Consortium* (IQ-CSRC) was formed to design a clinical study in healthy subjects to demonstrate that robust ECG monitoring and exposure-response analysis of data generated from first-in-human *single ascending dose* (SAD) studies can be used *in lieu* of the thorough QT study [94, 95]. This type of study would not include a pharmacological positive control, thus it would not be considered a thorough QT study. The exposure-response approach suggests that drug development costs would be reduced by waivers for conducting dedicated thorough QT studies. However, it is not clear whether or not the increase in complexity of early phase studies would make the overall drug development process less expensive. Lastly, this approach does not address the distinction between malignant and benign QTc prolonging drugs. Therefore, QTc prolonging drugs that do not actually cause torsade might be dropped from development or receive FDA labeling suggesting that the drug increases proarrhythmic risk, even though it may not be true. Currently, this approach is being discussed as an amendment to the ICH E14 guidance [96].

The other initiative is the *Comprehensive in vitro Proarrhythmia Assay* (CiPA), for which the FDA, the *Cardiac Safety Research Consortium* (CSRC), the *Health and Environmental Science Institute* (HESI), the *Safety Pharmacology Society* (SPS), the *European Medicines Agency* (EMA), Health Canada, *Japan National Institutes of Health Sciences* (NIHS), *Japan Pharmaceuticals and Medical Devices Agency* (PMDA),

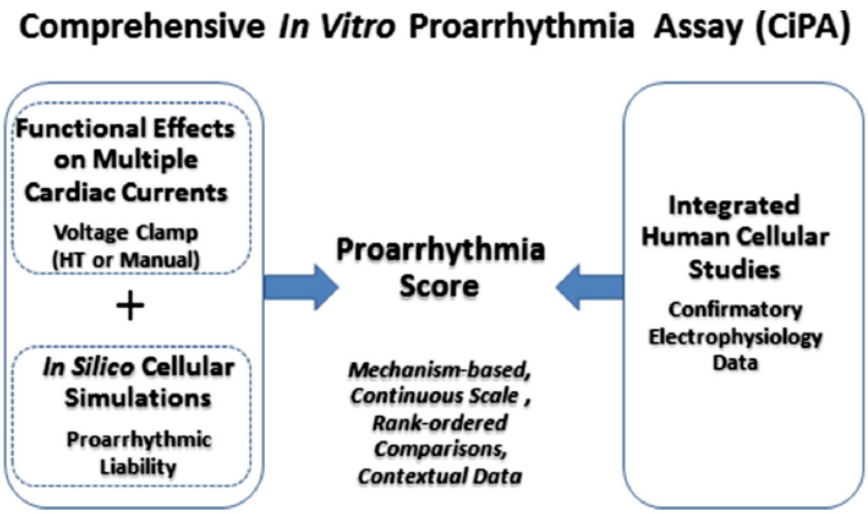

Figure 10.1: Schematic of the elements of the CiPA initiative. Abbreviations: HT, high throughput; Manual, manual patch voltage clamp. Reproduced from Sager et al with permission [97].

industry and academia are all involved. The goal of the CiPA initiative is to facilitate the adoption of a new paradigm for assessment of clinical risk of torsade that is not measured exclusively by potency of hERG potassium channel block and QTc prolongation. In particular, CiPA proposes a mechanistically driven assessment of (i) *in vitro* drug effects in multiple ion channels (ii) coupled with an *in silico* model of human cardiac myocytes with (iii) verification of predicted responses in *human induced pluripotent stem cell derived cardiomyocytes* (hiPSC-CM) (Figure 10.1). Implementation of this paradigm would likely include clinical confirmation that would include a careful ECG assessment in a phase 1 clinical study to confirm that no unanticipated clinical ECG changes are found [97]. The CiPA Phase I ECG sub-team is currently discussing the design of such confirmation package. The assessment of ECG biomarkers of this thesis will be presented in the "*Potential ECG biomarker approaches*" session at the "*CSRC/FDA Workshop: The Proarrhythmic Assessment of New Chemical Entities*" on April 2016.

Results of this thesis suggest that, while thresholds still have to be determined, the ability of J-T_{peak}c to detect inward current block in small sample sizes should be assessed and considered as a potential enhancement of the IQ-CSRC proposed paradigm. Moreover, J-T_{peak}c should be considered as a biomarker to detect $I_{Na,L}$ or $I_{Ca,L}$ current block in phase 1 clinical studies under CiPA.

APPENDIX A

Additional documentation

Cartas de aceptación, factores de impacto, áreas temáticas y contribución del doctorando

Factores de impacto, áreas temáticas y contribuciones del doctorando en cada una de las publicaciones incluidas en esta tesis

To support the research studies of this thesis, the PhD student played a lead role on the design and development of new ECG analysis tools (ECGlib [52] and ECGlab [53]). These tools are described in Section 9.2.1. Briefly, ECGlib is a C++ library for processing ECGs. It implements standard ECG signal processing methods that allow for automatic adjudication of ECGs. Its performance is comparable to state-of-the-art methods. ECGlib has a modular design and can be extended through plugins. ECGlab is a user friendly, graphical user interface for assessing results from automated analysis of ECGs in research environments. It is built on top of ECGlib library and plugins and allows for fast on-screen computer-assisted semi-automatic review and adjudication of large number of ECGs. ECGlib and ECGlab were developed using open source tools and libraries such us Armadillo [54], Boost [55], Qt [56] and Qwt [57]. The PhD student is working together with other ECGlib and ECGlab developers on making the these tools publicly available under an open source license.

For each study included in this thesis, the PhD student designed the study, analyzed the data and wrote the manuscript. A more detailed description of the PhD student contributions to each of the studies is outlined below:

1. Vicente J, Johannesen L, et al. Mechanisms of sex and age differences in ventricular repolarization in humans. *Am Heart J* 168(5):749–756, 2014

    - Factor the impacto: 4.463
    - Areas temáticas: Cardiac & cardiovascular systems.
    - Contribución del doctorado: The idea for this study came out of discussions between the student and Strauss and Johannesen. The design and planning of the study including software implementation and statistical analysis was carried out by the student. The manuscript was drafted by the student with help from Strauss and Johannesen and input from Galeotti. Journal correspondence was handled by the student and Strauss.

2. Vicente J, Simlund J, et al. Investigation of potential mechanisms of sex differences in quinidine-induced torsade de pointes risk. *J Electrocardiol* 48(4):533–538, 2015

    - Factor the impacto: 1.361

- Areas temáticas: Cardiac & cardiovascular systems.
- Contribución del doctorado: The idea for this study came out of discussions between the student and Strauss, Simlund, Johannesen and Wagner. The design and planning of the study including software implementation and statistical analysis was carried out by the student. Study data was curated by the student with help from Woosley and Johannesen. Semi-automatic adjudication of ECGs was performed by the student with help from Johannesen and Simlund. ECGs were assessed with ECGlab, which was developed by the student. Compartmental model (hysteresis) analysis was performed by Johannesen with help from the student. The manuscript was drafted by the student and Simlund with help from Strauss and Johannesen as well as input from all co-authors. Journal correspondence was handled by the student and Strauss.

3. Vicente J, Johannesen L, et al. Comprehensive T wave morphology assessment in a randomized clinical study of dofetilide, quinidine, ranolazine, and verapamil. *J Am Heart Assoc* 4(4):e001615, 2015

   - Factor the impacto: 4.306
   - Areas temáticas: Cardiac & cardiovascular systems.
   - Contribución del doctorado: The idea of assessing ECG biomarkers beyond QT and its subintervals was proposed by Strauss and further elaborated by the student together with Johannesen. The design and planning of the study including software implementation and statistical analysis was carried out by the student. The student and Johannesen performed analysis of all ECGs. ECG analysis software was developed with help from Johannesen. QTGuard+ (T-wave flatness, asymmetry and presence of notch) algorithms were provided by GE Healthcare and integrated in ECGlib by the student with help from Johannesen. The idea of plotting QT vs. other ECG biomarkers to visualize the ECG signatures of drugs was proposed by the student. Crumb conducted the voltage clamp experiments. The student analyzed the patch clamp data, fit Emax models and computed IC50 curves. Finally, the manuscript was drafted by the student with input from supervisors and all co-authors. Journal correspondence was handled by the student and Strauss.

4. Vicente J, Johannesen L, et al. Sex differences in drug-induced

changes in ventricular repolarization. *J Electrocardiol* 48(6):1081–1087, 2015

- Factor the impacto: 1.361
- Areas temáticas: Cardiac & cardiovascular systems.
- Contribución del doctorado: The idea of conducting sex-specific analysis came out of discussions between the student and Strauss and further elaborated by the student with input from Johannesen. Analysis of the ECGs was carried out by the student together with Johannesen. The statistical analysis plan was planned and carried out by the student with input from Johannesen. The student presented the results at the annual International Society for Computerized Electrocardiology (ISCE), where he received the "Best poster award" and was invited to submit a full manuscript to Journal of Electrocardiology. The manuscript was drafted by the student with input from supervisors and all co-authors. Journal correspondence was handled by the student.

5. Vicente J, Johannesen L, et al. ECG biomarkers for detection of drug-induced late sodium current block. *Manuscript* , 2015

- Factor de impacto: borrador.
- Areas temáticas: Cardiac & cardiovascular systems.
- Contribución del doctorado: The idea of assessing which biomarker would add value to assessing QTc alone was proposed by Stockbridge and further elaborated in discussions between the student, Strauss and Johannesen. The design and planning of the study including software implementation and statistical analysis was carried out by the student. The student and Johannesen performed analysis of all ECGs. ECG analysis software was developed with help from Johannesen. QTGuard+ (T-wave flatness, asymmetry and presence of notch) algorithms were provided by GE Healthcare and integrated in ECGlib by the student with help from Johannesen. The idea of using a ROC-AUC analysis was proposed by Johannesen and implemented and assessed by the student. The idea of using C4.5 decision tree was proposed by Hosseini and implemented and assessed by the student. The manuscript included in this thesis was drafted by the student with input from supervisors and all co-authors.

Lastly, the idea of the two FDA-sponsored prospective clinical trials was proposed by Stockbridge and led later by Strauss and Johannesen. The student played a lead role in both prospective clinical trials. The student contributed to the studies design, protocol, site initiation visits, data transfer and quality control, as well as follow-up with the clinic and making the data available through the Telemetric and Holter ECG Warehouse (`http://thew-project.org`, databases E-OTH-12-5232-020 and E-HOL-12-0109-021).

List of Figures

List of Tables

List of Acronyms

ADME absortion, distribution, metabolism and excretion 8

API Application Programming Interface 111

AUC area under the curve 103

CiPA Comprehensive *in vitro* Proarrhythmia Assay 129

CSRC Cardiac Safety Research Consortium 129

CSV comma separated values 113

EADs early afterdepolarizations 3

ECG electrocardiogram 1

EMA European Medicines Agency 129

FDA U.S. Food and Drug Administration 6

hERG human *ether-à-go-go* related gene 2

HESI Health and Environmental Science Institute 129

hiPSC-CM human induced pluripotent stem cell derived cardiomyocytes 130

i.v. intravenous 9

$I_{Ca,L}$ inward L-type calcium current 3

ICH International Conference on Harmonisation of Technical Requirements for Registration of Pharmaceuticals for Human Use 2

I_{Kr} rapid delayed outward rectifier potassium current 3

I_{Ks} outward slow delayed rectifier potassium current 5

$I_{Na,L}$ inward late sodium current 3

IQ-CSRC Consortium for Innovation and Quality in Pharmaceutical Development and the Cardiac Safety Research Consortium 129

J-T_{peak} early repolarization interval 9

J-T_{peak}c heart rate corrected early repolarization interval 6

LQT1 Long QT syndrome type 1 5

LQT2 Long QT syndrome type 2 5

LQT3 Long QT syndrome type 3 5

NIHS Japan National Institutes of Health Sciences 129

PD pharmacodynamic 122

PK pharmacokinetic 122

PMDA Japan Pharmaceuticals and Medical Devices Agency 129

QTc heart rate corrected QT interval 1

ROC receiver operating characteristic 103

SAD single ascending dose 129

SEM standard error of the mean 124

SNR signal-to-noise ratio 113

SPS Safety Pharmacology Society 129

SVG scalable vector graphics 114

TCRT total cosine R-to-T 6

torsade torsade de pointes 1

T_{peak}-T_{end} late repolarization interval 6

Bibliography

[1] US Food and Drug Administration. Guidance for industry E14 clinical evaluation of QT/QTc interval prolongation and proarrhythmic potential for non-antiarrhythmic drugs, 2005. URL `http://www.fda.gov/downloads/drugs/guidancecomplianceregulatoryinformation/guidances/ucm073153.pdf`.

[2] Stockbridge N, Morganroth J, et al. Dealing with global safety issues - was the response to QT-liability of non-cardiac drugs well coordinated? *Drug Saf* 36(3):167–82, 2013.

[3] Roden DM. Drug-induced prolongation of the QT interval. *N Engl J Med* 350(10):1013–22, 2004.

[4] International Conference on Harmonisation. ICH topic S7B the nonclinical evaluation of the potential for delayed ventricular repolarization (QT interval prolongation) by human pharmaceuticals., 2005. URL `http://www.ich.org/fileadmin/Public_Web_Site/ICH_Products/Guidelines/Safety/S7B/Step4/S7B_Guideline.pdf`.

[5] Wu L, Rajamani S, et al. Augmentation of late sodium current unmasks the proarrhythmic effects of amiodarone. *Cardiovasc Res* 77(3):481–8, 2008.

[6] Antzelevitch C, Belardinelli L, et al. Electrophysiological effects of ranolazine, a novel antianginal agent with antiarrhythmic properties. *Circulation* 110(8):904–10, 2004.

[7] Redfern WS, Carlsson L, et al. Relationships between preclinical cardiac electrophysiology, clinical QT interval prolongation and torsade de pointes for a broad range of drugs: evidence for a provisional safety margin in drug development. *Cardiovasc Res* 58(1):32–45, 2003.

[8] Zareba W and Cygankiewicz I. *Comprehensive Electrocardiology*, chapter The QT Interval, 834–57. Springer Science & Business Media, 2011.

[9] Trudeau MC, Warmke JW, et al. HERG, a human inward rectifier in the voltage-gated potassium channel family. *Science* 269(5220):92–5, 1995.

[10] Roden DM and Hoffman BF. Action potential prolongation and induction of abnormal automaticity by low quinidine concentrations in canine Purkinje fibers. relationship to potassium and cycle length. *Circ Res* 56(6):857–67, 1985.

[11] Hoekstra M, Mummery CL, et al. Induced pluripotent stem cell derived cardiomyocytes as models for cardiac arrhythmias. *Front Physiol* 3:346, 2012.

[12] January CT and Riddle JM. Early afterdepolarizations: mechanism of induction and block. a role for L-type Ca2+ current. *Circ Res* 64(5):977–90, 1989.

[13] Guo D, Zhao X, et al. L-type calcium current reactivation contributes to arrhythmogenesis associated with action potential triangulation. *J Cardiovasc Electrophysiol* 18(2):196–203, 2007.

[14] Duff HJ, Roden D, et al. Mexiletine in the treatment of resistant ventricular arrhythmias: enhancement of efficacy and reduction of dose-related side effects by combination with quinidine. *Circulation* 67(5):1124–1128, 1983.

[15] Duff HJ, Mitchell LB, et al. Mexiletine-quinidine combination: electrophysiologic correlates of a favorable antiarrhythmic interaction in humans. *J Am Coll Cardiol* 10(5):1149–1156, 1987.

[16] Giardina EGV and Wechsler ME. Low dose quinidine-mexiletine combination therapy versus quinidine monotherapy for treatment of ventricular arrhythmias. *J Am Coll Cardiol* 15(5):1138–1145, 1990.

[17] Johannesen L, Vicente J, et al. Late sodium current block for drug-induced long QT syndrome: Results from a prospective clinical trial. *Clin Pharmacol Ther* 99(2):214–223, 2016.

[18] Badri M, Patel A, et al. Mexiletine prevents recurrent torsades de pointes in acquired long QT syndrome refractory to conventional measures. *JACC Clin Electrophysiol* 1(4):315–322, 2015.

[19] Antzelevitch C and Shimizu W. Cellular mechanisms underlying the long QT syndrome. *Curr Opin Cardiol* 17(1):43–51, 2002.

[20] Moss AJ, Zareba W, et al. ECG T-wave patterns in genetically distinct forms of the hereditary long QT syndrome. *Circulation* 92(10):2929–2934, 1995.

[21] Andersen MP, Xue J, et al. A robust method for quantification of IKr-related T-wave morphology abnormalities. In *Comput Cardiol*, 341–344. IEEE, 2007.

[22] Graff C, Andersen MP, et al. Identifying drug-induced repolarization abnormalities from distinct ECG patterns in congenital long QT syndrome: a study of sotalol effects on T-wave morphology. *Drug Saf* 32(7):599–611, 2009.

[23] Couderc JP, McNitt S, et al. Improving the detection of subtle I(Kr)-inhibition: assessing electrocardiographic abnormalities of repolarization induced by moxifloxacin. *Drug Saf* 31(3):249–60, 2008.

[24] Couderc JP, Zhou M, et al. Investigating the effect of sotalol on the repolarization intervals in healthy young individuals. *J Electrocardiol* 41(6):595–602, 2008.

[25] Draper HW, Peffer CJ, et al. The corrected orthogonal electrocardiogram and vectorcardiogram in 510 normal men (Frank lead system). *Circulation* 30(6):853–864, 1964.

[26] Wilson F, Macleod A, et al. The determination and the significance of the areas of the ventricular deflections of the electrocardiogram. *Am Heart J* 10(1):46–61, 1934.

[27] Acar B, Yi G, et al. Spatial, temporal and wavefront direction characteristics of 12-lead T-wave morphology. *Med Biol Eng Comput* 37(5):574–584, 1999.

[28] Kardys I, Kors JA, et al. Spatial QRS-T angle predicts cardiac death in a general population. *Eur Heart J* 24(14):1357–1364, 2003.

[29] Whang W, Shimbo D, et al. Relations between QRS|T angle, cardiac risk factors, and mortality in the third national health and nutrition examination survey (NHANES III). *Am J Cardiol* 109(7):981–7, 2012.

[30] Vicente J, Johannesen L, et al. Comprehensive T wave morphology assessment in a randomized clinical study of dofetilide, quinidine, ranolazine, and verapamil. *J Am Heart Assoc* 4(4):e001615, 2015.

[31] Johannesen L, Vicente J, et al. Improving the assessment of heart toxicity for all new drugs through translational regulatory science. *Clin Pharmacol Ther* (95):501–508, 2014.

[32] Johannesen L, Vicente J, et al. Differentiating drug-induced multichannel block on the electrocardiogram: randomized study of dofetilide, quinidine, ranolazine, and verapamil. *Clin Pharmacol Ther* 96(5):549–58, 2014.

[33] Makkar RR, Fromm BS, et al. Female gender as a risk factor for torsades de pointes associated with cardiovascular drugs. *JAMA* 270(21):2590–2597, 1993.

[34] Fung M, Wu HHh, et al. Evaluation of the profile of patients with QTc prolongation in spontaneous adverse event reporting over the past three decades-1969-98. *Pharmacoepidemiol Drug Saf* 9(suppl 1):24–25, 2000.

[35] Abraham JM, Saliba WI, et al. Safety of oral dofetilide for rhythm control of atrial fibrillation and atrial flutter. *Circ Arrhythm Electrophysiol* 8(4):772–776, 2015.

[36] Bazett HC. An analysis of the time-relations of electrocardiograms. *Heart* 7:353–370, 1920.

[37] Rautaharju PM, Zhou SH, et al. Sex differences in the evolution of the electrocardiographic QT interval with age. *Can J Cardiol* 8(7):690–5, 1992.

[38] Bidoggia H, Maciel JP, et al. Sex differences on the electrocardiographic pattern of cardiac repolarization: Possible role of testosterone. *Am Heart J* 140(4):678–683, 2000.

[39] Jonsson M, Vos M, et al. Gender disparity in cardiac electrophysiology: implications for cardiac safety pharmacology. *Pharmacol Ther* 127(1):9–18, 2010.

[40] Bai CX, Kurokawa J, et al. Nontranscriptional regulation of cardiac repolarization currents by testosterone. *Circulation* 112(12):1701–1710, 2005.

[41] Yang PC, Kurokawa J, et al. Acute effects of sex steroid hormones on susceptibility to cardiac arrhythmias: a simulation study. *PLoS Comput Biol* 6(1):e1000658, 2010.

[42] Yang PC and Clancy CE. In silico prediction of sex-based differences in human susceptibility to cardiac ventricular tachyarrhythmias. *Front Physiol* 3:360, 2012.

[43] Dhingra R, Nam BH, et al. Cross-sectional relations of electrocardiographic QRS duration to left ventricular dimensions: the Framingham Heart Study. *J Am Coll Cardiol* 45(5):685–689, 2005.

[44] Yang PC and Clancy CE. Effects of sex hormones on cardiac repolarization. *J Cardiovasc Pharmacol* 56(2):123–129, 2010.

[45] Benton RE, Sale M, et al. Greater quinidine-induced QTc interval prolongation in women. *Clin Pharmacol Ther* 67(4):413–418, 2000.

[46] Rodriguez I, Kilborn MJ, et al. Drug-induced QT prolongation in women during the menstrual cycle. *JAMA* 285(10):1322–6, 2001.

[47] Darpo B, Karnad DR, et al. Are women more susceptible than men to drug-induced QT prolongation? concentration-QTc modelling in a phase 1 study with oral rac-sotalol. *Br J Clin Pharmacol* 77(3):522–31, 2014.

[48] Vicente J, Johannesen L, et al. Mechanisms of sex and age differences in ventricular repolarization in humans. *Am Heart J* 168(5):749–756, 2014.

[49] Vicente J, Simlund J, et al. Investigation of potential mechanisms of sex differences in quinidine-induced torsade de pointes risk. *J Electrocardiol* 48(4):533–538, 2015.

[50] Vicente J, Johannesen L, et al. Sex differences in drug-induced changes in ventricular repolarization. *J Electrocardiol* 48(6):1081–1087, 2015.

[51] Vicente J, Johannesen L, et al. ECG biomarkers for detection of drug-induced late sodium current block. *Manuscript* , 2015.

[52] Johannesen L, Vicente J, et al. ECGlib: Library for processing electrocardiograms. In *Comput Cardiol*, 951–954. IEEE, 2013.

[53] Vicente J, Johannesen L, et al. ECGlab: User friendly ECG/VCG analysis tool for research environments. In *Comput Cardiol*, 775–778. IEEE, 2013.

[54] Sanderson C. Armadillo: An open source C++ linear algebra library for fast prototyping and computationally intensive experiments, 2010. URL `http://arma.sf.net`.

[55] BOOST. C++ libraries. URL http://www.boost.org.

[56] Qt. Qt open source. URL https://www.qt.io/.

[57] Rathmann U and Wilgen J. Qwt - Qt widgets for technical applications. URL http://qwt.sourceforge.net/.

[58] Fridericia LS. Die systolendauer im elektrokardiogramm bei normalen menschen und bei herzkranken. *Acta Med Scand* 53(1):469–486, 1920.

[59] Drugs@FDA. Dofetilide label, 2013. URL http://www.accessdata.fda.gov/drugsatfda_docs/label/2013/020931s007lbl.pdf.

[60] DailyMed. Quinidine sulfate label, 2013. URL http://dailymed.nlm.nih.gov/dailymed/drugInfo.cfm?setid=a90a03b0-ffbe-4cf6-90b5-bfb0412a1cb2.

[61] Drugs@FDA. Ranolazine label, 2013. URL http://www.accessdata.fda.gov/drugsatfda_docs/label/2013/021526s026lbl.pdf.

[62] DailyMed. Verapamil label, 2014. URL http://dailymed.nlm.nih.gov/dailymed/drugInfo.cfm?setid=10881745-3a16-44c3-9b94-60433218f1d6.

[63] Williams E. Experimental designs balanced for the estimation of residual effects of treatments. *Aust J Chem* 2(2):149–168, 1949.

[64] Badilini F, Vaglio M, and Sarapa N. Automatic extraction of ECG strips from continuous 12-lead holter recordings for QT analysis at prescheduled versus optimized time points. *Ann Noninvasive Electrocardiol* 14(Suppl 1):S22–9, 2009.

[65] Galeotti L, Scully CG, et al. Robust algorithm to locate heart beats from multiple physiological waveforms by individual signal detector voting. *Physiol Meas* 36(8):1705, 2015.

[66] Goldberger AL, Amaral LAN, et al. PhysioBank, PhysioToolkit, and PhysioNet: Components of a new research resource for complex physiologic signals. *Circulation* 101(23):e215–e220, 2000.

[67] Badilini F and ISHNE Standard Output Format Task Force. The ISHNE Holter standard output file format. *Ann Noninvasive Electrocardiol* 3(3):263–266, 1998. ISSN 1542-474X.

[68] Marchesi C and Paoletti M. ECG processing algorithms for portable monitoring units. *The Internet Journal of Medical Technology* 1(2), 2004.

[69] Paoletti M and Marchesi C. Discovering dangerous patterns in long-term ambulatory ECG recordings using a fast QRS detection algorithm and explorative data analysis. *Comput Methods Programs Biomed* 82(1):20–30, 2006.

[70] Johannesen L and Galeotti L. Automatic ECG quality scoring methodology: mimicking human annotators. *Physiol Meas* 33(9):1479, 2012.

[71] Guldenring D, Finlay DD, et al. Transformation of the Mason-Likar 12-lead electrocardiogram to the Frank vectorcardiogram. *Conf Proc IEEE Eng Med Biol Soc* 2012:677–680, 2012.

[72] Lepeschkin E and Surawicz B. The measurement of the QT interval of the electrocardiogram. *Circulation* 6(3):378–388, 1952.

[73] Xue Q and Reddy S. Algorithms for computerized QT analysis. *J Electrocardiol* 30:181–186, 1998.

[74] Martínez JP, Almeida R, et al. A wavelet-based ECG delineator: evaluation on standard databases. *IEEE Trans Biomed Eng* 51(4):570–581, 2004.

[75] Badilini F, Maison-Blanche P, et al. QT interval analysis on ambulatory electrocardiogram recordings: a selective beat averaging approach. *Med Biol Eng Comput* 37(1):71–9, 1999.

[76] Yamaguchi M, Shimizu M, et al. T wave peak-to-end interval and QT dispersion in acquired long QT syndrome: a new index for arrhythmogenicity. *Clin Sci* 105(6):671–676, 2003.

[77] Emori T and Antzelevitch C. Cellular basis for complex T waves and arrhythmic activity following combined IKr and IKs block. *J Cardiovasc Electrophysiol* 12(12):1369–1378, 2001.

[78] Goldenberg I, Moss AJ, and Zareba W. QT interval: how to measure it and what is "normal". *J Cardiovasc Electrophysiol* 17(3):333–336, 2006.

[79] Antzelevitch C, Viskin S, et al. Does Tpeak-Tend provide an index of transmural dispersion of repolarization? *Heart Rhythm* 4(8):1114, 2007.

[80] Opthof T, Coronel R, et al. Dispersion of repolarization in canine ventricle and the electrocardiographic T wave: Tp-e interval does not reflect transmural dispersion. *Heart Rhythm* 4(3):341–348, 2007.

[81] Xia Y, Liang Y, et al. Tpeak-Tend interval as an index of global dispersion of ventricular repolarization: Evaluations using monophasic action potential mapping of the epi- and endocardium in swine. *J Interv Card Electrophysiol* 14(2):79–87, 2005.

[82] Diamant UB, Winbo A, et al. Two automatic QT algorithms compared with manual measurement in identification of long QT syndrome. *J Electrocardiol* 43(1):25–30, 2010.

[83] Couderc JP, Vaglio M, et al. Electrocardiographic method for identifying drug-induced repolarization abnormalities associated with a reduction of the rapidly activating delayed rectifier potassium current. *Conf Proc IEEE Eng Med Biol Soc* 1:4010–4015, 2006.

[84] Draisma HH, Schalij MJ, et al. Elucidation of the spatial ventricular gradient and its link with dispersion of repolarization. *Heart Rhythm* 3:1092–1099, 2006.

[85] O'Hara T, Virag L, et al. Simulation of the undiseased human cardiac ventricular action potential: model formulation and experimental validation. *PLoS Comput Biol* 7(5):e1002061, 2011.

[86] Van Oosterom A and Oostendorp TF. ECGSIM: an interactive tool for studying the genesis of QRST waveforms. *Heart* 90(2):165–168, 2004.

[87] Hall M, Frank E, et al. The WEKA data mining software: an update. *ACM SIGKDD explorations newsletter* 11(1):10–18, 2009.

[88] Leifke E, Gorenoi V, et al. Age-related changes of serum sex hormones, insulin-like growth factor-1 and sex-hormone binding globulin levels in men: cross-sectional data from a healthy male cohort. *Clin Endocrinol (Oxf)* 53(6):689–695, 2000.

[89] Van Dam PM, Oostendorp TF, and Van Oosterom A. ECGSIM: interactive simulation of the ECG for teaching and research purposes. In *Comput Cardiol*, 841–844. IEEE, 2010.

[90] Holford NH, Coates PE, et al. The effect of quinidine and its metabolites on the electrocardiogram and systolic time intervals: concentration–effect relationships. *Br J Clin Pharmacol* 11(2):187–95, 1981.

[91] Crumb W Jr, Pigott JD, and Clarkson CW. Description of a non-selective cation current in human atrium. *Circ Res* 77(5):950–956, 1995.

[92] DeLong ER, DeLong DM, and Clarke-Pearson DL. Comparing the areas under two or more correlated receiver operating characteristic curves: a nonparametric approach. *Biometrics* 44(3):837–845, 1988.

[93] Quinlan JR. *C4.5: programs for machine learning*. Morgan Kaufmann Publishers Inc., 1993.

[94] Darpo B, Sarapa N, et al. The IQ-CSRC prospective clinical phase 1 study: "can early QT assessment using exposure response analysis replace the thorough QT study?". *Ann Noninvasive Electrocardiol* 19(1):70–81, 2014.

[95] Darpo B, Benson C, et al. Results from the IQ-CSRC prospective study support replacement of the thorough QT study by QT assessment in the early clinical phase. *Clin Pharmacol Ther* 97(4):326–35, 2015.

[96] Darpo B, Garnett C, et al. Implications of the IQ-CSRC prospective study: Time to revise ICH E14. *Drug Saf* 38(9):773–80, 2015.

[97] Sager PT, Gintant G, et al. Rechanneling the cardiac proarrhythmia safety paradigm: a meeting report from the Cardiac Safety Research Consortium. *Am Heart J* 167(3):292–300, 2014.

José Vicente is a computer scientist (MSc 2003) and systems engineer (MSc 2011) working at the interface of pharmacology, experimental research, and regulatory science. He has experience in industry and academia, including software development, database design, systems administration, computers architecture, operating systems, signal processing and University teaching.

He joined the Biomedical Signal Interpretation and Computational Simulation (BSICoS) research group at University of Zaragoza (Spain) in 2010. During this period he learned cardiac electrophysiology as well as ECG signal processing techniques. He also contributed to the development of a detector of driver's degree of saturation and relaxation based on biological signals during driving simulation.

Since 2012, he is a research fellow at the U.S. Food and Drug Administration (FDA). His fellowship is supported by an appointment to the Research Participation Program at the Center for Devices and Radiological Health (CDRH) and the Center for Drug Evaluation and Research (CDER) administered by the Oak Ridge Institute for Science and Education (ORISE) through an interagency agreement between the U.S. Department of Energy and the U.S. FDA.

On September 2013, he enrolled in the Biomedical Engineering PhD program at University of Zaragoza, Spain. The main goal of his PhD is to assess whether an integrated analysis of the ECG, including novel T-wave morphology biomarkers, can differentiate multichannel blocking drugs with minimal proarrhythmic risk from selective hERG potassium channel blocking drugs with high proarrhythmic risk.

Through his research experience as an ORISE fellow at CDRH and CDER, he has applied his computer science engineering expertise to study drug effects on novel clinical and preclinical biomarkers to improve drug safety. His work has received several awards including the "Best Poster" award at the Annual meeting of the International Society for Computerized Electrocardiology in 2015, as well as the U.S. FDA "Excellence in Analytical Science " and "The Center for Devices and Radiological Health Director's Special Citation Award". His research has been published in multiple manuscripts in high-impact peer-reviewed journals, and it is part this PhD in Biomedical Engineering Thesis.